

THE UNIVERSITY OF HULL

The mineralogy and petrology of cement clinker and  
its influence on the quality of portland cement.

being a Thesis submitted for the Degree of

Doctor of Philosophy  
in the University of Hull

by

John Howard Medland, B.Sc., M.Sc.

List of samples supplied by Blue Circle.

For the samples marked with an asterisk , results of quality tests performed to BS 4550 were supplied by Blue Circle.

All the results supplied were analysed in the Trend Analysis.

The residence time of the clinker in the kiln and the detailed thermal history of the clinker was not known.

Works A.

Ordinary Portland cement clinker.\*

Works B.

Sulphate resisting cement clinker made with clay and chalk.

Sulphate resisting cement clinker made with pulverised fuel ash and chalk.

11 hourly samples from kiln 1 1930h-0530h

11 hourly samples from kiln 3 1930h-0530h

3 samples of raw kiln feed used during the production run.

Bulk sample of all the clinkers produced during this time.\*

Trial sulphate resisting cement clinker with additional PFA .

7 samples collected at intervals throughout trial at 0730, 1130\*, 1330, 1530\*, 1730, 1930, 2030\*.

Trial Low heat cement clinker

6 samples collected at intervals throughout the trial. 0900\*, 1200\*, 1300\*, 1400, 1500\*, 1600

1 sample of raw kiln feed used during the trial run.

Works C

Ordinary Portland Cement clinker.\*

Works D

Ordinary Portland Cement clinker.\*

Works E

Ordinary Portland Cement clinker.\*

Works F

White Portland Cement clinker.\*

Works G

Ordinary Portland cement clinker.\*

## ABSTRACT.

The relationships between the mineralogical, chemical and petrological characteristics of cement clinker minerals and the quality of the resultant Portland cement, is of great interest to producers and users of cement and concrete.

To examine these relationships, different types of cement clinkers from wet, semi-dry and dry process production kilns were analysed and then tested for quality using British Standard tests. The mineralogical and petrological properties of the calcium silicates, aluminates, ferrites and alkali sulphates were studied. From several thousand mineral analyses performed with an electron microprobe analysis unit, the substitution systems for the different minerals and polymorphs have been determined. The mineral analyses of the various cement clinkers have been plotted on ternary phase diagrams. The different mineral assemblages of the clinkers have been used to assess the effects of composition and production process on the cement clinkers.

All the analyses of the characteristics of the minerals and the quality of the cement have been compared using a trend analysis, developed by the author. This analysis establishes which characteristics have a significant effect on the strength of the Portland cement.

The role of potassium in the cement clinker and particularly its substitution into the belite phase, is crucial. The reasons for this influence and a relationship between the potassium substitution in the belite and the 28 day compressive strength of the cement is presented.

## Acknowledgements.

This research was undertaken with a Postgraduate scholarship from the University of Hull.

I would like to thank all the staff, technicians and research students of the Department of Geology, University of Hull for advice and assistance during the research. Especially Mr.R. Middleton for chemical and computing expertise, and Mr.F. Wilkinson for operation of the microprobe. I would also like to thank Blue Circle Industries for their permission to undertake the project. I would especially like to thank Messers. Sams, Smith, Ellis and Astrop of Northern area and Dr.Murray of Blue Circle Research , for information and guidance . Finally I would like to thank Prof.A.C.Dunham for supervising in all stages.

## Dedication

To my wife

for her patience and encouragement.

## CONTENTS.

### Chapter one.

Introduction.	1
History of Portland Cement	1
Manufacture of cement	1
Utilisation of cement	2
Reasons for research	2

### Chapter two.

Technology of cement manufacture .	4
Raw materials	4
Potential benefits in the use of PFA in cement manufacture.	6
Production methods	7
Cement clinker production processes	7
Manufacture of cement	7
Types of cement studied	9
Operation of cement kilns	11
Production of cement	13

### Chapter three.

The chemical and physical properties of cement clinker.	20
The chemistry of cement	20
X-ray fluorescence	22
Chemical and physical tests used to determine the quality of a cement	27
The requirements of a cement to comply with the British Standards.	27
Chemical tests	27
Physical tests	29

### Chapter four.

The crystallography and mineralogy of cement clinker.	34
---	----

Crystallography and composition of tricalcium silicate.	34
Solid solution of elements in alite.	35
Crystallography and composition of dicalcium silicate.	37
Belite in cement clinker	40
Crystallography and composition of the matrix phases.	42
Aluminate phases	43
Ferrite phases	47
Mineralogy of cement clinker	51
Identification of cement clinker minerals by X-ray diffraction	51
<u>Chapter five.</u>	
The petrology of Portland Cement clinker minerals.	63
Reflected and transmitted light petrology of cement.	65
Etching techniques	64
Alite	65
Belite	69
Belite polymorph classification system.	73
Tricalcium aluminate	74
Ferrite	73
Minor phases	77
The morpholgy of clinker minerals	77
The silicates	77
The matrix phases	79
The order of phase formation	81

## Chapter six

Descriptive petrology of the cement clinkers from the production works.	84
Works B SRC	84
Works B SRC and PFA	89
Works B LHC trial mix	93
Works A OPC	98
Works C OPC	99
Works D OPC	102
Works E OPC	103
Works F OPC	104
Works G OPC	105

## Chapter seven

The phase composition of cement clinker	110
Computational methods	110
Chemical determinations	112
Microscopical methods	112
Evaluation of the errors and accuracy of the determinative techniques.	118

## Chapter eight

The mineral chemistry of cement clinker phases.	121
Mineral analyses	121
Alite in clinker	123
Belite in clinker	137
Ferrite in clinker	149
Tricalcium aluminate in clinker	162
Alkali sulphate phases in clinker	168
The mineral assemblages in the quaternary system $\text{CaO-SiO}_2\text{-Al}_2\text{O}_3\text{-Fe}_2\text{O}_3$ .	173

Mineral assemblages in OPC	173
Dry process kilns	173
Semi-dry process kilns	177
Wet process kilns	182
Mineral assemblages in SRC, LHC and WPC.	182
<u>Chapter nine</u>	
The compressive strength and quality of Portland Cement.	193
Factors influencing the compressive strength of cement.	193
Phase composition	194
Microstructure	199
Multistatistical methods	200
Influence of minor phases	201
<u>Chapter ten</u>	
Analysis of the mineralogical, chemical and petrological characteristics influencing the quality of cement clinker.	208
Correlation coefficients	209
Trend analysis of the characteristics of the cement clinker	209
The influence of potassium on the compressive strength of cement.	215
<u>Appendices</u>	221

Locations of Tables of Results .

Chemical analyses by XRF of cement clinkers for which quality data was available. page 24

Chemical analyses of cement clinkers and kiln feeds from trial production runs at Works B. page 25 and 26

Qualitative assessment of phase composition of the cement clinkers by X-Ray diffraction. page 61

Properties of cement clinker minerals in reflected and transmitted light. page 83

Petrological characteristics of the cement clinker samples. page 109

Potential phase compositions of the cement clinkers. page 120

Mineral analyses (mean values) of alite in the cement clinkers from Works A,B,C,D,E,F,G. page 128

Mineral analyses (mean values) of alite in the cement clinkers from Works B. page 129

Mineral analyses (mean values) of alite in the trial cement clinkers from Works B. page 130

Mineral analyses (mean values) of belite in the cement clinkers from Works A,B,C,D,E,F,G. page 139

Mineral analyses (mean values) of belite in the cement clinkers from Works B. page 140

Mineral analyses (mean values) of belite in the trial cement clinkers from Works B. page 141

Mineral analyses (mean values) of ferrite in the trial cement clinkers from Works B. page 152

Mineral analyses (mean values) of ferrite in the cement clinkers from Works B. page 153

Mineral analyses (mean values) of ferrite and aluminate in the cement clinkers from Works A,B,C,D,E,F,G. page 54

Preferences of the cement clinker minerals for major and minor oxides. page 167

Mineral analyses of Alkali sulphate phases found in the cement clinkers.  
page 169

Trend analyses of the cement clinkers from Works A,B,C,D,E,F,G. pages 210, 211, 212

Mineral analyses of PFA page 24

Mineral analyses of the cement clinker phases by EMPA. pages 236 to 258

## Appendices

For Chapter two	
Appendix two. Characteristics of Pulverised fuel ash.	221
For Chapter three	
Appendix three. a. Sample preparation for element determination by XRF and AAS.	225
b. Chemical composition of SRC cement from chalk and clay.	225
For Chapter four.	
Appendix four. Instruments and operating conditions.	226
For Chapter five.	
Appendix Five. Preparation of polished surface specimens.	227
For Chapter seven.	
Appendix seven a. The Bogue calculation.	230
b. The matrix calculation method.	231
For Chapter eight.	
Appendix eight a. The operation of the electron microprobe.	232
b. Calculation of the mean analyses.	234
Appendix 12. Mineral analyses of cement clinker phases.	235
<u>References.</u>	259

Chapter one

PORTLAND CEMENT.

INTRODUCTION.

History of Portland cement.

The manufacture of Portland cement was patented by J. Aspdin in 1824.

The components for Portland cement were an argillaceous material typically clay or shale and a calcareous material usually limestone or chalk. Initially the raw materials were burnt in a vertical kiln with layers of coal. This was a slow process with intermittent production. To increase production and reduce labour costs, a rotary kiln was developed and patented by Ransome of England. This process used raw materials which had usually been ground wet. Since energy was becoming more expensive, energy efficient processes were developed. Notably semi-dry and dry process kilns with preheating systems to warm the incoming feed with the outgoing exhaust gases.

Manufacture of Portland cement.

The raw materials used are usually sedimentary rocks and they generally have some variation in their mineralogy and chemical composition. The kiln feed material is rapidly heated in the kiln and partial fusion of the mix occurs. This material is known as cement clinker. The clinker is a mixture of several mineral species. The four principal mineral phases are Tricalcium silicate (Alite), Dicalcium silicate (Belite), Tricalcium aluminate and a solid solution series of minerals between  $(Ca_2 Fe_2 O_5)$  and  $(Ca_6 Al_2 Fe_2 O_{15})$ , termed Ferrite.

The proportion of each of the minerals varies according to what

composition of raw mix was put into the kiln. The clinker phases are not in equilibrium and the individual phases do not have stoichiometric compositions. They all have some substitution for the major components in the mineral structure.

#### Utilisation of cement.

In 1981 the world cement industry produced over 7.5 million tonnes of cement. Over 50% of the output is used in the manufacture of concrete. The other major users are masonry and cement products. For these purposes one of the most important properties of the cement is its compressive strength. Differences in cement type, composition and behaviour of the cement clinker minerals causes variation in the strength of the cement. The substituting elements in the individual clinker phases can affect the behaviour of the mineral in its formation, stability and hydration. This in turn influences the properties of the cement when it is hydrated to produce mortar or concrete.

#### Reasons for the research.

There has been extensive research carried out on the properties of Portland cement clinker minerals and the variation in their composition, polymorphs and structural defects. Often this research has been carried out on one type of mineral. This <sup>Mineral</sup> phase may have been derived from a production cement clinker or more commonly from a laboratory scale furnace. This research is useful but it does not relate the clinker properties to the the performance of the cement. With the development of accurate mineral analysis techniques it has been possible to directly investigate the compositional and textural features of the minerals within the cement clinker. In some instances these properties have been related to the performance of the cement, such as hydration rate or strength development. However these experiments have frequently been made on cement clinker carefully prepared from mixes of pure reagents, with

different minor elements added one at a time to investigate their effects. In production cement clinker the minor elements are simultaneously present in the cement clinker. They have interrelated effects on a specific phase and between phases. The effects of these elements on the cement are complex. They control the stabilisation of different polymorphs, the formation of solid solutions, the presence or absence of lattice defects and the variation in the stoichiometric composition of the clinker minerals. These events do not take place individually but in combination. Thus to correlate the effects of the mineralogical and petrological changes on the quality of production cement clinker it is necessary to characterise all the mineralogical, chemical and textural features of different cement clinkers. From this it is then feasible to assess the scale of their effects on the quality of the cement, primarily the strength development.

Thus the aims of this research are -

1. To determine the mineral chemistry of the phases in different types of Portland cement.
2. To determine the petrological characteristics of the cement clinker minerals.
3. To determine the physical properties of the different cement clinkers.

With the objective of defining-

The mineralogical, petrological and chemical properties of the cement clinker which influence the quality and strength of Portland cement.

## Chapter two

### TECHNOLOGY OF CEMENT MANUFACTURE.

#### Introduction

The clinker specimens studied in this project were samples of production material from several works in the United Kingdom operated by Blue Circle Industries Limited.

#### Raw materials

The industrial works generally use suitable local raw material for preparation of the kiln feed . The feed stock consists of a calcareous rock, either chalk or limestone and argillaceous rock frequently clay or shale. The stratigraphic horizons worked by the individual cement works ranged from Devonian to Eocene in age . These raw materials provide the silica , lime , alumina and iron oxides which form the clinker minerals .

Frequently the correct blending of the raw mix to give the desired chemistry requires the addition of a small amount of high grade material, such as silica sand or iron oxide fines. In the production of some types of cement special raw materials are used . In white Portland cement a very low iron content is required ; to achieve this the iron bearing clay is replaced by kaolin . In some localities, waste materials can be used in the production of cement . At Works B, the clay component was replaced with pulverised fly ash ( P.F.A.) from a coal burning power station.

High grade raw materials.

Silica sand.

The silica sand used has a chemical composition of greater than 99% SiO<sub>2</sub>, pure quartz. The sand is used as an additive to raise the silica content of the kiln feed to the required silica modulus, or ratio.

Iron oxide fines.

The iron oxide fines have a chemical composition of about 70 % Fe<sub>2</sub>O<sub>3</sub>, 10 % SiO<sub>2</sub>, 10 % Al<sub>2</sub>O<sub>3</sub> and 10 % TiO<sub>2</sub>. The mineralogy is predominantly magnetite, haematite, ilmenite and a glass phase. The fines are usually termed "pyrites". The iron oxide is used to raise the iron content in the kiln feed to the required alumina-iron modulus, or ratio.

Pulverised fuel ash ( P.F.A. ).

The ash is produced by the burning of crushed coal in the steam generation furnaces at power stations. The chemical composition of PFA varies slightly depending on individual collieries supplying the power stations. However in general the composition of P. F. A. from a single major power station does not vary widely. The mineralogy is glass, magnetite, haematite, quartz, mullite and traces of unburnt fuel. ( A description of P.F.A. is given in Appendix 2 ).

The use of P.F.A. as a replacement for clay in cement has generally been restricted to the production of sulphate resisting Portland cement. This is because the iron content of the P.F.A. is too high to produce a kiln feed of suitable silica ratio and alumina ratio for ordinary portland cement.

A possible technique for upgrading PFA. for use in the manufacture of OPC.

An investigation by the author of the properties of P.F.A., provided a possible means of reducing the iron content to a suitable level for use in the production of Ordinary Portland Cement.

Using a very low power electromagnet, the magnetic particles were easily separated from the ash. These particles were dominantly magnetite

and haematite and were the principle iron bearing phase in the ash. The P.F.A. which had been magnetically separated was chemically analysed by X-ray fluorescence. The original total iron content of 10.07 % had been reduced to 6.8 % .

The magnetically treated P.F.A. has a suitably low iron content for use in Ordinary Portland Cement manufacture as a replacment for the clay or shale. (Typically OPC has  $\sim 2.7\%$   $Fe_2O_3$ )

#### Principal uses of PFA in the United kingdom.

There are very large quantities of P.F.A. produced by coal burning power stations . The production far exceeds the utilisation of the ash . Gutt ( 1974 ) noted that of the 9.9 million tonnes of P.F.A. produced in 1970-71, only 64 % was used. Of the 64 % utilisation , 73.4 % was used as landfill, 16.9 % in concrete blocks and 4.5 % as lightweight aggregate.

#### Potential benefits in the use of PFA in cement manufacture.

If the P.F.A. was upgraded and used as a clay replacement in Ordinary Portland Cement it would save some quarrying costs , reduce land loss, lower production costs of the cement and economise on the large areas of land which are used for P.F.A. storage by the Central Electricity Generating Board. The magnetite extracted from the P.F.A could be used as a source of iron. Alternatively it could be used in mineral preparation processes which require magnetite , for example the 'washing' of coal.

## PRODUCTION METHODS.

### Cement clinker production processes.

There are several different types of cement making processes and the preparation of the kiln feed varies . The main methods can be split into four types , known as dry , semi-dry , semi-wet and wet.

For the dry and semi-dry processes the individual raw material is crushed and mixed to an approximate kiln feed . The mixture is fine ground and homogenized in ball mills , final blending to the correct chemical composition taking place in silos . In the semi-dry process the prepared material is mixed with a small amount of water in a rotating dish to form nodules . These are dried and partly calcined by moving along a grate , heated by the hot exhaust gases from the kiln . In the dry process the raw meal is preheated in ducts by the hot exhaust gases and fed into the kiln, after separation from the gases by a suspension preheater .

In the wet and semi-wet processes the raw materials are slurried . For soft materials such as clay, soaking in water is sufficient . For harder materials such as chalk , shale and limestone, grinding is required. The slurries are blended to the correct chemical composition , with sufficient moisture to remain pumpable and fed to the kiln . For the semi-wet process the slurry is partially dewatered and the resulting filter cake is formed to nodules . These may be dried and partially calcined by a preheater before entry into the kiln .

### The production techniques for the specific cement works.

The cement clinker samples examined in this thesis were normal production materials from the works listed.

Works A , uses limestone and shale as raw materials in a semi-dry process with a grate preheater .

Works B , produced sulphate resisting portland cement using chalk and pulverised fuel ash as raw materials in a wet process.

Works C, uses limestone and shales for raw materials in a dry process with a suspension preheater .

Works D , uses chalk and clay as raw materials in a wet process.

Works E works, uses limestone and phyllite as raw materials in a dry process with a suspension preheater .

Works F, produces white Portland cement ("Snowcrete ") and uses chalk , kaolin and sand as raw materials in a wet process . The kiln is oil fired with a reducing atmosphere and the clinker output is water quenched.

Works G works, uses limestone and shale as raw materials in a semi-dry process with a grate preheater .

All works except F use coal for firing the kilns .

## Manufacture of cement.

### Introduction.

Most modern cement works use a rotary kiln to burn the cement raw feed. The rotary kiln is a steel cylinder lined with refractory bricks . The kiln rotates slowly at about one or two revolutions per minute . The long axis of the kiln is inclined away from the input end . As the kiln rotates the raw material slowly travels down the kiln from the cooler end, dehydrating and decarbonating . Finally as the material nears the flame in the sintering zone , partial melting takes place with reaction between the liquid flux and the unmelted fraction , producing the calcium silicates, aluminates and ferrites .

There are two major calcium silicate minerals. One is an impure form of tricalcium silicate termed alite and the other is a impure form of dicalcium silicate called belite. In cement mineralogy and chemistry the chemical formulae of the minerals are abbreviated. Thus tricalcium

silicate ( $3\text{CaO SiO}_2$ ) is termed  $\text{C}_3\text{S}$ . The dicalcium silicate phase ( $2\text{CaO SiO}_2$ ) is termed  $\text{C}_2\text{S}$ . The principle iron bearing phase is ferrite and this is often assumed to be tetra calcium aluminoferrite ( $4\text{CaO Al}_2\text{O}_3 \text{Fe}_2\text{O}_3$ ) or  $\text{C}_4\text{AF}$ . The actual composition of the ferrite can differ substantially from  $\text{C}_4\text{AF}$ ; it is dependent on the alumina/iron ratio of the cement. The major alumina bearing phase in portland cement is an impure form of tricalcium aluminate ( $3\text{CaO Al}_2\text{O}_3$ ) or  $\text{C}_3\text{A}$ .

The alite phase usually occurs in the cement clinker as angular pseudo-hexagonal crystals (Plate 2a.). The belite phase is generally smaller and rounded (Plate 2b.). The ferrite and aluminate are the matrix material and are formed from the liquid fraction of the clinker in the kiln. The ferrite frequently has a regular platy or dendritic form. (Plate 2b.). The aluminate phase is very small and irregular and it is not easily identified in between the ferrite crystals. The minor phases such as periclase ( $\text{MgO}$ ), alkali sulphates ( $\text{Na, K, CaSO}_4$ ) and free lime ( $\text{CaO}$ ) (Plate 2c.) occur in the matrix phases and the silicates.

The resulting clinker is discharged from the kiln and rapidly cooled in clinker coolers. The cement clinker is usually discharged from the kiln as distinct nodules. The size varies from fractions of a millimetre (dust) to large pieces up to 200 mm. The dominant size range is from 10 mm to 60 mm. The shape and surface texture vary depending on the type of cement being produced and to some extent the production methods used. The clinker is then ground with gypsum to produce cement. The gypsum is required to inhibit the rapid false setting of the cement after mixing with water.

#### TYPES OF CEMENT STUDIED.

##### Ordinary Portland Cement. (OPC)

This is manufactured to comply with British Standard (BS) 12. Ninety percent of cement used is OPC. This has a medium rate of hydration and is grey in colour.

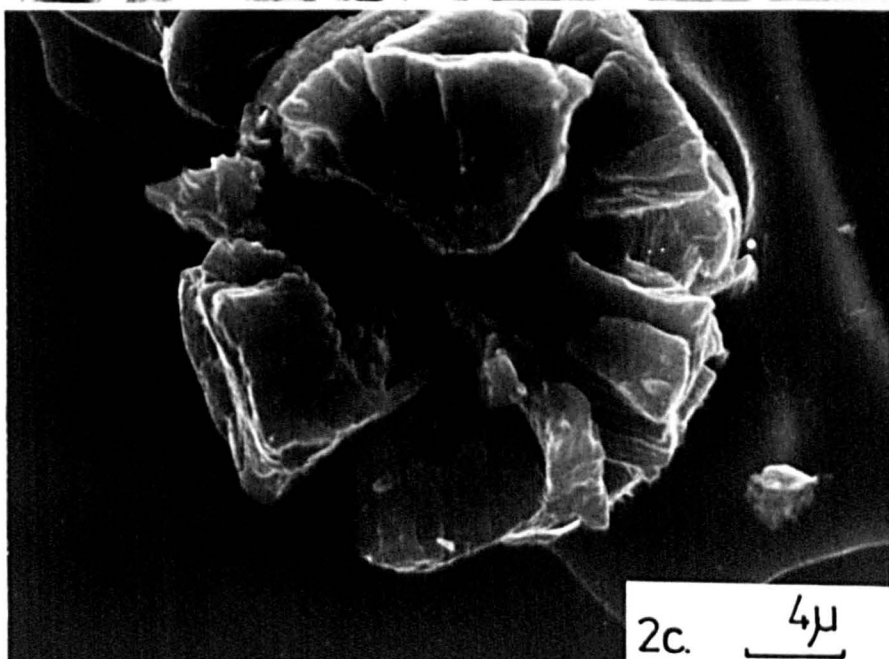
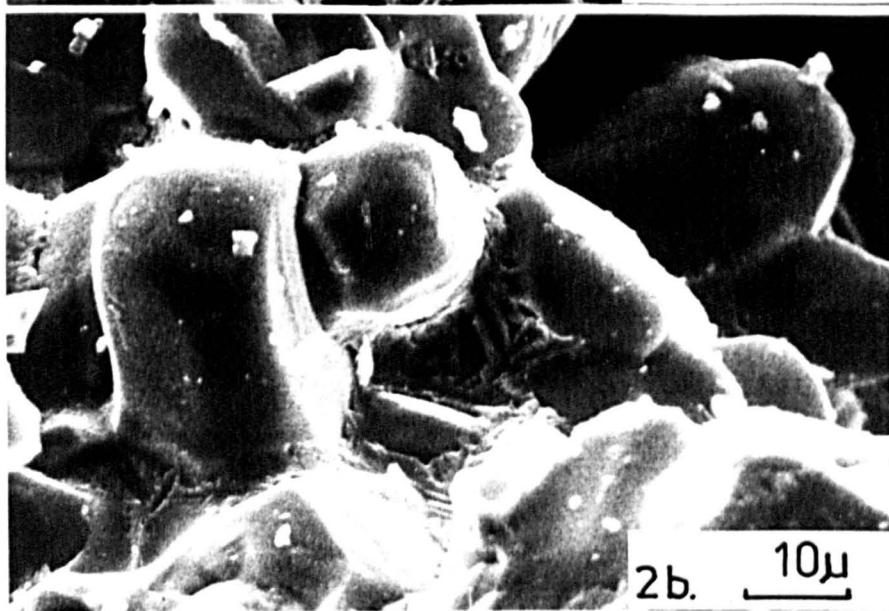
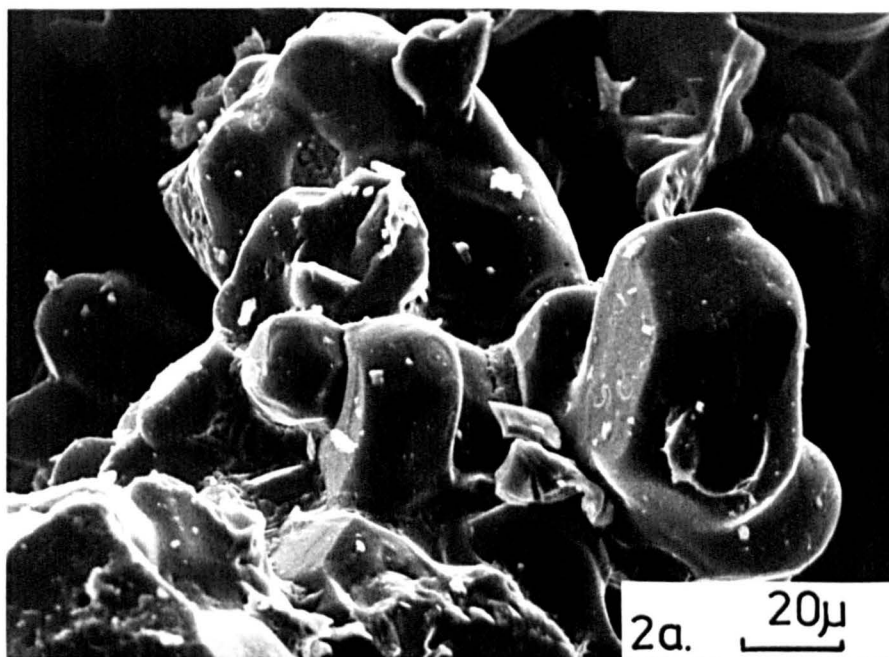
PLATE.2

Morphology of the cement clinker minerals by scanning electron microscopy.

Plate 2a. SEM of cement clinker. The large angular crystal (right hand side above figure number) is a typical alite grain. The rounded grain in the centre right is belite.

Plate 2b. SEM of cement clinker. The matrix material between the alite and belite is aluminate and ferrite. The ferrite grains frequently have a dendritic form.(centre).

Plate 2c. SEM of cement clinker. The rosette form is a partially hydrated frelime fragment. The frelime is extremely reactive with water.



Sulphate resisting portland cement.(SRC)

The susceptibility of Portland cement to sulphate attack is due to the reaction of the hydrated  $C_3A$  compounds with sulphate . To increase the resistance of the cement to sulphate attack , the  $C_3A$  level in the cement is reduced . This level must be lower than 3.5 % to comply with BS 4027 . The rate of hydration is less than OPC .

Low heat Portland cement (LHC)

This cement has less  $C_3S$  and more  $C_2S$  than OPC . The  $C_2S$  hydrates more slowly than  $C_3S$  and evolves heat less rapidly . This cement must comply with BS 1370 . The major use is in massive concrete construction projects or underground workings where a high rate of heat evolution would cause the build up of thermally induced stress in the hardening concrete . This would cause cracking and weakness in the structure.

White portland cement (WPC ) .

This cement is used where a white or coloured concrete is required for architectural reasons . The normal grey colour of OPC is due to the presence of the ferrite phase . To prevent the formation of ferrite , raw materials low in iron oxide are used . The strength of WPC is usually slightly lower than OPC . The cement meets BS 12 requirements and may be used instead of OPC . However it is more expensive because of the raw materials and the production process.

The operation of cement kilns.

Energy Consumption.

When the cement raw material is burnt , the type of process used , the fuel and the kiln conditions influence the final clinker product .

The cement production process has a very high ratio of energy cost to

total material cost , therefore modern kilns are designed to be energy efficient. To achieve this, preheater systems are installed which use the kiln exhaust gases to heat the incoming kiln feed. This has the effect of starting the calcining reaction in the feed before it reaches the kiln . This means that the kiln can be shorter and less heat is lost .

The fuel consumption during clinker production is largely determined by the moisture level of the kiln feed . The moisture content can vary from about 40 % for a wet process to nil for a dry process . The wet process , depending on the moisture content, consumes between 1400 to 1750 Kcal/kg , whilst the dry process with a suspension preheater may use about 850 Kcal/kg ( Jefferson 1978 ).

The heat exchanger system in a wet process kiln may consist of "curtains" of metal chains for about a quarter of the kiln length at the input end .

There are two main types of energy saving devices which are fitted to dry process kilns, the suspension preheater and the travelling grate preheater . The former consists of vertical cascades of cyclone separators, through which the kiln exit gases flow . The raw feed enters at the top and descends counter current to the hot gases and enters the kiln at approximately 760° C. The travelling grate preheater is sometimes termed a semi-dry process. The ground raw meal is mixed with water to form pellets , which are partially calcined on a slow moving grate using the hot exhaust gases .

The energy saving systems frequently cause an increased level of volatile elements such as K, P, Na and S, to be retained in the clinker . This is because the preheating of the raw feed by the exhaust gas allows the volatile elements in the gases to condense on the cooler incoming raw feed and be carried back into the kiln . This disadvantage can be overcome by using raw feed with a lower volatile content.

Kiln atmosphere and conditions.

The majority of cement kilns are designed to operate with an oxidising atmosphere , except kilns producing white cement. These operate with a reducing atmosphere . This preserves any iron content as  $Fe^{2+}$  rather than  $Fe^{3+}$  and prevents any discolouration to the white clinker due to oxidised iron . For heat economy in a normal kiln as little excess air as possible is used . Thus in certain parts of the kiln especially the burning zone , reducing conditions may occur which influence the quality of the clinker produced .

The influence of reducing conditions on the compressive strength of cement.

Sylla ( 1978 ) investigated the effect of a reducing atmosphere and rates of cooling on laboratory produced cement . He found that cement burned under slightly reducing conditions was characterised by a brown colour . It had lower compressive strengths than that produced under oxidising conditions which was a dark grey-green colour . This decrease in strength was thought to be due to the lowering of the alite content in clinkers burnt in reducing conditions ( Woermann 1960 ). The effects of different cooling rates were also found to be important . Brown clinker was produced if the nodules were burnt in reducing conditions and the clinker was cooled to below  $1200^{\circ}$  C. still under reducing conditions . This clinker produced a cement with low compressive strength due to the decrease in alite content . If the clinker was burnt in a reducing environment and was discharged at between  $1350^{\circ}$  C. to  $1200^{\circ}$  C. the clinker colour was grey-green. This was normally associated with clinker produced in oxidising conditions . The clinker however had a lower compressive strength than expected . If the clinker was discharged from the kiln at temperatures greater than  $1350^{\circ}$  C. the cement strength was not reduced, despite being burnt in reducing conditions .

Production of cement.

Fluxes and Mineralizers .

The action of fluxes is to reduce the temperature at which sintering

takes place . Mineralisers accelerate the reaction , Some compounds act as fluxes and mineralizers . The sintering of the cement raw mix takes place at about 1400° C. If the sintering temperature can be lowered, a significant reduction in energy consumption is possible . To achieve this reduction in sintering temperature different fluxes are used . The rate at which the sintering takes place is partially governed by the temperature. To increase the rate of reaction a suitable mineralizer can be used . There is no restriction to the use of flux and mineralizers as long as they do not unduly affect the setting time, strength and expansion of the cement.

The main fluxing materials already in use in Portland cement raw meal are  $Fe_2O_3$  ,  $Al_2O_3$  ,  $MgO$  and alkalis such as  $Na_2O$  and  $K_2O$ . Other fluxes which may occur in some cement raw meals are  $CaF_2$  ( fluorspar),  $P_2O_5$  ,  $ZnO$ ,  $ZnS$  and  $TiO_2$  .

Alternative materials which act as fluxes and, or mineralizers are :-

Sodium fluoride  $NaF$   
Magnesium fluoride  $MgF_2$   
Magnesium fluosilicate  $MgSiF_6$   
Calcium fluosilicate  $CaSiF_6 \cdot 6H_2O$   
Boric Oxide  $B_2O_3$   
Calcium chloride  $CaCl_2$   
Cryolite  $Na_3AlF_6$   
Sodium fluosilicate  $Na_3SiF_6$   
Chromium oxide  $Cr_2O_3$   
Calcium sulphate  $CaSO_4$   
( Gouda, 1980 )

The preceding list of compounds would generally be purposely added to the raw mix if desired .

#### The action and effects of fluxes and mineralizers.

The rate of clinker formation is a function of the amount and viscosity of the liquid formed . A decrease in viscosity lowers the sintering temperature required. The viscosity is lowered by the following compounds in reducing order of power ;  $MnO_2 > Fe_2O_3 > MgO > CaO > Na_2O > K_2O$  . This is the approximate order of the electronegativity of

the compound. Fluxes with small ions carrying high electrical charges are the most active ( Gouda , 1980 ). The viscosity is increased by  $\text{SiO}_2$  and to a lesser extent by  $\text{Al}_2\text{O}_3$ .

The  $\text{Fe}_2\text{O}_3$  and  $\text{Al}_2\text{O}_3$  in the kiln feed act as fluxes, they reduce the sintering temperature at which they combine with the  $\text{CaO}$  and  $\text{SiO}_2$  . They also increase the amount of liquid phase formed and assist in the formation of a high alite content without producing excess freelite ( $\text{CaO}$ ). The fluorspar (  $\text{CaF}_2$  ) has a dual role as both flux and mineralizer. When  $\text{CaF}_2$  is used as a flux, rapid cooling of the clinker is necessary to prevent decomposition of the cement compounds . The amount is critical because the compressive strength of the cement is reduced. Sodium fluoride has a similar effect .

Phosphorus pentoxide (  $\text{P}_2\text{O}_5$  ) is often naturally present in cement raw materials and up to 2.8 %  $\text{P}_2\text{O}_5$  will produce a sound cement ( Gutt and Smith, 1974 ). However the proportioning of the raw mix and the burning conditions have to be changed , because in the presence of  $\text{P}_2\text{O}_5$ , the alite phase decomposes to belite and freelite.

Magnesium fluosilicate (  $\text{MgSiF}_6$  ) is a by-product from the manufacture of phosphoric acid and super phosphate fertilizer . It is extremely reactive at a level of only 1 % , where it reduces the freelite whilst increasing  $\beta$  belite and alite levels (Flint , 1939 ). Generally fluoride or fluosilicate compounds, lower the eutectic temperature, accelerate the reaction to form alite and lower the freelite content. However they do cause a decrease in cement strengths if excess amounts are added.

The presence of boric oxide in  $\beta$  belite prevents the inversion to  $\gamma$  belite, but  $\text{B}_2\text{O}_3$  also inhibits the combination of  $\text{CaO}$ ,  $\text{SiO}_2$  and  $\text{Al}_2\text{O}_3$ .

Calcium sulphate (  $\text{CaSO}_4$  ) frequently occurs naturally in cement raw feed , but it may be added to assist the burning. Gutt and Smith ( 1968 ) have studied the effect of  $\text{SO}_3$  on the cement phases .They found that  $\text{SO}_4^{-2}$  and  $\text{Al}^{3+}$  ions hindered the formation of alite , thus belite was formed

preferentially. They also reported that the presence of  $Mg^{2+}$  counteracted the effect of  $SO_4^{-2}$ . Sarkar (1977), however could find no evidence to indicate that MgO in the presence of  $Al_2O_3$  and  $SO_3$ , significantly controlled the proportions of alite and belite in cement clinker. Knofel (1978) has shown that a small percentage of ZnS reduces the sintering temperature. The zinc was incorporated in the alite as a substitute for calcium. This caused the clinker to become darker. The compressive strength of the cement was increased but the setting time was retarded.

The presence of alkali oxides ( $LiO_2$ ,  $Na_2O$  and  $K_2O$ ), of which  $LiO_2$  is the most active, lowers the temperature at which the liquid phase<sup>forms</sup> and causes higher reactivity in the liquid phase. The alite content decreased and the amount of belite was increased. Frequently high alkali-content cement has been the cause of deleterious reactions with some types of aggregate used in concretes. Therefore the alkali-content is usually kept as low as possible.

Knofel (1977) found that 1%  $TiO_2$  reduced the sintering temperature by  $100^\circ C$ . Larger silicate crystals were formed especially of alite, but the belite content was increased and the alite level was decreased. An addition of 1%  $TiO_2$  lowered the alite level by 10%. However the compressive strength of the cement increased by 10%, despite the lower alite content. This was attributed to the enhanced strength development of the alite with Ti substitution. Unfortunately the increased  $TiO_2$  level retarded the initial set of the cement.

The best flux materials are  $Fe_2O_3$  and  $Al_2O_3$  since they reduce sintering temperature and increase the liquid phase without adverse effects on cement quality. The effects of small amount of the other fluxes and mineralizers frequently have as many adverse effects as beneficial ones. Thus the presence of various minor elements in cement must be considered as important factors in the investigation of cement clinker quality.

### Additions to the kiln .

During the burning process , materials other than the cement raw feed may be introduced into the kiln . This material may be purposely added or it may be a feature of the type of fuel used .

### Alkali rich dusts.

Most cement kilns produce a dust during the burning process . This dust is carried from the kiln by the exhaust gases . To prevent the discharge of the dust into the atmosphere , many kiln systems have gas cleansing precipitators . In some processes the collected dust is returned to a cement kiln . The dust is usually rich in alkalis , but it can be incorporated into the cement raw mix to produce a sound cement . However allowances have to be made in calculating the desired chemistry of the raw feed .

### Coal ash.

The majority of cement manufacturers in the U. K. use powdered coal to fire the cement kilns . Much of the ash produced is precipitated on the clinker nodules . The melting range of coal ash is between 1050° C to 1250° C thus at the sintering temperature of cement ( 1400° C ) the ash is molten . The ash precipitated on the nodules reacts with the clinker minerals .

The quantity and composition of the ash produced will vary depending on the coal used . On average the ash content of coal used is between 10 and 20 % ( Beaupre , 1981 ). The composition of the ash also varies depending on the source of the supply . The usual limits of variation are SiO<sub>2</sub>, 38 to 50 % , Al<sub>2</sub>O<sub>3</sub>, 20 to 40 % , Fe<sub>2</sub>O<sub>3</sub>, 6 to 16 % , CaO, 2 to 10 % , plus MgO , SO<sub>3</sub>, Na<sub>2</sub>O and K<sub>2</sub>O . The composition of the ash is almost identical to pulverised fuel ash ( P.F.A. ) which is produced by coal burning power stations .

The additions to the clinker of SiO<sub>2</sub> , Al<sub>2</sub>O<sub>3</sub> and Fe<sub>2</sub>O<sub>3</sub> from the ash causes a change in the calculated lime saturation factor (L.S.F.) . For a

high ash coal the L.S.F. can be lowered by 10 % , which has to be considered in proportioning the initial kiln feed . The feed must have a surplus of CaO ( L.S.F. > 100 ) to produce a clinker with the L.S.F. in the desired range ( 90 to 98 % ) .(L.S.F. definition p.28)

The molten ash has a very low viscosity and can penetrate very quickly from the outer surface, via cracks and pores into the clinker nodules . The ash is extremely lime deficient. In the contact areas the lime is transferred from the clinker to the ash layer. This causes the formation of large areas of belite in the ash layer and decomposition of the alite to belite in the contact zone of the clinker . Heilman ( 1960 ) found that most of the transport of CaO took place by diffusion through the solid phase . He found some evidence for minor transport of CaO by liquid diffusion . In some high lime clinker , freelite from deeper in the nodules could diffuse to the zones of belite which were lime deficient and would re-establish alite crystals . Such crystals were very large and contained inclusions of the original belite crystals . Heilman concluded that the main problem of using high ash coal lies in the greater tendency to ring formation in the kiln. There would also be a change in cement properties, notably strength and expansion due to the increase in the belite content .

Ash rings form in the kiln because the molten ash frequently cause the clinker nodules to stick together and to the lining of the kiln. Thus at the cooler end of the burning zone, the ash and clinker nodules could stick together and form a ring around the kiln which hampered the movement of the cement clinker along the kiln . This often meant that the kiln had to be shut down to clear the blockage. The lower the ash-content of the coal, the lower the probability of ring formation . The quicker the molten ash could penetrate the clinker, the less chance there was for the clinker surfaces to stick together because of the presence of the layer of molten ash . To overcome the problem of ring formation and the increase in belite content due to high ash coals, the following

procedures may be used. A higher kiln temperature increases the rate of ash assimilation and lessens the sticking action, but it requires more fuel. A higher silica ratio or a higher L.S.F. will counteract the tendency for ring formation because the burning temperature must be increased to sinter the kiln feed. Furthermore a high silica ratio increases the porosity of the clinker and permits the ash to penetrate rapidly into the clinker nodules. The higher silica ratio also increases the amount of belite formation. A higher LSF will counteract this. To produce a good clinker from a high ash coal the LSF should be increased slightly and the burning time lengthened.

Chapter three

THE CHEMICAL AND PHYSICAL PROPERTIES OF CEMENT CLINKER.

THE CHEMISTRY OF CEMENT.

Chemical analysis.

The major and minor elements of the cement clinker :  $\text{SiO}_2$  ,  $\text{Al}_2\text{O}_3$  ,  $\text{CaO}$  ,  $\text{Fe}_2\text{O}_3$  ,  $\text{TiO}_2$  ,  $\text{MnO}$  ,  $\text{MgO}$  ,  $\text{K}_2\text{O}$  ,  $\text{P}_2\text{O}_5$  ,  $\text{SO}_3$  and  $\text{Na}_2\text{O}$  were chemically analysed using X -ray fluorescence (XRF)<sup>spectroscopy</sup>. The advantage of the XRF technique is that it is rapid compared to wet chemical methods and is accurate providing that certain factors are taken into consideration.

Factors affecting X-ray Fluorescence.

In X-ray fluorescence analysis the intensity of the characteristic radiation , emitted by the sample in response to excitation by high energy X-rays , is a measure of the concentration of the particular element . However the intensity of the emitted X-rays is also affected by the physical and chemical conditions of the sample .

Absorption.

The most significant is the absorption of the X-rays in the sample . The greater this absorption , which increases with the increased atomic weight of the elements combined in the sample , the more the characteristic X-rays are weakened . This is because the irradiating X-rays penetrate less into sample containing elements with high atomic weights . Certain characteristic radiation emitted from some elements will in turn excite other elements to emission . These two influencing factors are known collectively as the inter-element effect.

### Grain size in powder samples.

For powder samples, the particle size distribution and packing density influence the emission of the X-rays . This is the grain size effect . For analysis of the major elements except Na , the grain size effect may be overcome by melting the ground cement with a flux, followed by rapid quenching of the sample to a glass.

### Use of flux to manufacture glass discs.

Ludwig and Richardz ( 1978 ) compared twelve commercially obtained fluxes for suitability to produce melts of low viscosity. These fluxes should solidify as a glassy tablet after a short fusion time. After slow annealing they are then serviceable. The use of some fluxes led to the crystallisation and cracking of the glass discs. In X-ray analysis the glass discs should absorb X-rays as little as possible and reduce inter-element effects to such an extent that they do not influence the analysis.

A major advantage of glass discs is that it is possible to analyse different types of cement and cement raw materials using the same calibration factors. Thus it is possible to achieve accurate results, despite significant variations in the mineralogical composition of the samples.

The flux used in the preparation of the discs in this research was Johnson Matthey Spectroflux 105.

### Sample preparation .

The samples received were visually inspected and non-cement fragments such as refractory brick and metal were removed . Each sample was crushed and then ground in a disc mill ( "Tema " ) for 2 X 30 sec. . The ground cement was suitable for glass disc preparation ( Appendix 3. ). For pressed pellet preparation, ( see Appendix 3.) the powder was hand ground

in a pestle and mortar until the " grittiness " was undetectable between pestle and mortar.

Accuracy of X-ray fluorescence analysis.

The accuracy of the cement clinker analyses from our XRF spectrometer were verified by analysing a Portland cement standard from British Chemical Standards (No.372) The same preparation method and instrumental conditions were used.

	<u>BCS</u>	<u>HULL</u>
SiO <sub>2</sub>	21.3	21.1
Al <sub>2</sub> O <sub>3</sub>	5.35	5.43
TiO <sub>2</sub>	0.33	0.31
Fe <sub>2</sub> O <sub>3</sub>	2.49	2.32
MnO	0.06	0.06
MgO	1.30	1.8 **
CaO	65.8	65.2
Na <sub>2</sub> O	0.21	0.19
K <sub>2</sub> O	0.62	0.63
P <sub>2</sub> O	0.19	0.20
SO <sub>3</sub>	.35	2.30
LOI		.54
Total	100.0	100.04

(\*\* The MgO was determined using Atomic Absorption spectroscopy because of the interference of the calcium background with the magnesium peak (Appendix 3).

Results of X-ray analysis of cement clinkers and kiln feed material from works A, B, C, D, E, F and G.

The analyses of the cement clinker and kiln feed shown in Tables (3.1, 3.2 and 3.3 ) are the average of two duplicate discs or powder pellets.

The error factors for the oxides were.  
(Maximum variation between four determinations)

SiO <sub>2</sub>	+/- 0.2 %	
Al <sub>2</sub> O <sub>3</sub>	+/- 0.1 %	
TiO <sub>2</sub>	+/- 0.01%	
Fe <sub>2</sub> O <sub>3</sub>	+/- 0.1 %	
MnO	+/- 0.01%	
MgO	+/- 0.01%	by AAS.
CaO	+/- 0.4 %	
Na <sub>2</sub> O	+/- 0.1 %	
K <sub>2</sub> O	+/- 0.04%	
P <sub>2</sub> O <sub>5</sub>	+/- 0.01%	
SO <sub>3</sub>	+/- 0.05%	

KEY

SRC = Production sulphate resisting cement made from chalk and PFA.

PFB = Trial SRC cement clinker with extra PFA, collected at 1030h.

PFC = Trial SRC cement clinker with extra PFA, collected at 1530h.

PFD = Trial SRC cement clinker with extra PFA, collected at 2030h.

LHA = Trial Low Heat cement clinker collected at 0900h.

LHB = Trial Low Heat cement clinker collected at 1200h.

LHC = Trial Low Heat cement clinker collected at 1300h.

LHD = Trial Low Heat cement clinker collected at 1500h.

OPC = Production Ordinary Portland cement clinker.

WPC = Production White Portland cement clinker.

(Table 3.1 ). X-ray fluorescence analyses of cement clinker from works A,B,C,D,E,F,G.

WORKS CEMENT	WRKS.B SRC	WRKS.B PFB	WRKS.B PFC	WRKS.B PFD	WRKS.B LHA	WRKS.B LHB	WRKS.B LHC
SiO2	20.85	20.93	21.15	19.87	20.36	21.08	20.81
Al2O3	4.05	4.81	4.72	4.18	4.54	4.33	4.56
TiO2	0.17	0.20	0.19	0.18	0.19	0.18	0.19
Fe2O3	4.87	4.81	4.66	4.72	5.21	5.60	6.16
MnO	0.06	0.06	0.05	0.08	0.07	0.06	0.08
MgO	0.55	0.53	0.55	0.55	0.54	0.52	0.52
CaO	66.58	63.51	64.64	65.15	65.64	64.99	64.79
Na2O	0.35	0.78	0.72	0.63	0.45	0.42	0.38
K2O	0.65	1.20	1.09	1.28	0.60	0.57	0.46
P2O5	0.17	0.15	0.15	0.14	0.18	0.19	0.19
SO3	0.71	2.92	1.46	2.29	0.64	0.33	0.24
F	n.d.						
LOI	0.50	0.71	0.86	0.58	0.13	0.88	0.67
TOTAL	99.51	100.61	100.24	99.65	98.55	99.15	99.05

WORKS CEMENT	WRKS.B LHD	WRKS.A OPC	WRKS.E OPC	WRKS.C OPC	WRKS.F WPC	WRKS.D OPC	WRKS.G OPC
SiO2	20.73	20.23	20.63	21.11	23.09	22.06	20.70
Al2O3	4.49	6.37	6.25	6.43	4.60	5.82	6.40
TiO2	0.19	0.26	0.26	0.29	0.01	0.33	0.31
Fe2O3	6.59	3.64	2.48	2.49	0.30	2.97	2.47
MnO	0.07	0.10	0.13	0.06	0.06	0.05	0.07
MgO	0.52	2.80	2.30	1.20	0.30	1.40	2.70
CaO	64.94	65.22	64.17	66.28	68.46	65.48	65.16
Na2O	0.46	0.19	0.38	0.48	0.28	0.35	0.42
K2O	0.62	0.41	1.48	0.51	0.19	0.47	0.52
P2O5	0.18	0.14	0.07	0.21	0.17	0.22	0.22
SO3	0.69	0.66	1.24	1.40	0.45	0.27	0.82
F	n.d.	0.07	0.05	0.27	0.03	0.10	0.04
LOI	0.20	0.62	1.50	0.28	2.03	0.16	0.59
TOTAL	99.68	100.71	100.94	101.01	99.97	99.68	100.42

KEY

K3 = Production Sulphate resisting cement ( SRC ) from kiln 3

PF = Trial SRC with PFA addition.

LH = Trial Low Heat cement clinker.

KF = Kiln feed for SRC clinker production.

LH.KFD = Kiln feed for Low Heat clinker.

The four digits after each sample identifier is the time of collection of the  
clinker.

(Table 3.2). X-ray fluorescence analyses of cement clinker and kiln feeds from works B. SRC. clinker (K3), SRC with PFA kiln additions (PF) and LHC trial mix (LH); (KF) is kiln feed.

Sample	K30530	KF2000	KF2300	KF0200	PF0730	PF1130	PF1330
SiO <sub>2</sub>	20.14	13.96	13.50	13.75	19.68	20.93	21.28
Al <sub>2</sub> O <sub>3</sub>	3.91	2.55	2.42	2.45	4.12	4.81	4.94
TiO <sub>2</sub>	0.17	0.10	0.10	0.10	0.17	0.20	0.21
Fe <sub>2</sub> O <sub>3</sub>	4.70	3.12	3.11	3.12	4.72	4.81	4.95
MnO	0.06	0.03	0.02	0.01	0.06	0.06	0.07
MgO	0.54	0.25	0.24	0.26	0.55	0.53	0.54
CaO	66.92	44.50	43.60	43.41	64.97	63.51	64.53
Na <sub>2</sub> O	0.45	0.15	0.17	0.16	0.87	0.78	0.72
K <sub>2</sub> O	0.78	0.42	0.41	0.40	1.18	1.20	1.10
P <sub>2</sub> O <sub>5</sub>	0.18	0.11	0.10	0.10	0.14	0.15	0.16
SO <sub>3</sub>	0.80	0.20	0.20	0.20	2.48	2.92	1.26
LOI	0.50	34.95	35.50	35.00	0.34	0.71	0.60
TOTAL	99.15	100.34	99.37	98.96	99.28	100.61	100.36

Sample	PF1530	PF1730	PF1930	PF2030	LH0900	LH1200	LH1300
SiO <sub>2</sub>	21.12	21.19	20.92	19.87	20.36	21.08	20.81
Al <sub>2</sub> O <sub>3</sub>	4.74	4.70	4.60	4.18	4.54	4.33	4.56
TiO <sub>2</sub>	0.19	0.20	0.20	0.18	0.19	0.18	0.19
Fe <sub>2</sub> O <sub>3</sub>	4.75	4.58	4.50	4.72	5.21	5.60	6.16
MnO	0.05	0.05	0.06	0.08	0.07	0.06	0.08
MgO	0.55	0.54	0.54	0.55	0.54	0.52	0.52
CaO	64.44	64.84	65.19	65.15	65.64	64.99	64.79
Na <sub>2</sub> O	0.73	0.71	0.71	0.63	0.45	0.42	0.38
K <sub>2</sub> O	1.18	0.99	1.10	1.28	0.60	0.57	0.46
P <sub>2</sub> O <sub>5</sub>	0.15	0.15	0.15	0.14	0.18	0.19	0.19
SO <sub>3</sub>	1.76	1.16	1.51	2.29	0.64	0.33	0.24
LOI	0.62	1.08	0.52	0.58	0.13	0.88	0.67
TOTAL	100.28	100.19	100.00	99.65	98.55	99.15	99.05

Sample	LH1400	LH1500	LH1600	LH.KFD
SiO <sub>2</sub>	20.32	20.73	20.11	13.48
Al <sub>2</sub> O <sub>3</sub>	4.32	4.49	4.60	2.47
TiO <sub>2</sub>	0.19	0.19	0.19	0.11
Fe <sub>2</sub> O <sub>3</sub>	6.26	6.59	6.20	3.01
MnO	0.09	0.07	0.09	0.03
MgO	0.51	0.52	0.54	0.25
CaO	63.50	64.94	65.33	43.51
Na <sub>2</sub> O	0.06	0.46	0.47	0.31
K <sub>2</sub> O	1.06	0.62	0.52	0.42
P <sub>2</sub> O <sub>5</sub>	0.17	0.18	0.17	0.10
SO <sub>3</sub>	1.79	0.69	0.59	0.18
LOI	0.83	0.20	0.45	35.91
TOTAL	99.10	99.68	99.26	99.78



KEY

K1 = Production Sulphate Resisting cement from Kiln 1.

K3 = Production Sulphate Resisting cement from Kiln 3.

The four digits indicate the time of collection of the clinker.

(Table 3.3 ). X-ray fluorescence analyses of cement clinker and kiln feeds from works B. SRC. clinker (K1,K3)

Sample	K11930	K12030	K12130	K12230	K12330	K10030	K10130
SiO2	21.26	21.10	21.43	21.57	21.60	22.05	21.55
Al2O3	4.07	4.30	4.29	4.34	4.30	3.88	4.01
TiO2	0.17	0.17	0.17	0.13	0.18	0.17	0.17
Fe2O3	5.06	5.04	5.22	4.47	5.23	4.73	5.04
MnO	0.04	0.06	0.05	0.03	0.07	0.09	0.08
MgO	0.53	0.53	0.50	0.58	0.54	0.55	0.56
CaO	66.19	66.10	66.44	65.89	65.81	66.15	66.04
Na2O	0.21	0.24	0.24	0.23	0.20	0.21	0.18
K2O	0.30	0.39	0.40	0.30	0.27	0.34	0.28
P2O5	0.17	0.15	0.17	0.14	0.14	0.14	0.14
SO3	0.10	0.03	0.10	0.02	0.04	0.06	0.04
LOI	0.60	0.85	0.53	0.32	1.10	0.79	0.86
TOTAL	98.70	98.96	99.54	98.02	99.48	99.16	98.95

Sample	K10230	K10330	K10430	K10530	K31930	K32030	K32130
SiO2	22.00	21.61	21.71	21.62	19.96	19.83	20.04
Al2O3	3.97	4.01	4.18	4.19	4.14	4.01	4.18
TiO2	0.17	0.17	0.18	0.17	0.18	0.17	0.17
Fe2O3	4.90	4.95	5.15	5.16	4.84	4.65	4.97
MnO	0.07	0.08	0.07	0.06	0.05	0.04	0.06
MgO	0.56	0.55	0.55	0.55	0.55	0.52	0.52
CaO	66.93	66.51	66.92	66.21	67.09	65.82	66.03
Na2O	0.18	0.17	0.23	0.22	0.37	0.73	0.56
K2O	0.27	0.34	0.32	0.31	0.87	1.77	1.27
P2O5	0.14	0.14	0.14	0.14	0.20	0.19	0.17
SO3	0.04	0.11	0.06	0.09	1.40	1.50	1.90
LOI	0.67	1.37	1.14	1.28	0.40	0.60	0.20
TOTAL	99.90	100.01	100.65	100.00	100.05	99.83	100.07

Sample	K32230	K32330	K30030	K30130	K30230	K30330	K30430
SiO2	20.07	20.09	20.18	20.15	20.06	20.11	20.48
Al2O3	4.00	3.98	3.85	3.95	3.94	3.78	3.84
TiO2	0.17	0.17	0.17	0.17	0.17	0.17	0.17
Fe2O3	4.74	4.88	4.71	4.79	4.72	4.67	4.52
MnO	0.03	0.07	0.07	0.05	0.06	0.07	0.08
MgO	0.55	0.56	0.57	0.55	0.54	0.55	0.53
CaO	67.12	67.09	66.73	67.30	66.73	67.90	67.01
Na2O	0.46	0.41	0.52	0.47	0.53	0.57	0.41
K2O	1.04	0.64	0.93	0.71	1.06	1.02	0.70
P2O5	0.19	0.19	0.18	0.19	0.19	0.36	0.19
SO3	1.70	0.90	1.50	0.90	1.40	1.80	0.70
LOI	0.32	0.51	0.55	0.60	0.40	0.05	0.60
TOTAL	100.39	99.49	99.96	99.83	99.80	101.05	99.23

The chemical and physical tests used to determine the quality of a cement.

The requirements of a cement to comply with the British Standards.

The quality of a cement was determined by a series of tests . These tests are strictly controlled procedures and precise details are given in British Standard ( BS ) 4550 'Methods of testing cement '. Many of these tests are usually made on daily samples of the cement production as a method of quality control . If a cement was produced as an experimental run , many cement samples were collected and tested using the procedures , to evaluate the quality of the cement.

Chemical tests.

The following chemical determinations are performed on cement clinker. They form part of the British Standard requirements. These determinations are: insoluble residue , total silica , ammonium hydroxide group , total calcium oxide , total alumina oxide , total iron oxide , magnesium sulphuric anhydride , sulphate present as sulphide , total sulphur , loss on ignition, minor constituents and free lime , pozzolanicity test for pozzolanic cement , sodium oxide and potassium oxide by flame photometry .

For routine quality control purposes at many cement works, the cement was usually analysed by XRF . The other chemical analyses usually performed, were for free lime , insoluble residue and loss on ignition determinations. The requirements for the different cements is shown in Table 3.4.

If a significant quantity of unusual elements are present in the cement , for example manganese or fluorine , the elements are determined by suitable methods such as selective ion determination .

Cement ratios and moduli.

After the chemical analysis of the cement, several calculations can be made to characterise the cement . These are-

Lime saturation factor. (LSF) .

This was calculated by the formula

$$LSF = \frac{CaO - 0.7(SO_3)}{2.8(SiO_2) + 1.2(Al_2O_3) + 0.65(Fe_2O_3)}$$

Each symbol in brackets refers to the total weight percentage of each oxide in the clinker . When the calculation was carried out on the kiln feed the  $SO_3$  content was not considered . Frequently the result was multiplied by 100 . The LSF of most cements was between 90 and 102 . The range for British cements is given in Table 3.4.

Silica ratio (SR) , Alumina ratio (AR).

These ratios are sometimes referred to as moduli in the literature .

The Silica Ratio was calculated by the formula

$$SR = \frac{SiO_2 \text{ total wt. \%}}{Al_2O_3 \text{ total wt. \%} + Fe_2O_3 \text{ total wt. \%}}$$

The Silica Ratio influences the proportions of  $C_3S$  and  $C_2S$  present in the cement . A high Silica Ratio generally favours the formation of  $C_2S$  , but it is also influenced by the Alumina Iron Ratio .

The Alumina Ratio or ( Alumina-Iron Ratio) was calculated by the formula

$$AR = \frac{Al_2O_3 \text{ total wt. \%}}{Fe_2O_3 \text{ total wt \%}}$$

The Alumina Ratio influences the temperature of burning and the rate of reaction. This is because the iron oxides and alumina oxides act as fluxes in the sintering process . The ratio also determines the amount of ferrite and aluminate formed . A low Alumina Ratio produces a clinker with a high ferrite and low  $C_3A$  content . A high Alumina Ratio produces the reverse effect.

There are no ranges given in the British Standards for Silica Ratios or Alumina Ratio . However the calculation is useful for prediction of burning behaviour and mineralogy . For cements in the U.K , the Silica Ratio was usually between 1.5 to 4.0 . The Alumina Ratio was between 1.4 to 3.5<sup>(Jefferson, 1979)</sup> except for white cements in which the Alumina Ratio was about 15.

#### Mineralogical Properties .

The British Standards only require the calculation of the C<sub>3</sub>A content of cement, calculated by the formula

$$C_3A = 2.65(Al_2O_3) - 1.69(Fe_2O_3)$$

The C<sub>3</sub>A content is used to determine the maximum permissible SO<sub>3</sub> content in OPC and LHC . For SRC the maximum C<sub>3</sub>A content was specified in the standard to minimise the weakening effects of sulphate attack on the aluminate. ( Table 3.4) .

#### Physical tests.

The physical tests were carried out on a batch ground cement made by grinding the clinker with good quality commercial gypsum to a target SO<sub>3</sub> content of 2.5%.

#### Fineness.

The fineness to which a cement was ground was dependant on the type of cement . This fineness was measured by the determination of the surface area . ( Table 3.5). The target level varied from works to works dependent on the actual reactivity of the cement produced .

#### Determination of surface area.

The surface area was determined by the Lea and Nurse method . This method was based on the principle that the ratio of flow through a bed of compacted powder was governed by the void structure of the bed . The structure was related to the fineness of the powder and thus the surface area . The rate of flow was measured by the fall in pressure between the

primary air input and the air output from the bottom of the cell with the cement in . The full procedure is given in BS 4550 : Part 3 : section 3 .

#### Setting times .

For this test an instrument known as the Vicat apparatus was used . This instrument measures the resistance of a paste of a standard consistency to the penetration of a needle under load. The initial setting time determined the length of time which the cement remained plastic and workable after mixing with about 25 % water content . This length of time varied due to the properties of the cement , principally fineness . The minimum time given in most standards for OPC was 45 minutes . The final setting time was when the paste became rigid and solid . This final setting time controlled the speed at which construction work could continue and a maximum of 8 to 10 hours was usually quoted .

#### Compressive strength tests .

The test measures the compressive strength of concrete or mortar after different periods of time. To minimise the effect of variables other than the cement itself , a standard procedure is used, ( BS 4550 : part 3 : section 3:4 ). The procedure involves the mixing of a sample of cement with a suitable coarse aggregate . These materials are mixed in specified proportions and the test specimens are made in the shape of cubes with 10 cm. sides. The test specimens are made by carefully filling , compacting and the striking off of the cube moulds . Usually batches of 12 cubes were made from one single batch of mixed concrete .

After filling the moulds ,the samples were placed in a moist curing room for 24 hours . Then the concrete cubes were removed from the moulds and marked for later identification. They were then stored in a curing tank filled with water at 20° C . The compressional strength of the cubes was tested after a specific time had elapsed usually 1 day , 3 days , 7 days and 28 days . Three cubes were tested each time.

The compressional force required to break the cubes was recorded to the nearest 0.5 N/mm<sup>2</sup> . If one of the results varied by more than +/- 5 % from the average of the set ,this value was discarded and the average recalculated. If two results varied by more than +/- 5 % the complete set of results was discarded . The compressive strength of cement could also be measured with 70.7 mm. cubes made of mortar ( sand and cement with no coarse aggregate ) . The mixture was vibrated to compact the cubes rather than the previous tamping method. The compressional strength test then proceeded as described previously.

#### Soundness and heat of hydration .

This test was not made as routine on samples , only on cement with a susceptibility to unsoundness . The presence of frelime ( CaO ) or periclase ( MgO ) could cause cracking of the hardened concrete due to delayed expansion of the two phases as they hydrated . The susceptibility of a cement to unsoundness due to frelime could be tested by hydrating the cement paste under water for 24 hours. The cement sample was then boiled in the water for 30 minutes. The expansion produced in the cement was measured . A large expansion indicated an unsound cement. This is the Le Chatelier test . This rapid test is unsuitable for detection of unsoundness due to MgO. This is because the temperatures in the cement kilns produce 'deadburnt' periclase. Thus it will only hydrate slowly over a period of years at normal temperatures. A suitable test for unsoundness due to MgO is the Autoclave test ( ASTM C 151 ). In this test the cement paste sample is treated in an autoclave for 3 hours at 295 P.S.I. The high temperature conditions in this test cause the hydration of MgO and CaO and gives an better indication of the potential unsoundness of the cement.

#### Heat of hydration ( BS 4550 part 3.8 ).

The heat of hydration of cement was measured calorimetrically and expressed as kilojoules per kilogram of anhydrous mass (Table 3.4) .

There are several rapid non standard semiquantitative methods which produce a good assessment. These tests measure the cumulative temperature rise of a hydrating cement sample over a short period of time. This is achieved by insulating the hydrating cement paste and recording the temperature of the paste every 30 minutes for about 12 hours. From the results, the rate of heat output can be determined.

TABLE(3.4)BRITISH STANDARD REQUIREMENTS FOR CEMENT.

Standard	OPC BS 12 (p2) (1971)	SRC BS 4027 (p2) (1972)	LHC BS 1370 (p2) (1979)
<b>CHEMICAL TESTS.</b>			
Lime saturation factor	66-102	66-102	66-88
Insoluble residue max wt.%	1.5	1.5	1.5
MgO Max. % total	4.0	4.0	4.0
SO <sub>3</sub> Max. % total			
with C <sub>3</sub> A content < 5 %	2.5	2.5	2.5
with C <sub>3</sub> A content > 5 %	3.0	-	3.0
Loss on ignition %			
temperate climate	3.0	3.0	3.0
tropical climate	4.0	4.0	4.0
<b>MINERALOGICAL TESTS.</b>			
C <sub>3</sub> A content % Max.	-	3.5	-
<b>PHYSICAL PROPERTIES .</b>			
Compressive strength MN/m <sup>2</sup> (min) on 10 cm.concrete cubes			
at 3 days	8.0	8.0	8.0
at 7 days	14.0	14.0	7.0
at 28 days	-	-	14.0
Fineness			
surface area, m <sup>2</sup> /Kg minimum	225.0	250.0	320.0
Setting time, Vicat apparatus			
inital set, not less than (mins)	45	45	60
final set, not more than (hours)	10	10	10
Soundness, expansion in mm. max.	10	10	10
Heat of hydration J/g ,max.			
7 days	-	-	250
28 days	-	-	290

The results of the chemical and physical tests made on the cement clinker from works A, B, C, D, E, F and G are presented in Table 3.5.

(Table 3.5). Compilation of values including British Standard tests used to determine quality of cement from the industrial works .

Works Cement	WKS.B SRC	WKS.B PFB	WKS.B PFC	WKS.B PFD	WKS.B LHA	WKS.B LHB	WKS.B LHC
LSF	100	92	94	100	100	96	96
Si Ratio	2.34	2.18	2.25	2.23	2.09	2.12	1.94
Al Ratio	0.83	1.00	1.01	0.89	0.87	0.77	0.74
Initial set	110	165	135	135	170	230	175
Final set (mins.)	200	225	195	190	250	310	230
Surface area (m <sup>2</sup> /Kg)	380	364	363	369	342	325	328
H2O %	28	27	27	29	26	26	27
SO3 %	2.3	2.5	2.5	2.5	2.5	2.5	2.5
Na2O/K2O	0.54	0.65	0.66	0.49	0.75	0.73	0.83
Equiv. K2O	0.53	1.18	1.09	0.95	0.68	0.64	0.58
Freelime %	1.6	1.2	2.5	5.1	2.8	2.1	1.0
COMPRESSIVE STRENGTHS ( in N/mm <sup>2</sup> )							
Day 1	11.9	13.3	14.8	11.4	10.9	9.7	12.5
Day 3	24.9	23.3	24.3	19.9	23.5	24.0	23.4
Day 7	32.0	30.9	31.0	24.2	31.0	34.4	30.4
Day 28	39.7	40.6	39.4	31.6	38.2	42.6	35.5

Works Cement	WKS.B LHD	WKS.A OPC	WKS.E OPC	WKS.C OPC	WKS.F WPC	WKS.D OPC	WKS.G OPC
LSF	96	99	97	97	97	94	98
Si Ratio	1.87	2.02	2.37	2.37	4.71	2.51	2.33
Al Ratio	0.68	1.75	2.52	2.58	15.32	1.96	2.59
Initial set	235	140	150	240	205	175	140
Final set (mins)	365	165	175	305	250	210	175
Surface area (m <sup>2</sup> /Kg)	329	352	354	354	355	354	347
H2O %	27	24	28	25	29	25	25
SO3 %	2.5	2.5	2.6	2.4	2.5	2.4	2.5
Na2O/K2O	0.74	0.46	0.26	0.94	0.31	0.74	0.81
Equiv. K2O	0.94	0.62	0.58	0.72	0.42	0.53	0.64
Freelime %	0.7	1.8	1.5	0.3	3.1	0.5	2.2
COMPRESSIVE STRENGTHS ( in N/mm <sup>2</sup> )							
Day 1	8.0	9.7	11.9	9.8	7.4	7.8	12.7
Day 2	21.5	20.1	23.3	28.2	18.6	21.2	24.6
Day 7	31.1	30.7	29.2	38.6	26.0	30.1	35.0
Day 28	40.9	49.6	35.3	51.3	39.3	44.7	46.2

Chapter four

THE CRYSTALLOGRAPHY AND MINERALOGY OF CEMENT CLINKER MINERALS.

CRYSTALLOGRAPHY OF CEMENT CLINKER MINERALS.

Crystallography and composition of tricalcium silicate  $C_3S$

Alite, the main constituent of cement clinker, was thought to be a solid solution of  $Ca_3SiO_5$  by Guttman and Gille (1931). Work by Jeffery (1952) determined the structure of  $Ca_3SiO_5$ . This consisted of Ca ions, isolated  $SiO_4$  tetrahedra and additional oxygens, the latter being coordinated to Ca only. Jeffery proposed three modifications for  $C_3S$ . Investigation by Bigare et al. (1967) showed that there were six polymorphs, three triclinic ( T1, T2, T3 ), two monoclinic ( M1, M2 ) and a trigonal high temperature form, often termed rhombohedral, ( R ). These polymorphs of pure  $C_3S$  had the following reversible transitions upto the decomposition temperature of 1250° C.

T1- 620° C -T2- 920° C -T3- 960° C -M1- 990° C -M2- 1050° C -R

Maki and Chromy (1978) using optical microscopy found an unidentified monoclinic phase M3 between M2 and R. The role of foreign atoms and the limits of solubility and the stabilization of the different polymorphs has been extensively investigated by Hahn et al. ( 1968 ). They found that pure  $Ca_3SiO_5$  was unstable with respect to  $Ca_2SiO_4$  and CaO below 1200° C. The effect of the substituting ions was to stabilize, to a certain extent the  $C_3S$  polymorphs. Their investigations established that pure tricalcium silicate was a stoichiometric compound of  $3CaO SiO_2$ . This disagreed with Boikova and Toropov (1964) who found an excess of 0.5 to 1.0 wt.% CaO in pure tricalcium silicate.

Solid solution of minor elements in alite.

Alite and alumina.

The alumina was incorporated in the lattice of  $C_3S$  as  $Al_2O_3$  or  $C_3A$ . Woermann et al ( 1963) distinguished two types of solid solution for  $Al_2O_3$ . Initially, up to 0.45%  $Al_2O_3$  , the  $Al^{3+}$  replaced  $Si^{4+}$  in tetrahedral sites and occupied the free octahedral sites , maintaining the electrostatic neutrality of the lattice. Secondly, for 0.45 % to 1 %  $Al_2O_3$  , the replacement was either as linked substitutions of Al for Si in tetrahedral sites and Al for Si in octahedral sites ; or by continuous balanced replacement of Si by Al, for the most part in the octahedral sites occupied by Ca and to a smaller extent in the vacant octahedral sites . Above 1 %  $Al_2O_3$  , tricalcium aluminate was formed as a separate phase. The solubility level was independent of temperature . Midgley and Fletcher (1963 ) found the same solubility results . However they maintained that the substitution of Al in the lattice was not due to  $C_3A$  in  $C_3S$  , but to a solid solution of the series  $C_3S - C_{4.5}A$ .

Alite and magnesia.

Jeffery ( 1952 ) proposed that alite had a definite composition with additional atoms in fixed lattice sites . The Mg substituted for Ca and 2 Si ions substituted for 2 Al ions plus one additional Mg ion in a vacant site to maintain the neutrality of the lattice . This had a compositional formula of  $Ca_{54} Mg Al_2 Si_{10} O_{90}$  (  $MgO = 0.96$  wt.% ).

Woermann et al ( 1963 ) proposed that Mg ions replaced an equal number of  $Ca^{2+}$  ions in the  $C_3S$  lattice . The solubility limit was up to 2% and was dependant on temperature .

Alite and iron.

Fletcher ( 1965 ) found that the solid solution was in the series

$C_3S-C_2F$ . In this substitution the  $3Ca^{2+}$  ions were replaced by  $3Fe^{2+}$  and  $6Si_4$  by  $6Fe^{3+}$ . The change was compensated for by one  $Fe^{3+}$  ion in an interstitial position. The limit of solubility of  $Fe_2O_3$  in  $C_3S$  was thought to be 1.1 % by Woermann et al ( 1963 )

Since Al and Fe ions occupy similar lattice positions their solubilities were interdependent .

#### Alite and sodium with potassium.

Woermann et al (1979) determined that the decomposition of pure  $C_3S$  to  $C_2S$  and  $CaO$  occurred at  $1180 \pm 10^\circ C$ . However this temperature increased greatly with  $K_2O$  substitution and slightly with  $Na_2O$  substitution. The level of alkali that could be incorporated in  $C_3S$  at  $1500^\circ C$  was 1.4 %  $K_2O$  and 1.4 %  $Na_2O$  .

#### Solid solution of other minor elements in alite.

##### Alite and Fluorine.

Welch and Gutt ( 1960 ) found that  $CaF_2$  (fluorspar) accelerated the formation of alite but reduced the hydraulicity . At levels greater than 0.74 % fluorine, the alite started to decompose to produce  $\alpha' C_2S$  and  $\alpha C_2S$ . Gutt and Osborne ( 1966 ) found two calcium silicofluorides  $3(Ca_3SiO_5)CaF_2$  and  $2(Ca_2SiO_4)CaF_2$  which they thought were intermediate compounds in the formation of  $C_2S$  and  $C_3S$  when fluorine was present in the cement raw materials.

##### Alite and Phosphorus.

Nurse ( 1952 ) showed that for each 1%  $P_2O_5$  present in the cement, the alite content was reduced by 9.9% and the belite level was raised by 10.9%. Welch and Gutt ( 1960 ) found that alite could take up to 1 %  $P_2O_5$  into solid solution involving a distortion of the lattice rather than true polymorphism .

### Alite and Titanium.

Kondo and Yoshida ( 1968 ) have shown that Ti substitutes for Si in alite to a limit of 0.6 % at 1500-1600° C .

Manganese. Kondo and Yoshida (op. cite.) found that  $Mn_2O_3$  was soluble in alite up to 0.7% at 1500 - 1600° C.

### Alite and Sodium.

Yamaguchi et al ( 1962 ) found that  $Na_2O$  substituted for  $CaO$  in the alite lattice up to a limit of 0.3 % .

The existance of these different types of solid solutions indicate that alite is not a compound with a definite composition.

### Crystallography and composition of Dicalcium silicate $C_2S$ .

#### Polymorphic forms of $C_2S$

There has been very extensive study of the polymorphism of dicalcium silicate using high temperature X-ray diffraction (X.R.D) and differential thermal analysis (D.T.A) . From these investigations five well defined polymorphs have been found.( Midgley, 1974 )

( High temperature ) alpha ( $\alpha$ )  $C_2S$  -- alpha dash high ( $\alpha'H$ )  $C_2S$  -- alpha dash low ( $\alpha'L$ )  $C_2S$  -- beta ( $\beta$ )  $C_2S$  -- gamma ( $\gamma$ )  $C_2S$  ( low temperature ).

Some researchers claim the existance of other modifications , but there is no overall agreement . The principal  $C_2S$  polymorph present in Portland cement is the  $\beta$  form with occasionally some  $\alpha$  and  $\alpha'$  belite. The  $\gamma$  phase is non hydraulic and is generally a very minor component in cement except in unusual conditions.

Polymorphic transformations in dicalcium silicate.

The temperature stability fields of the polymorphs are variable due to the stabilizing effect of certain elements on individual polymorphs . The system of C<sub>2</sub>S transformations was shown schematically by Niesel and Thormann (1967).

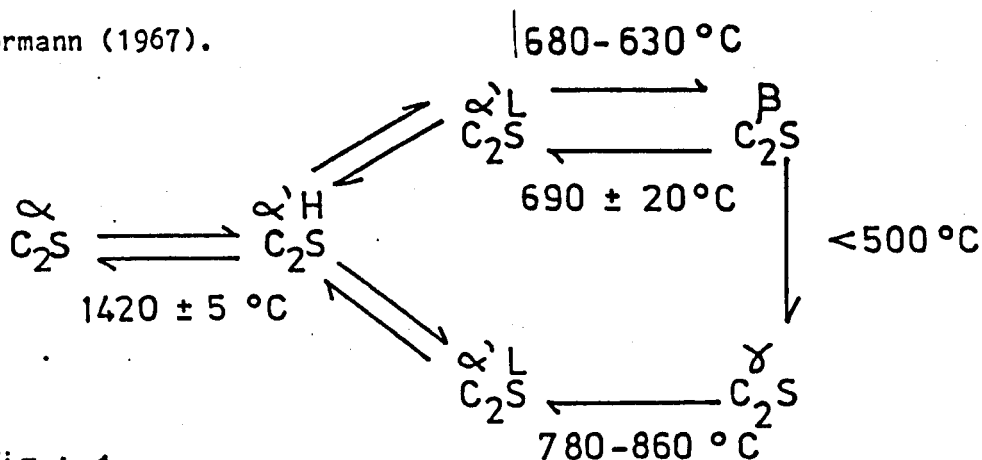


Fig.4.1

SCHMATIC DIAGRAM OF C<sub>2</sub>S TRANSFORMATIONS  
From Niesel and Thormann (1967)

Alpha belite to alpha dash phase change.

At temperatures greater than  $1420^\circ\text{C}$  the  $\alpha$  phase was stable, but with decreased temperature the  $\alpha$  phase changed to  $\alpha'$ H , a change reversible without hysteresis . The structural changes could not be precisely defined. Smith et al (1961) suggested that half the SiO<sub>2</sub> tetrahedra rotated so that their apices pointed in opposite directions at the phase change.

Alpha dash to beta phase change.

The  $\alpha'$  to  $\beta$  phase change occurred at approximately  $650^\circ\text{C}$ . This transformation was reversible with a hysteresis of  $25^\circ\text{C}$  . Smith proposed that the tranformation involved a rotation of SiO<sub>4</sub> tetrahedra and a change in the Ca ion coordination . This changed from 8 fold in the  $\alpha'$  phase to a variable 8 or 9 in the  $\beta$  form. This irregular coordination made the  $\beta$  form the most hydraulically reactive of the C<sub>2</sub>S polymorphs.

Beta to gamma phase change.

The  $\beta$  to  $\gamma$  phase change was a monotropic transition ,with a transformation of primary coordination ( Yannaquis and Guinier, 1959 ).

This involved a considerable increase in volume ,causing the 'dusting' of the cement clinker. Smith et al (1965) thought that the transition involved a rotation of the  $\text{SiO}_4$  tetrahedra . Because of the large movements of some of Ca atoms it was semi reconstructive . The temperature of the  $\beta$  to  $\gamma$  transformation has been observed at different values by various researchers.

Nurse (1952 ) proposed that the change occurred at  $525^\circ \text{C}$  . Whilst Wolf and Hille (1959) said that the transformation occurred at  $300^\circ \text{C}$  . One of the major problems with defining the temperature was that the transformation was extremely slow and never reached completion.

#### Solubility and stabilization of $\text{C}_2\text{S}$

The most stable phase at ambient temperature was  $\gamma \text{C}_2\text{S}$  , however for cement use the  $\beta$  form is the most important. There are several factors influencing the  $\beta$  to  $\gamma$  transformation. Yannaquis and Guinier (1959) have reported that the crystallite size affected the stability of  $\beta \text{C}_2\text{S}$ . Microscopic examination of the phase has shown that  $\beta \text{C}_2\text{S}$  crystals were stable at room temperature were never larger than  $5\mu\text{m}$ . Grains of  $\gamma \text{C}_2\text{S}$  derived from  $\beta \text{C}_2\text{S}$  were generally between  $10\mu\text{m}$  to  $100\mu\text{m}$  . They thought that this was due to the mechanism of the  $\beta$  to  $\gamma$  transformation, which was by nucleation and growth . If after the  $\alpha' \text{C}_2\text{S}$  to  $\beta \text{C}_2\text{S}$  transformation the crystals were large , there was a high probability that each crystal would contain a  $\gamma$  nucleus . Thus as the temperature decreased the  $\beta$  crystals would change to  $\gamma$  . If the  $\beta$  crystal size was small , many grains would not contain a  $\gamma$  nucleus and could not transform during cooling.

## Belite in cement.

### Variation in the stoichiometric composition of belite in cement.

In the case of  $\beta$   $C_2S$  generally found in cement, the stabilization of the phase was by solid solution with foreign ions and by variance from the stoichiometry. Guinier and Regourd (1968) reported that a maximum of 1% excess CaO could be incorporated into  $C_2S$ . This stabilized the  $\beta$  phase at room temperature. They found that the effect of excess  $SiO_2$ , the solubility of which in  $C_2S$  was between 1.5% and 2%, was to produce the  $\gamma$  phase.

In the production of cement, excess silica produces large crystals of belite which favour the transformation of  $\beta$   $C_2S$  to  $\gamma$   $C_2S$ .

### Substitution of minor elements in belite.

The effect of alkalis such as  $Na_2O$  and  $K_2O$  was to stabilize the  $\beta$  form. Thilo and Funk (1953) noticed that the lowest effective level of  $Na_2O$  was between 0.17% and 0.27%.

Midgley's investigation (reported in Gutt and Nurse, 1974) of stabilizing elements found that any of the following elements would completely stabilize the  $\beta$   $C_2S$  polymorph; potassium 0.83%, sodium 1.75%, vanadium 2.20%, chromium 1.24%, manganese 0.88% and the following oxides; phosphorus pentoxide 0.08% and sulphur trioxide 5.0%. Midgley also found that Al,  $Fe^{3+}$ , Mg and Ti did not stabilize  $\beta$   $C_2S$ .

Eramin et al (1970) found that the limit of solubility of the following oxides in  $C_2S$  was;  $Na_2O$  0.6%,  $Fe_2O_3$  1.8%,  $TiO_2$  0.5% and MgO 1.0%. However Eramin did not give details of which polymorph of  $C_2S$  had been studied.

Belite in cement clinker is similar to  $\beta$   $C_2S$  but the lattice is slightly modified by the addition of various atoms. The XRD pattern of

belite from cement has some broad reflections and slightly displaced lines when compared to synthetic  $\beta$  C<sub>2</sub>S. The belite differs because it is a product of imperfect crystallization and non-equilibrium.

#### Stabilization of the belite polymorphs by minor element substitution.

Butt and Timashev (1974) found that in the C<sub>2</sub>S lattice, Ca<sup>2+</sup> could be substituted by Al<sup>3+</sup>, Mg<sup>2+</sup>, K<sup>+</sup>, Na<sup>+</sup>, Ba<sup>2+</sup>, Cr<sup>3+</sup>, Mn<sup>2+</sup> and Fe<sup>3+</sup>. For the (SiO<sub>2</sub>)<sub>4</sub> group, Nurse (1952) proposed that (PO<sub>4</sub>)<sup>3-</sup> or (SO<sub>4</sub>)<sup>2-</sup> could be substituted. An attempt by Forest (1967) to produce belites similar to those found in clinker, produced an oxygen defective structure with substitutions for Si. The general formula was (Ca<sub>2</sub> M<sub>x</sub>) (Si-x O<sup>-x/2</sup>).

The M ions were Fe<sup>3+</sup> and Al<sup>3+</sup>. Gutt (1968) found that a high P<sub>2</sub>O<sub>5</sub> or SO<sub>3</sub> content would stabilise the  $\alpha'$  and  $\beta$  polymorphs. However for the  $\beta$  C<sub>2</sub>S phase, K<sub>2</sub>SO<sub>4</sub> and CaSO<sub>4</sub> were most effective.

#### The influence of the kiln conditions on the stabilization of the belite polymorphs.

In an investigation of the factors affecting the stability of belite, Sasaki (1960) discovered that the burning conditions in the kiln were important. If the belite had ions substituting for Si and was burnt in reducing conditions, then the  $\beta$  C<sub>2</sub>S form was stabilized. If the belite had ions substituting for Ca, for example Fe<sup>2+</sup> replacing Ca<sup>2+</sup>. Then burning the clinker in reducing conditions produced a solid solution of FeO and C<sub>2</sub>S. In these circumstances the  $\beta$  C<sub>2</sub>S to  $\gamma$  C<sub>2</sub>S inversion proceeded rapidly.

#### The influence of stabilizing ions on the hydration rates of $\beta$ C<sub>2</sub>S.

Pritts and Daugherty (1976) studied the effects of different stabilizing elements on the hydration characteristics of  $\beta$  C<sub>2</sub>S. They found that the change in hydration rate was broadly related to the

charge/radius ratio of the stabilizing elements. Ions with large charge/radius ratios (C/R) substituted for  $\text{Si}^{4+}$  (C/R = 9.5), those with a small C/R substituted for  $\text{Ca}^{2+}$  (C/R = 2.0). The ions which had intermediate C/R ratios occupied interstitial lattice positions and did not stabilize the  $\beta$   $\text{C}_2\text{S}$ . The effects of the stabilizers substituting for silicon in  $\beta$   $\text{C}_2\text{S}$  were studied. The stabilizers tried were  $\text{V}_2\text{O}_5$  ( $\text{V}^{5+}$ ),  $\text{Cr}_2\text{O}_3$  ( $\text{Cr}^{6+}$ ),  $\text{B}_2\text{O}_5$  ( $\text{B}^{3+}$ ) and  $\text{SO}_3$  ( $\text{S}^{6+}$ ). In all cases the substituted  $\beta$   $\text{C}_2\text{S}$  hydrated more slowly than the pure  $\beta$   $\text{C}_2\text{S}$ . As the C/R ratio increased the hydration rate decreased. The effects of the stabilizers substituting for calcium in  $\beta$   $\text{C}_2\text{S}$  was also studied. There were only two stabilizers,  $\text{Na}^+$  or  $\text{K}^+$  which substituted for  $\text{Ca}^{2+}$ . The vaporization of the stabilizers made concentration control difficult. However the results indicated that as the C/R ratio of the substituting ion increased, the hydration rate decreased. This was similar to the effect of the stabilizers substituting for Si. From this evidence Pritts and Daugherty concluded that it was not possible to use metal oxide doped  $\beta$   $\text{C}_2\text{S}$  to replace  $\text{C}_3\text{S}$  in portland cement and keep the same rate of hydration.

The advantage of a cement with low  $\text{C}_3\text{S}$  and high  $\text{C}_2\text{S}$  content would have been that it required less energy to produce, because the sintering temperature would be reduced.

#### Crystallography and composition of the matrix phases.

The interstitial material between the alite and belite grains usually consisted of two phases, aluminate and ferrite.

#### Crystallography and composition of the aluminate phases.

The presence or absence of the different aluminate phases in the clinker was dependent on the type of cement examined. Robson (1968)

presented a survey of the compounds present in the CaO - Al<sub>2</sub>O<sub>3</sub> system. These were C<sub>3</sub>A , C<sub>12</sub>A<sub>7</sub> , CA , CA<sub>2</sub> , and CA<sub>6</sub> . The major aluminate phase in ordinary portland cement was C<sub>3</sub>A with minor amounts of C<sub>12</sub>A<sub>7</sub>. The other aluminates usually only occur in aluminous or high alumina cements.

#### Composition of aluminates present in Portland Cement.

##### Calcium aluminate C<sub>12</sub>A<sub>7</sub>

The 12CaO.7Al<sub>2</sub>O<sub>3</sub> phase has several unusual characteristics . Welch (1960) observed that the compound absorbed atmospheric moisture at high temperatures . Welch found that this caused variation in the cell volume, density and refractive index. Nurse et al (1965) found that the maximum uptake of moisture occurred at 950 to 1000° C and caused an increase in weight of 1.3% , compared to the anhydrous compound. The chemical composition was C<sub>12</sub>A<sub>7</sub>H . The lattice was thought to be under considerable strain and the 6-oxygen coordination shell of the calcium ions was very irregular.

Robson (1968) thought that the presence of large structural holes and several vacant sites in the lattice was the cause of the rapid hydration behaviour of the aluminate. Robson proposed that the uptake of the hydroxyl ions at high temperature was linked to the structural arrangement of the aluminate.

##### Tricalcium aluminate C<sub>3</sub>A.

##### The polymorphic forms of C<sub>3</sub>A.

The occurrence of four polymorphic forms of C<sub>3</sub>A was proposed by Boikova et al (1972) . These were cubic, orthorhombic, monoclinic and the high temperature tetragonal form. These polymorphs had different limits of solid solution with Na<sub>2</sub>O, which were as follows ; cubic up to 2% , orthorhombic from 3.8% to 4.6% and monoclinic from 4.6% to 5.7%. Later

research by Maki (1973) and Cervantes Lee and Glasser (1979) has shown that the existence of the tetragonal form is doubtful. Regourd (1978) reported the occurrence of a monoclinic polymorph of  $C_3A$ , but it was only found occasionally in commercial cement clinker. Varma and Wall (1981) found that an industrial clinker with high potassium and low sodium levels, had monoclinic  $C_3A$ . An electron microprobe analysis of monoclinic  $C_3A$  by Regourd (1978) gave values of 3.7 % for  $K_2O$  and 1.6 % for  $Na_2O$ . The entry of  $K^+$  into this  $C_3A$  lattice was related to the disordering effect of  $SiO_2$  and  $MgO$  on the structure. This permitted the large  $K^+$  ions to replace the smaller  $Ca^{2+}$  ions.

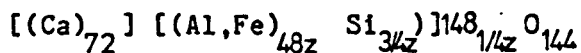
#### Substitution of iron in tricalcium aluminate.

The solid solution between  $C_3A$  and iron has been extensively investigated because of the partition of alumina between the  $C_3A$  and the ferrite phase. This is very important, since the  $C_3A$  content of cement is critical because of the susceptibility of  $C_3A$  to sulphate attack. The solid solution series  $C_3(A_{1-x}F_x)$  has been investigated by several researchers. There was some variation in the results obtained. The principal method used was to measure the differences in the cell parameter 'a'. No evidence was found to indicate a change to a non cubic cell, due to replacement of Al by Fe. However Majumdar (1965) and Moore (1966) found that parameter 'a' increased with additional iron content beyond the limiting composition. Thus equilibrium had not been reached.

Tarte (1965) found that the parameter 'a' remained constant when the Fe/Al+Fe ratio exceeded 10%. Schault and Roy (1965) found that the limiting concentration of  $C_3F$  in  $C_3A$  decreased as the temperature decreased. This was based on the composition at which a ternary phase was formed, not on a change in unit cell parameters. The difference in results is probably due to the compositions measured not having reached a state of equilibrium.

Substitution of silica in tricalcium aluminate.

In the solid solution  $C_3A - SiO_2$ , the Si replaces the Al. Moore (1966) proposed that if there was a simple Si replacement for Al, the structure would have to accommodate an extra oxygen for every two replaced Al atoms. An alternative replacement would consist of four Al atoms substituting for three Si atoms leaving an occasional vacant Si/Al site. Moore found that with increasing Si content the cell parameter 'a' decreased. This occurred to a limiting Si/Al+Si ratio of 5 to 6%. Han et al (1981) proposed that Si substituted for Al and Fe in the aluminate by the following formula.



Substitution of magnesium in tricalcium aluminate.

In the solid solution  $C_3A$  with MgO the CaO was replaced by MgO to a limit of 2.5 Wt.% ( Muller and Schwiete , 1956 ). Moore (1966) suggested that the MgO in the cement concentrated preferentially in the  $C_3A$ .

Substitution of sodium in tricalcium aluminate.

In the solid solution  $C_3A - Na_2O$  the Ca atom was replaced by two Na atoms. Brownmiller and Bogue (1932) proposed that the compound had the composition  $Na_2O \cdot 8CaO \cdot 3Al_2O_3$  ( $NC_8A_3$ ). Fletcher et al (1965) found that there was not a solid solution between  $C_3A$  and  $NC_8A_3$ . The limiting composition for CaO replacement by  $Na_2O$  was approximately 6.5 wt.%. The compound  $NC_8A_3$  had 7.6 wt.% of  $Na_2O$  in its composition. The lattice parameter 'a' decreased with the addition of  $Na_2O$ . At 3%  $Na_2O$  there was a change of symmetry from cubic to orthorhombic. This was necessitated by the presence of the additional Na atoms. Han et al (1981) proposed that the substitution of Ca by Na was linked to the Al and Fe replacement by Si, following the formula.



Shin and Glasser ( 1983 ) have investigated the interdependence of sodium and potassium substitution in  $C_3A$  . The cubic form of  $C_3A$  was stable if the  $Na_2O$  level was below 2%. Between 2 and 4%  $Na_2O$  , orthorhombic and cubic forms existed. Above 4.5% only the monoclinic form was present. The limit of potassium solubility in  $C_3A$  at  $1050^\circ C$  to  $1200^\circ C$  was between 0.75% and 1.0%  $K_2O$ . The  $C_3A$  saturated with  $K_2O$  was in the cubic form. The solubility of K in  $C_3A$  increased, if  $Na_2O$  was present at a level greater than about 2%. This limit of solubility for  $K_2O$  was about 2.5 wt.%. Shin and Glasser concluded that the partition of alkali elements between the phases present in the clinker was partially controlled by the Na/K ratio. If the ratio was high, the  $C_3A$  crystallized in the orthorhombic form and contained most of total alkali content. If the Na/K ratio was low , cubic  $C_3A$  was formed and the alkalis were partitioned into the other phases in the cement, notably belite.

The author believes that this is an over generalisation. The factors affecting the mobility of the alkali elements should be taken into account. If there is abundant sulphate available the alkali sulphate phases will form preferentially and there will be less alkali available to substitute into the tricalcium aluminate. Thus the use of high and low ratios of  $Na_2O/K_2O$  to predict the type of tricalcium aluminate that forms , may give inaccurate results.

#### Substitution of potassium in tricalcium aluminate.

In the solid solution  $C_3A$  with  $K_2O$ , Suzukawa (1956) found that the potassium compound  $KCa_3Al_3$  was isomorphous with  $NaCa_3Al_3$  , however a linked substitution with Si was necessary for the formation of the solid solution. Moore (1966) found that in the absence of silica only a trace of potassium could be taken up by the  $C_3A$  . This was because the K atom had a large ionic radius and the space it required could only be made available by replacing the large Al ions with smaller Si atoms.

Crystallography of tricalcium aluminate in cement.

The lattice parameter 'a' for  $C_3A$  in cement was lower than for pure  $C_3A$ , because of the effect of substitutions. The  $C_3A$  in white cement had the lowest 'a' value. This was due to the aluminate containing the maximum amount of  $SiO_2$ ,  $MgO$  and  $Na_2O$  which all reduce the cell size. The  $Fe_2O_3$  content which would caused an increase in cell size was low. The effect of different element substitution on  $C_3A$  in cement was semi additive. The interaction of the elements was complex and affected the limiting concentrations. The replacement of large Al ions by smaller Si ions made extra space available to accommodate very large ions such as Fe.

Minor aluminate compounds.

The work of Halstead and Moore (1962) confirmed the existence of an aluminate compound with the formula  $Ca_4(Al_6O_{12})(SO_4)$ . They suggested that it could be formed in portland cement when a high sulphur content fuel was used. This compound reacted readily with water to produce mainly calcium alumina hydrates and a calcium alumina sulphate, an expansive hydrate. If the clinker was interground with lime, gypsum and a low  $C_3A$  portland cement, a shrinkage compensated cement was produced.

Crystallography and composition of ferrite in cement.

The orthorhombic alumino-ferrite phases occurred as solid solutions in the  $CaO - Al_2O_3 - Fe_2O_3$  series, with the general formula  $C_2(F_{1-p}A_p)$  where p was between 0 and 0.7.

In a study of the solid solutions by Woermann et al. (1965), two discontinuities in the variation of molar fractions of Al ions were discovered. These were detected by variations in the lattice constants in the  $C_2F$  to the hypothetical ' $C_2A$ ' series. Smith (1962) linked these changes which occurred at  $p=0.33$  to a change in symmetry. Initially Al would replace the tetrahedral Fe, when about half the the tetrahedral

sites were filled , Al would enter tetrahedral and octahedral sites equally. When p was about 0.33 a change in the space group occurred. This involved a contraction and rotation of the tetrahedra , with a displacement of the Ca atoms. Smith found that the limit of Al substitution was reached at 69 mol.%  $Al_2O_3$ . When Tarte (1965) used infra red spectroscopy to investigate the  $C_2 (F_{1-p} A_p)$  series, he observed a steady increase in wave number up to  $C_2 F_{0.3} A_{0.7}$ , then there was no change . The position of some of the lines changed due to the formation of the aluminate phases  $C_3A$  and  $C_{12}A_7$  .

#### Substitution of magnesium in ferrite.

The MgO to ferrite solid solution was studied in detail by Woermann et al (1965) . The presence of MgO changed the normal red-brown colour of ferrite in transmitted light to a dark green. It had been previously thought that the Mg substituted for Ca . However Woermann detected two types of solid solution . The solid solution MgO-ferrite had a higher lime content than ferrite . For every three atoms of MgO substituted , two additional atoms of CaO were combined. The limit of solid solution was the formation of periclase. The formula of the hypothetical end member of the solid solution series was " $Ca_2Mg_3O_5$ ". The solid solution of Mg in  $C_2F$  was a substitution of  $Mg^{2+}$  for  $Fe^{3+}$  .

Investigation of  $Ca_2 Fe Al O_5$  (p=0.50) by Woermann gave different results to those described previously , because additional CaO was combined by incorporation of MgO to a solubility limit of 1.5%. The substitution ratio of Ca to Mg changed from  $Ca/Mg = 2/3$  to  $Ca/Mg = 1/3$  at p = 0.45 to 0.50 . This abrupt change was thought to be due to a discontinuity in the ferrite series.

Kato (1959) studied the MgO - ferrite solid solution and found that  $SiO_2$  and MgO substituted for  $(Al,Fe)_2O_3$  in the ferrite to a level of about 10% .

The interrelationship between aluminate and ferrite.

The interaction between synthetic  $C_3A$  and  $C_4AF$  phases was investigated by Tarte (1965). In a mixture of  $C_3A$  and  $C_4AF$  heated to  $1300^\circ C$ , the two phases exchanged Fe and Al to produce a solid solution  $C_3(AF)$  with a limiting composition of  $C_3(A_{0.9}F_{0.1})$ . Several poorly crystalline phases formed with the displacement of some of the XRD reflections and broadening of high angle peaks. The same occurred for the infra-red absorption bands. Tarte deduced that the crystallization of the phases was incomplete. He thought that this was related to the formation of a glassy phase when the solid solution had a high alumina content. A sample of composition  $C_2(A_{0.8}F_{0.2})$  had a diffuse infra-red absorption spectrum and no XRD reflections. If the Al/Fe ratio was close to unity the crystallization was complete.

Compositional variation in the ferrite solid solution series.

In commercial cement, the composition of the ferrite is as dependant on the production methods as the Al/Fe ratio of the kiln feed, because in all cases equilibrium is not attained. Hansen et al (1928) proposed that there was complete miscibility between  $C_2F$  and " $C_2A$ " to a limit of  $C_4AF$ . However later studies by Yamauchi (1937) and Newkirk and Thwaite (1958) established that the ferrite phase was not limited to  $C_4AF$ . The composition could extend to solid solutions richer in Al, the  $Al_2O_3/Fe_2O_3$  ratio of which was 2.2 to 2.3, an equivalent of  $p=0.70$  in the series  $C_2A_pF_{1-p}$ .

Midgley et al (1964) investigated the XRD traces of magnetically separated ferrite from cement. They found that there was a broadening of the 141 reflection caused by an expansion of the crystal lattice due to the substitution of iron. The average composition they obtained from XRD analysis of several cements, was very close to  $C_4AF$ . Midgley and Grove (1970) reported that there was a correlation between the molar ratio  $Fe_2O_3/(Fe_2O_3 + Al_2O_3)$  of the ferrite phase and the cement in

which it had crystallized. If the molar ratio was greater than 0.37 , the following equation was solved to give q .

This was substituted in the formula  $Ca_2 ( Fe_q Al_{1-q} )_2 O_5$  .

$$q = 0.27 - 0.74 ( f / ( 1.57a + 5 ) )$$

where  $f = \text{wt.} \% Fe_2O_3$

$a = \text{wt.} \% Al_2O_3$

This equation does not take into account the influence of the different production methods for cement, on the composition of the ferrite.

Copeland et al (1959) studied the compositions of ferrite from cement clinker . They found that the compositions lay between  $C_6 A_{1.22} F_{1.78}$  and  $C_6 A_{1.77} F_{1.23}$  . Schwartz (1967) separated the ferrite phase from cement by chemical solution and analysed them by XRF . He found that the ferrites were stoichiometrically depleted in CaO up to 5% . This lime deficiency increased if  $K_2O$  ,  $Na_2O$  and  $MgO$  were present . If  $SiO_2$  was present the deficiency diminished . Schwartz determined that the solubility limits of minor elements in the ferrite phase from cement was  $K_2O=3\%$  ,  $MgO=4\%$  and  $SiO_2=7\%$  . Regourd and Guinier (1974) reported that Ti, Mn and Cr could also be incorporated into the  $C_2(AF)$  lattice.

THE MINERALOGY OF CEMENT CLINKER.

Introduction.

The technique of x-ray diffraction ( XRD ) provides an accurate and rapid method of determining the mineralogical composition of cement or concrete . The use of XRD for quantitative analysis of phase composition is discussed in chapter 8 .

Identification of the cement clinker mineral phases by X-ray diffraction.

The X-ray diffraction analytical technique for cement was widely adopted in the late 1950's . Midgley ( 1957 ) published a compilation of X-ray data for cement clinker minerals and hydrated cement minerals . The principle problem with the XRD method is that several of the phases have reflections which partially or fully overlap each other . For this reason it is often necessary to use reflections which are not the strongest for each phase .

Identification of Alite in clinker

Midgley ( 1957 ) recognised two types of tricalcium silicate , pure  $3\text{CaO} \cdot \text{SiO}_2$  and alite which has  $\text{Al}_2\text{O}_3$  and  $\text{MgO}$  in solid solution with the  $\text{C}_3\text{S}$ .

Alite had a single reflection at  $1.761 \text{ \AA}$  whilst pure  $\text{C}_3\text{S}$  had doublets.

Guinier and Regourd ( 1968 ) described six different modifications which could be determined by the reflections occurring between  $2.885 \text{ \AA}$  to  $2.714 \text{ \AA}$  and  $1.791 \text{ \AA}$  to  $1.759 \text{ \AA}$  . The first range was unusable in clinker investigations because of peak overlapping . Using the latter set , the alite modifications were distinguishable . The triclinic modification only occurred in slowly cooled clinker . The position of the peaks varied slightly due to minor element substitution, especially  $\text{Mg}$  and to some

extent Fe and Al .

#### Identification of Belite in clinker .

Midgley (1974) established that there were four polymorphic forms of  $C_3S$ .

These were alpha ( $\alpha$ ), alpha dash ( $\alpha'$ ), beta ( $\beta$ ) and gamma ( $\gamma$ ) .

Midgley proposed that the beta phase was the most likely phase to occur in cement. However if the clinker was burnt at lower temperature than usual, the low temperature gamma form was frequently formed. The identification of the different polymorphs was complex because many of the belite reflections almost coincided with alite or aluminate reflections . In many instances only weak reflections were clear of overlapping effects . When Midgley et al (1960) made a study of the quantitative compositions of cement they used a weak line at 2.87 Å to measure the amount of  $\beta C_3S$  present in the sample.

Guinier and Regound (1974) proposed that identification by XRD of the belite form was possible if the belite content was above 12 %. The presence of orthorhombic  $C_3A$  in the cement could complicated the analysis.

Pritts and Daugherty (1976) used the 3.008 Å peak of  $\gamma C_2S$  and the 3.048 Å peak of  $\beta C_2S$  to determine the presence of each phase within mixtures used in their studies of  $\beta C_2S$  hydration ratios . Kristmann (1977) attempted to identify the belite modifications in the range 2.495 Å to 2.368 Å but was unsuccessful even after separating the silicate phases from the ferrite and aluminate by magnetic separation .

#### Identification of Tricalcium aluminate in clinker.

Midgley (1957) recommended that the 2.7 Å reflection was used for the identification of  $C_3A$  . However Kantro et al (1964) showed that the  $C_3A$  peak was partially overlapped by the major ferrite peak . The position of the ferrite peak varied considerably because of the effects of the solid solution . This had to be compensated for if an estimation of phase content was to be made .

Regourd et al (1973) proposed that tricalcium aluminate could occur in three different modifications, cubic, orthorhombic and tetragonal. The existence of the tetragonal form has not been generally accepted. The cubic form was characterised by a single peak at 2.70 Å, 1.907 Å and 1.556 Å. The orthorhombic form had a double peak at 2.70 Å and triple peaks at the other values. These triple peaks were only detectable on very high resolution XRD instruments.

Mander et al (1974) used the small peak at 4.08 Å to estimate the amount of  $C_3A$  present in cement. If there was a high alkali content in the cement and  $NC_8A_3$  and  $KC_8A_3$  were present, these peaks overlapped with the  $C_3A$  peak.

Regourd (1978) reported the occurrence of a monoclinic  $C_3A$  polymorph, however it is only rarely found in commercial cement clinker. Varma and Wall (1981) studied several industrial clinkers and found that a clinker with a high potassium and low sodium content, contained monoclinic  $C_3A$ . The monoclinic  $C_3A$  has reflections with higher 'd' spacing values than the other forms. This indicates an expansion in the lattice which is due to the presence of the large  $K^+$  ions. The stabilization of the cubic form was due to the substitution of the potassium.

#### Identification of Ferrite in clinker .

The ferrite phase is a solid solution and the lattice spacing of the ferrite changes with the composition. The strongest reflection occurs at 2.62 Å for  $C_6A_2F$  and 2.67 Å for  $C_2F$ . The 2.60 Å reflection of alite partially overlaps the  $C_6A_2F$  reflection.

Kanto et al (1964) produced a series of diffractograms showing the complete variation in 'd'-spacing for the solid solution series  $C_2F$  to  $C_6A_2F$ . To accomplish this the ferrite was magnetically separated from ground cement clinker.

Mander et al (1974) used a maleic acid-methanol solution to leach the

silicates and freelite from cement and concentrate the aluminates and ferrite . They used the reflections at  $2.08 \text{ \AA}$  for  $C_2F$  ,  $2.053 \text{ \AA}$  for  $C_4AF$  and  $2.04 \text{ \AA}$  for  $C_6A_2F$  . This was the most suitable interference free area for both intensity and peak shift measurements .

Kristmann (1977) found that sometimes the ferrite peaks were broad and difficult to measure . He thought that this was caused by the small crystallite size of the ferrite. He also thought that variation in the composition of the ferrite within a single sample would cause peak broadening.

#### Identification of the minor phases in clinker .

Midgley (1957) found that freelite could be detected if there was about 2 % present. Periclase could be detected if there was more than 1.5% present. The  $1.39 \text{ \AA}$  reflection of freelite was best because the stronger reflection at  $2.405 \text{ \AA}$  was masked by  $C_2S$  . The periclase was best detected by the strongest reflection at  $2.106 \text{ \AA}$

If a leaching solution was used to remove the silicate phases, other minor cement phases could be detected. One of these was calcium sulphoaluminate (  $C_4A_3SO_4$  ) . This compound expands on hydration and produces a shrinkage compensating cement . Mander et al (1974) used the  $3.754 \text{ \AA}$  reflection to measure the amount of this compound present in cement.

#### The procedure used by the author for analysis of cement clinker by X-ray diffraction techniques.

Approximately 10g. of the clinker, which had been ground in a 'Tema' mill, was mixed with half a gram of pure quartz powder. This mixture was then ground in a small agate mortar until there was no trace of roughness between the mortar and the pestle. The quartz was used as an internal standard. The fine powder was packed into a aluminium cavity mount.

The sample was irradiated using a cobalt tube operating at 40 Kv and 25Ma.

The instrumental conditions are given in Appendix 4.

Data processing of the X-ray results of the cement from Works A,B,C,D,E,F and G.

The diffractograms of the different cement clinker samples are shown in Figures 4.3, 4.4, 4.5 and 4.6.

No physical phase separation was attempted for individual analysis of the different phases. A qualitative assessment<sup>of</sup> the phase composition of the cement clinker samples is given in Table 4.1. The presence or absence of the different phases and polymorphs was assessed by using the characteristic reflections listed in Table 4.2.

These reflections were selected from the X-ray data of d spacing and intensity published by Midgley ( 1957).

To select suitable reflections for each phase or polymorph, the d spacings and intensities, for all the cement clinker minerals was plotted on a graph as shown in Figure 4.2 .

By using this technique, characteristic reflections could be selected for the seventeen different phases and polymorphs. If there was overlap from adjacent reflections, the degree of interference could be assessed from the intensity values of the individual reflections. Thus it was possible to derive a series of reflections which could be used to determine whether a specific phase or polymorph was present.

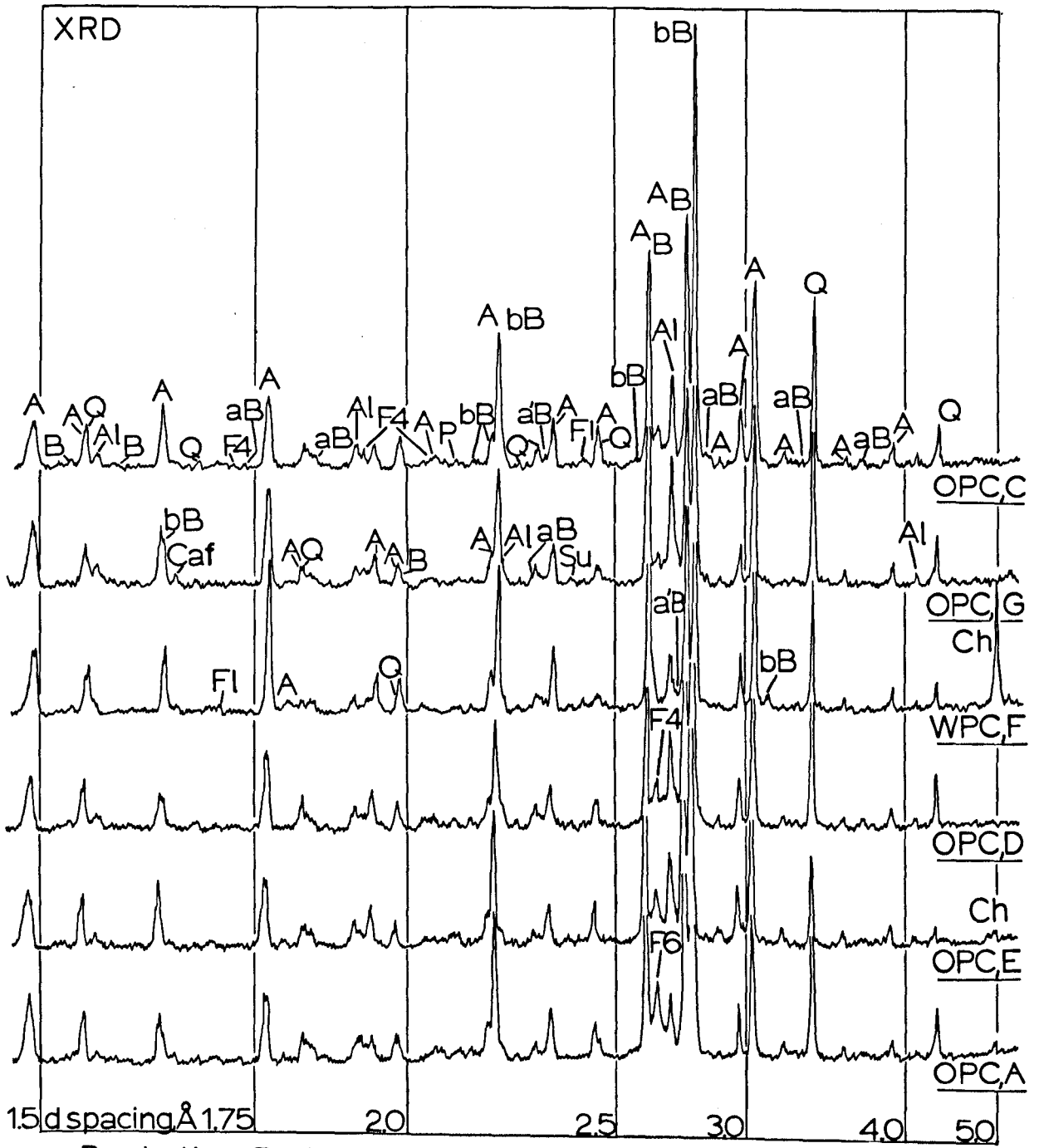


KEY for X-Ray diffractograms.

- A = Alite
- A1 = Tricalcium aluminate
- B = Belite (undifferentiated)
- aB = Alpha belite
- bB = Beta belite
- Ca<sub>12</sub>F = Calcium aluminate (C<sub>12</sub>A<sub>7</sub>)
- Ch = Calcium silicate hydrate (CSH)
- F4 = Ferrite (C<sub>4</sub>AF) solid solution
- F6 = Ferrite (C<sub>6</sub>A<sub>2</sub>F) solid solution
- F1 = Freeline
- P = Periclase
- Q = Quartz (internal standard)
- Su = Gypsum

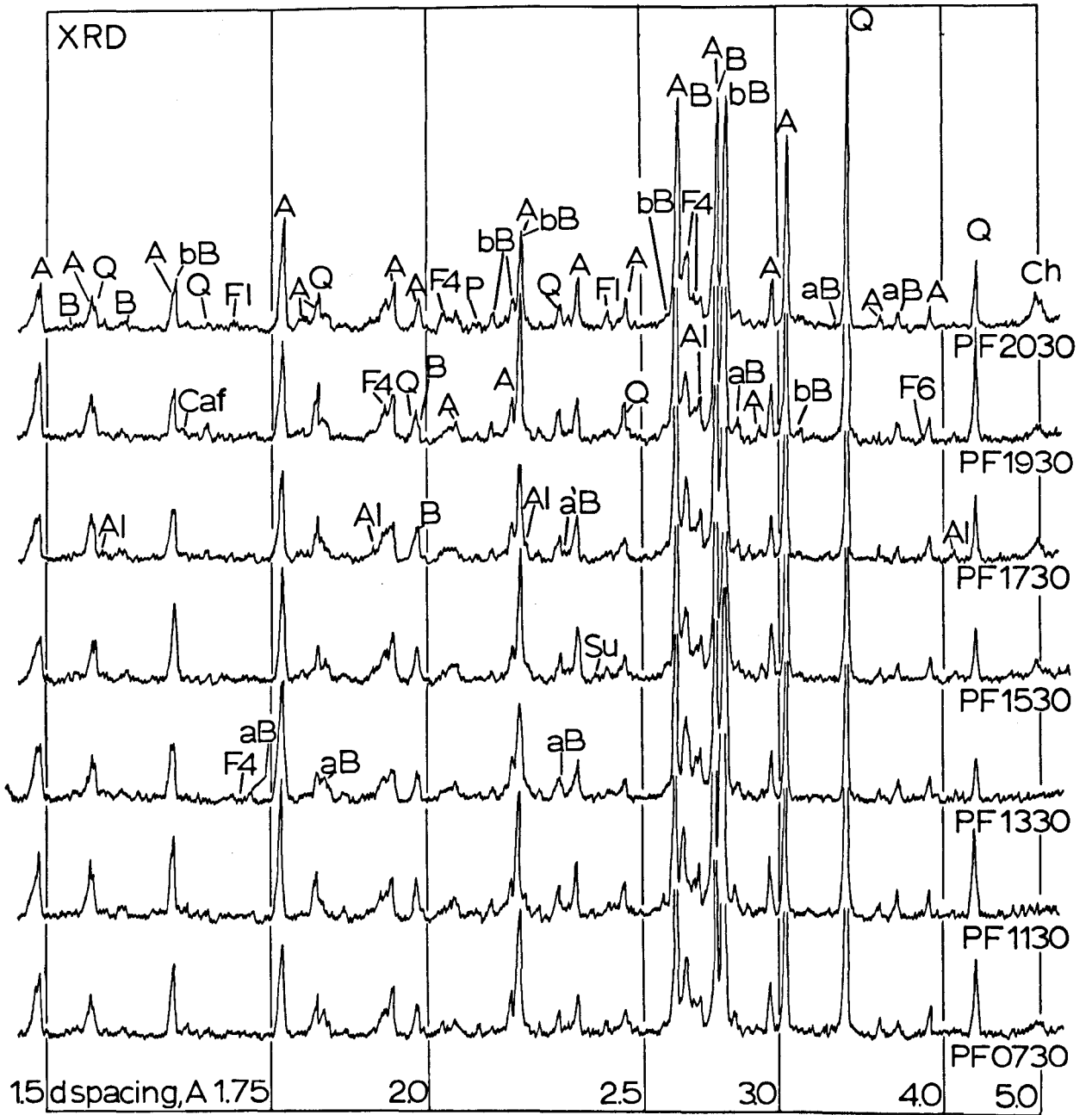
The absence of annotation on each of the individual diffractograms does not imply that the specific phase is not present. The annotated peaks are examples of reflections which were useful in the identification of each phase or polymorph.

The instrumental conditions used during the X-ray diffraction analysis are given in Appendix 4.



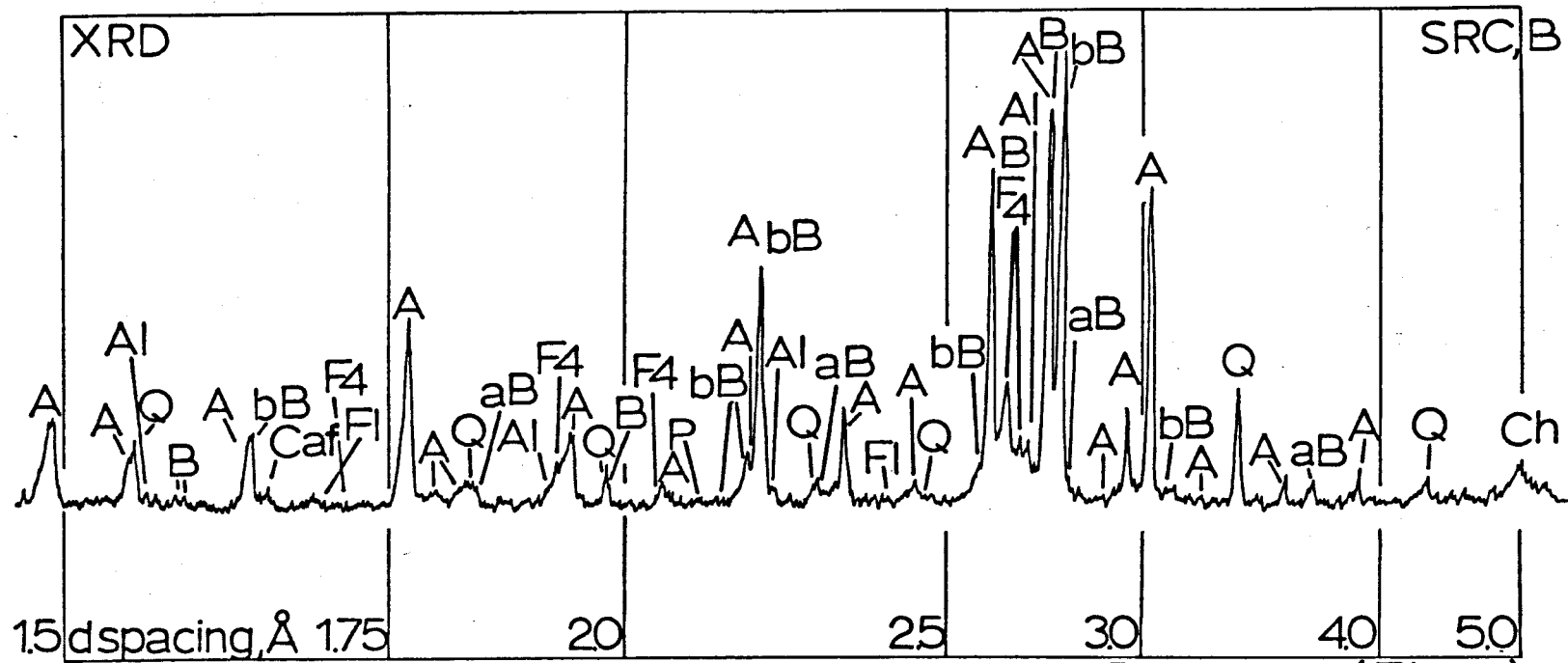
Production Portland cement, Works A,C,D,E,F,G

(Fig.4.3)



Trial PFA addition to Sulphate resisting cement , Works B ( Fig4:4)





Production Sulphate resisting cement, Works B

(Fig. 4.6)

KEY

SRC = Production sulphate resisting cement made from chalk and PFA.

PFB = Trial SRC cement clinker with extra PFA, collected at 1030h.

PFC = Trial SRC cement clinker with extra PFA, collected at 1530h.

PFD = Trial SRC cement clinker with extra PFA, collected at 2030h.

LHA = Trial Low Heat cement clinker collected at 0900h.

LHB = Trial Low Heat cement clinker collected at 1200h.

LHC = Trial Low Heat cement clinker collected at 1300h.

LHD = Trial Low Heat cement clinker collected at 1500h.

OPC = Production Ordinary Portland cement clinker.

WPC = Production White Portland cement clinker.

(Table 4.1 ). The phase composition of the cement clinkers by X-ray diffraction analysis .

WORKS CEMENT		WKS.A OPC	WKS.E OPC	WKS.C OPC	WKS.F WPC	WKS.D OPC	WKS.G OPC	WKS.B SRC	WKS.B PFB	WKS.B PFC	WKS.B PFD	WKS.B LHA	WKS.B LHB	WKS.B LHC	WKS.B LHD
PHASE	POLYMORPH OR FORMULA														
ALITE	Rhombohedral R	n/d.	n/d.	major	minor	n/d.	major	trace	n/d.						
ALITE	Monoclinic M3	major													
ALITE	Monoclinic M1	minor													
ALITE	Triclinic T	n/d.													
BELITE	Alpha high a'	n/d.	trace	trace	minor	trace	n/d.	n/d.	trace						
BELITE	Alpha a	minor	minor	major	major	major	major	trace	minor	minor	trace	minor	minor	minor	trace
BELITE	Beta β	major	major	minor	minor	minor	minor	major							
BELITE	Gamma γ	n/d.	trace	n/d.	n/d.	trace	n/d.	n/d.	n/d.	n/d.	trace	n/d.	n/d.	n/d.	n/d.
ALUMINATE	C <sub>3</sub> A Cubic	major	major	major	major	minor	n/d.	minor	minor	minor	minor	trace	trace	minor	trace
ALUMINATE	Orthorhombic	n/d.	n/d.	n/d.	n/d.	major	major	n/d.							
ALUMINATE	C <sub>12</sub> A <sub>7</sub>	minor	trace	trace	trace	minor	trace								
FERRITE	C <sub>4</sub> A <sub>F</sub>	minor	minor	minor	n/d.	major	minor	major							
FERRITE	C <sub>6</sub> A <sub>2</sub> F	major	major	major	trace	minor	major	n/d.	n/d.	trace	trace	n/d.	n/d.	n/d.	n/d.
FREELIME	CaO	trace	trace	trace	minor	trace	trace	trace	trace	trace	minor	trace	trace	trace	trace
PERICLASE	MgO	minor	minor	trace	trace	trace	trace	trace	minor	trace	trace	trace	trace	trace	trace
GYPSUM	CaSO <sub>4</sub> ·2H <sub>2</sub> O	trace	trace	minor	trace	trace	trace	minor	trace	minor	trace	trace	trace	minor	minor
CALCIUM SILICATE HYDRATE		trace	trace	trace	major	n/d.	minor	minor	trace	minor	major	minor	trace	trace	n/d.

(Table 4.2 ). Compilation of X-ray diffraction reflections used to identify the individual phases and polymorphs in the cement clinkers .

PHASE	POLYMORPH OR FORMULA	POSITION OF PEAK IN Å	INTENSITY 1 TO 10	SPECIAL FEATURES
ALITE	Rhombohedral R	1.79 to 1.76	9	Single peak
ALITE	Monoclinic M3	1.79 to 1.76	9	Double peak, equal height
ALITE	Monoclinic M1	1.79 to 1.76	9	Double peak, unequal height
ALITE	Triclinic T	1.79 to 1.76	9	Triple peak
BELITE	Alpha high a'	2.25	8	
BELITE	Alpha a	2.83	10	
BELITE	Beta β	2.61	10	
BELITE	Gamma γ	4.32	4	
ALUMINATE	C <sub>3</sub> A Cubic	2.71	10	Single peak
ALUMINATE	Orthorhombic	2.71	10	Double peak
ALUMINATE	C <sub>12</sub> A <sub>7</sub>	1.605	7	
FERRITE	C <sub>4</sub> AF	2.63	10	
FERRITE	C <sub>6</sub> A <sub>2</sub> F	2.62	10	
FREELIME	CaO	2.405	10	
PERICLASE	MgO	2.106	10	
GYPSUM	CaSO <sub>4</sub> ·2H <sub>2</sub> O	2.39	4	
PORTLANDITE	Ca(OH) <sub>2</sub>	4.90	7	

Chapter five.

THE PETROLOGY OF PORTLAND CEMENT CLINKER MINERALS.

Introduction.

In Portland cement clinker , eight phases may be readily determined . The major minerals are alite, belite, tricalcium aluminate and ferrite. The minor phases are freelite , periclase , alkali sulphates and aluminates.

Techniques for the microscopical examination of Portland cement clinker.

The scanning electron microscopy of the cement clinker provides an excellent method of examining the morphology of the cement clinker phases. (Plate 2, Chapter 2). For detailed petrographic microscopy of cement clinker, the reflected light microscopy techniques are very useful . The method of preparation of polished block specimens is given in Appendix 5 . Some of the samples were prepared as polished thin sections . For this the preparation technique was more complicated . In electron microprobe analysis the thin sections are easier to study because they may be examined using transmitted light as well as reflected light . They are however more susceptible to damage and suffer from degradation caused by partial hydration.

Similar methods with variations are given in Midgely ( 1964 ) and in Insley and Frechette ( 1952 ) . The technique used is generally determined by the existing 'in house' section preparation system .

The technique developed by the author has the advantage that the finished sections are ideal for electron microprobe analysis . If desired these can be ground to make polished surface thin sections which are also suitable for probe analysis.

The prepared samples were examined using a Zeiss "Ultraphot " microscope with Epi lenses in the reflected light mode . After the final polishing of each sample , many microphotographs were taken in reflected light for use in the location of suitable phases for electron microprobe analysis . Prior to probe analysis the polished surfaces were coated with a layer of carbon , to prevent electrical charging of the specimen by the microprobe beam. The carbon layer obscured all the grain boundaries.

After probe analysis the carbon layer was removed by polishing with  $1/4 \mu\text{m}$  diamond paste . To aid the identification of some of the different clinker minerals ,the polished sections were treated with etching agents , either distilled water or alcohol with 1 %  $\text{HNO}_3$  (Nitric acid ). The etching process was not used on the samples before probe analysis because of the effect of surface roughening and contamination.

#### Etching techniques .

To etch the phases for photomicrographs , a solution of distilled water of pH 6.5 or a solution of 1 %  $\text{HNO}_3$  in alcohol ( Nital) was used .

A drop of the etching solution was put on the polished specimen surface and allowed to stand for several seconds. For distilled water an etch time of 50 to 100 seconds produced the best results. For the Nital etch a period of 10 to 15 seconds was best . The exact time varied , because the longer the specific etch was left on the surface the greater the etching effect . The drop was then blotted off the surface ,to leave the specimen dry.

Reflected and transmitted light petrology of cement.

Tricalcium silicate (  $\text{Ca}_3\text{SiO}_5$  )  $\text{C}_3\text{S}$  , Alite.

The tricalcium silicate in portland cement has incorporated in it a small amount of tricalcium aluminate in solid solution . Jeffery ( 1952 ) has shown that aluminium and magnesium may be substituted for silicon . Because of the substitutions and solid solutions possible in the tricalcium silicate , the term alite is used to denote this mineral phase in cement. The effect of the solid solution on the microscopic properties is principally to cause biaxial interference and to zone individual crystals .

In reflected light microscopy , the alites were usually pale grey , euhedral to subhedral pseudo hexagonal crystals . The size varied from 5  $\mu\text{m}$  to 200  $\mu\text{m}$  . Generally the crystals were between 20-50  $\mu\text{m}$  . The small alites frequently appeared to be coalescing to form larger crystals (Plate 3a. ) . The very large crystals were idiomorphic with irregular outlines ( Plate 3b. ) . Occasionally the alite crystals had corroded edges and small blebs of secondary belite formed along the boundaries. (Plate 3d.) This was caused by the loss of  $\text{CaO}$  from the alite during slow cooling . The presence of fluorine in the cement clinker promotes the decomposition of alite to belite and  $\text{CaO}$ . The fluorine level is usually kept as low as possible to prevent the excessive decomposition of alite. In some cements , especially those with a high alkali content , the alite crystals had serrated outlines . This was probably due to the alite reacting with the liquid phase on cooling . In the majority of the clinker samples the the alite crystals had several straight fractures parallel to the long axis of the grain .( Plate 3g.) These cracks were associated with the rapid cooling of the clinker and were due to stress caused by shrinkage of the alite which was unable to transform to a lower temperature polymorph . Some samples were very cracked , other samples

PLATE 3.

Plate 3a. Works B SRC clinker.

The belite grains are rounded and have the characteristic curved fracture around the edge of the grain. ( right )  
The alite grains are very small and poorly formed because of low CaO levels . There is only a small amount of the pale coloured phase, which is ferrite.

Plate 3b. Works B SRC clinker.

The dark grey phase is alite. The medium sized alite grains are the typical pseudohexagonal shape. The largest alite grains have characteristic straight fractures.

Plate 3c. Works B SRC with PFA clinker, Nital etch.

The etch solution shows the zoning in the angular alite grains. The light zoned areas have been less susceptible to the etch solution. The rounded belite grains have a mottled appearance . The ferrite is unaffected by the etch.

Plate 3d. Works C OPC clinker , Nital etch.

Many of the angular alite grains have a thin layer of very small blebs of secondary belite around them. This is caused by the loss of CaO from the alite during cooling.

Plate 3e. Works B SRC with PFA clinker, H<sub>2</sub>O etch.

Only the alite and aluminate are etched by the distilled water. The aluminate has etched to a greater extent than the alite. The belite grains are unaffected. ( bottom right )

Plate 3f. Works B SRC clinker.

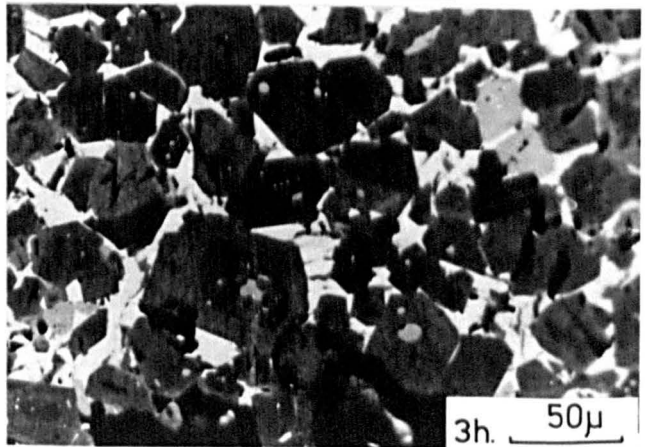
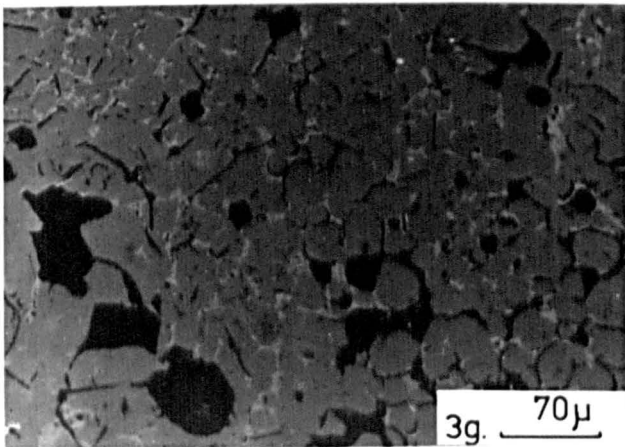
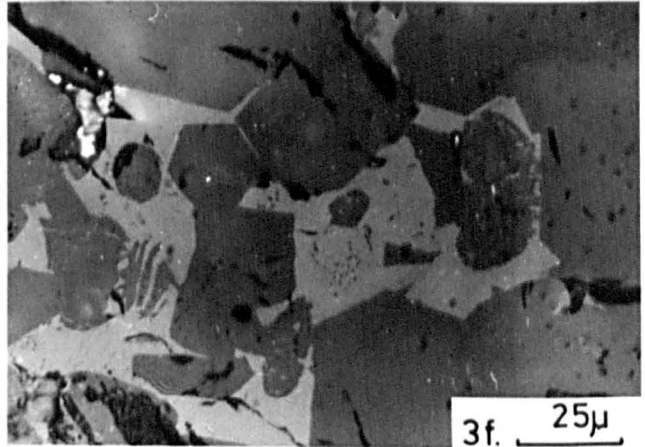
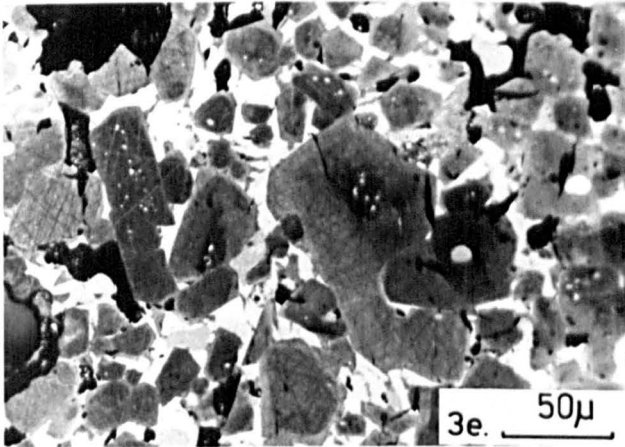
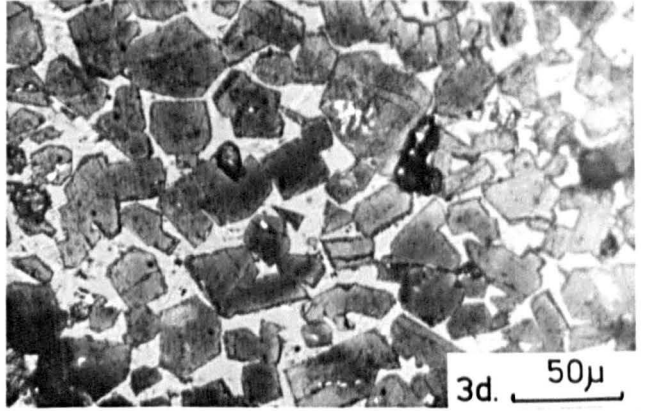
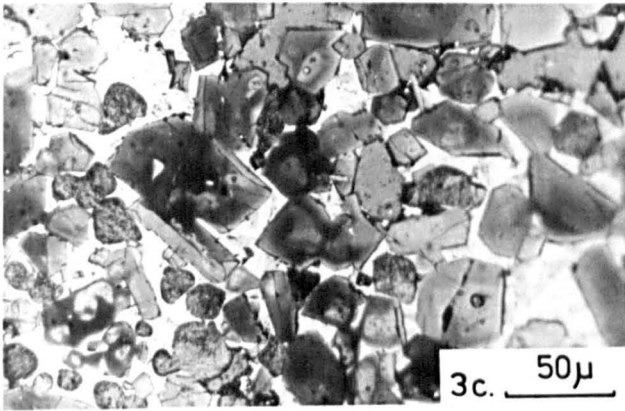
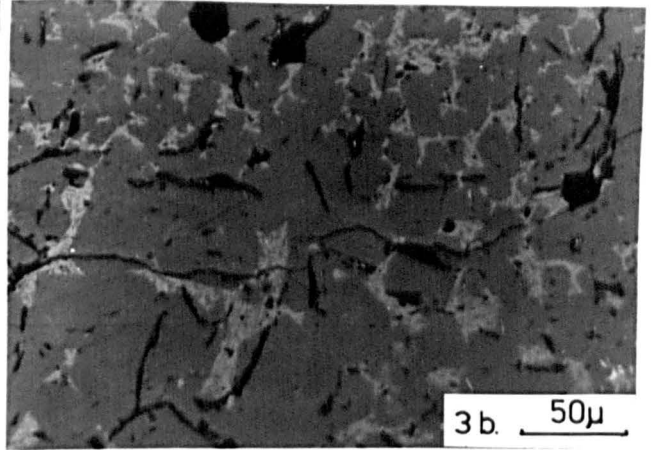
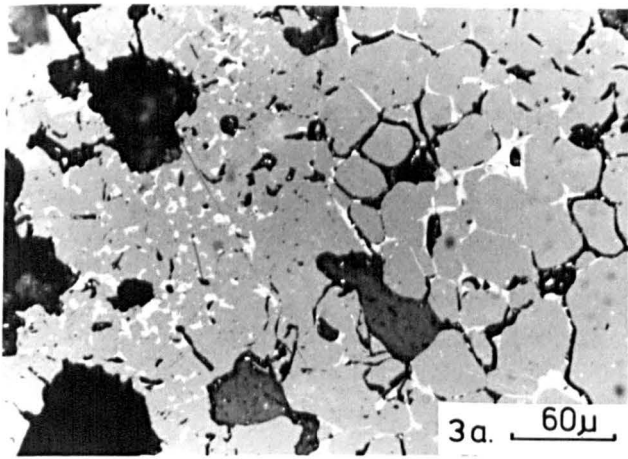
The angular alite grains have abrupt boundaries with the ferrite matrix . Many of the belite grains are comprised of small crystallites, ( centre bottom and right ). These agglomerates of belite contain several inclusions of ferrite and alite. The boundaries between the belite grains and the matrix are diffuse and show an intergrowth texture.

Plate 3g. Works B SRC clinker.

The alite crystals are angular and have the typical long straight fractures. The belite grains ( right ) are rounded and have curved fractures. These fractures are caused by the contraction of the phases, which are unable to invert to a lower temperature polymorph during the rapid cooling of the clinker.

Plate 3h. Works B SRC clinker, H<sub>2</sub>O etch.

The alite grains have been highly etched by the water. The small unetched areas within the alites are blebs of belite. These blebs are remnants of the early formed belite grains which have been engulfed by the later alite. The alite was then partially remelted. The light-dark boundaries represent the solid-liquid interface.



only had a few fractures . In some samples the fractured alites were restricted to the outer area of the clinker nodules .

The smaller alite crystals rarely showed any fracturing . This was probably due to the larger alite crystals fracturing and relieving the tensional stress in the area. Frequently the alite crystals contained many inclusions of belite , ferrite and occasionally freelite . These inclusions were 'armoured' by the alite against reaction with the other phases .( Plate 3h.) It was generally thought that these belite inclusions were remnants of belite which had undergone partial diffusion by calcium ions to form alite . However Skalny et al ( 1975 ) showed that the inclusions of belite had thin shells of ferrite surrounding them. This ' armoured ' the belites against further reaction . These belites were then engulfed by the later forming alite .

#### Effects of chemical etching on alite.

The distilled water etch produced a layer of calcium silicate hydrate (CSH) on alite . The thickness of the CSH layer was indicated by the colour of the alite in reflected light. The colour varied from a light blue to dark blue to brown , the colour was dependent on duration of the etch and the reactivity of the alite polymorph. ( Plate 4a. colour ) The alite crystals often showed zones after etching due to the varying degree of etch anisotropy . These zones were either straight divisions of the crystal ( Plate 3e. ) or concentric zones ( Plate 3h. ) sometimes parallel to the outer boundaries of the crystal.

The degree of reactivity of the alite to water is related to the number of lattice defects in the the individual crystals. The number of defects is reduced if the cement clinker is cooled slowly. This is because the annealing processes can operate for a longer time. Thus rapid cooling produces the most reactive alite.

The belite and ferrite inclusions within the alite were easily identified because they did not etch .

PLATE 4.

Colour plates

Plate 4 a. Works G OPC clinker, H<sub>2</sub>O etch.

The alite crystals are angular and have a blue to magenta colour. Some of the crystals have irregular boundaries because of the loss of CaO during cooling. The outer portion of the crystals have inverted to belite. The pale grey rounded grains are belite, which have not been etched by the distilled water. Several of the alites have small inclusions of belite. The lath shaped phase is tricalcium aluminate in the orthorhombic form. This has etched to a pale brown grey. The very pale grey phase between the other phases is ferrite which is not etched by the distilled water.

Plate 4b. Works C OPC clinker, Nital etch.

The pseudo-hexagonal alite crystals are predominantly orange with some blue to purple fringes. The colours are partially dependent on the reactivity of the alite and partially on chemical reactions that occur to the etch solution. If there are crystals of free lime exposed on the surface, the acidic etch solution is weakened or neutralised and the etched layer is thinner. The more reactive alite develops a thicker layer of etched surface. The thickness can be estimated by the etching colour. The blue to purple layer is thicker than the orange layer. If there are patches of blue on alite crystals which are mostly orange, then the effects are chemical. If the alite is predominantly blue to purple the alite is more reactive to the etch ( as in Plate 4 c.) and thus has a thicker etched layer.

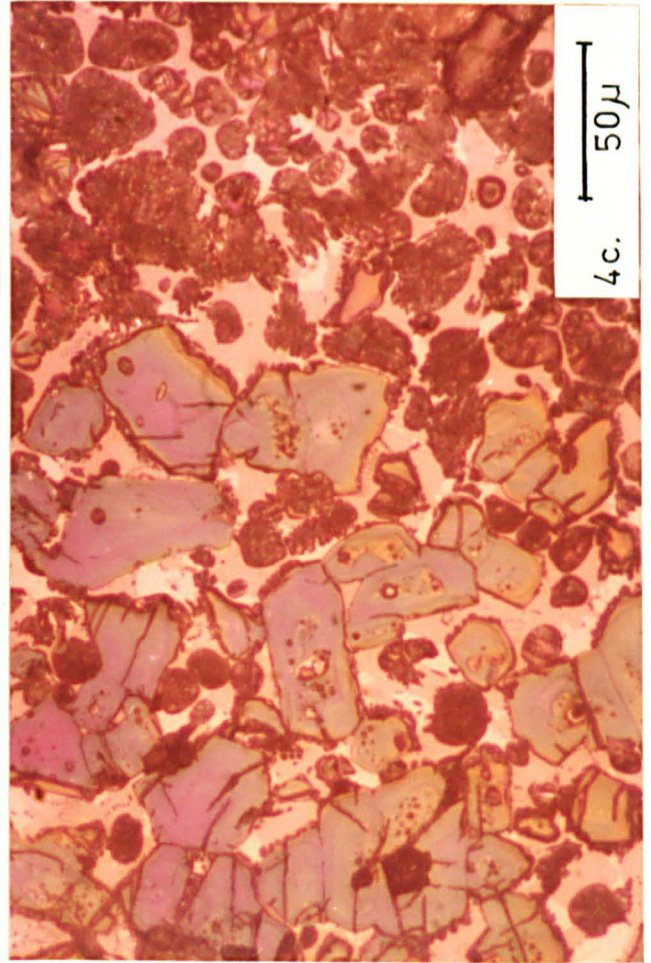
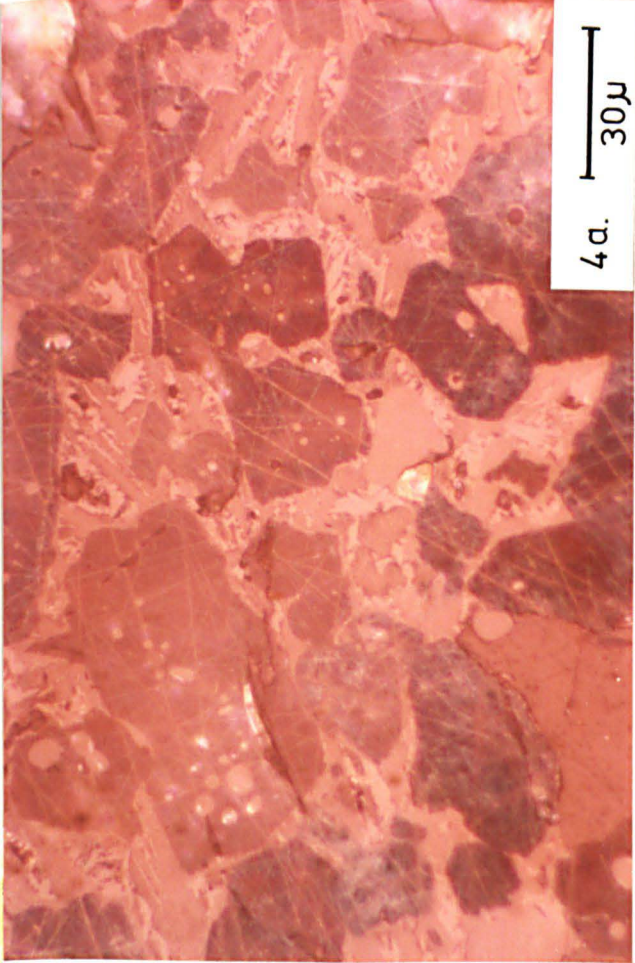
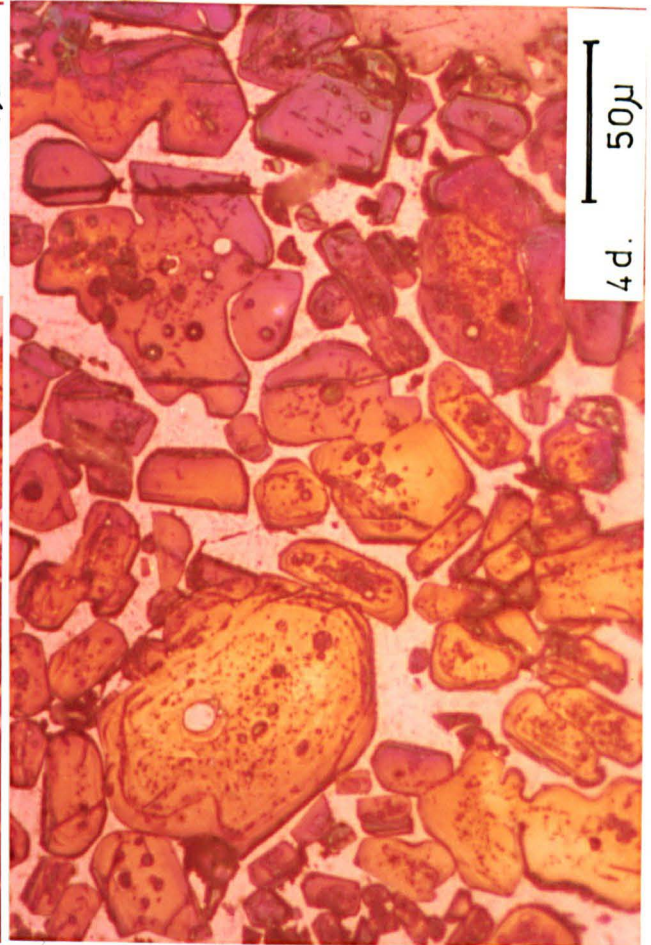
The Nital solution strongly etches the belite grains and shows the twinning structures. ( left ). The rounded belite grains with only one or two twinning planes are Type 1 (  $\alpha$  belite ). The irregular belite grains with multiple twinning planes are Type 2 (  $\alpha'$  belite ). Around some of the alites there are some secondary belites. ( bottom ).

Plate 4 c. Works G OPC clinker, Nital etch.

The alite crystals have etched a blue purple colour ( left ). Some of the individual crystals show zoning. There are several very small inclusions of ferrite and belite in the central areas of the many of the grains. There is extensive development of secondary belites around the alite. The belite grains have etched to a dark blue-black and no discrete lamellae can be indentified. These grains often appear mottled. This is type 3 belite (  $\beta$  belite ). Many of these belites show an intergrowth texture with the matrix phases. In some cases the belite 'grains' are agglomerates of many small crystallites. ( centre ). Thus the individual crystal size of these belites is extremely small. The tricalcium aluminate phase has etched to a very pale brown. The ferrite is not etched.

Plate 4 d. Works A OPC clinker, Nital etch.

Many of the alite crystals in this clinker are larger or smaller than usual. In several examples the clusters of very small alite crystals have coalesced to form a large irregular shaped grain. ( eg. bottom right ). These grains contain many small inclusions of belite and ferrite. The very large pseudo-hexagonal alite ( centre left ) has a trace of the solid-liquid interface formed by the partial melting of the first generation alite. The inner zone which remained solid has inclusions of belite and matrix, which it engulfed during formation. The outer zone, which is the second generation of alite, has no inclusions. This is because the original inclusions were remelted.



The Nital solution also etched the alite crystals. The colour ranged from yellow to orange to purple to blue, depending on the duration of the etching time and the reactivity of the alite. ( Plate 4b. and 4c. colour )

Dicalcium silicate , (  $\text{Ca}_2\text{SiO}_4$  ) ,  $\text{C}_2\text{S}$  , Belite.

The dicalcium silicate phase in portland cement contains several other minor oxides and is termed belite . The pale grey crystals were generally smaller than the alite , from 5 to 30  $\mu\text{m}$  , although grains up to 80  $\mu\text{m}$  were occasionally found . The belite crystals occurred in several forms : as individual rounded crystals amongst alite and interstitial material. These were etched with Nital and frequently had slightly diffuse boundaries with the interstitial phases . The belite occurred as loose flocks of rounded crystals with interstitial phases between the crystals ( Plate 5c. and 5e.) or as clusters of closely packed polygonal crystals with only traces of the interstitial phase between them and usually centered around a void or a large irregular mass of belite . These clusters and flocks were frequently surrounded by smaller than average alites ( Plate 5b. ). Midgley ( 1968 ) thought that the belite clusters centred around voids may have been due to the presence of high potassium content flue gases in the voids. The potassium stabilized the belite phase .

In many of the clinker samples the belite crystals were characterised by a curved fracture around the boundary of the grain . These fractures were probably due to stress which was caused by the shrinkage of the belite structure which was unable to transform to a lower temperature polymorph due to rapid cooling. Occasionally the cracking around the belite grains was restricted to the outer zone of the clinker nodules .

Small blebs of belite commonly occurred in alite crystals frequently concentrated in the inner regions of the alite crystals . Small belite crystals sometimes occurred as a thin skin around the alite crystals or as discrete unevenly dispersed blebs around the alite, ( Plate 5g. ).

Plate 5

Plate 5a. Works B LHC clinker, H<sub>2</sub>O etch.

The belite grains are filling many of the gaps between the subhedral alite crystals. This indicates that these belites were formed after the alite. ( Note. There are many fine scratches on the surface of the specimens. This was not from the original polishing process . These scratches were caused by the removal of the carbon coating after microprobe analysis, to allow etching.)

Plate 5b. Works B SRC with PFA addition clinker, H<sub>2</sub>O etch.

The belite cluster ( centre ) has many angular grains and extensive grain to grain contact. The dark irregular shaped phase within the belite cluster is an aluminate and it has been strongly etched. The belite cluster is due to the presence of a siliceous particle in the kiln feed, probably flint.

Plate 5c. Works B LHC clinker, H<sub>2</sub>O etch.

The string of rounded grey belite grains is caused by the penetration of some molten coal ash into the clinker. The liquid coal ash is lime deficient and reacts with the alite , which is lime rich, to form belite.

Plate 5d. Works D OPC clinker, H<sub>2</sub>O etch.

The irregular angular dark grey phase between the alite and belite crystals is tricalcium aluminate. The aluminate is in the cubic polymorph. It is highly reactive with water and has been strongly etched. Many of the belite grains have a distinctive intergrowth texture with the matrix . This is often associated with a lower viscosity liquid phase which can be due to the presence of minor elements such as manganese. A high burning temperature could produce similar effects to a lesser extent.

Plate 5e. Works B SRC with PFA addition Clinker, Nital etch.

The pseudo-hexagonal alite and the rounded belite crystals have been etched by the Nital solution. The belites have little or no trace of twinning and are classified as type 1. (  $\alpha$  belite).

Plate 5f. Works C OPC clinker, Nital etch.

The subhedral alite crystals have less distinctive boundaries than the alite crystals in Plate 5e. This is because the alite phase is more reactive and a thicker etch layer has developed. There is also extensive development of secondary belite around the edges of the alite. The primary belite phase occurs in two forms: As large rounded grains with intergrowths into the matrix and ; as small 2 to 3 $\mu$ m. micro grains within the aluminate ( pale grey ) and the ferrite ( white ).

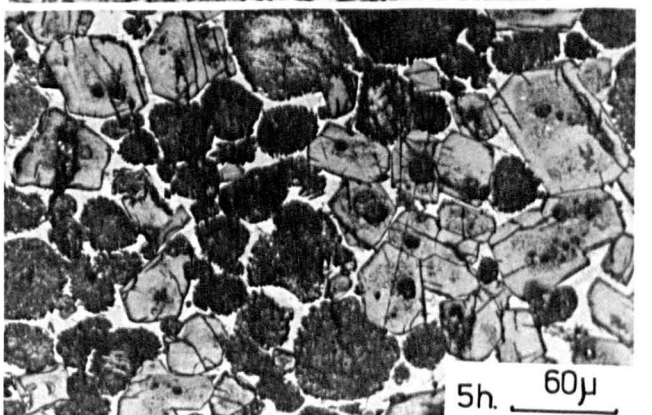
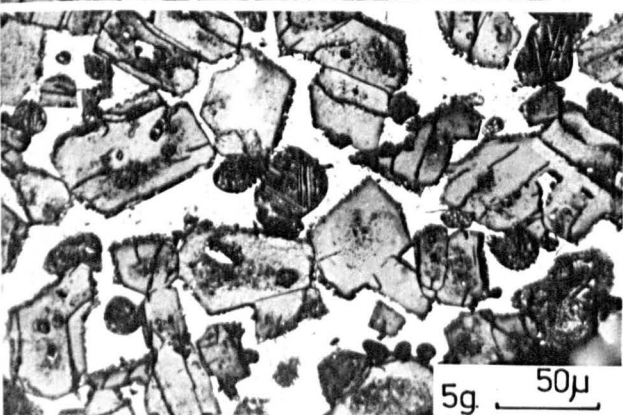
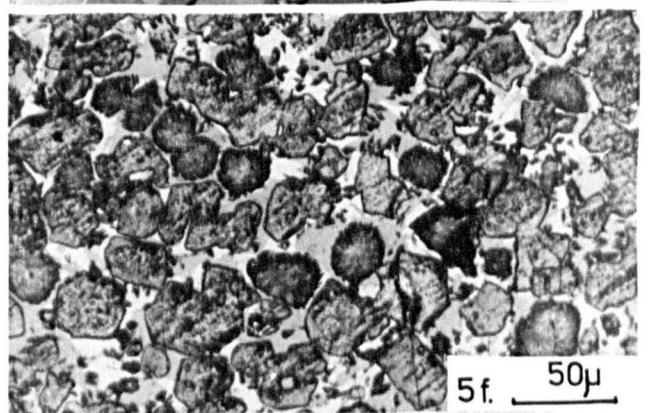
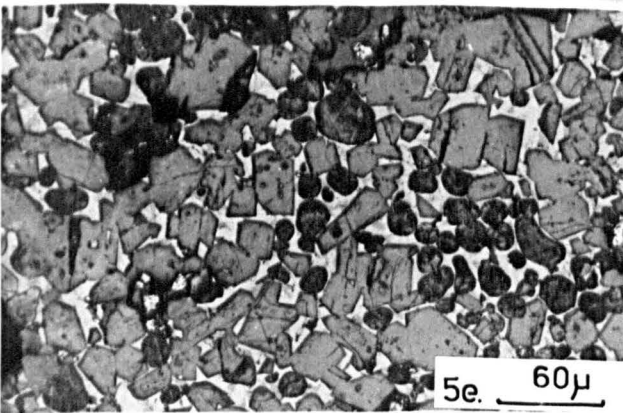
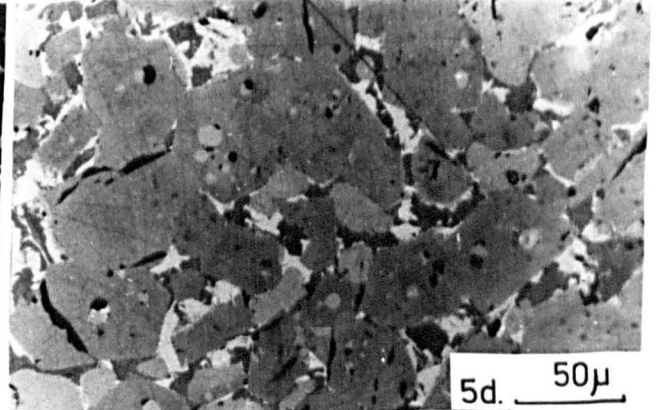
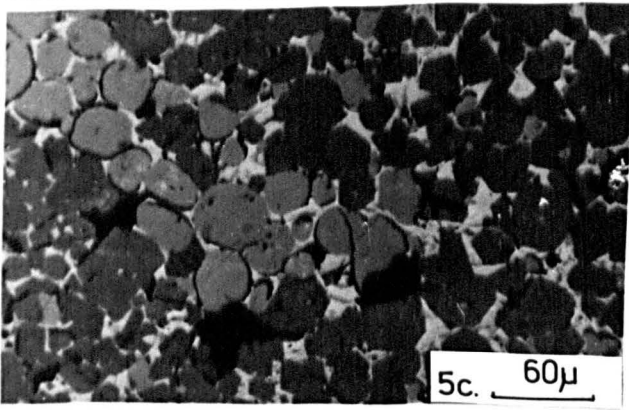
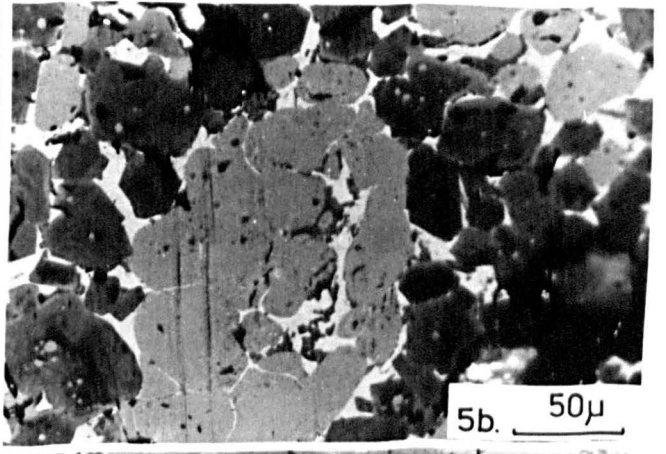
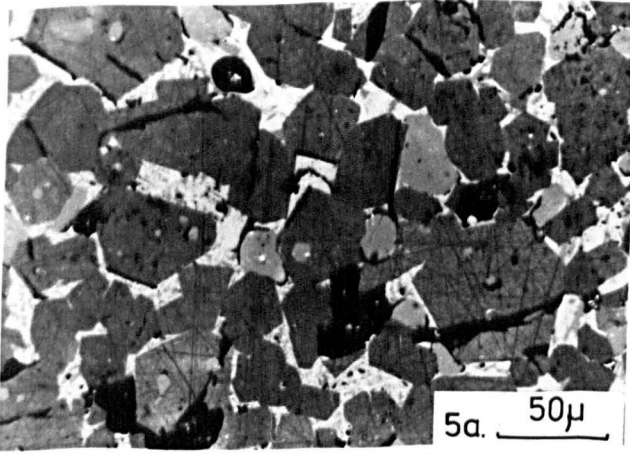
Plate 5g. Works D OPC clinker, Nital etch.

The belite crystals have distinctive lamellae twinning in several orientations, these are characteristic of type 2 belites (  $\alpha'$  to  $\beta$  belite ).

The euhedral alites have inclusions of belite and frelime in the central areas of the crystals. Around many of the alites there are borders of small secondary belite crystals. There is an abundance of ferrite and aluminate. The silicate grains are almost 'floating' in the matrix

Plate 5h. Works D OPC clinker, Nital etch.

The different crystals are closely packed together. There are extensive areas of belite ( left ). These belites have a mottled appearance and are typical of type 3 belite (  $\beta$  belite ). Many of the belites have an intergrowth texture with the matrix phases ( centre ). Most of the alite grains have many inclusions in the inner zones. The larger inclusions are belite. The very small dust like inclusions within the alite are frelime.



Occasionally the belite crystals were deformed round the alite crystals, (Plate 5a.).

The belite crystals frequently had small fine inclusions of freelite. At high magnification the belite crystals frequently had an intergrowth texture with the interstitial phases . ( Plate 5d. ) The texture sometimes developed to such an extent that the belite grains appeared to be formed of a series of elongated blebs . ( Plate 5f. ) The belite grains were not usually etched by distilled water , but were highly etched by the Nital solution . ( Plate 4c. colour ) The etching behaviour of the belites was extremely useful to identify some of the belite polymorphs by differential etching of the twinning structure of the various polymorphs.

#### Twinning in belite crystals.

The presence or absence of these twinning features was used in a classification system by Insley (1936). This consisted of three types:

Type I. This belite type was present in clinker heated to above 1450 °C and quickly quenched . The grains had complex striations and Insley considered the belite to be  $\alpha$  C<sub>2</sub>S .

Type II. This belite type occurred in clinker heated to 1420 °C . The grains had a single set of polysynthetic bands.

Type III. These belites were irregularly shaped and frequently showed an elongated lath like structure . Insley interpreted this interfingering structure as a result of late crystallization during cooling .

Chromy ( 1967 ) also devised a classification scheme for belites and used the following characteristics.

Belite type 'a' had polysynthetic twins of  $\beta$  C<sub>2</sub>S.

Belite type 'b' had intersecting wide lamellae of  $\beta$  C<sub>2</sub>S and contained inclusions .

Belite type 'c' had complex narrow lamella of  $\alpha'$  C<sub>2</sub>S .

Later Chromy ( 1970 ) modified and revised his classification system. He suggested that the stabilisation of the  $\alpha'$   $C_2S$  phase led to the formation of rounded untwinned grains with smooth surfaces . Chromy also reported that rapid quenching caused an imperfect  $\alpha C_2S$  to  $\alpha'$   $C_2S$  transformation . This was identifiable from the lamellae of the  $\alpha'$  form in the  $\alpha C_2S$  matrix. This transformation could proceed to  $\beta C_2S$  resulting in fine polysynthetic twinning . The presence of optically distinguishable lamellae in polysynthetic twinning was characteristic of  $\beta C_2S$  .

Ono et al ( 1968 ) classified the belites as two types :

Type 1 with rounded grains and complex cross lamellae developed from the  $\alpha$  to  $\alpha'$   $C_2S$  inversion , together with minute polysynthetic twinning due to the  $\alpha'$  to  $\beta C_2S$  inversion .

Type 2 belites formed as irregular grains with distinct parallel striations ( polysynthetic twinning ) .

The occurrence of the elongated interfingering texture has been studied by several researchers . Metzger ( 1953) suggested that the interfingering was caused by the faster growth of every second lamella . Investigation of several different specimens by the author does not support this theory because the lamellae appeared to spread in a radial pattern .

Sarkar ( 1977 ) suggested that the structure was caused by partial solution rather than crystallization . The differential solution was due to varying amounts of impurities in the crystals . This was unlikely as the detailed optical examination showed that apparent single belite crystals actually consisted of many smaller grains which did not show evidence of partial solution . ( Plate 3f. ) The distinct boundaries between the micrograins and the matrix were more indicative of crystal growth rather than solution .

Tsuboi and Ogawa ( 1972 ) suggested that the elongate belite lamellae were associated with high MgO levels in cement . They found that ZnO had

a similar effect . Since both MgO and ZnO act as mineralizers they reduced the viscosity of the melt . Thus it was likely that the elongated lamellae development was due to the lowered viscosity rather than a particular element . This supports the theory that the interfingering texture was a growth structure rather than a dissolution texture .

The previous classification systems for the belite polymorphs were not directly applicable to belite present in cement from production kilns. Therefore in this investigation , the author classified the belite grains as follows :

Belite polymorph classification system.

Type 1. These belite grains have an absence of twinning features. ( Plate 5e. ) . This type was dominantly  $\alpha$  C<sub>2</sub>S . ( If there was some  $\alpha$  to  $\alpha'$  C<sub>2</sub>S transformation present, traces of twinning were visible ) .

Type 2. These belite grains have wide distinctive lamellae with two or three orientations ( Plate 5g. and 4b. colour ) . This type was principally  $\alpha'$  C<sub>2</sub>S .( There may be some  $\alpha'$  C<sub>2</sub>S inversion to  $\beta$  C<sub>2</sub>S ).

Type 3. These belite grains have many fine indistinct lamellae with multiple orientations. The grains often appeared mottled, ( Plate 5h. and 4c. colour). This type was dominantly  $\beta$  C<sub>2</sub>S .

This system was similar to the classification used by Dorn (1978), who investigated cement from production kilns.

Tetracalcium alumino-ferrite. ( Ca<sub>4</sub> Al<sub>2</sub> Fe<sub>2</sub> O<sub>10</sub> ) , C<sub>4</sub> AF , Ferrite.

The major iron bearing constituent in Portland cement is termed Ferrite. Generally the formula of this phase is assumed to be Ca<sub>4</sub> Al<sub>2</sub> Fe<sub>2</sub> O<sub>10</sub>

which is the mineral Brownmillerite. This is in the solid solution series which ranges from  $6\text{CaO} \cdot 2\text{Al}_2\text{O}_3 \cdot \text{Fe}_2\text{O}_3$  to  $2\text{CaO} \cdot \text{Fe}_2\text{O}_3$ , ( $\text{C}_6\text{A}_2\text{F} - \text{C}_2\text{F}$ ). The actual composition of the ferrite phase within cement varies considerably within the solid solution series. The term ferrite is generally used to describe phases in this solid solution series.

The ferrite was readily identified by its highly reflective pale grey colour, distinguishing it from the duller and darker grey alites and belites. The ferrite usually formed the predominant interstitial phase. The interstitial phases represented the melt that was formed in the sintering process. Frequently the ferrite formed small irregular crystals. (Plate 6b and 6c.) In some cements the ferrite developed a dendritic structure with calcium aluminates between the ferrite crystals. (Plate 6a.) The ferrite was unaffected by either etch solution.

#### Tricalcium aluminate ( $\text{Ca}_3\text{Al}_2\text{O}_6$ ), $\text{C}_3\text{A}$ .

Tricalcium aluminate is a common component of Ordinary portland cement clinker. In a low alkali or slowly cooled cement the  $\text{C}_3\text{A}$  crystals developed as square or rectangular grains. The  $\text{C}_3\text{A}$  occurred primarily as small 2 to 5  $\mu\text{m}$  crystals. (Plate 10a.) In normally cooled cement with a high alkali content, the tricalcium aluminate was stabilized by the alkalis and occurred as long prismatic crystals between the alite and belite. (Plate 6e.) The  $\text{C}_3\text{A}$  etched very readily in distilled water producing a yellow to orange to dark brown colour. The colour of the etch was dependent on the duration of etch. The prismatic form was more reactive to the distilled water etch than the cubic form. This would indicate that the orthorhombic (prismatic) form of  $\text{C}_3\text{A}$  had a higher reactivity than the other forms.

#### Calcium oxide, ( $\text{CaO}$ ) or Freeline.

Freeline always occurred in the Portland cement clinker due to minor inhomogeneities in the raw mix. If the percentage of freeline exceeded 3%,

PLATE 6

Plate 6a. Works B SRC with PFA clinker, H<sub>2</sub>O etch.

The ferrite phase which is white and unetched has developed a dendritic texture with the aluminate phase, which has etched to give a dark colour.

Plate 6b. Works B SRC clinker, unetched.

In this cement the ferrite has formed as fine laths with irregular orientations. There are some small angular crystals of aluminate probably C12A7. The large pale grey crystals are alite or belite.

Plate 6c. Works B SRC with PFA clinker, H<sub>2</sub>O etch.

Detail of matrix phases. The ferrite phase is in the dendritic form. The fine irregular aluminate is between the dendrites. The small rectangular fragments (centre right) are alite.

Plate 6d. Works D OPC clinker, H<sub>2</sub>O etch.

The dark amorphous phase between the large crystals (centre) is alkali sulphate. This phase is very reactive with water. The grey phase with a slight striped appearance (bottom left) is tricalcium aluminate in the orthorhombic form. There are a few small rounded grains of belite which have not etched. The diffuse pale patch (right) is due to internal reflections.

Plate 6e. Works G OPC clinker, H<sub>2</sub>O etch. The pale grey laths between the darkly etched euhedral alites, are tricalcium aluminate. This is in the orthorhombic form and has been stabilized by the substitution of Na. The ferrite content in this nodule is very low.

Plate 6f. Works B SRC clinker, H<sub>2</sub>O etch.

The dark grey rectangular crystals are alite. They are small and closely packed. This is a characteristic of clinker which has been fired at slightly lower temperature than normal.

Plate 6g. Works G OPC clinker, H<sub>2</sub>O etch.

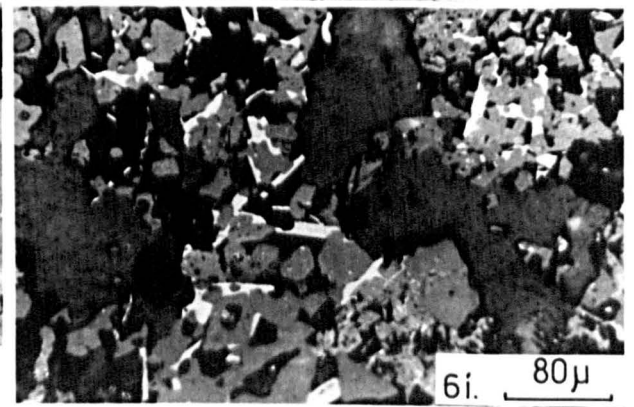
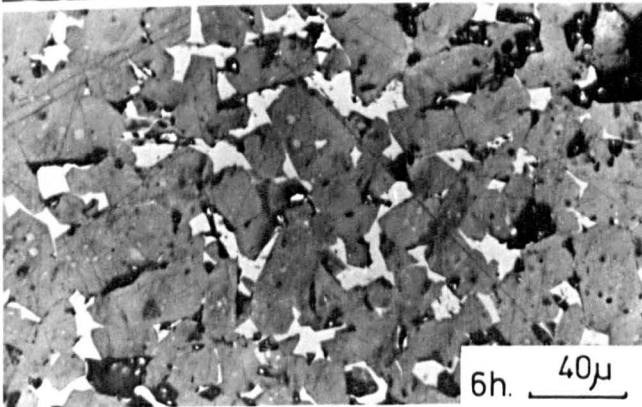
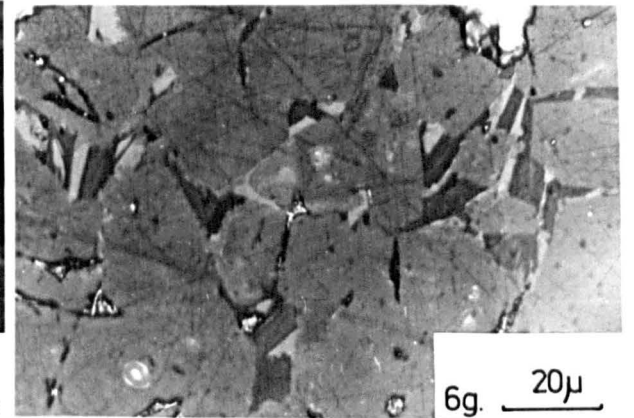
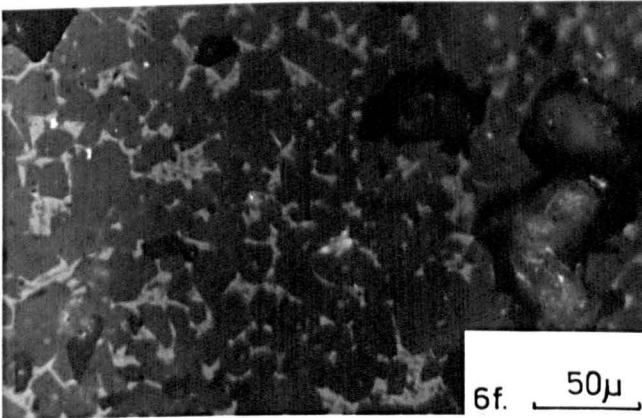
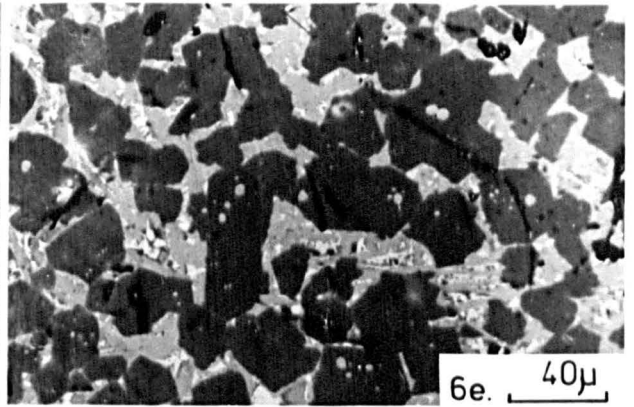
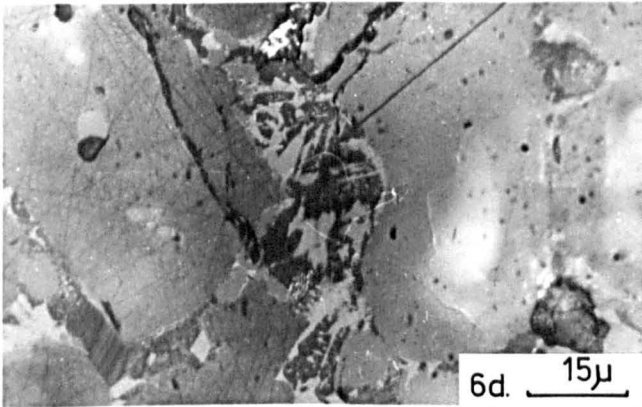
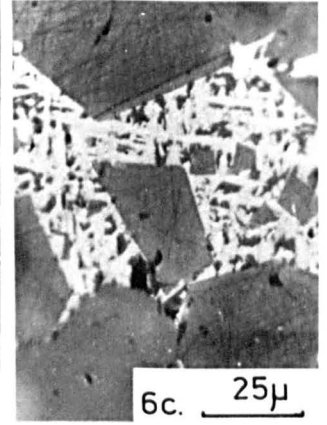
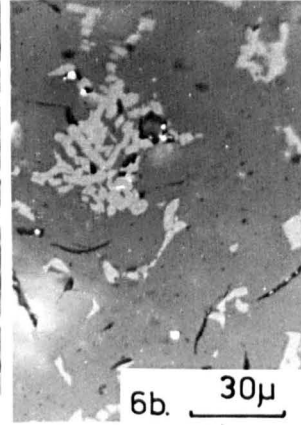
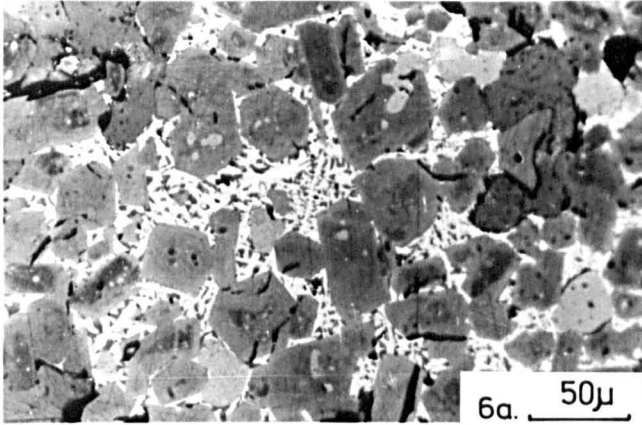
The subhedral alite crystals have a border of secondary belite. The matrix is predominantly orthorhombic tricalcium aluminate. This is in the form of laths which are zoned longitudinally and have a striped appearance. There are some very small periclase grains which are bright spots (2 to 4µm.) with a thin black outline. (top right).

Plate 6h. Works B SRC clinker, H<sub>2</sub>O etch.

The euhedral alite crystals have only etched lightly and do not show any zoning which indicates that their reactivity is low. There are some very small inclusions of belite. The matrix is ferrite with no trace of aluminate. The irregular black areas are pores.

Plate 6i. Works B SRC clinker, unetched.

This clinker was burnt at lower temperature than normal at about 1450° C. It was also cooled very slowly. The alite crystals are small and poorly developed. The belite grains are pale grey in colour and are clustered together. (area just to left of figure number). They are small and contain many voids and inclusions. Due to the slow cooling the ferrite has crystallized as large laths between the alite and belite grains. Overall the clinker is extremely porous. The extensive areas of irregular dark grey material are holes in the clinker nodule filled with mounting resin.



the kiln feed may have been too high in CaO content or there was poor burning in the kiln . The incomplete firing in the kiln did not allow complete reaction of the CaO with the other components of the clinker. In polished sections the crystals of CaO always occurred as spheroidal particles in the other major cement phases The free lime always etched very rapidly with distilled water , to small black blebs frequently clustered together .

#### Magnesium oxide , ( MgO ) , Periclase.

The presence of periclase was dependent on the amount of MgO in the kiln feed . In the clinker the MgO often crystallised as small rectangular grains in the ferrite , because ferrite was one of the later forming minerals . In polished sections, the periclase could be identified by the high relief from the flat surface because of its high hardness value. The high thermal expansion of the periclase caused a narrow fracture around the edge. Thus in reflected light it appeared as a bright raised grain with a thin black outline . ( Plate 6g. )

#### Alkali sulphates.

The alkali ( Na,K, ) content of the clinker was distributed either , as substitution elements in the alites , belites and ferrites or if the alkalis were in excess they occurred as alkali sulphates . In polished sections these appeared as very irregular low reflectance minerals . The minerals were usually very soft and were scratched due to the polishing. Otherwise they appeared very similar to the mounting resin . The chemical composition could only be determined by electron microprobe analysis ( see Chapter 8 ) . After etching with distilled water the alkali sulphates darkened and became uneven (Plate 6d.) due to the phase hydrating very rapidly .

#### Other alkali phases.

In some of the cement clinker studied, there were crystals which had the characteristics of belite, but were etched by the distilled water .

Brown (1948) thought that this type of belite had the chemical composition  $23\text{CaO} \cdot \text{K}_2\text{O} \cdot 12\text{SiO}_2$ . Nurse (1960) concluded that this was not a distinct compound but a potassium stabilized form of  $\alpha'$   $\text{C}_2\text{S}$ . Its X-ray pattern differed from  $\beta$ - $\text{C}_2\text{S}$  only in the intensity of some of the lines.

In the authors' opinion the difference in reactivity to water of the two phases is due to the presence of defects in the lattice of the potassium rich belite. These defects are caused by the substitution of calcium ions ( $\text{Ca}^{2+} = 0.99\text{\AA}$ ) by the larger potassium ions ( $\text{K}^+ = 1.33\text{\AA}$ ).

#### Minor matrix phases .

The interstitial areas in the cement clinker were often thought to contain a "glass" phase. This "glass" content of the clinker was always very low. Some workers, notably Insley and Frechette (1952) studied the refractive index of the "glasses" and found that the refractive index was dependent on its composition; principally the  $\text{Al}_2\text{O}_3$  and  $\text{Fe}_2\text{O}_3$  content. The high iron "glass" had a higher refractive index than the alumina glass. The "glass" etched with Nital. Studies by Hofmann (1975) showed that this "glass" was cryptocrystalline and became microcrystalline under slow cooling conditions.

The author supports the latter view that the material referred to as "glass" is an aluminate phase with a low, but variable iron content.

### THE MORPHOLOGY OF THE CEMENT MINERALS.

#### THE SILICATES

The most variable features of the alite crystals was the size range and the crystal morphology. Several workers have investigated the causes of the different features.

Tsuboi and Ogawa (1972) found that if the clinker had been well burnt, the alite grains were well defined euhedral crystals larger than  $20\mu\text{m}$ .

An increased burning time and increase in temperature resulted in a more uniform distribution of evenly sized alite crystals .

The size of the raw material grains influenced the size of the alite crystals . Large siliceous particles caused clusters of belite crystals which were lime deficient areas and conversely in other regions of the clinker , there were areas of lime excess , resulting in free lime formation. Heilman ( 1952 ) found that 1 % of coarse quartz resulted in the same free lime production as 6 % excess limestone .

Dorn (1978) reported that belite formation in the lime poor zones led to a lime excess at the edges of the cluster . This caused large alites to form in the vicinity . Dorn also found that a highly viscous liquid phase due to alkali or sulphate frequently caused large alites . Brown (1948) proposed that instant quenching produced straight angular alite and rounded belite . Angular belite was produced under moderate cooling conditions . Maki and Goto ( 1982 ) found that burning at high temperatures caused high supersaturation conditions over large areas of the clinker and many nuclei formed. This favoured the formation of small alite crystals . At low burning temperature the supersaturation of the alite remained low . The low nucleation rate favoured the development of large alite crystals .

In the present investigation it was observed that the alite crystal morphology produced by different formation conditions did not match with the previous descriptions . The author found that around the belite clusters , the alite grains were frequently smaller than the belite crystals .( Plate 3g. and 5a.) In hard burnt cement clinker with a high sulphate and alkali content, The alite size was extremely variable from 10 to 60  $\mu\text{m}$ . This does not agree with the observations of Dorn ( 1978).

In clinker that was burnt at a lower temperature than usual ,there were extensive areas of very small, 5 to 10  $\mu\text{m}$ . long, subhedral alite laths and stubby alites up to 60  $\mu\text{m}$ . long. ( Plate 6f. ) This conflicts with the supersaturation and nucleation theory of Maki and Goto ( 1982 ) .

In well burnt clinker that was slowly cooled, the alite crystals were larger, up to 50  $\mu\text{m}$ . and dominantly euhedral . ( Plate 6h. ) In the lightly burnt , slowly cooled clinker , the alites were smaller about 20 $\mu\text{m}$ . and had no fractures . The belite grains were also small about 10 $\mu\text{m}$ . and irregularly shaped with a porous texture. ( Plate 6i. ) The ferrites had developed as long discrete laths up to 40  $\mu\text{m}$ . ( Plate 6i. ) This was not seen in normally cooled cements . In the very rapidly quenched cement clinker, the central area of the clinker nodules were bright green . This green area consisted almost entirely of irregular shaped belite grains with traces of matrix . ( Plate 7c.right ) The green colour was due to the iron in the matrix phase being in the ferrous state. The dark brown outer region was dominantly alite with some belite. (Plate 7c.left) The alite grains were small and subhedral.( Plate 7a. ). This contrasted with the observations by Brown ( 1948 ) . The differences were particularly apparent in the sulphate resisting cement clinkers and the low heat cement clinkers . These features were also noticeable in the Ordinary Portland cement clinkers .

#### The morphology of the matrix phases.

##### Ferrite.

The ferrite phase in cement is in the solid solution series  $\text{C}_6\text{AF}_2$  to  $\text{C}_6\text{A}_2\text{F}$ . This caused the characteristics to vary depending on the composition of the phase in the different types of cement . The reflectivity of the ferrite was determined by the iron content . High reflectivity was due to a high iron content . This was controlled by the total iron content of the clinker . The apparent reflectivity of the ferrite could be reduced due to the inclusion of crystals of the other matrix phases if the crystal size was very small . In the sulphate resisting cement and the low heat cement , the ferrite often crystallized with a distinct dendritic texture, with the aluminate phase between the branches. The ferrite was unetched by distilled water or Nital .

PLATE 7

Plate 7a. Works B SRC clinker , rapidly quenched.

The cluster of irregular shaped large belite grains ( left ), has only traces of matrix phases between the grains. The alite crystals are smaller than normal and are also closely packed. ( right ) Rapidly quenched cement clinker often has large areas of matrix deficiency.

Plate 7b. Works D OPC clinker . H<sub>2</sub>O etch.

The pale grey rounded belite grains are well dispersed. The grey alite grains are subhedral and contain many inclusions of belite. The aluminate phase has etched to a dark grey and is irregular in shape. This is typical of the cubic polymorph of tricalcium aluminate.

Plate 7c. Works B SRC clinker, rapidly quenched, H<sub>2</sub>O etch.

The massive cluster of angular belite grains ( right ) has a very sharp boundary against the pack of alite crystals ( left ) The belite grains had formed a central zone in the clinker nodules and were bright green in colour. This large zone of belite indicated that the clinker in this area was extremely lime deficient. The matrix in this zone was tricalcium aluminate with no ferrite phase detectable. Thus all the matrix etched to a dark grey. The alite crystals were anhedral and small. The matrix was predominantly aluminate with traces of ferrite. In the outer regions of the nodules the matrix was mostly ferrite e.g. Plate 7a . Generally throughout the nodules there was a deficiency in matrix.

Plate 7d. Works G OPC clinker, H<sub>2</sub>O etch.

The alite crystals are surrounded by small secondary belite grains. The long lath like crystals with traces of striping are tricalcium aluminate in the orthorhombic form. These aluminate crystals have developed after the formation of the secondary belite.

Plate 7e. Works B LHC Trial clinker, H<sub>2</sub>O etch.

The euhedral alite crystals contain many inclusions of belite and very small particles of freelite. These are concentrated in the central zones of the crystals. The alite was very reactive to the water and has been strongly etched. The aluminate phase in the matrix is probably C<sub>12</sub>A<sub>7</sub> and has only etched slightly.

Plate 7f. Works B SRC clinker.

This clinker has been burnt at a lower temperature than normal. The alite crystals (right) are anhedral and there is a low matrix content. The belite crystals clustered around the pore (black) are poorly developed and have many very small holes in their structure. This type of belite was very susceptible to degradation, due to the  $\beta$  to  $\gamma$  phase transformation.

Plate 7g. Works B LHC Trial clinker, H<sub>2</sub>O etch.

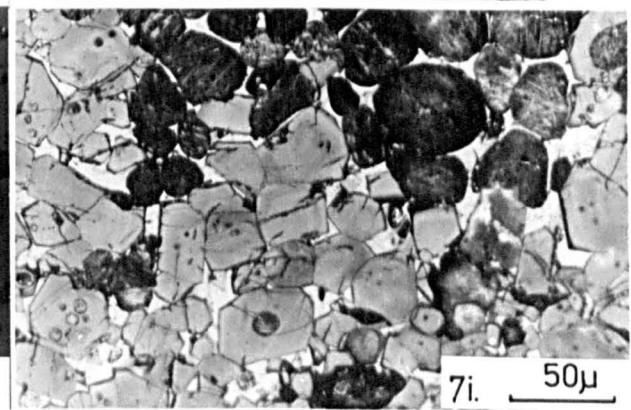
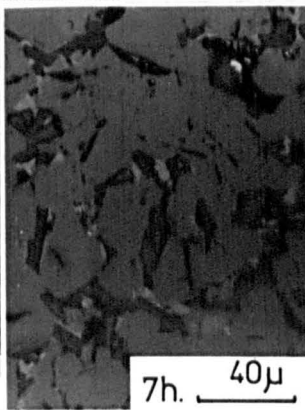
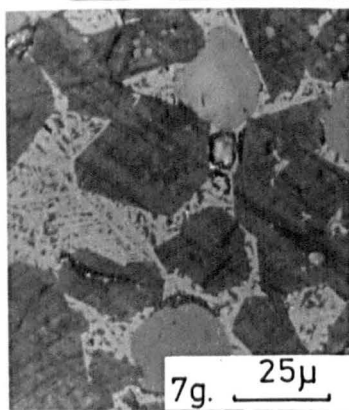
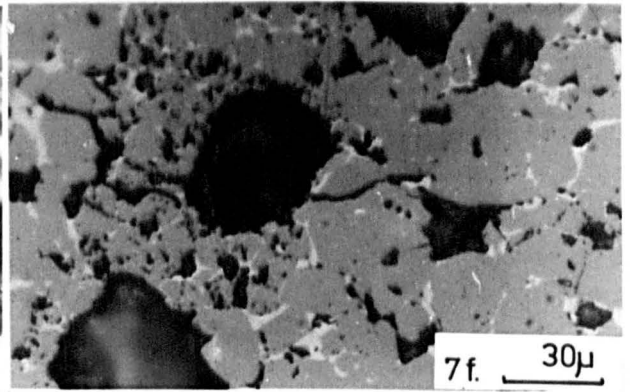
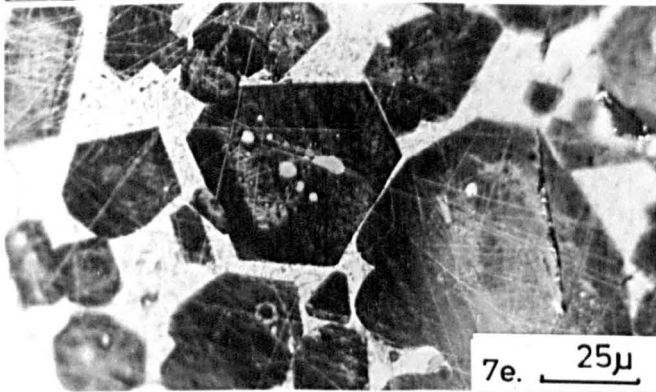
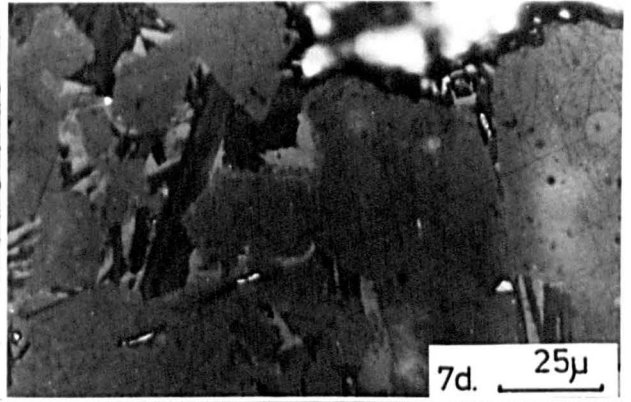
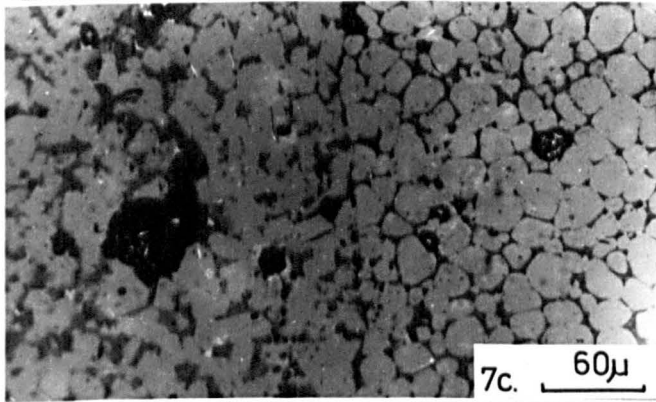
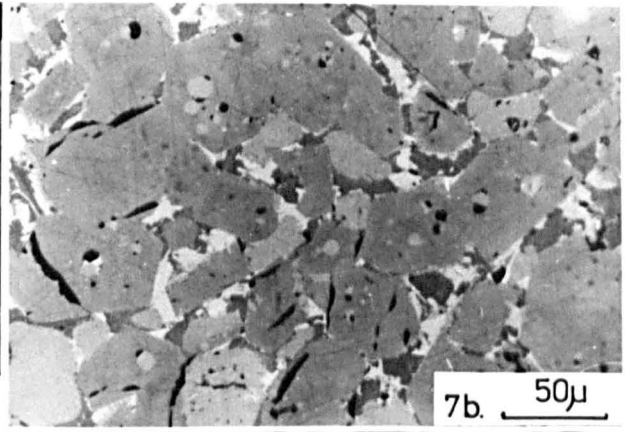
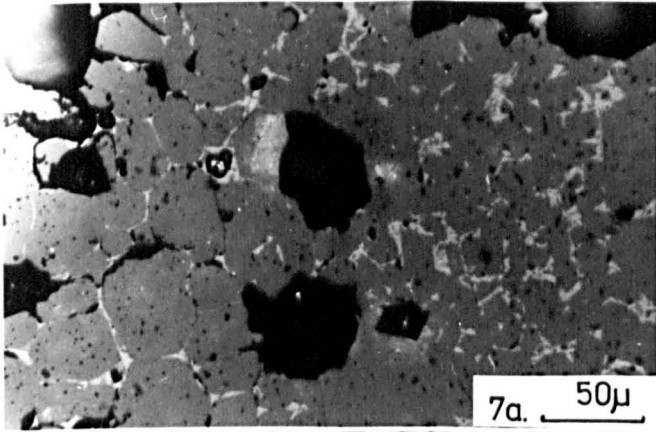
The euhedral alites and rounded belites are surrounded by abundant matrix. This principally consists of ferrite in the dendritic form and traces of the aluminate phase.

Plate 7h. Works G OPC clinker, H<sub>2</sub>O etch.

The subhedral alite crystals are in a matrix which consists almost entirely of tricalcium aluminate. The alite crystals are only slightly etched. The aluminate which is in the orthorhombic form has been strongly etched.

Plate 7i. Works B SRC with PFA addition, Nital etch.

The subhedral alite crystals are closely packed and show traces of zoning. The inclusions are principally belite and are only in the central areas of the alite. These are the relics of the early forming alite polymorph. The later overgrowth does not contain any belite inclusions. The belites ( top ) have multiple lamellae which are often indistinct. Thus most of the belite is type 3, with a few type 2 grains. Some of the large belite inclusions in the alite crystals have etched and show traces of twin lamellae.



### Aluminate.

The major aluminate phase in the ordinary portland cement was usually tricalcium aluminate,  $C_3A$ . The  $C_3A$  occurred intergrown with the ferrite in one of two forms: either as small angular, often triangular crystals. (Plate 7b.) This was the cubic form. The presence of alkalis or  $MgO$  at a level greater than 3 wt.%, caused the  $C_3A$  to form as long lath shaped crystals. (Plate 7d.) These crystals were of the orthorhombic form. Both forms were rapidly etched by distilled water and lightly etched by the Nital solution.

In sulphate resisting cement and low heat cement the formation of  $C_3A$  was suppressed by the addition of extra iron oxide. Under certain production conditions an aluminate phase occurred as a very fine indistinct phase amongst the ferrite. (Plate 7e.) If the alumina content of the clinker was slightly higher, a more distinct, small irregularly shaped aluminate phase crystallized amongst the ferrite. (Plate 7g.) These latter two phases have been termed glass by earlier researchers. However the etching behaviour in distilled water was very similar to that of  $C_3A$ .

### THE ORDER OF PHASE FORMATION.

In the clinker samples investigated there was evidence of several episodes of alite formation and belite development in the production cycle. After the initial formation of the liquid phase, dominantly  $Ca$ ,  $Fe$  and  $Al$ , belite crystals started to nucleate. These were usually very irregular in shape and contained small voids. (Plate 7f.) Then at about  $1200^{\circ}C$  the alite crystals started to form by solid state reaction between  $CaO$  and the belite. These alite crystals frequently engulfed the smaller remnant belite crystals and matrix material. (Plate 7e.) With continued heating the early alite crystals, which were probably the  $M1$  polymorph, partially

dissolved in the molten phase . Then after cooling from the sintering temperature, a higher temperature polymorph, possibly M2, M3 or R formed as an overgrowth on the earlier formed alite. ( Plate 7i. ) This formation and remelting process provides an explanation for the frequent occurrence of large alite crystals with inclusions of belite and matrix only in the inner regions of the crystal. ( Plate 7i. ) Etching clearly shows a boundary between the alite with inclusions and the inclusion free alite . (Plate 4d. colour ) The zone boundary is probably the solid-liquid interface on the remelting of the first formed alite . This process of crystallization and remelting provides an explanation of the textures in the different phases . The later and higher temperature polymorph forms were euhedral crystals . They did not have extensive competition for space from the belite grains . As cooling continued the belite crystals formed quickly and did not have enough time to fully equilibrate . They frequently contained very small inclusions of matrix and free lime . These belites filled the voids between the existing alites. Often the belite grains formed around the alite crystals .( Plate 7g. )

Occasionally if there was a lack of Ca or excess of Si, very small blebs of belite formed around the edges of the alite crystals .( Plate 4c. colour). This was due to the loss of CaO from the alite as the clinker cooled. As the cooling continued, the interstitial phases differentiated . The concentration of iron in the melt finally resulted in the formation of a ferrite phase . The ferrite crystallized as irregular shaped laths or as dendritic crystals in between the alite and the belite .( Plate 7g.) If there was a sufficiently high alumina content in the melt , discrete angular or prismatic crystals of  $C_3A$  formed amongst the ferrite. ( Plate 7h. ) If the alumina content was low , a fine indistinct aluminate phase crystallized between the dendritic ferrite crystals. ( Plate 7e. ).

The microscopical properties of the cement clinker minerals are summarised in Table 5.1.

(TABLE 5-1) PROPERTIES OF CEMENT MINERALS IN REFLECTED AND TRANSMITTED LIGHT.

	TRICALCIUM SILICATE		DICALCIUM SILICATE		TETRA CALCIUM ALUMINO-FERRITE	TRICALCIUM ALUMINATE		CALCIUM OXIDE	MAGNESIA OXIDE	ALKALI-SULPHATES
CHEMICAL FORMULA	$Ca_3SiO_5$		$Ca_2SiO_4$		$Ca_4Al_2Fe_2O_{10}$	$Ca_3Al_2O_6$		CaO	MgO	(K, Na, CaSO <sub>4</sub> )
ABBREVIATION	$C_3S$	$\alpha C_2S$	$\alpha' C_2S$	$\beta C_2S$	$C_4AF$	$C_3A$				
CRYSTAL SYSTEM	Hexagonal	Hexagonal	Orthorhombic	Monoclinic	Orthorhombic	Cubic	Orthorhombic	Cubic	Cubic	
CEMENT PHASE FORM	Alite	$\alpha$ Belite	$\alpha'$ Belite	B Belite	Ferrite	Aluminate	Aluminate	Freelite	Periclase	Alk. sulphate
TRANS. LIGHT COLOUR	Colourless	Pale yellow	Pale yellow	Yellow-orange	Red-brown	Irregular	Irregular	Rounded	Rounded	Irregular
PLEOCHROISM		Slight	Slight	Slight	Yellow-brown	None		None	None	Opaque
X-POLAR. LIGHT INTERFERENCE COLOUR	First order grey	First order yellow-red	First order yellow-red	Second order yellow	Third order	Isotropic		Isotropic	Isotropic	
REFLECT. LIGHT FORM	Angular-pseudo hexagonal	Rounded	Irregular polygonal	Rounded	Irregular or dendritic	Irregular triangular	Irregular oblong	Rounded	Sub-angular	Irregular
COLOUR	Pale grey	Pale grey	Pale grey	Pale grey	White to grey	Pale grey	Pale grey	Dark grey	White	Dark grey
BIREFLECTANCE				Slight	Slight	Pale brown				
REFLECTANCE	Medium	Medium	Medium	Medium	High	Medium-high	Medium-high	Low	Very high	Very low
USUAL SIZE RANGE	5um to 120um	2um to 80um	2um to 80um	2um to 80um	Variable	5um to 10um	5um to 30um	2um to 8um	2um to 5um	5um to 50um
CHEMICAL ETCH COLOURS ( Time )										
DISTILLED WATER ( 20 to 30 sec.)	Blue to magenta to brown	Nil	Nil	Nil	Nil	Green-yellow to blue	Yellow-blue to brown	Black	Nil	Hydrates rapidly
ALCOHOL ( 5 min.)	Nil	Pale pink	Pale pink	Pale pink	Nil	Nil	Nil	Nil	Nil	Nil
NITAL ( 10 to 15 sec.)	Yellow-orange purple to blue	Blue	Dark blue	Dark blue	Nil	slight	slight	Black	Nil	Nil
OTHER FEATURES	Longitudinal fractures. May show etch zones	Absence of twins after Nital etch	Distinct twins two or three orientations.	Complex twins are indistinct and mottled	Part of solid solution $C_2^F$ - $C_6A_2F$ . The low iron phase etchs slightly in $H_2O$			Reacts fast in water	Very hard High relief	Very soft Scratches

Chapter six.

DESCRIPTIVE PETROLOGY OF CEMENT CLINKER  
FROM PRODUCTION KILNS AT WORKS A,B,C,D,E,F AND G

Descriptive petrology of the Sulphate Resisting Cement clinker from Works B  
kiln No.1.

Source of the raw materials.

The raw materials used for cement manufacture at Works B were chalk and pulverised fuel ash (PFA). The PFA was from coal burning power stations. Some high grade materials were used such as silica sand and iron oxide to adjust the feed chemistry to the desired alumina and silica ratios.

Clinker morphology.

Samples of Sulphate Resisting Cement clinker were collected from number one kiln at hourly intervals from 1930 to 0530 .

The clinker was usually ' hard burnt ' and the irregularly shaped nodules had a fine grained smooth outer rim . The central region was granular with a high porosity (15 to 20 % ). Many of the nodules had small ' islands ' of brown clinker surrounded by grey green material . This indicated that the clinker had been burnt in a reducing atmosphere in a section of the kiln . At a later stage , reoxidation occurred in most of each nodule . The brown areas were remnants of the reduced clinker.

Clinker petrology.

The alite crystals were generally euhedral to subhedral . The size ranged from 20  $\mu\text{m}$ . to 140  $\mu\text{m}$  . The dominant size was 60  $\mu\text{m}$ . by 20  $\mu\text{m}$ . Most of the alite grains were extensively fractured parallel to the long

side of the crystals due to the contraction of the alite on cooling. (Plate 8a.)

The belite crystals were rounded and smaller than the alite crystals . In the SR clinker they frequently occurred as large clusters up to 2 mm. across . This was caused by the characteristics of the raw materials used . The chalk contained flint nodules which had different crushing and grinding behaviour compared to the chalk . The flint fragments from the crushing plant were larger than the crushed chalk . These flint particles were regions of very high silica content in the kiln feed . During the firing process , belite was preferentially formed in these regions . Occasionally the region was so rich in silica , that the belite formed as large irregular shaped grains . Tsuboi and Ogawa ( 1972 ) , found similar characteristics in clinker produced from kiln feed with other siliceous components. The size of the belite crystals in the clusters varied from 5  $\mu\text{m}$ . to 60  $\mu\text{m}$ . , the dominant size was about 30  $\mu\text{m}$  . There was extensive fracturing around the boundaries of the belite grains due to contraction of the crystals on cooling . (Plate 8g.) There were occasional belite grains as inclusions in the large alite crystals . Frequently very small blebs of secondary belite were surrounded by alite . The primary belites were principally type 3 with some type 2 .

The matrix between the alite and belite consisted almost entirely of high reflectivity ferrite . At the edges of the nodules in the fine grained rim , an irregular shaped phase was intergrown with the ferrite. (Plate 8b. ) This phase was thought by the author to be a calcium aluminate , because it was rapidly etched by distilled water .

Several of the clinker samples , notably K1 2030 to K1 2230 had different features . The clinker nodules were small and dusty . The alite crystals were euhedral to anhedral and very small , the dominant grain size was about 10  $\mu\text{m}$  . Frequently groups of these small crystals appeared to be coalescing to form larger alite crystals (Plate 8d. ) A few large

PLATE 8

Plate 8a Works B SRC clinker, K1 0430,1 unetched.

The alite crystals were very variable in size. The larger crystals usually had fractures parallel to the longest sides. Many of the smaller alite grains did not have fractures.

Plate 8b. Works B SRC clinker, K1 2330, H<sub>2</sub>O etch.

After etching the clinker with H<sub>2</sub>O, the aluminate phase etchs strongly and appears as irregular angular crystals. This aluminate frequently only occurred in the outer parts of the clinker nodules.

Plate 8c. Works B SRC clinker, K1 0130, H<sub>2</sub>O etch.

This clinker was 'hard burnt', it was fired at a higher temperature than required. This allowed a longer crystallization period for the phases. The alite crystals are euhedral and the aluminate grains are larger than the aluminate in Plate 8b. There is greater definition between the ferrite and the aluminate phase.

Plate 8d. Works B SRC clinker, K1 2230, unetched.

This clinker was 'under burnt', the temperature was slightly lower than usual. The alite crystals were extremely variable, from very large 90µm (bottom centre) to small poorly formed alites in a cluster. (centre left)

Plate 8e. Works B SRC clinker, K3 0130, unetched.

The belite grains are clustered around a void (centre). They are very angular and irregular in shape. These clusters of belite are often caused by a fragment of siliceous material in the kiln feed. This produces an area of lime deficiency in which the belite forms. Adjacent to the belite cluster there are clusters of very small anhedral alite crystals.

Plate 8f. Works B SRC clinker with PFA kiln addition, H<sub>2</sub>O etch.

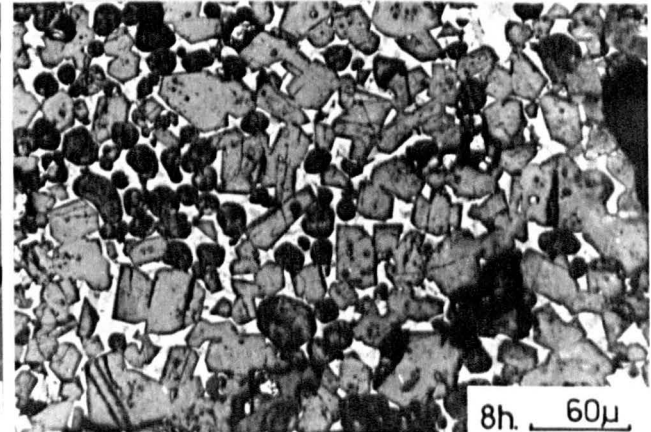
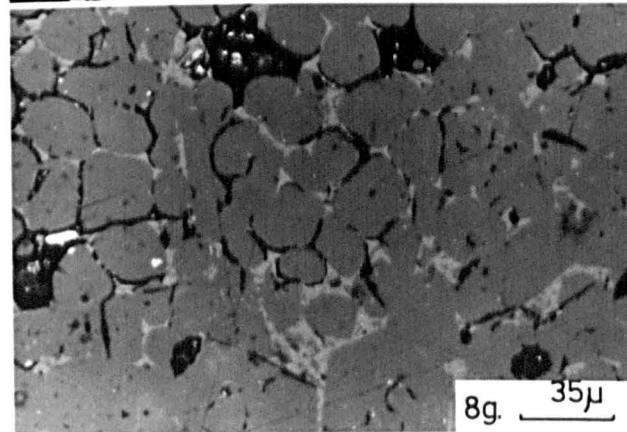
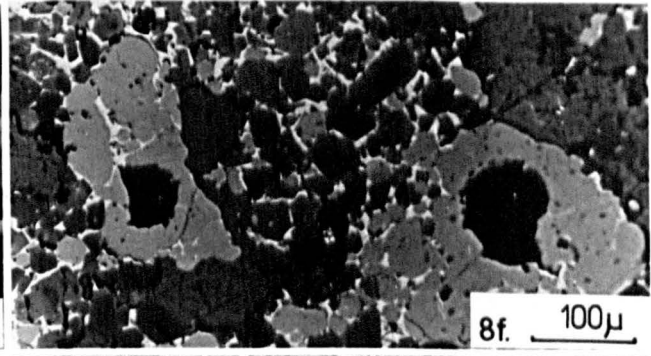
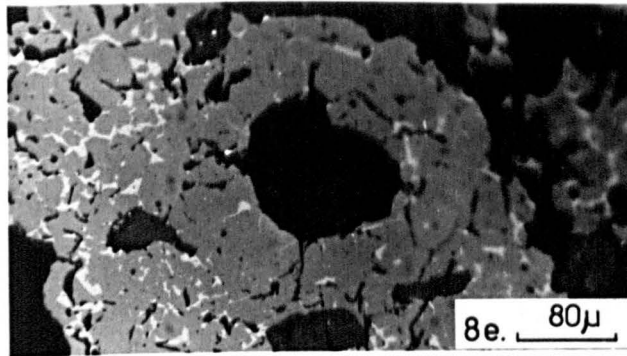
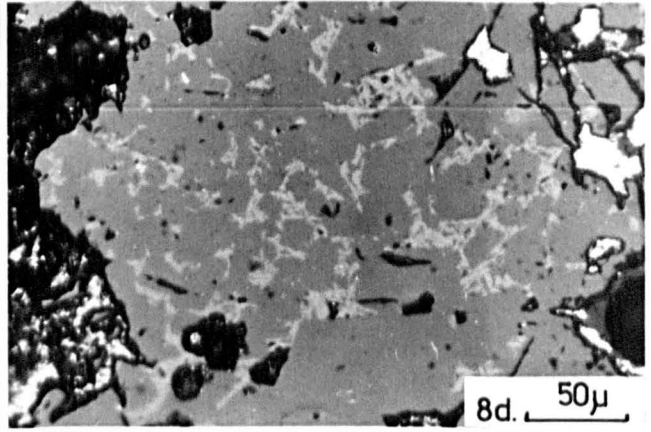
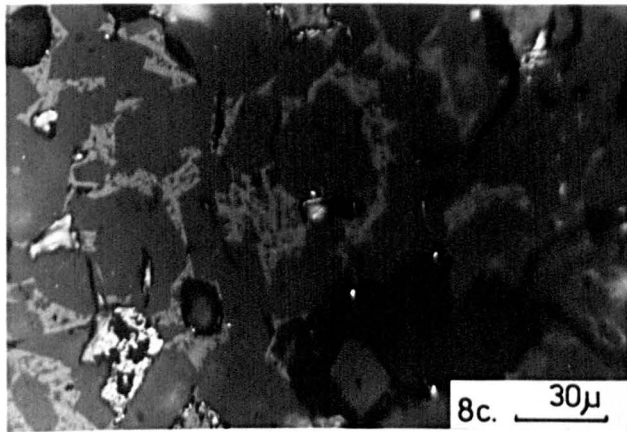
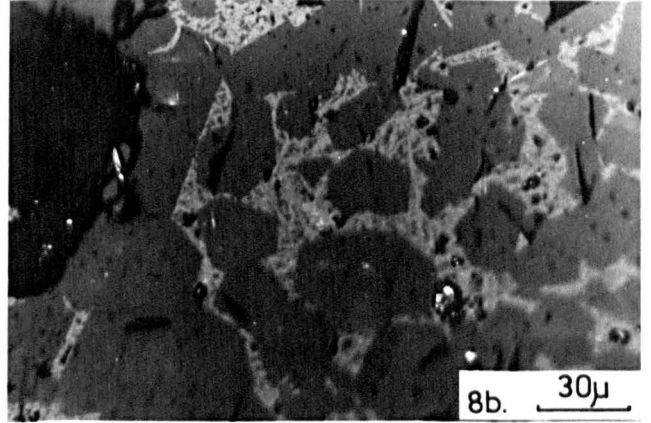
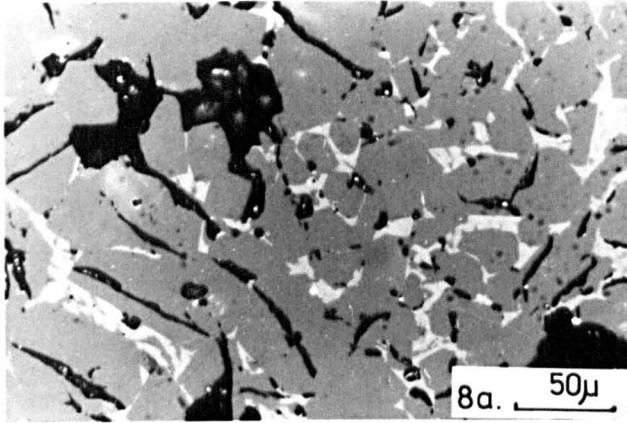
The shape of the clusters of belite (pale grey) frequently indicate the origin of the siliceous fragment. The elongate clusters (this Plate) with distinct corners are often derived from flint or chert fragments which occur in the calcareous feedstock. The rounded clusters (Plate 8e) can be relicts from quartz sand grains. These may be from the lithologies worked for the feed or from silica sand added in the blending process to achieve the correct Silica Ratio. If the belite grains occur as a long thin streamer in the clinker (Plate 5c), the probable source is the coal ash from the kiln. If PFA is added to the kiln it has an effect similar to a high ash coal.

Plate 8g. Works B SRC clinker, K1 0230, unetched.

The belite grains are bounded by circular fractures, which are due to the contraction of the grains during the cooling process.

Plate 8h. Works B SRC clinker with PFA kiln addition, Nital etch.

The alite crystals are euhedral and in several areas they are coalescing to form large subhedral grains. The belite grains are variable in size and generally rounded in shape. These belite grains are dominantly type 3 with some type 2 grains. The aluminate portion of the matrix has etched very slightly and is distinguishable from the unetched white ferrite.



alite crystals were about 150  $\mu\text{m}$ , showed extensive fracturing . The belite grains were similar to the belite in the previous samples . The matrix however was different; there was more of the dendritic aluminate phase throughout the nodules .

These latter samples of clinker were the products of either , a low burning temperature in the kiln , a short residence time in the burning zone , or a combination of both . The alite , belite and ferrite phases were further from the state of equilibrium than the phases in the correctly burnt clinker . Many of these samples deteriorated , despite storage in a dessicator . This was probably due to the inversion of  $\beta$  belite to  $\gamma$  belite which involved a volume increase of about 12 % .

#### Influence of kiln conditions on the clinker.

The Sulphate Resisting Cement from number 3 kiln had different production conditions to the clinker from kiln number 1.

The fine dust produced by all the kilns at Works B was collected from the exhaust gases by cyclones and mixed with water to form a slurry . This was fed through a spray drier and injected into kiln 3 with the normal slurry . The dust from the kilns was high in alkalis and produced a cement with high alkali and sulphur content . The input of the exhaust dust was not constant . The return dust system was usually switched in or out every two or three hours . Thus the alkali and sulphur content of the clinker varied . The normal slurry feed system was also a cause of variation to the feed for kiln 3 . The slurry was pumped from the stirred storage ponds to the kilns . Since kiln 3 was the furthest from the storage tank , slight separation occurred with the larger and heavier particles . Thus the sand and flint particles and the 'pyrites' dust tended to separate from the kiln feed . Therefore the feed to the kiln 3 was lower in  $\text{SiO}_2$  and  $\text{Fe}_2\text{O}_3$  than the slurry to kiln 1 .

Clinker morphology.

The clinker nodules from kiln 3 were more variable than kiln 1. The size of the clinker nodules was smaller and the clinker was more dusty. The outer surface of the nodules had a rough texture.

Clinker petrology.

The alite crystals were on average smaller than those from kiln 1. They were very acicular and the dominant size was about 20  $\mu\text{m}$ . by 7  $\mu\text{m}$ . There were only a few large stubby crystals 70  $\mu\text{m}$ . by 50  $\mu\text{m}$ . These large crystals usually contained some belite inclusions, but the small alites did not. The boundaries were sharp and there was very little fracturing.

Some of the clinker samples K3 2030 to K3 2230 were characterised by large areas of small anhedral poorly formed alite. ( These clinker samples suffered the same deterioration after a few months as those from kiln number 1 ).

The belite crystals were rounded and had a variable size range from 5  $\mu\text{m}$  to 60  $\mu\text{m}$ . The dominant size was 25  $\mu\text{m}$ . These belites generally occurred as very large clusters due to the coarse silica feed. There was some slight fracturing along the edges of the grains. The boundary between the belite crystals and the matrix was frequently irregular, possibly due to corrosion of the belite phase by the matrix. After etching with Nital the belite grains were mostly type 3 ( $\beta$ ) with some type 2 ( $\alpha'$  to  $\beta$  transformation).

The matrix was principally ferrite. The matrix of the larger nodule clinker samples was usually highly reflective with only a few traces of dendritic aluminate phase at the edges of the nodules. In the smaller nodule clinker, the dendritic aluminate was much more prevalent, especially in the outer zone of the nodules. (Plate 8c.) This was because the entire nodule could be quenched very rapidly. This dendritic phase closely resembled the phase which Insley and Frechette ( 1952 ) referred to as a dark interstitial glass.

The presence of the high sulphate and alkalis levels in the kiln led to the formation of alkali sulphate phases. These were small irregular shaped grains with low reflectivity .

Descriptive petrology of Sulphate Resisting Cement with pulverised fuel ash addition , from Works B.

In June 1980 a short trial was carried out to reduce the Lime Saturation factor ( L S F ) on kiln 3 at Works B by adding Pulverised fuel ash ( P F A ). The P F A was fed into number 3 kiln via the dust return system. The kiln dust return had an L S F varying from 130 to 180 . This high L S F caused a high frelime content in the clinker from the kiln. The P F A was lime deficient and the addition of the ash to the dust return would tend to counteract the high L S F of the recycled dust . The P F A was introduced into the return dust feed at half a tonne per hour. Samples of clinker output were taken at hourly intervals .

Clinker morphology, PF 0730 sample.

This was the first clinker sample taken with the PFA addition . The nodules varied from about 30 mm. to dust , the dominant size was about 10 mm. The nodules were rounded with a rough surface.

Clinker petrology.

The subhedral alite grains were usually long and thin , 60  $\mu\text{m}$  by 15  $\mu\text{m}$ .

The larger alites contained many belite inclusions in the inner zone . Some of the nodules had a few patches of very small euhedral alites , 10  $\mu\text{m}$  to 15  $\mu\text{m}$  . The belite grains were rounded and occurred either as small groups of 5 to 10 grains , or as very large clusters , the relics of siliceous fragments (Plate 8e.) . The dominant grain size was between 20 and 30  $\mu\text{m}$  . The belite was principally type 3 with some type 2 grains present .

The ferrite was highly reflective with only traces of the fine aluminate phase in the outer zone of the nodules .

Clinker morphology, PF 1130 sample.

As the trial proceeded the PFA addition significantly reduced the clinker LSF from 101 to 95 . The clinker sample at 1130 was extremely hard burnt and consisted of very large rounded nodules and some dust.

Clinker petrology.

Many of the alite grains were very large , 150  $\mu\text{m}$  . Generally however the size was between 50 to 60  $\mu\text{m}$  . The distilled water etch showed a zonation in many of the alite grains . The inner zone was etched to a darker colour . The author noticed that the amount of etching was partially dependant on the calcium content of the alite . the low calcium content alites had a paler etching colour . Since the PFA was lime deficient, the clinker LSF was reduced and this favoured the formation of belite . Thus the later forming alite had less CaO available.

The individual belite crystals were between 25 to 35  $\mu\text{m}$ . and occurred in very large clusters up to 1 mm. across , or as long streamers upto 0.5 mm. long (Plate 8f.) . The strings of belite were probably caused by the molten PFA penetrating the clinker along cracks in the nodules . The molten PFA reacted with the alite phase and formed belite . After etching with Nital the belite grains were identified as type 1 ( $\alpha$  to  $\alpha'$ ) belite , the high temperature polymorph of belite. Most of the belites were type 2 belite, with some type 3 . (Plate 8h.)

There was extensive matrix crystallisation and the aluminate phase appeared very distinctively against the ferrite, after etching with distilled water. ( Plate 9a. ). The crystallisation of the aluminate phase was due to the extreme hard burning of the clinker . This increased the duration of time in which the matrix phases could equilibrate and crystallize .

Clinker morphology PF 1530 to 1830 sample.

The clinker samples collected were not as hard burnt as the 1130 sample. The nodules were variable, the size ranged from 100 mm. to dust.

The predominant size was 20 to 30 mm. The nodules were rounded with a very rough surface. The porosity of the nodule was about 10 % which was lower than previous samples. The clinker nodules broke easily and the dusting increased after a short period of dry storage, probably due to the  $\beta$  to  $\gamma$  inversion of the belite.

Clinker petrology.

The alite crystals were smaller, 20 to 60  $\mu\text{m}$ ., than the previous samples. Some nodules had areas of small, 10 to 15  $\mu\text{m}$ ., long euhedral alite crystals with very few longitudinal cracks.

The belite crystals 15 to 40  $\mu\text{m}$ ., generally occurred as very large clusters up to 0.5 mm. across and in thin strings. The belite was mostly type 3 with some type 2. There were frequent belite inclusions in the larger alite grains. Occasionally in some nodules, the action of the molten P F A on alite crystals partially changed the alite grains to belite.

The matrix in the inner zone of the nodule was highly reflective ferrite with no aluminate phase. In the outer zone of the nodule a few traces of the irregular dendritic aluminate phase were visible. There were several small clusters of freelite, which etched black with distilled water.

Clinker morphology PF 2030 to 2130 sample.

The final sample was collected after PFA addition had ceased. The clinker was under burnt and was a pale grey colour. The nodules were very friable. The clinker nodules were small from about 30mm to dust and the surface was extremely rough.

Clinker petrology.

The alite crystals were variable in size from 5  $\mu\text{m}$ . to 50  $\mu\text{m}$ . and most of the grains were either 5 or 50  $\mu\text{m}$  . The small crystals were euhedral and tended to occur in clusters (Plate 9b.) . The larger alites had a few fractures and a few small belite inclusions .

The belite crystals frequently occurred as large clusters up to 0.5 mm. across. The individual grain sizes varied from 4 to 30  $\mu\text{m}$ . They were usually rounded , but some had a more angular outline . The belite was dominantly type 3 , with a small amount of type 2.

The matrix was high reflectivity ferrite in the centre of nodules with only a trace of the irregular shaped aluminate phase in the outer zone . The porosity was high 15% to 20%. The nodules deteriorated very quickly and disintergrated into dust .

The effect of PFA addition on the Sulphate Resisting Cement clinker.

The duration of the trial was limited and did not allow the kiln conditions to stabilize . The PFA did reduce the high LSF in kiln 3, but it caused a significant increase in belite content . In the hard burnt clinker, the matrix crystallisation led to the formation of aluminate which would be unacceptable in Sulphate Resisting Cement.

The addition of PFA was similar to using a high ash coal . However the benefits were that the unburnt coal in the PFA reduced the quantity of fuel that was normally required and the clinker was easier to burn . The PFA addition increased the tonnage of clinker produced by about 80 tonnes per week, ( providing the PFA was added at 0.5 tonnes per hour , excluding water content , and assuming a 4 % loss on ignition for the PFA).

The compressive strength of the cement produced during the actual PFA addition was very similar to the normal production SRC . The exceptions were that the initial and final sets were later and the slump was greater .

The crystallisation of the aluminate phases could have been lessened by rapid quenching and burning at a lower temperature .

Recommendations for the utilisation of PFA to control clinker chemistry.

To reduce the high belite content of the clinker and the large belite crystals, the quantity of PFA addition should be restricted to 0.25 tonnes/hour . This would produce a cement of consistent quality , with the requisite lower LSF .

Descriptive petrology of the Low Heat cement clinker production trial at Works B.

In August 1980 a test run was made ; to produce low heat cement . This used the Sulphate Resisting Cement kiln feed with P F A and iron oxide additions. The test was run from 0930 to 1400 , the P F A was added at 0.30 tonne per hour and the iron oxide at 0.36 tonne per hour , ( the moisture loss on the iron oxide was 16.7 % , thus the actual rate of iron oxide addition was 0.3 tonne per hour ) .

Clinker morphology. LH 0900 sample.

The sample was collected before the PFA and iron oxide addition . The nodules were extremely variable in size from very coarse 80 mm to the smaller sizes from 20 mm to 1 mm . The nodules were rounded with a slightly uneven surface texture. The nodules were frequently very porous about 15% void volume.

Clinker petrology

The alite crystals were very variable with large subhedral crystals 100  $\mu\text{m}$  and very small euhedral crystals 5  $\mu\text{m}$  . The dominant size was small about 30  $\mu\text{m}$  . There was only a few fractures in the large alites.

The rounded belite crystals were between 5  $\mu\text{m}$  and 30  $\mu\text{m}$  , they often occurred in clusters about 100 to 200  $\mu\text{m}$  across , due to the presence of large siliceous particles in the kiln feed. The belite crystals were mostly type 3.

The matrix was extremely variable in some nodules . The ferrite was relatively bright with only traces of any aluminate phases except in the very outer zone of the nodules (Plate 9d.) . There were often patches of free lime.

#### Clinker morphology LH 1200 sample.

The clinker sample at taken at 1200 hours was collected during the addition of the trial kiln feed . The clinker was hard burnt and the surface of the nodule was glassy . The nodules were about 20 mm with some fine dust . The core of the nodule was a brown-orange colour rather than the usual dark green-grey . This was indicative of reducing conditions having prevailed in the burning zone of the kiln .

#### Clinker petrology.

The alite crystals had a very wide size range from small euhedral crystals of 10  $\mu\text{m}$  to the anhedral crystals of 100  $\mu\text{m}$  . The dominant size was between 20 to 25  $\mu\text{m}$  . The boundaries of the crystals were sharp with no interaction visible between the alite and the matrix phases.

The belite grains ranged in size from 5 to 35  $\mu\text{m}$  . These were either in loosely packed flocks of rounded grains or tightly packed clusters of angular crystals. (Plate 9e.) Generally the nodules were very heterogeneous. Some of the belite grains had an intergrowth texture with the matrix phases . The belite crystals were dominantly type 3 .

The matrix in the brown-orange areas of the nodules was a bright ferrite . However the matrix in dark green-grey areas was ferrite with abundant aluminate development .(Plate 9c ) . The porosity was about 13 % and no significant frelime was visible .

PLATE 9

Plate 9a. Works B SRC clinker with PFA addition, H<sub>2</sub>O etch .

Many of the pale grey belite inclusions in the alite crystals show evidence of partial dissolution and replacement by alite. ( top right ) The belite grain in the centre is a later generation than the inclusions . This grain is deformed around a euhedral alite . There is extensive development of aluminate phase within the matrix . This was due to hard burning of the clinker.

Plate 9b. Works B SRC clinker with PFA ,unetched.

The alite crystals in the centre are smaller than usual and there is extensive grain to grain contact. In this clinker the small crystals have remained discrete and have not coalesced. There are normal sized alites on the left.

Plate 9c. Works B LHC Trial clinker, H<sub>2</sub>O etch .

The ferrite phase is in the form of distinct laths . The pale grey aluminate phase fills the interstitial areas. The bright patches in the alite are caused by internal reflections.

Plate 9d. Works B LHC Trial clinker, unetched.

The crystallization of the aluminate phase in this clinker was very localized. ( left ) It usually only occurred in the outer areas of the nodules . There is little or no aluminate detectable in the matrix on the right.

Plate 9e. Works B LHC Trial clinker, H<sub>2</sub>O etch.

The overall grain size of all clinker minerals is small. The belite clusters are closely packed with rounded or subangular grains. The adjacent alite crystals have extensive grain to grain contact. The matrix content in this clinker is low .

Plate 9f. Works B LHC Trial clinker, H<sub>2</sub>O etch.

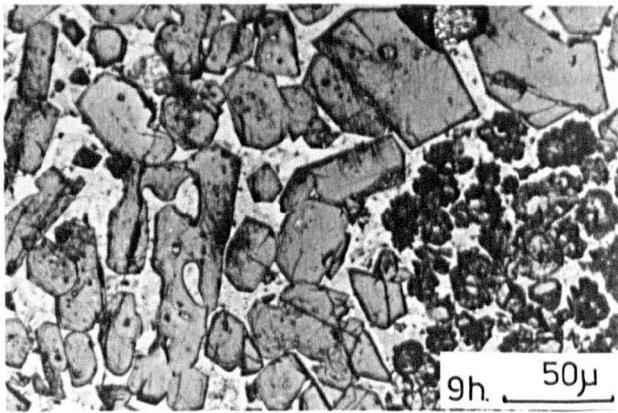
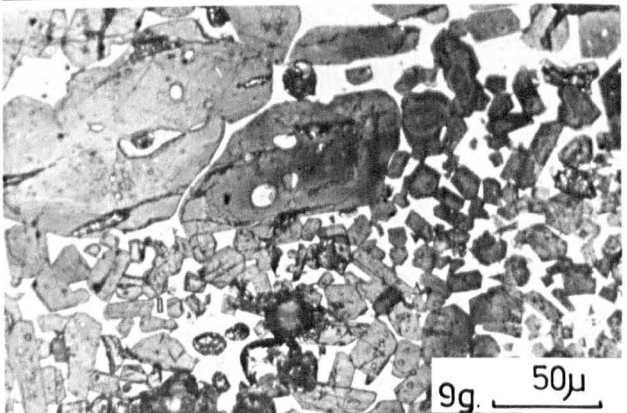
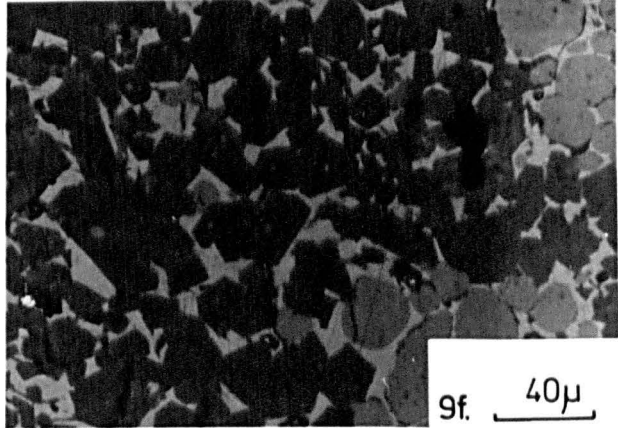
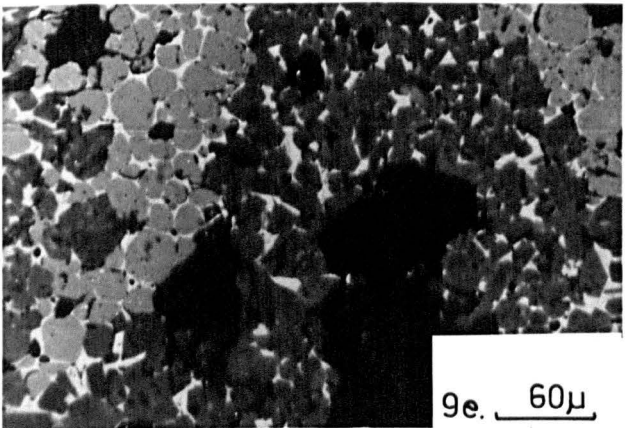
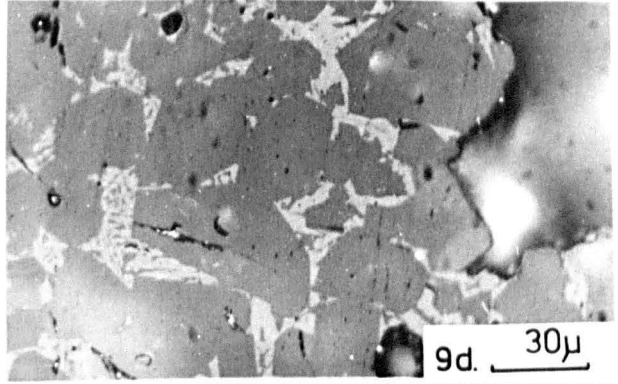
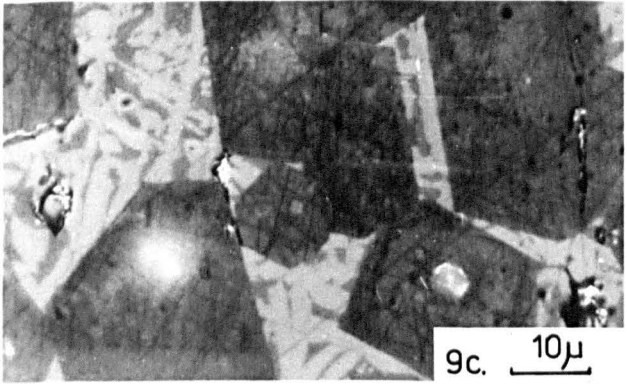
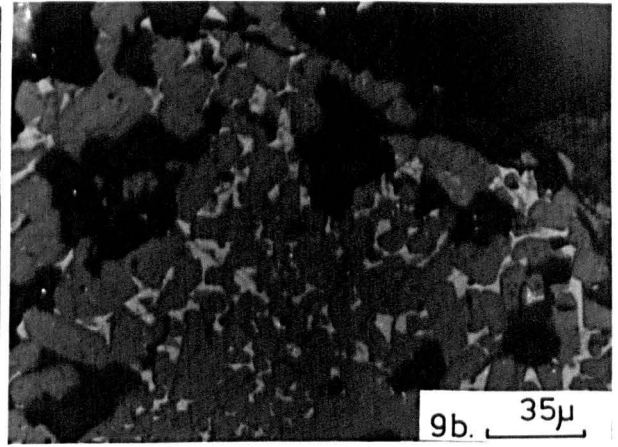
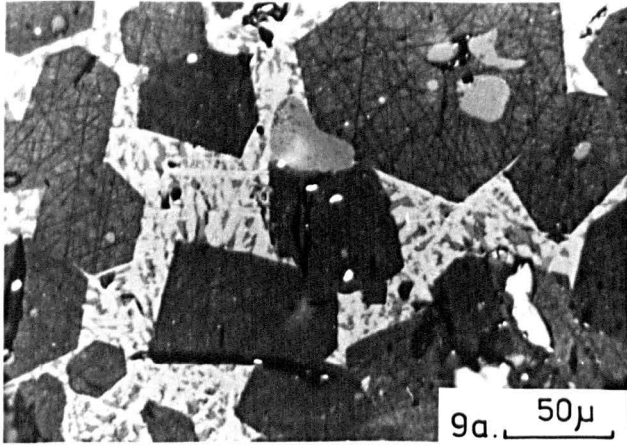
This clinker has been 'hard burned' and because of this has a higher matrix content. The alite crystals are substantially larger and euhedral. One of the large alites crystals ( middle left ) has an embayment of matrix. This was caused by several smaller alites coalescing to form a large crystal.

Plate 9g. Works A OPC clinker, Nital etch.

There is a very wide size range between the large ameoba-like alite grains and the small euhedral alites. The large grains have been formed by the coalescing of many of the small grains. These large alite grains contain several inclusions of ferrite or belite. Only the small alite crystals show any trace of zoning.

Plate 9h. Works A OPC clinker, Nital etch.

The large ameoba-like alites ( left ) with inclusions and embayments of matrix are accompanied by the more common subhedral alite crystals. (centre ) The cluster of belite grains ( right ) show extensive intergrowth texture and are mostly type 3 . Many of the irregular shaped crystals appear to be made up of micro grains. This preponderance of small grains of belite and alite is indicative of a high nucleation rate in the clinker. This produces a reactive clinker which usually has good compressive strengths.



Clinker morphology LH 1330 sample.

The clinker sample was hard burnt . These nodules were rounded and rough textured . The size varied from 100 mm to 1 mm and the dominant size was about 40 mm . Most of the nodules were grey-green and the outer surface was glassy . The inner zone was coarser and frequently orange-brown in colour because of reducing conditions in the burning zone . The porosity was low , about 8 % .

Clinker petrology.

The alite crystals varied from 10  $\mu\text{m}$  to 90  $\mu\text{m}$  . The dominant size was 30 to 40  $\mu\text{m}$  . The larger crystals were always cracked and contained small belite blebs .

The belite crystals occurred in large tightly packed clusters or loosely arranged flocks . The size of the crystals ranged from 5 to 30  $\mu\text{m}$ ., the dominant size was about 25  $\mu\text{m}$  . After etching with Nital solution most of the belites had a mottled appearance , typical of type 3 belite . However some had the distinctive lamellae of type 2 .

The matrix had similar characteristics to the 1200 sample . The brown-orange clinker had bright ferrite whilst the grey-green clinker had ferrite with a very fine 'feathery' formed aluminate phase intercrystallised . There were only a few traces of freelite visible .

Clinker morphology LH 1600 sample.

This was the last clinker sample was collected from the trial . Overall it was hard burnt . The nodule size varied from 150 mm to 1 mm, the dominant size was about 40 mm . Most of the nodules were grey-green with only very small areas of brown-orange material . The porosity was about 10 % .

Clinker petrology.

The alite crystals ranged from 10  $\mu\text{m}$  to 100  $\mu\text{m}$  . The dominant size was about 50  $\mu\text{m}$  and the crystals were euhedral . (Plate 9f. ) There was more alite in this sample than in the previous samples .

The belite grains commonly occurred in small clusters frequently centered around voids . The size of these individual belite crystals varied from 10 to 60  $\mu\text{m}$  , the dominant size was about 40  $\mu\text{m}$  . The belite grains were mostly type 3 . The size of the clusters was between 50 to 120  $\mu\text{m}$  . , smaller than in the previous samples .

The matrix was dominantly ferrite with only traces of the aluminate phases .

The PFA and oxide addition had ceased two hours before the last sample was collected . Thus the effects of the addition had diminished and the clinker was very similar to the sulphate resisting clinker . The alite content had increased and the belite content had decreased. The very large belite clusters were very rare . Generally the belite occurred in small clusters of 20 to 30 grains . The amount of reduction which had occurred to this clinker was low when compared with the preceding samples . There was less fine aluminate phase than in the normal SRC clinker .

Descriptive petrology of the Ordinary Portland Cement clinker from Works A.

Source of raw materials.

The raw materials of limestone and shale , for the Works A are quarried from Carboniferous sedimentary rocks . The occurrence of dolomitic zones within the limestone caused variations in the MgO content of the kiln feed. To overcome this problem the limestone was analysed regularly to prevent the incorporation of any high MgO content limestone into the semi dry process kiln.

Clinker morphology Works A, OPC.

The size of the clinker nodules supplied varied from about 50 mm to 20mm.

The dominant size was about 35 mm. The nodules were dark green-grey with a brown-orange core . The nodules were rounded and had a very rough surface .

Clinker petrology.

The smaller , 10 to 30  $\mu\text{m}$ . alite grains were subhedral . There were occasional clusters of very small , 5 to 10  $\mu\text{m}$ . euhedral alites which often appeared to be coalescing to form larger alite crystals . The large 100  $\mu\text{m}$ . alite crystals were frequently irregular in shape , with inclusions of matrix phases and belite. (Plate 9g.). These large alite crystals generally occurred in the brown-orange clinker . The small subhedral and euhedral crystals were typical of the normal grey-green clinker . The alite in the brown zone produced a paler etch colour with distilled water , than the alite in the dark green clinker zone . The author found that the overall difference in etch colour was frequently indicative of the

reactivity of the mineral phase . The darker the etch colour of a distilled water etch , over a fixed duration of time , the greater the reactivity of the mineral with water . This indicated that the alite in the dark green clinker produced in oxidising conditions , was more reactive than the alite in the brown-orange clinker produced in reducing conditions . Many of the large alite crystals were fractured .

In the green-black clinker , the belite crystals were between 5 and 40  $\mu\text{m}$ .

These occurred as individual grains or small flocks of ten to twenty grains . The flocks of belite were caused by siliceous fragments possibly from sandstone horizons which occurred in the limestone. There were two types of belite distinguishable after etching with Nital . The type 2 belite grains had sharp outlines and two or three sets of lamellae. The type 3 belite grains frequently had an irregular boundary with an elongated intergrowth texture with the matrix. (Plate 9h. ) These belite grains had a mottled appearance with no visible lamellae. In the brown-orange clinker there was only a few rounded primary belite crystals type 3 . However there was extensive secondary belite phase development around most alite grains in the form of small blebs . At high magnification the alite crystal boundaries appeared to be corroded by the secondary belite development.

The matrix was pale grey rather than the highly reflective ferrite found in Sulphate Resisting cement clinker . This was due to the lower iron content in the ferrite and the presence of tricalcium aluminate . The cubic tricalcium aluminate occurred as very small 5 to 15  $\mu\text{m}$ . angular crystals . After etching with distilled water the tricalcium aluminate developed a green-yellow etch layer.

#### Descriptive petrology of the Ordinary Portland Cement clinker from Works C.

##### Source of raw materials.

Works C produces cement by the dry process . The raw materials were

Carboniferous limestone and shale. The limestone quarry is transected by many mineral veins containing fluorite, calcite, galena and sphalerite. The presence of fluorspar ( $\text{CaF}_2$ ) or sphalerite ( $\text{ZnS}$ ) in small quantities generally acts as a mineraliser and facilitates clinker production at a lower temperature. Welch and Gutt (1960) have shown that a fluorine level above 0.74%, reduces the compressive strength. Thus the fluorine not only acts as a mineraliser but it induces changes in the alite which reduces its hydraulicity. Therefore the fluorine level in the limestone had to be monitored and if a high fluorine level was detected, the limestone was rejected. Variation in the silica content of the shale was balanced by working two shales alternatively and blending the material to produce a suitable shale feed.

#### Clinker morphology Works C OPC.

The cement clinker was rounded and had a rough surface texture. The nodules were almost totally dark grey-green clinker with only slight traces of brown-orange clinker. The overall porosity of the clinker was about 10%.

#### Clinker petrology.

The alite crystals were generally small, 5 to 30  $\mu\text{m}$  and were euhedral to subhedral. The subhedral grains often had many inclusions of belite and matrix phases. In the brown orange clinker many of the alite crystals had been corroded by belite, (Plate 10b.) which had formed around the pre-existing alite. Generally the alite grains had only slight fracturing because they were small.

The belite crystals were between 5 to 30  $\mu\text{m}$ , rounded and occurred in small flocks. The individual grain size was small. In the grey-green clinker the belites were dominantly type 2. Some of the large belites had an untwinned zone in the centre of the crystal, possibly type 1 belite, the high temperature a belite polymorph. (Plate 10f.) In the brown-orange clinker the belite crystals often had an intergrowth texture

PLATE 10

Plate 10a. Works A OPC reduced clinker nodule, H<sub>2</sub>O etch.

The alite crystals are subhedral and often have irregular boundaries. The alite grains are only slightly etched. This indicates that these alite crystals have a low reactivity with water. The belite crystals (centre) are extremely irregular. The tricalcium aluminate phase has crystallized as large, very irregular crystals, typical of the cubic form. These crystals have etched to a dark grey.

Plate 10b. Works C OPC clinker, H<sub>2</sub>O etch.

The alite crystals have etched normally. Many of the crystals contain small inclusions of belite. The primary belites are unetched (centre). In several areas the alite crystals have a corroded contact with belite. This is caused by the removal of CaO from the alite.

Plate 10c. Works C OPC clinker H<sub>2</sub>O etch.

The alite crystals are euhedral and have sharp boundaries with the matrix phase. The contacts with the belite grains are extremely irregular. The tricalcium aluminate crystals are in the cubic form and are well distributed throughout the interstitial areas.

Plate 10d. Works D OPC clinker H<sub>2</sub>O etch. The pale grey belite crystals (left and centre) show an intergrowth texture with the ferrite and especially with the alite. Several of the alite crystals are surrounded by small secondary belite grains. The tricalcium aluminate phase has etched to a dark grey and is very irregular.

Plate 10e. Works D OPC clinker from reduced zone, Nital etch.

The large alite crystals are very irregular with inclusions of belite and ferrite. The fine dark speckling in the alite is very small inclusions of free lime. The belite grains are very irregular. Many of the apparent grains are clusters of very small grains of belite. The very pale faint grey phase in the interstitial areas is tricalcium aluminate in the cubic form.

Plate 10f. Works C OPC clinker, Nital etch.

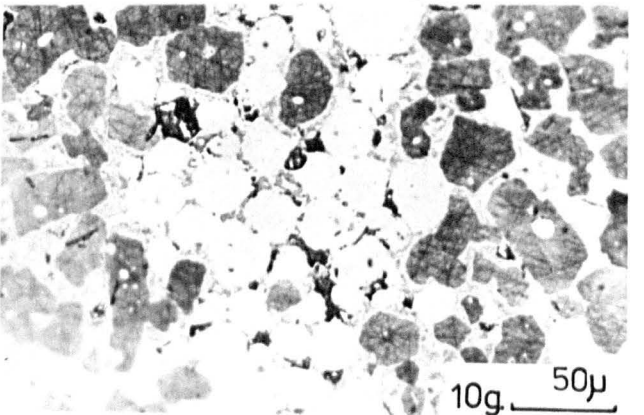
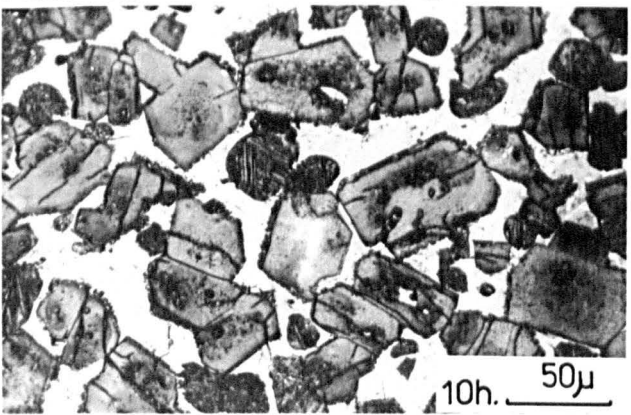
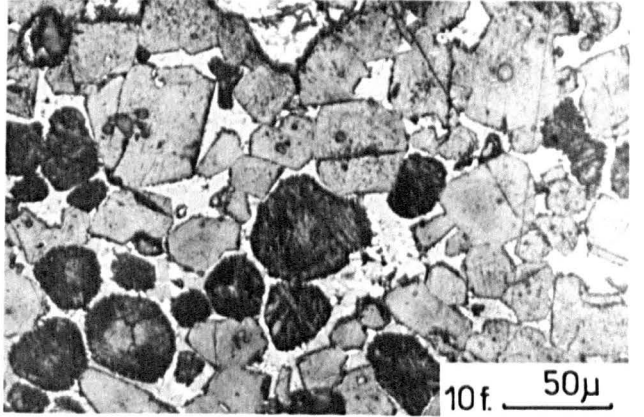
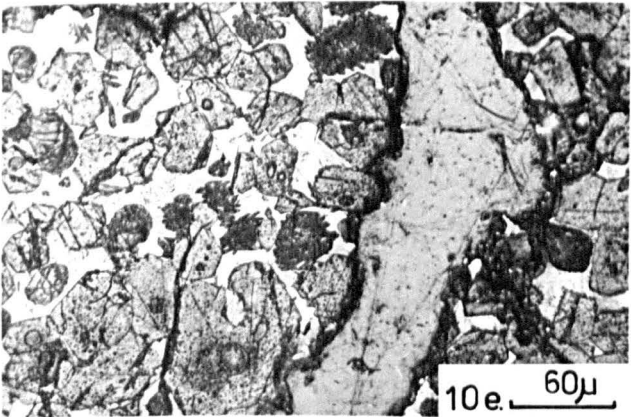
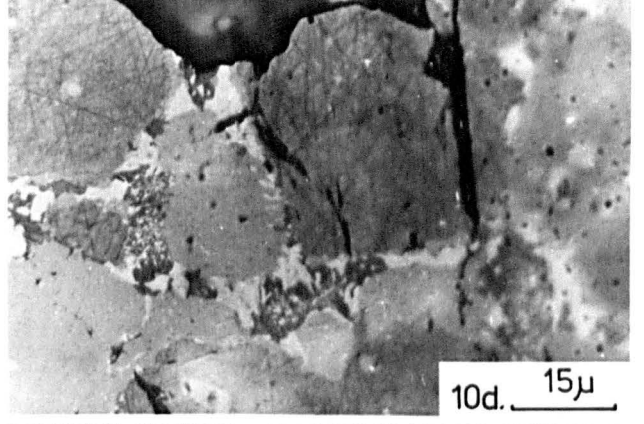
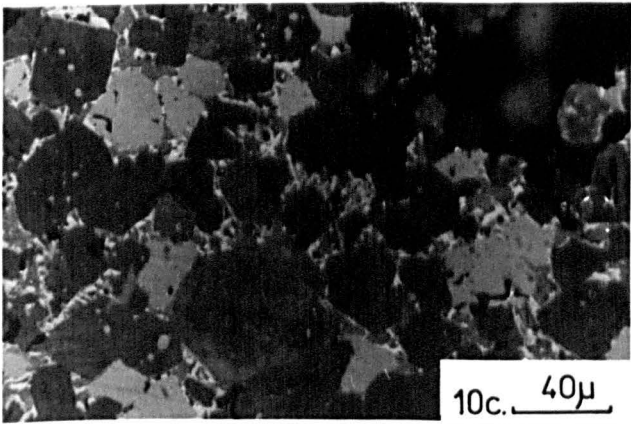
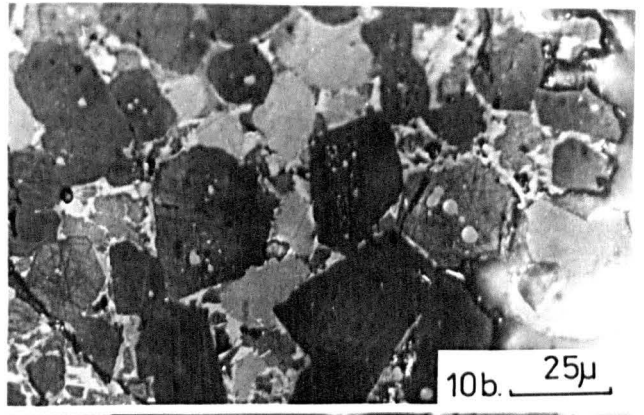
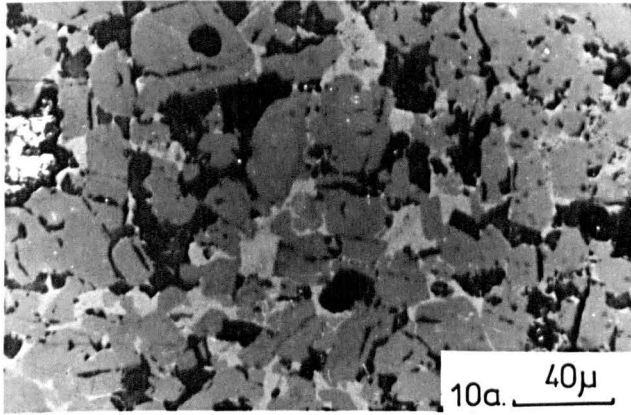
The belite crystals (centre) have distinct lamellae, typical of type 2 belite. Some of the belites have no lamellae in the central zones of the grain. These are type 1 belite, the high temperature A form, with a border of type 2. Many of the euhedral alite crystals are surrounded by very small secondary belite grains.

Plate 10h. Works D OPC clinker from the oxidising zone, Nital etch.

This clinker contrasts with the cement in Plate 10e, which was from a reduced clinker. The alite crystals are euhedral and have distinct zones of inclusions. There are small secondary belite grains surrounding most of the alite crystals, which do not show corrosion. The belite grains have distinct lamellae and are type 2 belite. Only a few of the belite grains show any intergrowth textures. This contrasts sharply with the clinker from the reduced nodule. There is a high matrix content and the calcium silicate grains are 'floating' in the ferrite.

Plate 10g. Works E OPC clinker, H<sub>2</sub>O etch.

The matrix is comprised mostly of small irregular aluminate crystals in the cubic form. The ferrite content is low. The alite crystals are subhedral and closely packed. Many of the crystals have contacts with extensive corrosion. Some of the alite has been replaced by belite. The principal belite grains are in a tight cluster. This is indicative of large siliceous particles in the kiln feed.



with the interstitial phases. The belites were dominantly type 3. Frequently there were small secondary belite blebs forming around the alite grains.

The matrix phases were more easily identified after etching with distilled water. The ferrite was unaltered, but the tricalcium aluminate crystals etched a yellow-green colour. The crystals were small and angular. (Plate 10c.) This indicated that the tricalcium aluminate was in the cubic form.

#### Descriptive petrology of Ordinary Portland Cement clinker from Works D.

##### Source of the raw materials.

Cement Works D produced cement by the wet process. The raw materials used were chalk and clay. The wet process was used because of the ease of transporting the clay by pipeline and the relative ease of removing the flint from the chalk by screens after wet milling. If the flints were not removed the fragments caused high silica concentrations in the clinker.

##### Clinker morphology, Works D OPC.

The cement clinker was rounded and had a coarse textured surface. About 15 % of each nodule was brown-orange clinker in the central area. The remainder of each nodule was grey-green. The overall porosity of the clinker was about 12 %.

##### Clinker petrology.

The alite crystals varied in size from 5  $\mu\text{m}$  to 50  $\mu\text{m}$ . The crystals were euhedral to subhedral. The larger alites contained many small inclusions of belite and matrix phases. In the brown-orange clinker many of the alite crystals were larger and had been corroded at the ends. (Plate 10d.).

The rounded belite crystals , 10 to 40  $\mu\text{m}$ . , were well distributed with only a few large clusters . In the brown-orange clinker , the belite grains were dominantly type 3 and had intergrown with the matrix phases. (Plate 10e.) In the grey-green clinker the belite grains were principally type 2 with some type 3 grains. (Plate 10h.) .

The matrix phases in the grey-green clinker were very abundant and the calcium silicates were 'floating' in the matrix. The tricalcium aluminate crystals were lath shaped , characteristic of the orthorhombic form . The ferrite was unaffected by the etch solution . In the brown-orange clinker there was less matrix phase and the tricalcium aluminate was more angular and irregular, typical of the cubic form.

#### Descriptive petrology of the Ordinary Portland Cement clinker from Works E.

##### Source of the raw materials.

Cement Works E used limestone and phyllite to produce cement by the dry process. There is a high potassium level in the phyllite and the limestone feed has a high magnesia content. Therefore the feed has to be monitored to prevent excessively high levels of  $\text{MgO}$  and  $\text{K}_2\text{O}$  from being included in the kiln feed because these elements cause substantial loss in the compressive strength and durability of cement.

##### Clinker morphology, Works E.

The cement clinker was generally rounded and had an uneven surface texture . There were several fragments of refractory brick included with the clinker . The nodules were usually about 60 % grey-black clinker , the remainder was orange or brown-orange .

##### Clinker petrology.

The alite crystals were generally small , 5 to 40  $\mu\text{m}$  , euhedral to subhedral . The alite grains in the brown-orange clinker had belite

inclusions and often a well developed fringe of secondary belite grains around the edges . These alite crystals usually had corroded boundaries. (Plate 10g.)

The belite crystals occurred as rounded grains ranging from 5  $\mu\text{m}$  to 30 $\mu\text{m}$ .

The belite was frequently present as small flocks . In the grey-green clinker large closely packed clusters were common . After etching with Nital solution, the primary belites were identified as type 3. The large belite inclusions in the alite crystals had widely spaced lamellae and were typical of type 2 belite.

The matrix phases were very indistinct until the sample had been etched with distilled water . In the brown-orange and pale orange clinker, the tricalcium aluminate etched to a green-yellow colour and appeared lath shaped ( orthorhombic ) . There was also another calcium aluminate phase which was very angular and etched to a dark blue . There was only a few small areas of ferrite detectable in the matrix . In the dark green clinker the angular crystals of tricalcium aluminate etched to a yellow-green. The ferrite was unaffected by either etch solution.

#### Descriptive petrology of White Portland Cement clinker from Works F .

##### Source of the raw materials.

Works F produced a white cement for decorative purposes . The raw materials were chalk and china clay . The cement was produced by a wet process with a reducing atmosphere in an oilfired kiln .

##### Clinker morphology, Works F.

The cement clinker was white and rounded with a smooth fine grained surface texture . The porosity of the clinker nodule was very high at 20%.

##### Clinker petrology.

The phases were extremely difficult to identify until the clinker had

been etched with distilled water . The alite crystals were small, 5  $\mu\text{m}$  to 30  $\mu\text{m}$  and generally subhedral . The alite grains etched very slowly , after about 30 minutes only a pale etch colour was developed . This indicated that the reactivity to water of this alite polymorph in the white Portland Cement was very low . This was because the alite had formed in a reducing atmosphere.

The belite crystals were small, well rounded and had distinct boundaries . The size varied from 5 $\mu\text{m}$  to 25  $\mu\text{m}$  . The belite grains were frequently in very large clusters up to 1mm. After etching with Nital, most of the belites appeared to be type 1 or type 2 .

There was a low matrix content and extensive grain to grain contact , many grains had an interlocking texture. The matrix etched with distilled water to a dark green . The major interstitial phase was tricalcium aluminate in the cubic modification.

#### Descriptive petrology of the Ordinary Portland Cement clinker from Works G.

##### Source of the raw materials.

Cement Works G produced cement by the semi-dry process . The raw materials were limestone and shale from Carboniferous rocks. The quarrying operations had to be carefully controlled to ensure that a balanced raw feed was sent to the cement works . The MgO content of the raw feed had to be monitored to prevent the occurrence of excessive amounts of periclase in the clinker .

##### Clinker morphology, Works G.

The clinker nodules varied from 1mm to 150 mm and were generally rounded with a rough surface . The central zone of the nodules was usually brown-orange. The outer zone had been reoxidized and was green grey in colour. The nodules were very hard and had been 'hard burnt'.

Clinker petrology.

The alite crystals varied from 10 to 70  $\mu\text{m}$  , the larger grains were subhedral . After etching with distilled water the alites in the brown-orange areas were shades of blue. The alite grains in the grey green clinker were blue to brown . All of the larger alite crystals contained many small inclusions of belite and ferrite .

The belite crystals varied in size from 5 to 30  $\mu\text{m}$ . They were well dispersed and clusters were rare . The belites frequently were deformed around existing alite grains and seemed to have " squeezed " into the available space. (Plate 11a.) In the brown-orange clinker many of the alite crystals had a fringe of secondary belite grains around them .

The lath shaped tricalcium aluminate in the interstitial areas etched with distilled water to a green-yellow. (Plate 11b.) The ferrite remained unetched and was light grey . There were several very small crystals of periclase , identifiable by their reflectivity and hardness indicated by the surface relief caused by polishing.

In the dark grey-green areas there was more primary belites and less secondary belite fringes around the alite crystals . The definition between the alite , belite and ferrite grains was better than the brown-orange areas . After etching with distilled water the tricalcium aluminate crystals appeared as blue-brown laths as opposed to the green-yellow colour of the reduced clinker . When the sample was etched with Nital , about 80 % of the primary belites had distinct lamellae in several orientations which was characteristic of type 2. (Plate 11c.) The other belites had a mottled appearance and were type 3 grains. On examining the sample with crossed polarised light after the Nital etch , many of the alite crystals and some of the belite crystals had a bright zone around them . At high magnification the outer edge of the bright zone appeared to be the original outline of the crystal . The alite or belite crystal had been altered for 1 to 2  $\mu\text{m}$  and replaced by a specular

PLATE 11

Plate 11 a. Works G OPC clinker, H<sub>2</sub>O etch.

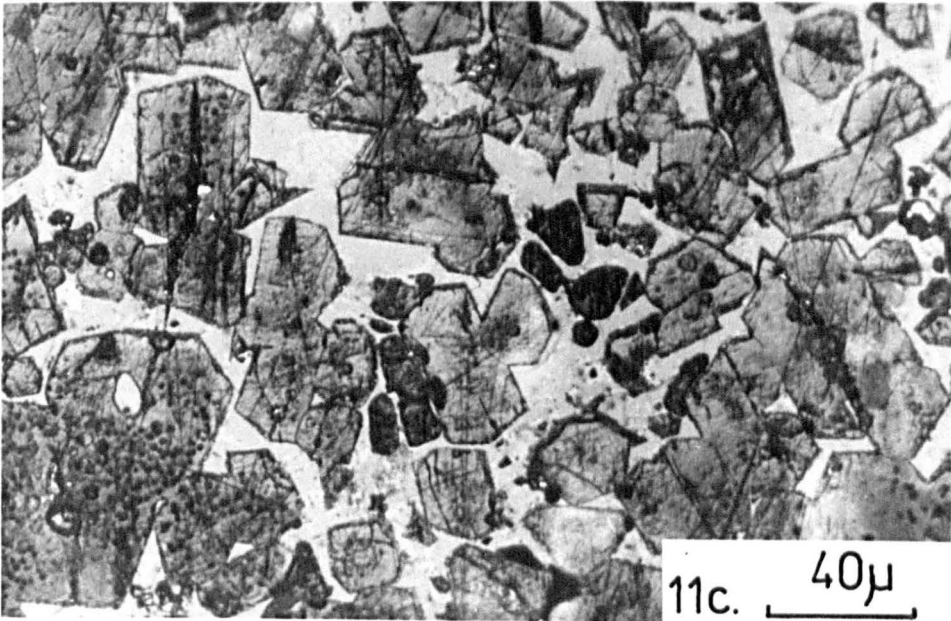
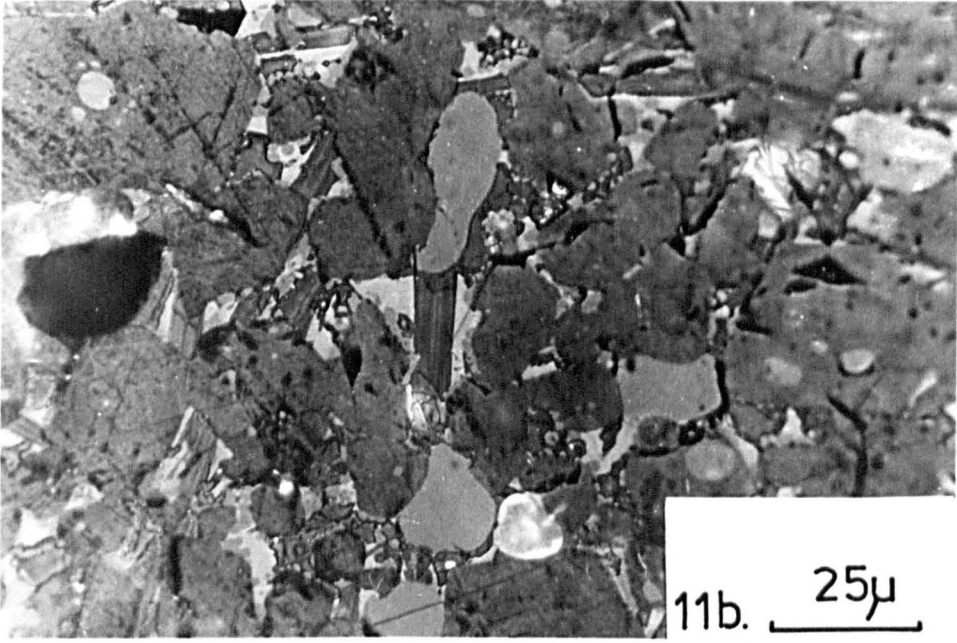
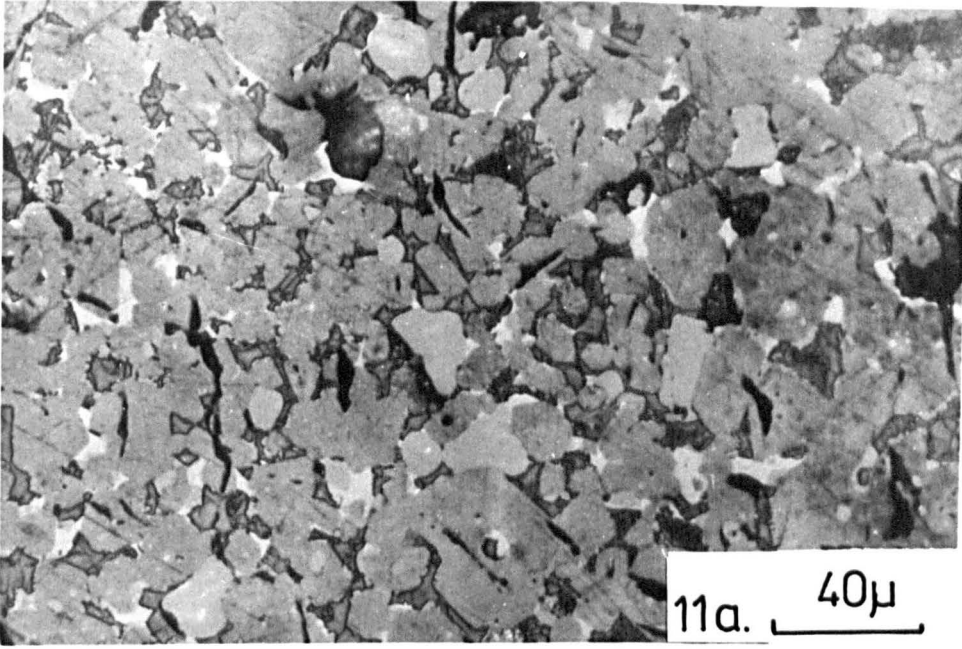
The aluminate has etched dark grey between the grey angular alite and the pale grey rounded irregular belite. Many of the belite grains are distorted around and between the alite crystals.

Plate 11 b. Works G OPC clinker , H<sub>2</sub>O etch.

Many of the alite crystals have irregular boundaries because there has been replacement of the alite by secondary belite . The long laths are aluminate in the orthorhombic form and show longitudinal zoning.

Plate 11 c. Works G OPC clinker, Nital etch.

The belite grains have etched to a very dark grey. They are extremely angular and do not show any intergrowth texture. There are two or three different lamellae orientations and this is typical of Type 2 belite . The alite crystals are euhedral and have inclusions of ferrite and belite in the central areas. Some of the alites have a speckled appearance of dark spots, which are freelite.  
(bottom left ) . Several of the alite crystals have irregular boundaries because of the development of secondary belite.



phase. This was because the etch solution had penetrated along the grain boundaries and reacted with the silicate to form a thin etched layer . The petrological characteristics used in the Trend analysis ( Chapter 10) for all the cement clinkers from the different works are summarised in Table 6.1.

KEY

SRC = Production sulphate resisting cement made from chalk and PFA.

PFB = Trial SRC cement clinker with extra PFA, collected at 1030h.

PFC = Trial SRC cement clinker with extra PFA, collected at 1530h.

PFD = Trial SRC cement clinker with extra PFA, collected at 2030h.

LHA = Trial Low Heat cement clinker collected at 0900h.

LHB = Trial Low Heat cement clinker collected at 1200h.

LHC = Trial Low Heat cement clinker collected at 1300h.

LHD = Trial Low Heat cement clinker collected at 1500h.

OPC = Production Ordinary Portland cement clinker.

WPC = Production White Portland cement clinker.

( Table 6.1) Petrological characteristics of the cement clinker samples.

Sample	Wks.B	Wks.B	Wks.B	Wks.B	Wks.B	Wks.B	Wks.B	Wks.B	Wks.A	Wks.E	Wks.C	Wks.F	Wks.D	Wks.G
Cement	SRC	PFB	PFC	PFD	LHA	LHB	LHC	LHD	OPC	OPC	OPC	WPC	OPC	OPC
Phase composition of the clinker by point counting.														
Alite %	67	58	57	51	67	68	69	67	65	63	61	67	60	67
Belite %	12	21	27	24	11	12	7	10	8	13	16	15	14	9
Ferrite %	11	11	7	12	13	13	16	17	9	8	8	0	10	6
Aluminate % (cubic)	4	3	3	5	3	2	3	2	13	9	10	11	2	0
Aluminate % (ortho)	0	0	0	0	0	0	0	0	0	0	0	0	8	12
Sulphate %	1	4	2	3	1	1	1	2	1	2	2	2	1	1
C12A7 %	3	1	2	2	3	2	3	2	4	3	3	3	4	3
Freelite %	2	1	1	4	1	1	1	1	1	1	1	2	1	1
<b>TOTAL</b>	<b>100</b>	<b>99</b>	<b>99</b>	<b>101</b>	<b>99</b>	<b>99</b>	<b>100</b>	<b>101</b>	<b>101</b>	<b>99</b>	<b>101</b>	<b>100</b>	<b>100</b>	<b>99</b>
Size range of the individual phases. ( in microns )														
Alite upper size	140	150	60	50	100	100	90	100	100	40	30	30	50	70
Alite lower size	20	10	15	5	5	10	10	10	5	5	5	5	5	10
Alite general size	60	60	45	20	30	25	35	50	30	30	20	20	30	40
Belite upper size	60	35	40	30	30	35	30	50	40	30	30	25	40	30
Belite lower size	5	10	5	5	5	5	5	10	5	5	5	5	5	5
Belite general size	30	25	25	20	20	20	25	40	30	20	15	15	25	15
Polymorph of belite in clinker ( in % of total belite )														
Belite Type 1	0	20	0	0	0	0	0	0	0	0	10	30	0	0
Belite Type 2	20	30	20	5	10	10	20	5	40	20	70	60	80	80
Belite Type 3	80	50	80	95	90	90	80	95	60	80	20	10	20	20
Characteristics of the clinker														
Porosity (volume %)	15	10	15	20	10	13	8	10	15	15	10	20	12	10
Reduction (volume %)	15	5	20	5	50	60	50	15	20	40	3	95	5	20

Chapter seven.

THE CALCULATION OF THE PHASE COMPOSITION OF CEMENT CLINKER.

Computational methods.

The Bogue method.

The accurate analysis of the phase composition of cement has been attempted by many methods . One of the oldest methods , but still the most widely used , is the Bogue estimation . This is a computational method of determining the phase composition and was developed by Bogue (1929) . This method relies on the assumption that the phases are in equilibrium and there is no minor element substitution . The Bogue calculation is shown in Appendix ( 7 ) . The main disadvantage with the Bogue calculation is that the composition of the ferrite is assumed to be  $C_4AF$ , which it is not. The alite and belite values obtained by the calculation are extremely sensitive to variations in the CaO/SiO ratio. Thus accurate determination of the freelite content of the cement is essential. The effects of minor element substitution also cause variation in the calculated alite and belite contents . In an attempt to correct these variations , Hansen ( 1968 ) assumed that equilibrium had been established and crystallisation was complete . He proposed that the ferrite composition was  $C_6A_2F$  and that the aluminate was  $C_3(A_{0.9}F_{0.1})$  . The  $Al_2O_3$  total was also corrected for  $TiO_2$  and  $P_2O_5$  by adding them to  $Al_2O_3$  .

When the Hansen calculations were carried out on some cements , the  $C_3A$  value obtained was zero , however XRD analysis showed that  $C_3A$  was present.

Hansen attributed this error to equilibrium not being attained.

#### The simultaneous equation method.

Midgley ( 1970 ) analysed several cement clinkers and then determined the composition of the individual phases by electron microprobe . The major mineral phases in the cement were expressed in the terms of their oxide components . Midgley calculated equations to indicate the oxide percentages in a specific phase from the bulk composition of the cement . From these values Midgley prepared a series of equations for alite , belite , ferrite and aluminate which could be solved simultaneously . Midgley concluded that the simultaneous equation method was only marginally better than the Bogue method and only as accurate as a modified Bogue method which used a ferrite composition calculated from the bulk analysis of the cement.

In a review of the phase composition of cement , Gutt and Nurse (1974) concluded that there was no method available at the time that was statistically superior to the Bogue calculation .

#### The matrix recalculation method.

The matrix recalculation method requires the accurate analysis of the chemical compositions of the cement clinker. The calculation uses a series of simultaneous equations to calculate the potential phase composition of individual cement clinkers. The composition of the mineral phases was determined by electron microprobe analysis. The chemical analysis of the clinker was determined by X-ray Fluorescence. The MgO content of the clinker was analysed by Atomic Absorption Spectroscopy to overcome element interference problems. To compensate for the presence of free lime in the clinker , the free lime level was determined by the titrimetric method.

The process for the matrix calculation method is shown in Appendix 7b.

Evaluation of the accuracy and errors of methods for the determinative analysis of the phase composition of cement.

Chemical determination.

Aldridge and Eardley ( 1973 ) reported that variations within the standard deviation of a chemical analysis on cement could cause substantial errors in the Bogue calculation . They recommended more specific procedures for the determination of alumina and a wider use of standard samples .

Microscopy determination.

An alternative method of quantitatively analysing the phase content of cement is by microscopy . In this technique the clinker samples are impregnated with resin and a polished surface of the sample is prepared . Insley et al. ( 1938 ) and Brown ( 1948 ) proposed several methods of identifying and measuring the different phases . This involved the recognition of the mineralogical properties and the use of various chemicals to etch the phases. Chayes and Fairburn ( 1951 ) introduced the point counting technique which was then used by many microscopists .

There were several problems associated with this technique . The resolution of the microscope sometimes prevented the accurate identification of very small phases especially in the matrix . The results were also subject to a high statistical error if too few determinations were made . So as a consequence to achieve accurate results, this method of phase estimation was slow and laborious . Brown (1948 ) concluded that " the accuracy of the analysis depended on the nature and preparation of the specimens as well as the perception and skill of the operator " .

### X-ray diffraction determination.

The X-ray diffraction method for analysis of cement was adopted in the 1950's . This technique was developed to overcome the problems of computational and microscopical methods for the determination of the phase composition .

The principle problem with the XRD method was caused by variation in the ferrite composition from the assumed  $C_4AF$  . The second problem was that substitution of minor elements into the cement phases. This changed the crystal lattice parameters and altered the XRD patterns. Midgley (1954 ) suggested that the composition of the ferrite phase in Portland cement could be determined by comparing the X-ray diffraction data of ferrites from different cements with ferrites made from synthetic mixes . However due to the resolution of the X-ray instrument available at the time measurements could only be made on magnetically concentrated samples . Later with improved XRD instruments , Midgley ( 1958 ) attempted to find a correlation between the ferrite composition and the  $Al_2O_3:Fe_2O_3$  ratio in the clinker . This was unsuccessful as no good correlation was found. Midgley et. al. ( 1964 ) proposed a method for the determination of the phase composition of cement by XRD . The cement samples were ground in isopropyl-alcohol to a particle size of less than  $5 \mu m$  . To measure the variation in the intensities of the cement minerals , an internal standard of KBr was used . This standard had X-ray diffraction reflections which did not interfere with the cement mineral reflections . The samples were loosely packed in a cavity mount to avoid preferred orientation . Mechanical mixtures of alite , belite , tricalcium aluminate and ferrite were made. From these mixtures, standard diffraction traces were plotted . the calibration graphs obtained used the intergrated areas of the peaks . There were problems with overlapping peaks and variations in the XRD patterns .

Kantro et. al. ( 1964 ) proposed a method for the quantitative

determination of the major phases in the cement. This method measured the of height of the peaks from the cement minerals against an internal standard of silica .

The position of the ferrite peaks varied depending on the composition of the ferrite and they frequently overlapped to some extent with the aluminate peaks . Similar problems occurred with partial overlap of belite and alite peaks . To overcome this problem , calibration equations were produced with compounds of known composition . The constants in the equations were evaluated by the method of least squares . The accuracy of the values obtained for the composition of the cements were erratic .

Combined chemical, X-ray and computational determination.

Yamaguchi and Takagi ( 1968 ) investigated many different cements . The clinker was chemically analysed and part was separated by heavy liquid techniques to give an alite and belite fraction . These were then analysed individually by chemical and X-ray analysis . Then the composition of the alites and belites was calculated . The interstitial fraction was also separated from part of the original sample . The ferrite and aluminate compositions were determined . From these standard formulae the average composition of alite , belite , ferrite and aluminate were obtained in wt.% oxide. Thus-

	SiO <sub>2</sub>	Al <sub>2</sub> O <sub>3</sub>	Fe <sub>2</sub> O <sub>3</sub>	CaO	MgO	Na <sub>2</sub> O	K <sub>2</sub> O
Alite	24.83	1.24	0.49	72.23	0.98	0.09	0.14
Belite	32.50	2.36	1.03	62.83	0.52	0.20	0.30
Ferrite	3.61	24.51	22.08	44.50	4.36	0.37	0.57
Aluminate	3.88	27.43	7.81	53.48	1.97	2.27	1.15

These values , ignoring the alkalis , were then used in a series of equations which were solved by the least squares method .

Yamaguchi and Takagi then attempted to determine the phase composition of the cement by other methods , notably point counting , Bogue calculation

and X-ray diffraction .

The estimates for alite and belite by the various methods were similar. The greatest variation was in the ferrite and aluminate values . The simultaneous equation method gave low values for the aluminate content.

High resolution X-ray diffraction to determine the composition of ferrite.

Midgley and Moore ( 1970 ) used high resolution X-ray diffraction equipment to find a correlation between the  $Al_2O_3:Fe_2O_3$  ratio in the cement and the ferrite composition . They established that assuming there was a solid solution between  $C_2F$  and the hypothetical " $C_2A$ ", the composition of the ferrite could be calculated by reference to the unit cell dimensions.

In cement with an  $Fe_2O_3 / Al_2O_3 + Fe_2O_3$  molar ratio greater than 0.37 , an estimation of the ferrite composition could be calculated from the chemical analysis by the formula -

$$q=0.27+0.74(f/(1.57a+f))$$

where  $f$  = % by wt. of  $Fe_2O_3$

$a$  = % by wt. of  $Al_2O_3$

in the formula  $Ca_2 (Fe^q Al_{1-q} )_2 O_5$

Phase extraction and calibration method to determine aluminate and minor element content.

Mander et. al. ( 1974 ) presented a quantitative method to determine some of the phases in Portland cement clinker . The procedure used a maleic acid-methanol solution to remove the silicate phases . This eliminated the interference from the silicates . The calibration curves plotted were tricalcium aluminate (  $C_3A$  ) , alkali modified  $C_3A$  ( either  $NC_3A_3$  or  $KC_3A_3$  ) , periclase (  $MgO$  ) , calcium sulpho-aluminate (  $4CaO_3 3Al_2 O_3 SO_4$  ) , freelite (  $CaO$  ) and the ferrite solid solution found in cement

from  $C_2F$  to  $C_6A_2F$ . The individual calibration curves of peak height against percentage of phase present were prepared by addition of known amounts of each phase to cements that were free of those phases. To evaluate the accuracy of the method, two specially prepared samples with known percentages of the various phases added were analysed and the results compared with the percentages added. The comparison was good except for  $C_3A$ . This was because the calibration curve had a shallow slope and small variations in peak height gave large differences in calculated phase content.

The method was restricted in usage because the calibration curves were specific to the actual instrument used. The errors caused by the shallow slope for the  $C_3A$  curve would have to be minimised because the accurate determination of  $C_3A$  is crucial in some cements. The method also does not indicate the percentage of alite and belite present in the cement.

#### The accuracy of the XRD method in determining the phase composition.

Aldridge (1982 a) investigated the accuracy and precision of the XRD method for determining the phase composition of cement. The study analysed 150 cements that were produced in New Zealand. Aldridge found that there was no significant differences between the accuracy of the compositions determined by the Bogue calculation or good X-ray diffraction methods. He concluded that with the X-ray diffraction methods available the analysis was probably not absolutely accurate but it could be used to give relatively accurate compositions within a series of cements.

#### Comparison of computational, chemical, XRD and XRF determinative techniques.

From an interlaboratory study of the same cements by microscopy, X-ray diffraction and Bogue calculation, Aldridge (1982 b) investigated the level of accuracy and precision of the techniques attained by different laboratories. The original samples were carefully subdivided and sent to

several laboratories throughout the world . The Bogue calculation , X-ray diffraction and wet chemical analysis were made on the cement . The microscopical determination was made on the clinker . Some of the laboratories used X-ray fluorescence analysis ( XRF ) to determine the bulk chemistry of the cement in addition to using wet chemical methods . The XRF technique is used by many cement works as part of the quality control process . The precision of the XRF technique was only slightly less than the wet chemical method. However XRF analysis was quicker with 15 to 20 samples per day compared with 5 to 10 for wet chemistry. The accuracy of the wet chemical analysis was very dependant on the experience of the analyst and the laboratory. The accuracy of the microscopical analysis of the clinker was influenced by the resolution of the microscope , sampling error , identification of phases and the experience of the microscopist . Aldridge calculated that with the exception of aluminate phases the sampling error was more significant than the identification error . The main error in the aluminate phase analysis was because aluminate, periclase and freelite were not always correctly identified .

Aldridge reported that the errors in the X-ray diffraction analysis of cement could be caused by three factors .

- I. The variation in the intensity of X-rays. This could be due to the wrong alignment of the diffractometers , the packing of the sample in the holder , insufficient grinding of sample or the use of an unsuitable internal standard .
- II. The difficulty in separating the many X-ray reflections of the cement minerals that overlap and cause interference with each other.
- III. The standardisation error caused by the substitution of minor elements in many of the cement minerals. This varied the X-ray diffraction patterns of the cement minerals from the published data.

Only one laboratory in the study had a satisfactory method of X-ray analysis for the phase composition . In this laboratory the cement samples were ground with silicon which was the internal standard . The sample was

scanned and the peak positions were closely matched to the range of standards . Those standards with the correct polymorphic forms were selected . In the final analysis certain peaks were chosen and the peak areas were determined. A quartz monochromator, temperature controlled to  $\pm 1^{\circ}\text{C}$  was used to filter the X-rays for analysis .

After a comparison of the methods for analysing cement composition , Aldridge concluded that optical analysis by an experienced cement microscopist gave the most accurate composition and correlated with the Bogue composition . However great care had to be taken to minimise the possible errors .

The current methods of X-ray diffraction analysis are in general unsatisfactory for analysing the phase composition of cement . It is however the only analytical method for directly determining the amount of compound present in a cement clinker. With further development and the establishment of suitable standards, the XRD technique could become an effective method of determining the phase composition of cement clinker.

#### Conclusions and evaluation of the techniques for determination of the phase composition of cement clinker.

The results of the phase composition determinations for the cement clinker from the works studied is given in Table 7.1. A qualitative determination of the phases composition of the clinkers by X-ray diffraction is given in Table 4.1 (Chapter four. )

The different methods for determining the cement compound compositions have different errors for the various phases. In the point counting method there is a tendency to under-estimate the amount of belite and over-estimate the alite level. This occurs especially if the belites are small and well dispersed throughout the clinker, because they are difficult to identify. If the belite is large and clustered, the error is

less. The freelite is consistently under-estimated because of its very small size. ( The titrimetric method for determining freelite is most accurate and relatively quick.) The Bogue calculation is reasonably accurate for alite and belite proportions. The aluminate and ferrite values are less accurate because of the effects of solid solution on the compositions of these phases. The matrix calculation relies on obtaining accurate analyses of all the phases , both major and minor, in the clinker. This is extremely difficult because of the small size of some of the phases. If accurate analyses can be obtained, the calculation of the potential phase composition should be better overall than the Bogue or microscopical methods.

Summary. (the best techniques for different phases.)

The X-ray technique is best for determining the tricalcium aluminate, ferrite and magnesia phase contents. The alite and belite phases are most accurately determined by point counting with a high resolution microscope.

The matrix recalculation method requires the acquisition of the chemical compositions of all of the mineral phase in the clinker for an accurate calculation. The Bogue calculation is much more rapid but less accurate. However for production control at an individual cement plant the Bogue method is relatively useful. The effects of production changes can be rapidly determined by the variation in the Bogue composition of the cement. This usually reflects the changes in the actual phase composition of the cement.

KEY

SRC = Production sulphate resisting cement made from chalk and PFA.

PFB = Trial SRC cement clinker with extra PFA, collected at 1030h.

PFC = Trial SRC cement clinker with extra PFA, collected at 1530h.

PFD = Trial SRC cement clinker with extra PFA, collected at 2030h.

LHA = Trial Low Heat cement clinker collected at 0900h.

LHB = Trial Low Heat cement clinker collected at 1200h.

LHC = Trial Low Heat cement clinker collected at 1300h.

LHD = Trial Low Heat cement clinker collected at 1500h.

OPC = Production Ordinary Portland cement clinker.

WPC = Production White Portland cement clinker.

ATEPC = Alite % in sample by Point counting

BTEPC = Belite % in sample by Point counting

FERPC = Ferrite % in sample by Point counting

ALUPC = C3A % in sample by Point counting

GYPPC = Gypsum % in sample by Point counting

FLPC = Freelite % in sample by Point counting

C12A7 = C12A7 % in sample by Point counting.

ATEB = Alite % in sample by Bogue

BTEB = Belite % in sample by Bogue

FERB = Ferrite % in sample by Bogue

ALUB = C3A % in sample by Bogue

GYPB = Gypsum % in sample by Bogue

LOI = Loss on ignition

ATEM = Alite % in sample by Matrix recalculation

BTEM = Belite % in sample by Matrix recalculation

FERM = Ferrite % in sample by Matrix recalculation

ALUM = C3A % in sample by Matrix recalculation

MGM = Periclase % in sample by Matrix recalculation

FLC = Freelite % in sample by Titration.

GYPM = Gypsum % in sample by Matrix recalculation

(Table 7.1) Phase composition determinations of the cement clinker from works A,B,C,D,E,F and G.

Sample Cement	WKS.B LHD	WKS.A OPC	WKS.E OPC	WKS.C OPC	WKS.F WPC	WKS.D OPC	WKS.G OPC
Phase composition of the cement clinker by point counting							
ATEPC	67	65	63	61	67	60	67
BTEPC	10	8	13	16	15	14	9
FERPC	17	9	8	8	0	10	6
ALUPC	2	13	9	10	13	10	12
GYPCC	2.0	1.0	2.0	2.0	0.5	1.0	1.0
FLPC	1.0	1.0	1.0	0.5	2.0	1.0	1.0
C12A7	2	4	3	3	3	4	3
TOTAL	101.0	101.0	99.0	100.5	100.5	100.0	99.0
Phase composition of the cement clinker by the Bogue calculation							
ATEB	63	56	51	57	58	53	51
BTEB	12	17	22	17	22	24	22
FERB	20	11	8	8	0	9	8
ALUB	1	11	12	13	13	11	13
GYPB	2	1	3	3	1	1	2
FLC	0.7	1.8	1.5	0.3	3.1	0.5	2.2
LOI	0.2	0.6	0.2	0.3	2.3	0.2	0.6
TOTAL	98.9	98.4	97.7	98.6	99.4	98.7	98.8
Phase composition of the cement clinker by the matrix method							
ATEM	54	61	55	58	57	51	49
BTEM	23	12	18	19	29	28	23
FERM	17	19	16	17	1	12	10
ALUM	4	4	6	4	9	8	12
MGM	0	1	1	1	0	1	2
FLC	0.7	1.8	1.5	0.3	3.1	0.5	2.2
GYPM	1	1	3	2	0	0	2
TOTAL	99.9	99.8	100.4	100.9	99.0	100.4	100.2
Sample Cement	WKS.B SRC	WKS.B PFB	WKS.B PFC	WKS.B PFD	WKS.B LHA	WKS.B LHB	WKS.B LHC
Phase composition of the cement clinker by point counting							
ATEPC	67	58	57	51	67	68	69
BTEPC	12	21	27	24	11	12	7
FERPC	11	11	7	12	13	13	16
ALUPC	4	3	3	5	2	2	3
GYPCC	1.0	4.0	2.0	3.0	1.0	1.0	1.0
FLPC (freelime)	1.5	1.0	1.0	4.0	1.0	1.0	1.5
C12A7	3	1	2	2	5	2	3
TOTAL	99.5	99.0	99.0	101.0	100.0	99.0	100.5
Phase composition of the cement clinker by the Bogue calculation							
ATEB	70	47	51	54	62	59	62
BTEB	7	25	23	16	13	17	13
FERB	15	15	14	15	17	17	19
ALUB	3	5	5	4	3	2	2
GYPB	2	6	3	5	1	1	1
FLC	1.6	1.2	2.5	5.1	2.1	2.1	1.0
LOI	1.2	0.7	0.9	0.6	0.1	0.9	0.7
TOTAL	99.8	99.9	99.4	99.7	98.2	99.0	98.7
Phase composition of the cement clinker by the matrix method							
ATEM	69	50	47	53	57	52	55
BTEM	9	24	28	15	20	24	21
FERM	15	14	16	19	16	17	18
ALUM	3	5	4	3	4	4	3
MGM	0	0	0	0	0	0	0
FLC	1.6	1.2	2.5	5.1	2.1	2.1	1.0
GYPM	1	6	3	5	1	1	1
TOTAL	98.7	100.2	100.6	100.1	99.7	99.8	99.1
(FLC is freelime by titration)							

Chapter eight.

THE MINERAL CHEMISTRY OF CEMENT CLINKER PHASES.

Introduction.

One of the best techniques for investigating the mineral chemistry of the cement clinker phases is electron microprobe analysis (EMPA). The advantages of this technique over chemical analysis are immense, especially in mineral chemistry studies. The small size of the electron beam enables a series of analyses to be made across a specific crystal in a clinker nodule. This scale of analysis is especially useful because it can provide information on substitution of elements into the mineral structure. The detailed analysis of the cement clinker minerals can indicate how a minor element is partitioned between the main phases of the clinker. These minor elements often act as stabilizers to polymorphs of the clinker minerals which are out of equilibrium conditions when discharged from the kiln. This can include the stabilisation of high temperature polymorphs which vary considerably in their reactivity towards water, from the usual polymorphic forms produced. Thus accurate analyses of the clinker minerals provides data on the potential performance of the cement.

Electron microprobe analysis of cement clinker.

The use of EMPA for investigating cement clinker developed in the early 1960's. The electron microprobe chemically analyses material by bombarding the specimen with a beam of electrons. The X-ray spectrum produced was analysed by crystal spectrometers. Later development in microprobe analysis techniques produced an energy dispersive system. In

this process the full spectrum from the specimen is analysed by a solid state lithium 'doped' silicon solid state detector .

The electron beam used to generate the X-ray spectra from the specimen can be focused to a spot approximately 1  $\mu\text{m}$  in diameter. The small size of the electron beam enables a quantitative analysis to be made on selected phases in the specimen . For a quantitative analysis the specimens must have been carefully prepared. ( See Appendix 5 ) The surface should be level and have a good polish . To prevent charging of the specimen by the electron beam , the surface is coated with a very thin conducting layer. Elements with a low atomic number are not usually detected by the analysis system , thus carbon is usually chosen ( Atomic No. 6 .).

For accurate analysis of the chemistry of a specific phase , it is best if the phase selected is large enough to avoid the unintentional analysis of another phase below or adjacent to the crystal under investigation . This is because the electron beam penetrates the specimen to a variable depth and produces an electro-solid interaction zone which is larger than the beam . The size of this zone is dependent on the power of the beam . It is usually about 10  $\mu\text{m}$  in diameter at normal operating conditions ( Appendix 8 ) . It is possible to gain useful information from phases which are smaller than the diameter of the beam . This was achieved by plotting the EMPA analyses on ternary phase diagrams. It was then possible to deduce compositional trends from the phase diagrams. Electron microprobe analysis of cement clinker provides a means of investigating the stoichiometry of the clinker phases and the partitioning of the minor elements in the individual phases.

The rate of hydration of the clinker minerals is dependent on the nature and proportion of the minor elements present in the individual minerals . The incorporation of these elements in solid solutions can be either by replacement of the major elements, by occupation of vacant sites in the lattice , or a combination of the two .

Early microprobe analyses were presented as electron intensity maps of individual elements in the different cement minerals ( Midgley , 1964 ) . A pilot study with the electron probe on the aluminate phase by Moore (1965 ) , used the output of a detector which was sensitive to back scattered electrons to produce images of the element distribution by atomic number. Moore attempted to obtain some quantitative measurements of the magnesium content in some of the cement phases . This was achieved by holding the electron beam stationary and recording the X-ray count for a fixed time period. A sample of olivine with known MgO content was used as a standard . However the high value of 13 % noted for C<sub>3</sub>A was due to the unintentional analysis of some periclase within the aluminate . Peterson ( 1967 ) gave values for Al<sub>2</sub>O<sub>3</sub> , K<sub>2</sub>O , Na<sub>2</sub>O<sub>3</sub> and SO<sub>3</sub> in alite and belite grains , but the results were variable and had uncertain correction procedures .

Yamaguchi and Takagi ( 1968 ) made a very comprehensive study of Japanese portland cement clinker . They used EMPA to measure the Al<sub>2</sub>O<sub>3</sub> , Fe<sub>2</sub>O<sub>3</sub> , MgO , Na<sub>2</sub>O , and K<sub>2</sub>O in alite and belite using standard samples made from lithium borate glasses with 50% by weight of the constituent added to the specific phase to calibrate the analyser . The values of the analyses were very variable. To give reproducible results, the standards and samples had to be analysed at the same time with the same sample holder.

In the late 1960's it became feasible , due to improvements in detectors and correction procedures , to achieve detailed quantitative chemical analyses of the major and minor phases in cement.

#### Mineral chemistry of alite in cement clinker.

Midgley (1968) used an electron microprobe to determine the chemical composition of an alite in a commercial portland cement . The average

analyses of the alites is given in Table 12.1 in Appendix 8. The standards used were synthetic preparations of the cement minerals with specific additions of minor elements. To calculate the molar ratios, Midgley used the unit cell of Jeffery (1952) for the alite. This had 180 oxygens per unit cell with the formula  $Ca_{108} Si_{36} O_{180}$ . To calculate the structural cell from the molar ratios, silicon and titanium (34.59) were assigned to the tetrahedral positions (36.00 required). The balance was made up from the alumina, leaving a balance of alumina (0.51).

The remainder of the cations (Fe, Mg, Na, K, Mn) were used to fill the calcium sites, the total was 107.72 which was 0.28 short of the total 108.00. This was filled by the available aluminium leaving 0.23 to occupy the interstitial sites. This formula differs from the one proposed by Jeffery because he assigned magnesium to the interstitial positions. Midgley believed that there was no reason to suppose that the aluminium occupied the interstitial position rather than magnesium. However it did support the idea that interstitial sites were not filled by specific ions. The charge balance was thus maintained by cation substitution in the interstitial sites. The substituting elements were partially dependent on the environment prevailing at the time of formation.

Midgley (1968 b.) made a more extensive study of alite and belite. Four different clinker specimens were used of varying bulk chemical compositions. Midgley calculated the coefficients of variation from the alite compositions. He found that the differences in composition between the individual alite grains was real, since the coefficients of variation were higher than would have been expected from analytical variation.

The mineral compositions of the alite in the cement clinkers from the works A, B, C, D, E, F and G, that were investigated by the author are shown in Tables 8.2, 8.3 and 8.4. (All oxide values are in weight percent oxide, unless otherwise stated.)

KEY

XRF analyses from pages 24,25,26

EMP analyses for Alite from pages 128,129,130

EMP analyses for Belite from pages 139,140,141

(Fig.8.1) CEMENT CLINKER ANALYSIS (XRF) V ALITE AND BELITE ANALYSIS (EMP)

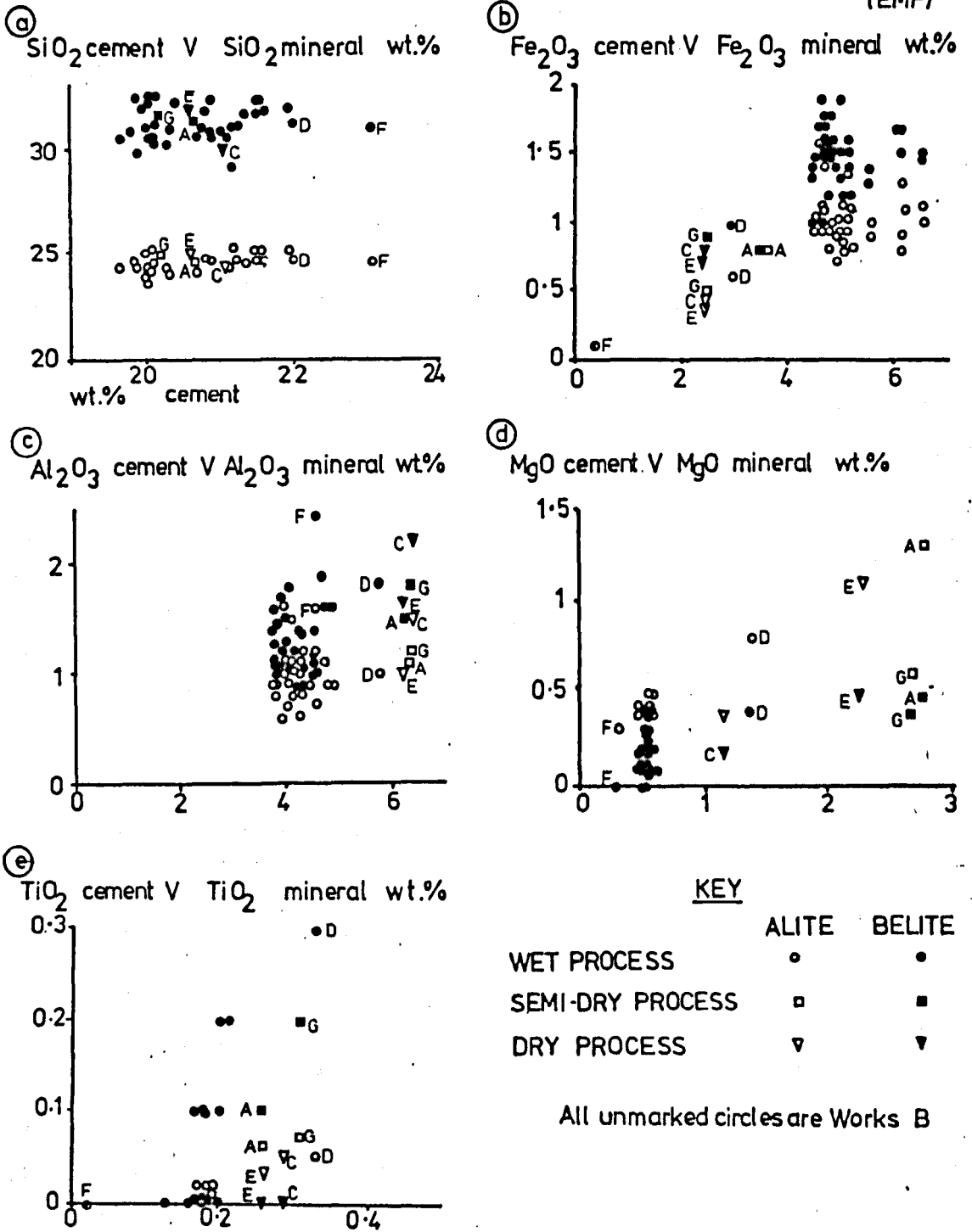


(Fig.8.1 continued) ALITE AND BELITE

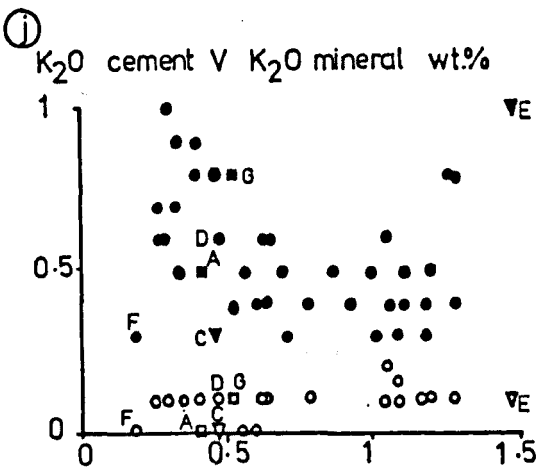
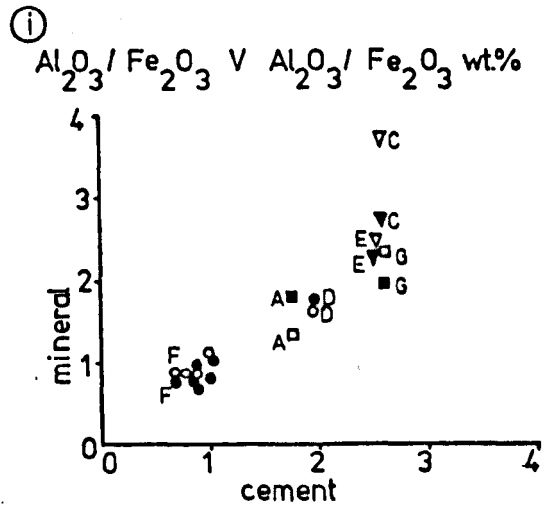
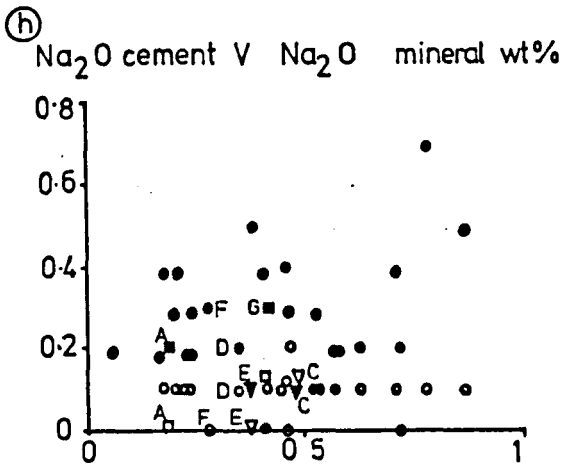
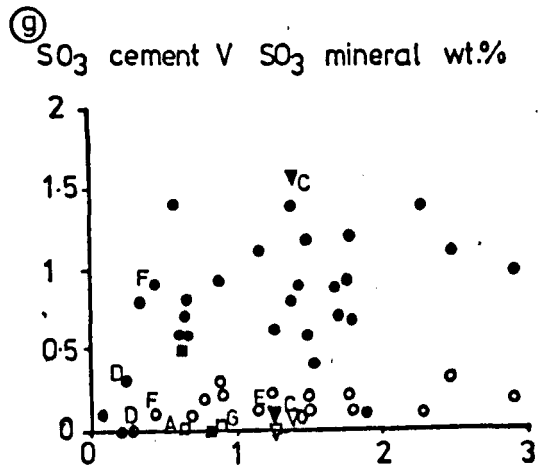
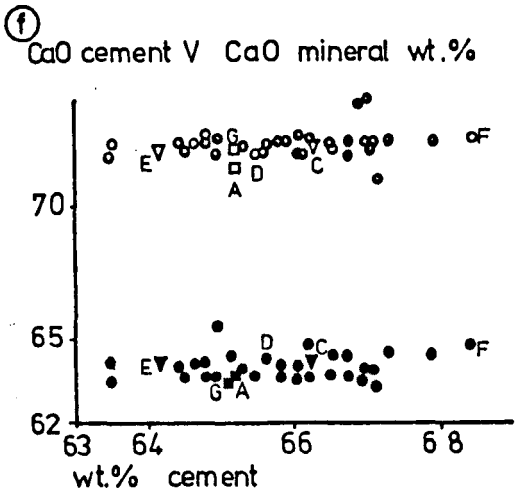


( Table 8.1 ) The variation in the levels of element substitution in Alite determined by electron probe analysis. ( in wt.% oxide)

Cement Alite type	OP alite	SR alite	Alite	Rhom.alite	Mono.alite	Alite
Author Midgley	Midgley	Midgley	Hornain	Kristmann	Kristmann	Ghose & Barnes
Year	1968	1968b	1968b	1971	1977	1977
Al <sub>2</sub> O <sub>3</sub>	1.2	1.26	1.19		1.0	1.0
TiO <sub>2</sub>	0.11	0.12	0.11	0.6		
Fe <sub>2</sub> O <sub>3</sub>	1.39	0.43	1.39		1.0	1.0
MnO		0.02	0.02			
MgO	0.86	0.09	0.86		0.5	2.1
Na <sub>2</sub> O	0.30	0.2	0.3			0.1
K <sub>2</sub> O	0.10	0.06	0.10			0.1
SO <sub>3</sub>						0.25
CuO				0.74		
V <sub>2</sub> O <sub>5</sub>				0.70		
ZnO				0.68		
NiO				0.63		
Cr <sub>2</sub> O <sub>3</sub>				0.57		
CoO				0.31		

KEY

SRC = Production sulphate resisting cement made from chalk and PFA.

PFB = Trial SRC cement clinker with extra PFA, collected at 1030h.

PFC = Trial SRC cement clinker with extra PFA, collected at 1530h.

PFD = Trial SRC cement clinker with extra PFA, collected at 2030h.

LHA = Trial Low Heat cement clinker collected at 0900h.

LHB = Trial Low Heat cement clinker collected at 1200h.

LHC = Trial Low Heat cement clinker collected at 1300h.

LHD = Trial Low Heat cement clinker collected at 1500h.

OPC = Production Ordinary Portland cement clinker.

WPC = Production White Portland cement clinker.

(Table 8.2). Electron microprobe analyses (mean values)  
of Alite from works A,B,C,D,E,F, and G .

Works Cement	WKS.B SRC	WKS.B PFB	WKS.B PFC	WKS.B PFD	WKS.B LHA	WKS.B LHB	WKS.B LHC
SiO2	24.8	24.7	24.4	24.6	24.1	24.5	24.7
Al2O3	0.9	0.9	1.1	1.0	1.1	0.9	0.7
TiO2	0.0	0.0	0.0	0.0	0.0	0.0	0.0
Fe2O3	1.0	0.8	1.0	1.0	1.2	1.0	0.9
MnO	0.0	0.0	0.0	0.0	0.0	0.3	0.0
MgO	0.4	0.4	0.4	0.5	0.4	0.3	0.3
CaO	72.2	72.3	72.4	72.2	72.3	72.6	72.7
Na2O	0.1	0.1	0.0	0.1	0.1	0.1	0.0
K2O	0.1	0.1	0.2	0.1	0.0	0.0	0.0
P2O5	0.0	0.0	0.0	0.0	0.0	0.0	0.0
SO3	0.1	0.2	0.1	0.1	0.0	0.0	0.0
TOTAL	99.6	99.5	99.6	99.6	99.2	99.7	99.3

Works Cement	WKS.B LHD	WKS.A OPC	WKS.E OPC	WKS.C OPC	WKS.F WPC	WKS.D OPC	WKS.G OPC
SiO2	24.2	24.9	25.0	24.3	24.6	24.7	24.6
Al2O3	0.9	1.1	1.0	1.5	1.6	1.0	1.2
TiO2	0.0	0.1	0.0	0.1	0.0	0.1	0.1
Fe2O3	1.1	0.8	0.4	0.4	0.1	0.6	0.5
MnO	0.0	0.0	0.0	0.0	0.0	0.0	0.0
MgO	0.3	1.3	1.1	0.4	0.3	0.8	0.6
CaO	72.5	71.4	71.9	72.3	72.6	72.0	72.1
Na2O	0.0	0.0	0.0	0.1	0.0	0.1	0.1
K2O	0.1	0.0	0.1	0.0	0.0	0.1	0.1
P2O5	0.0	0.0	0.0	0.0	0.0	0.0	0.1
SO3	0.0	0.0	0.0	0.1	0.1	0.0	0.0
TOTAL	99.1	99.6	99.5	99.1	99.3	99.3	99.4

KEY

K1 = Production Sulphate Resisting cement from Kiln 1.

K3 = Production Sulphate Resisting cement from Kiln 3.

The four digits indicate the time of collection of the clinker.

(Table 8.3 ). Electron microprobe analyses (mean value) of  
Alite from SRC clinker (K1,K3)

Sample	K11930	K12030	K12130	K12230	K12330	K10030	K10130
SiO <sub>2</sub>	25.4	24.4	24.6	24.7	25.0	24.6	25.3
Al <sub>2</sub> O <sub>3</sub>	0.7	1.2	1.0	0.8	0.6	0.8	0.7
TiO <sub>2</sub>	n.d						
Fe <sub>2</sub> O <sub>3</sub>	0.8	1.1	1.1	0.9	0.8	1.0	0.8
MnO	n.d	n.d	n.d	n.d	n.d	0.1	n.d
MgO	0.4	0.4	0.4	0.4	0.4	0.4	0.4
CaO	72.6	72.0	72.3	72.5	72.6	72.2	72.7
Na <sub>2</sub> O	n.d	n.d	n.d	n.d	0.1	0.1	n.d
K <sub>2</sub> O	n.d	0.1	0.1	0.1	n.d	0.1	n.d
P <sub>2</sub> O <sub>5</sub>	n.d						
SO <sub>3</sub>	n.d						
TOTAL	99.9	99.2	99.5	99.4	99.5	99.3	99.9

Sample	K10230	K10330	K10430	K10530	K31930	K32030	K32130
SiO <sub>2</sub>	25.2	25.2	24.8	24.8	24.3	24.3	25.1
Al <sub>2</sub> O <sub>3</sub>	0.6	0.9	0.8	0.8	0.9	1.1	0.8
TiO <sub>2</sub>	n.d						
Fe <sub>2</sub> O <sub>3</sub>	0.7	1.0	0.9	1.0	0.9	1.1	0.9
MnO	n.d						
MgO	0.3	0.4	0.4	0.4	0.4	0.4	0.4
CaO	72.3	72.3	72.6	72.1	72.5	72.6	72.1
Na <sub>2</sub> O	n.d	0.1	0.1	0.1	n.d	n.d	n.d
K <sub>2</sub> O	0.1	n.d	n.d	n.d	n.d	n.d	n.d
P <sub>2</sub> O <sub>5</sub>	n.d						
SO <sub>3</sub>	n.d	n.d	n.d	n.d	n.d	0.2	n.d
TOTAL	99.2	99.9	99.6	99.2	99.0	99.7	99.3

Sample	K32230	K32330	K30030	K30130	K30230	K30330	K30430
SiO <sub>2</sub>	23.7	24.4	24.7	24.5	24.1	24.4	24.1
Al <sub>2</sub> O <sub>3</sub>	1.6	1.0	0.9	0.9	1.2	0.9	0.9
TiO <sub>2</sub>	n.d						
Fe <sub>2</sub> O <sub>3</sub>	1.6	0.8	0.9	0.9	1.4	0.9	1.0
MnO	n.d						
MgO	0.4	0.4	0.3	0.4	0.4	0.4	0.4
CaO	71.1	72.4	72.5	72.6	71.9	72.5	72.3
Na <sub>2</sub> O	0.2	0.1	0.1	0.1	0.1	0.1	n.d
K <sub>2</sub> O	0.2	n.d	n.d	n.d	0.1	0.1	n.d
P <sub>2</sub> O <sub>5</sub>	n.d						
SO <sub>3</sub>	0.7	0.2	n.d	n.d	0.1	0.1	n.d
TOTAL	99.5	99.3	99.4	99.4	99.3	99.4	98.7

KEY

K3 = Production Sulphate resisting cement ( SRC ) from kiln 3

PF = Trial SRC with PFA addition.

LH = Trial Low Heat cement clinker.

(Table 8.4). Electron microprobe analyses (mean value) of Alite from SRC clinker (K1,K3), SRC with PFA kiln addition clinker (PF) and L H trial mix (LH) .

Sample	K30530	PF0730	PF1130	PF1330	PF1530	PF1730	PF1930
SiO2	25.2	24.3	24.7	24.8	24.4	24.4	24.6
Al2O3	0.9	1.1	0.9	0.9	1.1	1.1	1.2
TiO2	n.d						
Fe2O3	0.9	1.1	0.8	0.9	1.0	1.0	1.0
MnO	n.d						
MgO	0.4	0.4	0.4	0.4	0.4	0.4	0.5
CaO	72.9	72.0	72.3	72.3	72.4	72.4	72.2
Na2O	0.1	0.1	0.1	n.d	n.d	n.d	0.1
K2O	0.1	0.1	0.1	n.d	0.1	n.d	0.1
P2O5	n.d						
SO3	n.d	0.3	0.2	0.2	0.1	0.1	0.1
TOTAL	100.5	99.4	99.5	99.5	99.5	99.4	99.8

Sample	PF2030	LH0900	LH1200	LH1300	LH1400	LH1500	LH1600
SiO2	24.6	24.1	24.5	24.7	24.3	24.2	24.2
Al2O3	1.2	1.1	0.9	0.7	1.1	0.9	1.0
TiO2	n.d						
Fe2O3	1.0	1.1	0.9	0.8	1.1	1.0	1.3
MnO	n.d						
MgO	0.5	0.4	0.3	0.3	0.4	0.3	0.3
CaO	72.2	72.3	72.6	72.6	71.9	72.5	72.3
Na2O	0.1	0.1	0.1	n.d	n.d	n.d	n.d
K2O	0.1	n.d	n.d	n.d	0.1	0.1	n.d
P2O5	n.d	n.d	n.d	n.d	0.1	n.d	n.d
SO3	0.1	n.d	n.d	n.d	0.2	n.d	n.d
TOTAL	99.8	99.1	99.3	99.1	99.2	99.0	99.1

Variation in the stoichiometric ratios of SiO<sub>2</sub> and CaO in alite.

The SiO<sub>2</sub> content of the alite showed a slight increase as the SiO<sub>2</sub> level in the cement increased (Figure 8.1,a) . Most of the variation was due to the different substitutions of the minor elements in the cements. The same reason applied for the CaO content of the alite against the CaO content of the cement (Figure 8.1,f).

Substitution of MgO in alite.

Regourd and Guinier (1974) used EMPA to investigate the partitioning of elements in the clinker phases. (Table 8.1) . The alites had a distinct partitioning of MgO . The rhombohedral (trigonal) alites had a low MgO level (0.5%) and the monoclinic alites had a high MgO content (2.0%). Kristmann (1977) investigated a wide range of clinkers from many different production methods and burning processes. (Table 8.1) . His results for MgO concurred with those of Regourd and Guinier (1974) . Kristmann also found alite crystals with MgO contents between the high and low levels. He concluded that these crystals were either monoclinic alites with low MgO or a mixture of trigonal and monoclinic alite. The distribution of the minor elements in coexisting alites and belites agreed with Midgley ( 1968 b ). Kristmann proposed that Mg was preferentially incorporated into the alite.

Ghose and Barnes (1980) studied the distribution of the minor elements in the clinker phases and their relationship to the bulk chemistry of the clinker . (Table 8.1). They found that the MgO content of alite increased linearly with an increase in the MgO level in the clinker. They did not investigate the distribution of MgO between the different alite polymorphs.

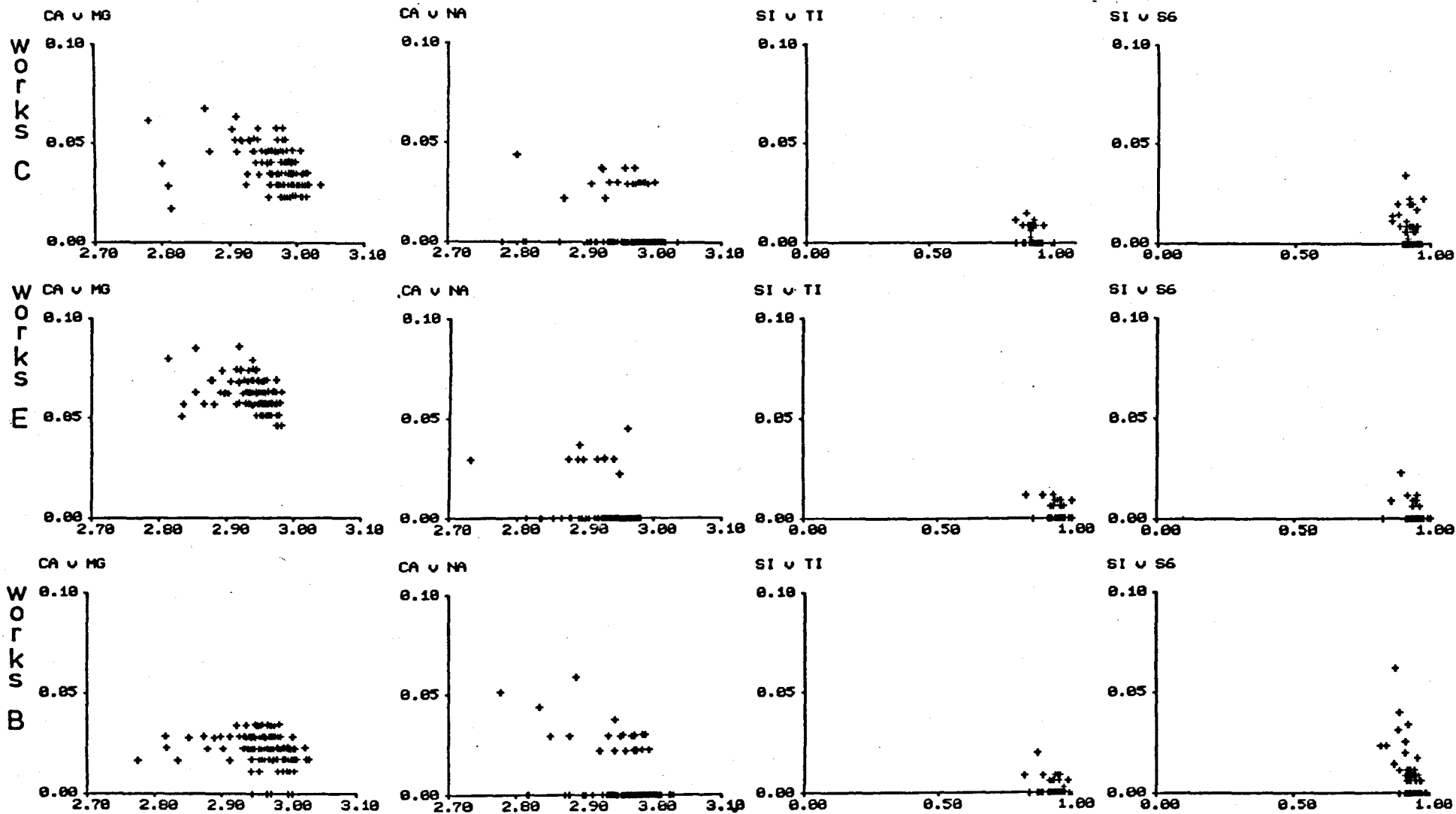
Figure (8.1,d) shows the MgO content of the cement clinker against the substitution of MgO in the alite and belite phases of the clinker investigated by the author. This indicates that the MgO was preferentially incorporated in the alite. The overall trend indicated for the monoclinic alite, was a linear increase with increased clinker MgO. The two values that did not lie on the general trend, indicated that the alite in that specific clinker was in a different polymorphic form. The alites in these clinkers, one from a semi dry process kiln (Works G) and one from a dry process kiln (Works C) were in the rhombohedral (trigonal) form. The Mg ions replaced the Ca ions.(Figure 8.2 Ca v Mg). The limit of substitution depended on which polymorphs of alite were in the cement clinker.

#### Substitution of $Al_2O_3$ and $Fe_2O_3$ in alite.

Kristmann (1977) found that alites contained appreciable amounts of Fe and Al. He proposed that the partition of Al was related to the production process. In the wet process the Al was partitioned into the alite phase, whilst for the dry process, the Al was incorporated into the belite phase.

The level of  $Al_2O_3$  in the alite and belite against the  $Al_2O_3$  in the clinker from the different works showed an overlap. (Figure 8.1,c). The partition of Al between alite and belite from wet process kilns had a substantial overlap. The alites and belites from the dry and semi-dry process kilns did not show any distinct partitioning. There was an overall general increase with increasing levels of  $Al_2O_3$  in the clinker. The Al ions substituted for the Si ions. The proposal by Jeffery (1952) that the Mg substitution for the Ca ions was linked to the Al substitution for Si, is not supported by the author. This is because in Figure (8.3) the Si v Al plot would have to show a greater level of Al substitution when there was a increased amount of Mg substitution. ( Figure 8.2, Ca v Mg).

(Figure 8-2). Number of ions substituted versus number of ions substituted in alite calculated on 5 oxygens .



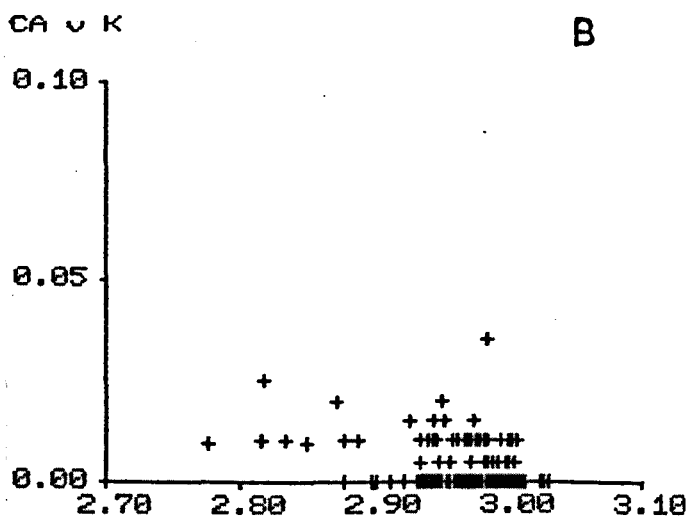
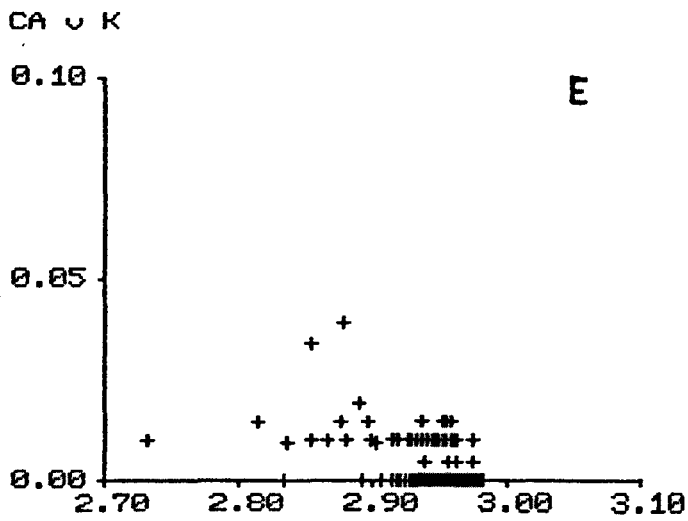
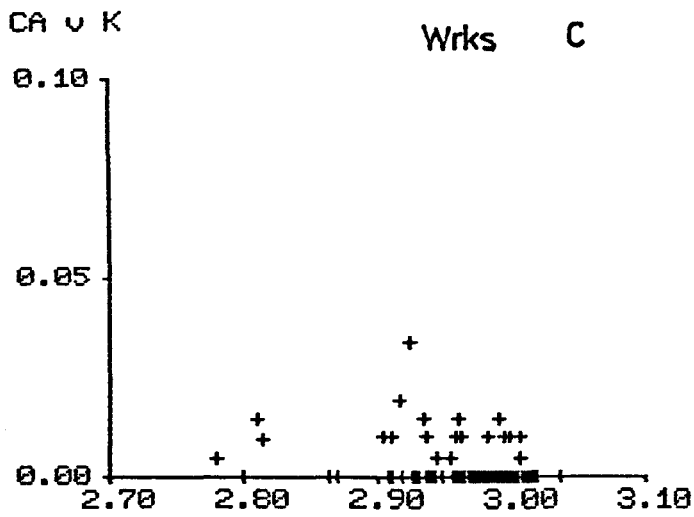
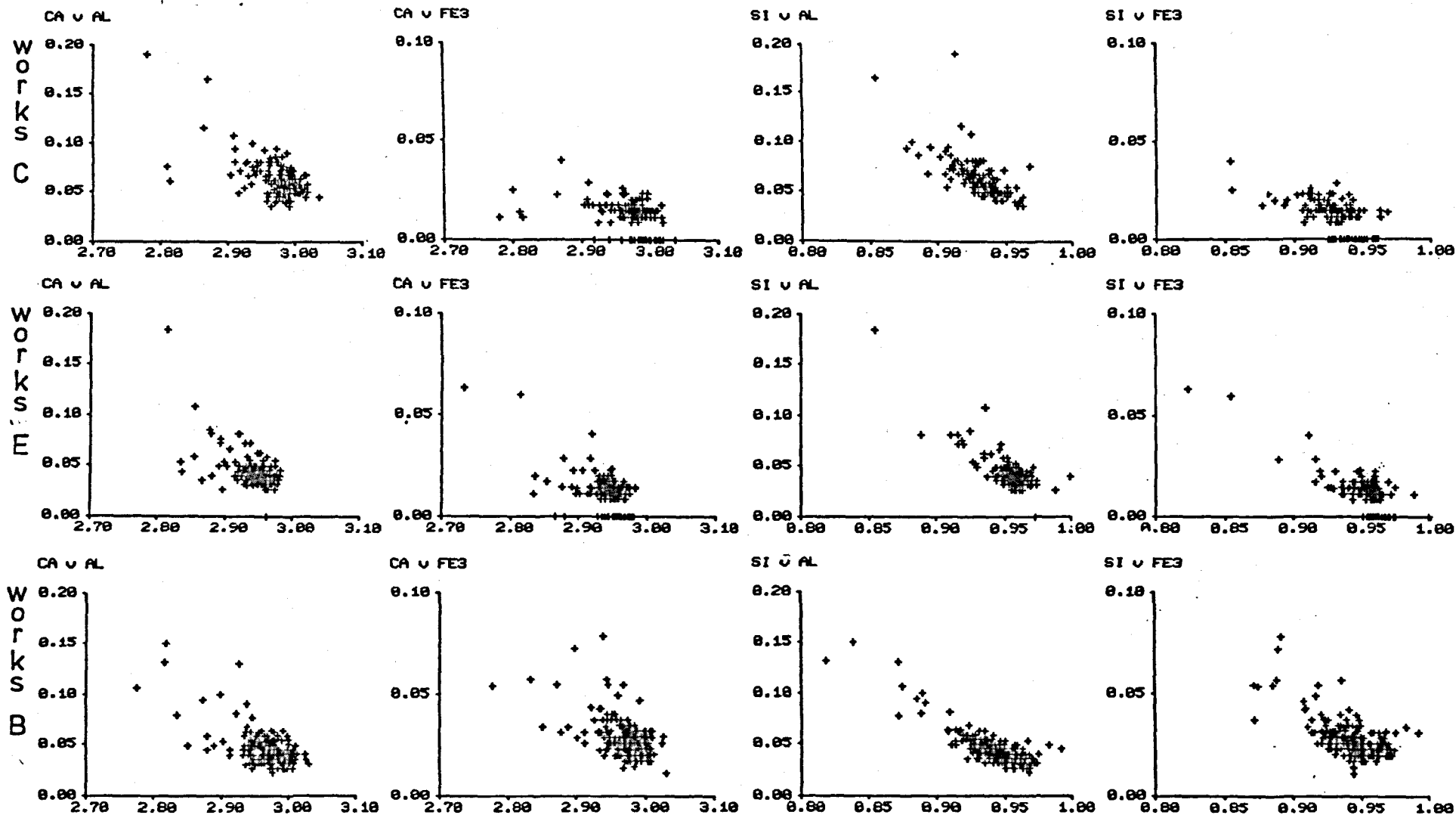


(Figure 8-3). Number of ions substituted versus number of ions substituted in alite calculated on 5 oxygens .



this is not shown in the substitution system.

The  $\text{Fe}_2\text{O}_3$  level in the alite (Figure 8.1,b) had a similar distribution to  $\text{Al}_2\text{O}_3$ . The overall control on the  $\text{Al}_2\text{O}_3$  and  $\text{Fe}_2\text{O}_3$  content of the alite was the  $\text{Al}_2\text{O}_3/\text{Fe}_2\text{O}_3$  ratio of the clinker. (Figure 8.1,1). The  $\text{Fe}^{3+}$  ions appeared to substitute for Ca ( Figure 8.3, Ca v Fe ) in some of the clinkers, or for Si in other clinkers ( Figure 8.3, Si v Fe). This was probably due to the presence of zones of reduction in some cement clinkers.

Fletcher (1965) has proposed that  $\text{Fe}^{2+}$  ions substituted for  $\text{Ca}^{2+}$  on a one for one basis. The  $\text{Si}^{4+}$  ions were replaced by  $\text{Fe}^{3+}$  ions . From the microprobe analyses obtained it was not possible to differentiate between iron in the ferrous or ferric state. All the iron values were calculated in the ferric state , because it was the state of oxidation in normal clinker. This caused the apparent dual substitution of  $\text{Fe}^{3+}$  for Si and Ca.

#### Substitution of the minor elements, $\text{Na}_2\text{O}$ , $\text{K}_2\text{O}$ , $\text{SO}_3$ and $\text{TiO}_2$ .

Kristmann's (1977) microprobe analyses of alites had only small quantities of  $\text{Na}_2\text{O}$  and  $\text{K}_2\text{O}$  in them. (Table 8.1). Ghose and Barnes (1980) found that the average  $\text{K}_2\text{O}$  content for alite was low (0.1%). This was because the  $\text{K}_2\text{O}$  in alite disrupts the crystal lattice. The maximum level of  $\text{K}_2\text{O}$  present (Figure 8.1,j ) supports this theory .

The  $\text{Na}_2\text{O}$  content of alite was similar to the  $\text{K}_2\text{O}$  level at about 0.1%. (Figure 8.1,h). The Na and K ions both substitute for Ca . (Figure 8.2, Ca v Na and Ca v K)

Hornain (1971) studied the distribution of some transition elements in cement clinker. (Table 8.1) He proposed that  $\text{Ni}^{2+}$ ,  $\text{Cu}^{2+}$  and  $\text{Zn}^{2+}$  replaced  $\text{Ca}^{2+}$  directly. The  $\text{Ti}^{4+}$  ions substituted for  $\text{Si}^{4+}$  at the tetrahedral sites . The other elements which had variable valencies , V ,Cr , Mn and

Co, had combined substitutions for Ca or Si and in the vacant interstitial sites. In the case of the elements with higher atomic numbers, Co, Ni, Cu and Zn, the  $Al_2O_3$  content of the alite was reduced. This was due to the partial replacement of the Al ions in the octahedral sites.

The only transition element that normally occurred in alite in a detectable quantity was titanium. The  $TiO_2$  content of the alites analysed by the author, was between 0 and 0.1%. (Figure 8.1,e). There was a general increase with increased  $TiO_2$  levels in the cement. However the  $TiO_2$  content of the alite was also controlled by the amount of ferrite present in the clinker. Thus clinker with a high ferrite content such as sulphate resisting or low heat cement, contains alite with a low  $TiO_2$  content. Those cements which have a lower ferrite content have alites with a higher  $TiO_2$  content. The Ti ions substituted for the Si ions. (Figure 8.2, Si v Ti)

The  $SO_3$  content of the alite grains was very low (0.1%). Any values above this level caused the alite to dissociate to CaO and  $C_2S$ . The  $SO_3$  content of the alites from the works studied was consistently low. (Figure 8.1,g) The S ions substituted for the Si ions. (Figure 8.2, Si v Ti).

The mineral chemistry of belite in cement clinker.

Fletcher (1968) investigated the composition of belite crystals from ordinary portland cement and sulphate resisting cement. ( Table 12.1). Fletcher found that the ratio of  $\text{Al}_2\text{O}_3$  to  $\text{Fe}_2\text{O}_3$  in the belite grains corresponded closely to the  $\text{Al}_2\text{O}_3 / \text{Fe}_2\text{O}_3$  ratio in the cement . He proposed that the belite formed from a liquid in which the Al/Fe ratio was the same as that of the clinker. The  $\text{C}_2\text{S}$  lattice had no apparent selectivity for  $\text{Al}^{3+}$  or  $\text{Fe}^{3+}$ . In portland cement the amount of  $\text{Fe}^{2+}$  was usually very low unless extensive reduction had occurred in the burning process . If  $\text{Fe}^{3+}$  was present it replaced  $\text{Ca}^{2+}$  . If there was extensive replacement of  $\text{Ca}^{2+}$  by  $\text{Fe}^{2+}$  , dusting of the clinker occurred . This was caused by the inversion of  $\beta \text{C}_2\text{S}$  to  $\gamma \text{C}_2\text{S}$  because the  $\beta \text{C}_2\text{S}$  with  $\text{Fe}^{2+}$  replacement<sup>15</sup> unstable . He calculated the molar ratios of the analyses on the unit cell of  $\beta \text{C}_2\text{S}$  with 16 oxygens (  $\text{Ca}_8 \text{Si}_4 \text{O}_{16}$  ) . The probable substitutions for Ca were K , Na and Mg in the octahedral sites . The replacements for Si were Fe , Ti , Mn and Al in the tetrahedral sites . To maintain the electroneutrality a proportion of the minor elements had to occupy interstitial sites. The composition of belite crystals from different types of cement clinker were investigated by Midgley (1968). (Table 12.1). He found that the  $\text{Na}_2\text{O}$  ,  $\text{Al}_2\text{O}_3$  ,  $\text{K}_2\text{O}$  and  $\text{Fe}_2\text{O}_3$  levels were higher in belite than alite and the MgO content was lower. Midgley also investigated the distribution of minor elements between coexisting alite and belite . There was a considerable lack of homogeneity in the samples with some of the values for minor elements differing by a factor of four between similar phases in the same sample. This was probably due to inhomogeneity in the kiln feed and to solid state reactions which had not reached equilibrium.

( Table 8-5) The variation in the levels of element substitution in Belite determined by electron probe analysis.  
( in wt.% oxide )

Cement type	OP belite	SR belite	OP belite	SR belite	Belite	$\beta$ belite	$\alpha'$ belite	$\beta$ belite	$\alpha'$ belite	Belite max	Belite	Belite min.	Belite max,	Belite	K def. Belite
Author	Fletcher	Fletcher	Midgley	Midgley	Hornain	Hjorth	Hjorth	Regourd & Guinier	Regourd & Guinier	Sarkar	Kristmann	Barnes & Jeffery	Barnes & Jeffery	Ghose & Barnes	Ghose & Barnes
Year	1968	1968	1968	1968	1971	1971	1971	1974	1974	1977	1977	1978	1978	1980	1981
Al <sub>2</sub> O <sub>3</sub>	1.7	1.1	1.19	2.04				2.6	1.9		2.0	0.18	7.82		
TiO <sub>2</sub>	0.3	0.2	0.18	0.12	1.20						1.5				
Fe <sub>2</sub> O <sub>3</sub>	0.8	1.5	2.16	0.69								0.16	8.62		
MnO	0.03	0.06	0.06	0.03	0.41					0.01					
MgO	0.4	0.2	0.56	0.50						3.45	0.5	0	3.45	0.33	
Na <sub>2</sub> O	0.3	0.3	0.9	1.0						2.28	0.7				
K <sub>2</sub> O	0.3	0.5	0.75	0.50		3.1	4.3	0.78	1.42	1.92	1.9	0	1.92	1.0	40.0
P <sub>2</sub> O <sub>5</sub>	0.15	0.15								2.0		0	2.17		
SO <sub>3</sub>	0.10	0.1								3.55		0	3.5	1.7	
CuO					0.2										
V <sub>2</sub> O <sub>5</sub>					2.13										
ZnO					0.03										
NiO					0.25										
Cr <sub>2</sub> O <sub>3</sub>					1.1					0.01					
CoO					0.33										

KEY

- SRC = Production sulphate resisting cement made from chalk and PFA.
- PFB = Trial SRC cement clinker with extra PFA, collected at 1030h.
- PFC = Trial SRC cement clinker with extra PFA, collected at 1530h.
- PFD = Trial SRC cement clinker with extra PFA, collected at 2030h.
- LHA = Trial Low Heat cement clinker collected at 0900h.
- LHB = Trial Low Heat cement clinker collected at 1200h.
- LHC = Trial Low Heat cement clinker collected at 1300h.
- LHD = Trial Low Heat cement clinker collected at 1500h.
- OPC = Production Ordinary Portland cement clinker.
- WPC = Production White Portland cement clinker.

(Table 8.6 ). Electron microprobe analyses (mean values)  
of Belite from works A,B,C,D,E,F and G .

Works Cement	WRKS.B SRC	WRKS.B PFB	WRKS.B PFC	WRKS.B PFD	WRKS.B LHA	WRKS.B LHB	WRKS.B LHC
SiO <sub>2</sub>	31.7	30.6	30.5	32.4	30.9	30.5	30.9
Al <sub>2</sub> O <sub>3</sub>	1.2	1.6	1.6	1.0	1.0	1.2	1.4
TiO <sub>2</sub>	0.0	0.2	0.0	0.1	0.0	0.0	0.0
Fe <sub>2</sub> O <sub>3</sub>	1.5	1.8	1.5	1.0	1.4	1.3	1.7
MnO	0.0	0.0	0.0	0.0	0.0	0.0	0.0
MgO	0.1	0.3	0.2	0.2	0.1	0.0	0.1
CaO	64.5	63.4	64.2	64.5	64.4	65.6	63.7
Na <sub>2</sub> O	0.2	0.7	0.2	0.2	0.1	0.0	0.5
K <sub>2</sub> O	0.6	0.5	0.3	0.4	0.4	0.5	0.8
P <sub>2</sub> O <sub>5</sub>	0.0	0.0	0.0	0.1	0.0	0.0	0.1
SO <sub>3</sub>	0.6	1.0	0.9	1.4	0.6	0.8	0.3
TOTAL	100.4	100.1	99.4	101.3	98.9	99.9	99.5

Works Cement	WRKS.B LHD	WRKS.A OPC	WRKS.E OPC	WRKS.C OPC	WRKS.F WPC	WRKS.D OPC	WRKS.G OPC
SiO <sub>2</sub>	30.5	31.5	31.7	29.9	30.8	31.0	31.2
Al <sub>2</sub> O <sub>3</sub>	1.2	1.5	1.6	2.2	2.4	1.8	1.8
TiO <sub>2</sub>	0.0	0.1	0.0	0.0	0.0	0.3	0.2
Fe <sub>2</sub> O <sub>3</sub>	1.5	0.8	0.7	0.8	0.0	1.0	0.9
MnO	0.1	0.0	0.0	0.0	0.0	0.0	0.0
MgO	0.0	0.5	0.5	0.2	0.0	0.4	0.4
CaO	63.7	63.8	64.2	64.3	64.9	63.8	63.5
Na <sub>2</sub> O	0.4	0.2	0.1	0.1	0.3	0.2	0.3
K <sub>2</sub> O	0.6	0.5	1.0	0.3	0.3	0.6	0.8
P <sub>2</sub> O <sub>5</sub>	0.0	0.0	0.0	0.0	0.0	0.1	0.3
SO <sub>3</sub>	0.8	0.5	0.1	1.6	0.9	0.3	0.0
TOTAL	98.8	99.4	99.9	99.4	99.6	99.5	99.4

KEY

K1 = Production Sulphate Resisting cement from Kiln 1.

K3 = Production Sulphate Resisting cement from Kiln 3.

The four digits indicate the time of collection of the clinker.

(Table 8.7 ). Electron microprobe analyses (mean values) of  
Belite from SRC clinker (K1,K3)

Sample	K11930	K12030	K12130	K12230	K12330	K10030	K10130
SiO <sub>2</sub>	31.0	30.8	31.6	32.1	31.7	31.2	32.3
Al <sub>2</sub> O <sub>3</sub>	1.3	1.4	1.1	0.9	1.0	1.3	1.1
TiO <sub>2</sub>	0.1	0.1	0.1	n.d	n.d	0.1	n.d
Fe <sub>2</sub> O <sub>3</sub>	1.5	1.9	1.6	1.3	1.4	1.9	1.3
MnO	n.d	n.d	n.d	n.d	n.d	0.1	n.d
MgO	0.1	0.2	0.2	0.1	0.1	0.3	0.1
CaO	65.1	64.0	64.2	64.0	64.4	63.8	64.3
K <sub>2</sub> O	0.6	0.9	0.8	1.0	0.7	0.9	0.7
P <sub>2</sub> O <sub>5</sub>	n.d						
SO <sub>3</sub>	0.1	0.1	n.d	n.d	0.1	n.d	n.d
TOTAL	99.8	99.4	99.6	99.4	99.4	99.6	99.8

Sample	K10230	K10330	K10430	K10530	K31930	K32030	K32130
SiO <sub>2</sub>	32.0	32.3	31.9	32.0	29.8	30.8	32.0
Al <sub>2</sub> O <sub>3</sub>	1.1	1.1	0.9	0.9	1.8	1.5	1.2
TiO <sub>2</sub>	n.d	0.1	n.d	n.d	n.d	n.d	n.d
Fe <sub>2</sub> O <sub>3</sub>	1.5	1.4	1.2	1.5	1.2	1.6	1.5
MnO	n.d	n.d	n.d	n.d	0.3	n.d	n.d
MgO	0.1	0.1	n.d	0.1	0.1	0.1	0.2
CaO	63.9	64.1	64.0	64.2	64.2	64.3	63.9
K <sub>2</sub> O	0.6	0.5	0.7	n.d	0.5	0.4	0.8
P <sub>2</sub> O <sub>5</sub>	n.d	n.d	n.d	n.d	n.d	n.d	0.1
SO <sub>3</sub>	n.d	n.d	n.d	n.d	1.4	1.2	0.1
TOTAL	99.2	99.6	98.7	98.7	99.3	99.9	99.8

Sample	K32230	K32330	K30030	K30130	K30230	K30330	K30430
SiO <sub>2</sub>	30.5	30.6	30.2	31.2	31.1	30.3	32.2
Al <sub>2</sub> O <sub>3</sub>	1.7	1.2	1.6	1.2	1.2	1.4	1.0
TiO <sub>2</sub>	n.d						
Fe <sub>2</sub> O <sub>3</sub>	2.1	1.6	1.7	1.6	1.6	1.7	1.4
MnO	n.d						
MgO	0.1	0.4	0.2	0.1	0.1	0.2	0.1
CaO	63.7	64.1	64.8	64.9	64.1	64.8	64.3
K <sub>2</sub> O	0.4	0.4	0.4	0.3	0.6	0.3	0.5
P <sub>2</sub> O <sub>5</sub>	0.1	n.d	n.d	n.d	n.d	n.d	n.d
SO <sub>3</sub>	0.9	0.9	0.6	0.3	0.8	0.7	0.1
TOTAL	99.5	99.2	99.5	99.6	99.5	99.4	99.6

KEY

K3 = Production Sulphate resisting cement ( SRC ) from kiln 3

PF = Trial SRC with PFA addition.

LH = Trial Low Heat cement clinker.

(Table 8-8 ) . Electron microprobe analyses (mean values ) of Belite from SRC clinker (K1,K3), SRC with PFA kiln addition clinker (PF) and LHC trial mix (LH) . .

Sample	K30530	PF0730	PF1130	PF1330	PF1530	PF1730	PF1930
SiO <sub>2</sub>	32.4	30.5	30.6	31.1	30.5	29.1	32.3
Al <sub>2</sub> O <sub>3</sub>	1.1	1.5	1.6	1.6	1.6	1.9	1.0
TiO <sub>2</sub>	n.d	n.d	0.2	0.2	n.d	n.d	0.1
Fe <sub>2</sub> O <sub>3</sub>	1.5	1.8	1.8	1.5	1.6	1.5	1.0
MnO	n.d	n.d	0.0	n.d	n.d	n.d	n.d
MgO	0.1	n.d	0.3	0.3	0.2	0.4	0.2
CaO	64.1	63.8	63.4	63.8	64.2	64.4	64.6
K <sub>2</sub> O	0.4	0.4	0.5	0.5	0.3	0.5	0.4
P <sub>2</sub> O <sub>5</sub>	n.d	n.d	n.d	n.d	n.d	n.d	0.1
SO <sub>3</sub>	0.2	1.1	1.0	0.6	0.9	1.1	0.4
TOTAL	99.8	99.1	99.4	99.6	99.3	98.9	100.1

Sample	PF2030	LH0900	LH1200	LH1300	LH1400	LH1500	LH1600
SiO <sub>2</sub>	32.4	30.9	30.5	31.0	30.2	30.6	30.7
Al <sub>2</sub> O <sub>3</sub>	1.0	1.0	1.1	1.4	1.4	1.2	1.1
TiO <sub>2</sub>	0.1	n.d	n.d	n.d	n.d	n.d	n.d
Fe <sub>2</sub> O <sub>3</sub>	1.0	1.2	1.4	1.7	1.7	1.5	1.5
MnO	n.d						
MgO	0.1	0.1	n.d	0.1	0.1	0.1	0.3
CaO	64.5	64.5	65.6	63.8	64.3	63.8	64.1
K <sub>2</sub> O	0.4	0.4	0.5	0.8	0.4	0.6	0.4
P <sub>2</sub> O <sub>5</sub>	n.d	n.d	n.d	1.0	n.d	n.d	n.d
SO <sub>3</sub>	1.4	0.7	0.8	0.3	1.2	0.8	1.4
TOTAL	100.9	98.8	99.9	100.1	99.3	98.6	99.5

(Figure 8.4). Number of ions substituted versus number of ions substituted in belite calculated on 4 oxygens .

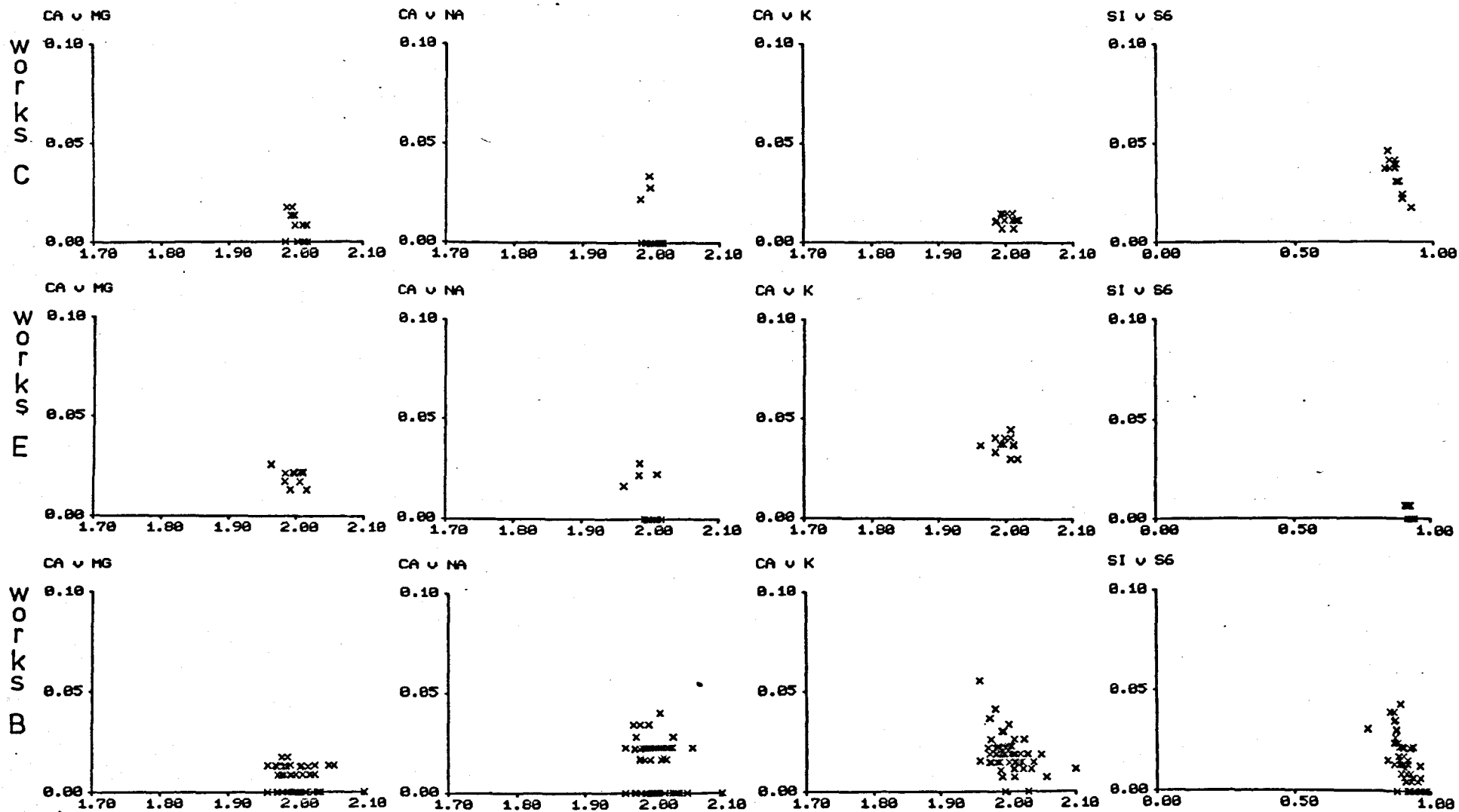
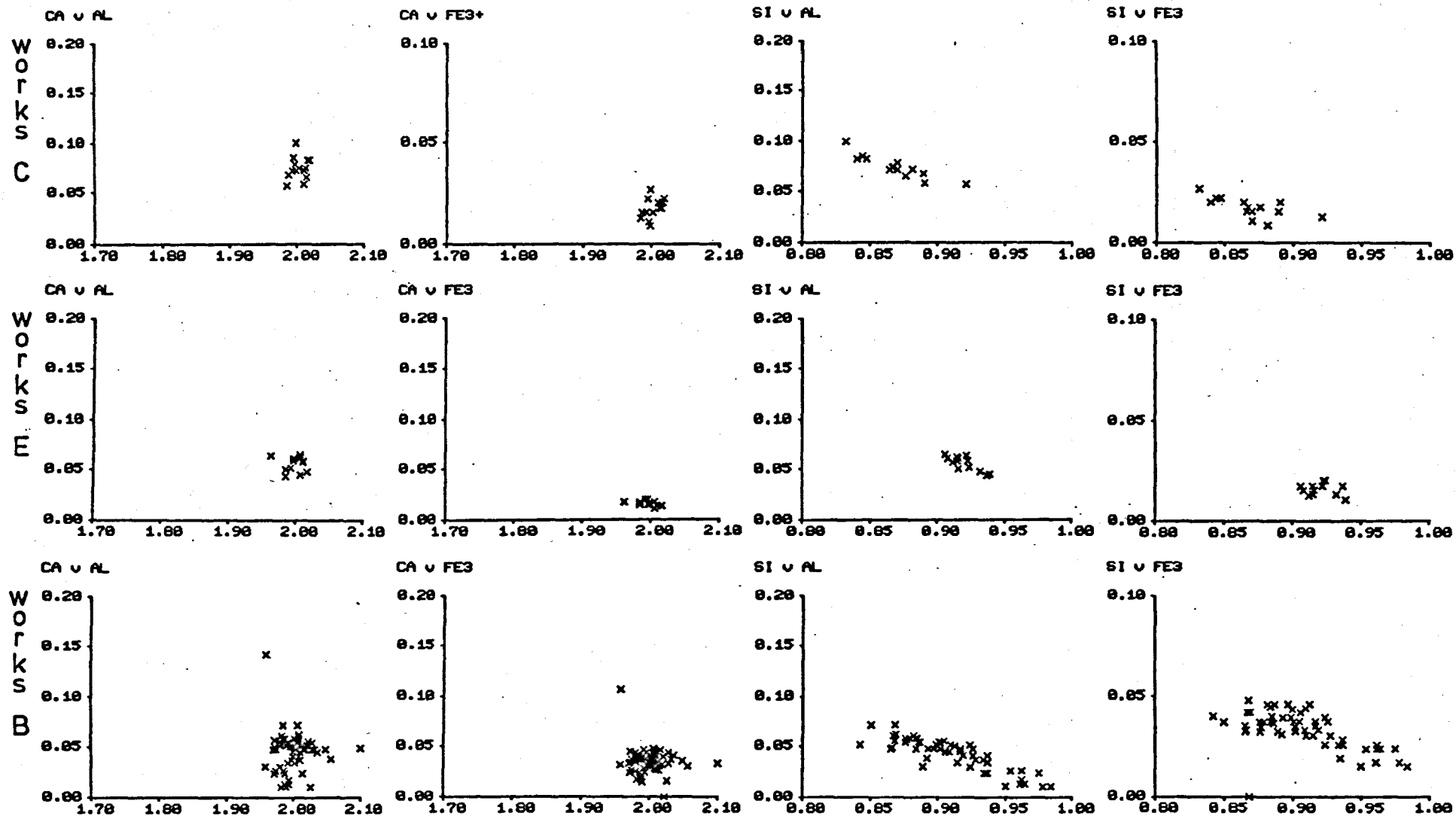


(Figure 8-5). Number of ions substituted versus number of ions substituted in belite calculated on 4 oxygens .



The mineral compositions of the belite in the cement clinkers from works A, B, C, D, E, F and G that were investigated by the author are shown in Tables 8.6, 8.7 and 8.8.

#### Substitution of MgO in belite.

Sarker (1977) found that the range of MgO in belites he analysed was between 0 and 3.5 wt.%. (Table 8.5). Barnes et al (1978) found similar values. (Table 8.5). When Ghose and Barnes (1980) made analyses of MgO levels in belite (Table 8.5), they proposed that there was a linear increase in the MgO content of the belite with increased MgO in the clinker. When Kristmann (1977) investigated the mineralogical properties of production clinker, he found that the variation of MgO in belite was between 0 and 0.5%. (Table 8.5).

The MgO content of belites from production cement clinker studied by the author, varied from 0 to 0.5%. (Figure 8.1,d) The increase was not linear, because when the MgO level in the clinker was above 2% there was no increase in the MgO content of the belite. This was because the periclase phase usually formed preferentially. The overall level of MgO in cement clinker was usually kept to less than 3%, to prevent 'unsoundness' in cement. The Mg ions substituted for Ca. (Figure 8.4 Ca v Mg).

None of these values approached the level of substitution of MgO in the bredigite ( $\alpha$ -L  $C_2S$ ) studied by Midgley and Bennett (1971). They used EMPA to analyse larnite and bredigite from Scawt Hill in Larne, Northern Ireland. These minerals are natural  $C_2S$  polymorphs. The analyses showed that the principle difference between larnite and bredigite was in the amount of calcium replaced by magnesium. In larnite there was no replacement, whilst in bredigite the amount of MgO substitution was about 13%. They concluded that larnite ( $\beta$   $C_2S$ ) could be stabilised for geological time by a very small quantity of minor elements. The bredigite phase could coexist with larnite, if it had the major substitution of magnesium for calcium.

### Substitution of $Al_2O_3$ and $Fe_2O_3$ in belite.

An extensive investigation of the mineral chemistry of belite from different manufacturing processes was carried out by Barnes et al (1978) using EMPA. ( Table 8.5) The maximum values given for some of the elements especially Fe and Al was probably due to the unintentional sampling of phases surrounding the belite crystals.

### Substitution of $Al_2O_3$ in belite.

The author has found that the level of  $Al_2O_3$  in belite against the total  $Al_2O_3$  in cement showed an overall increase with increased  $Al_2O_3$  in the cement. ( Figure 8.1,c ).

The proposal by Kristmann (1977) that Al was partitioned into the alite in a wet process kiln and into belite in a dry kiln, is not supported. If clinker D (wet) and clinker E (dry) are compared, belite D should have a lower  $Al_2O_3$  level than belite E, which it does not.

The Al ions appear to substitute for Si ( Figure 8.5, Si v Al ) rather than for Ca ( Figure 8.5, Ca v Al ), which Butt and Tismashev (1974) proposed.

### Substitution of $Fe_2O_3$ in belite.

For iron oxide there was an apparent overlap between the  $Fe_2O_3$  in the cement and the  $Fe_2O_3$  in the belite and alite (Figure 8.1,b). However if each cement was considered individually there was a preference for the  $Fe_2O_3$  to substitute in the belite phase. There was a general increase in the  $Fe_2O_3$  content of the belite with increased  $Fe_2O_3$  in the cement. The amount of substitution of Fe was controlled by the  $Al_2O_3/Fe_2O_3$  ratio of each of the individual cement clinkers.(Figure 8.1,1). The Fe ions substituted for the Si ions. ( Figure 8.5, Si v  $Fe_3$  ). If the clinker was burnt in reducing conditions, the  $Fe^{2+}$  substituted for  $Ca^{2+}$  in the belite.

### Substitution of Na<sub>2</sub>O and K<sub>2</sub>O in belite.

Ghose and Barnes (1980) studied the relationship between the distribution of minor elements and the bulk composition of the cement . They found that S, K and Fe appeared to increase linearly with increased levels in the cement. ( Table 8.5). The type of process influenced the K content of the belite . Those produced by a wet process had higher K<sub>2</sub>O values than those from a dry or semi dry process . The Na<sub>2</sub>O was generally more abundant in the matrix phases than in the alite or belite crystals .

Several researchers have tried to establish a correlation between the different polymorphs of belite and the amount of minor element substitution. Hjorth (1971) used EMPA to determine the composition of belites from cement. ( Table 8.5). Hjorth discovered that  $\beta$  C<sub>2</sub>S contained less K<sub>2</sub>O than  $\alpha'$  C<sub>2</sub>S . Regourd and Guinier (1974) found that  $\alpha'$  C<sub>2</sub>S had a higher K<sub>2</sub>O content than  $\beta$  C<sub>2</sub>S and a lower Al<sub>2</sub>O<sub>3</sub> level. ( Table 8.5). They used these differences to classify the belite polymorphs.

Sarkar (1977) thought that Regourd and Guinier's (1974) classification was over simplified. He investigated the mineralogical characteristics of belites from cement with XRD , microscopy and EMPA. Sarkar found that belite crystals, classified as  $\beta$  C<sub>2</sub>S by Regourd and Guinier's system, were determined as  $\alpha'$  C<sub>2</sub>S by XRD and microscopy.

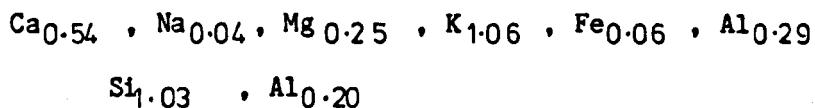
### Substitution of K<sub>2</sub>O in belite.

The level of K<sub>2</sub>O in the belite from different works varied considerably. (Figure 8.1,j). A possible explanation is that the variation was caused by the unintentional sampling of small inclusions of alkali sulphate within the belite grains. This was unlikely because the belite in clinker from Works E, which had a substantial amount of alkali sulphate phases , had low Na<sub>2</sub>O and SO<sub>3</sub> contents.(Figure 8.1,h and g ). The cause of the variation in K<sub>2</sub>O was that the partitioning of the K<sub>2</sub>O in the clinker was partially controlled by which polymorph of C<sub>3</sub>A was in the

clinker. If the aluminate was present in the cubic form the  $K_2O$  substituted preferentially into the tricalcium aluminate. ( e.g. Figure 8.6,j Works A and Figure 8.1,j Works A ) If the aluminate was in the orthorhombic form more  $K_2O$  was available for substitution in the belite. (e.g. Figure 8.6,j Works G and Figure 8.1,j Works G ). The  $K^+$  ions substituted for Ca , ( Figure 8.4,Ca v K).

This is the principal reason why Regourd and Gunier's (1974) classification of belite by  $K_2O$  and  $Al_2O_3$  content is unreliable.

An unusual phase was found by Ghose and Barnes (1981) . This was a form of belite with a very high potassium level. The atomic composition of the K-rich belite was :-



Ghose and Barnes found that only if the K was included as replacement for Ca was an acceptable calcium to silica ratio produced. They concluded that the K rich belite was a very defective  $C_2S$  structure with the potassium solubility level much higher at  $K = 1.06$  than the previously accepted level of  $K = 0.17$  .

#### Substitution of $Na_2O$ in belite.

The  $Na_2O$  content of belite was also controlled by the tricalcium aluminate polymorph present in the clinker. Thus the level of substitution of  $Na_2O$  into the belite was not directly related to the  $Na_2O$  in the clinker, except when there was little or no tricalcium aluminate present. The cements produced by Works B (Figure 8.1,k ,solid circles ) had a very low aluminate content. In these belites the  $Na_2O$  level in the belites increased linearly with increased  $Na_2O$  content in the clinker. The Na ions substituted directly for Ca. ( Figure 8.4, Ca v Na ).

#### Compositional variation in belite due to zoning.

The chemical composition of belites within a single clinker could vary

because of the different generations of crystal formation.

Skalny et al (1975) used a scanning electron microscope (SEM) with an energy dispersive x-ray analysis spectrometer (EDS) to study partially and selectively dissolved cement clinkers. The belite grains were identified by their Ca/Si ratio. Some of the belite grains were embedded in large alite crystals. These belites had a thin shell surrounding them. When this shell was analysed, the main elements were Ca, Al and Fe. Skalny proposed that they were early forming belites which had been engulfed by later alite formation. The alumina-ferrite shell had prevented reaction between the early belite and the surrounding later alite crystals.

A mineralogical study of clinker by Kristmann (1977) using EMPA showed that belite could incorporate higher levels of Na<sub>2</sub>O and K<sub>2</sub>O than the alite, ferrite or aluminate. Kristmann suggested that this indicated that the belite system closed after that of the aluminates and ferrite, because of the high ionic mobility of the alkalis. However Lehmann et al (1964) thought that the aluminate and ferrite systems were the last to crystallize.

From the features observed from microscopy and detailed mineralogical analysis the author supports the latter view that the ferrite and the aluminate phases were the last to crystallize.

These results show that the behaviour of sodium and potassium was complex. Predictions based on ionic mobility models could be misleading.

#### Substitution of transition elements in belite.

Hornain (1971) investigated the substitution of some transition elements in belite. ( Table 8.5 ). He found that V and Cr were preferentially partitioned into the belite phase. The Ti, V and Cr ions replaced Si. The elements with a higher atomic number such as Ni, Cu and Zn replaced Ca, the Mn and Co ions substituted for Ca or Si.

The only transition element that occurred in detectable quantities in belite, from the clinkers analysed by the author was titanium. The TiO<sub>2</sub>

was preferentially partitioned into the belite rather than the alite. (Figure 8.1,e). However the level of substitution was controlled by the production process. The belite in clinker from dry process kilns had very low  $TiO_2$  levels. The belite in clinker from the semi-dry and wet process kilns had higher  $TiO_2$  levels.

#### Substitution of $SO_3$ in belite.

The  $SO_3$  content of the belite varied considerably. (Figure 8.1,g). Overall there was an increase in the  $SO_3$  in the belite with an increased level of sulphate in the clinker. The principal cause of the variation was the availability of the alkalis necessary for the formation of alkali sulphate phases. If these phases formed there was less  $SO_3$  to substitute into the belite. This was shown by the low level of sulphate substitution in belite from Works E which had a substantial quantity of alkali sulphate phases present. The  $S^{6+}$  ions substituted directly for the Si ions. (Figure 8.4, Si v  $S^{6+}$ ).

#### The mineral chemistry of ferrite and aluminate in cement.

##### The ferrite solid solution series.

The early investigations into the composition of ferrite with EMPA in the mid 1960's produced very variable results. The best conclusion drawn was that the composition of the ferrite in cement was between  $C_4AF$  and  $C_6A_2F$ .

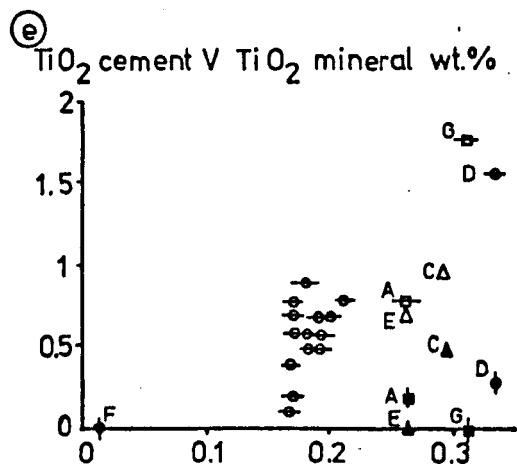
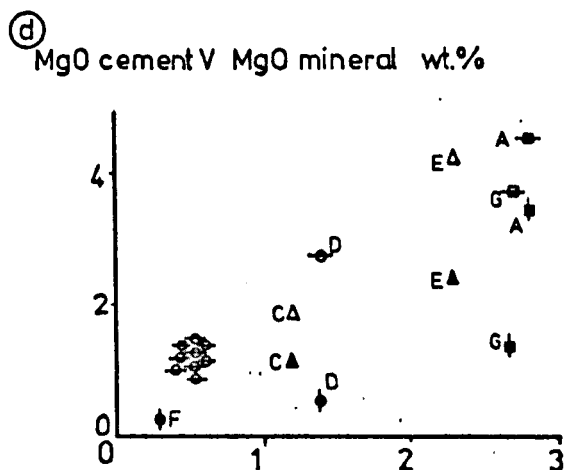
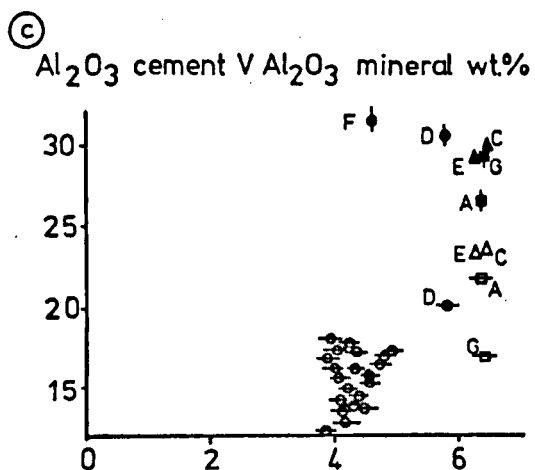
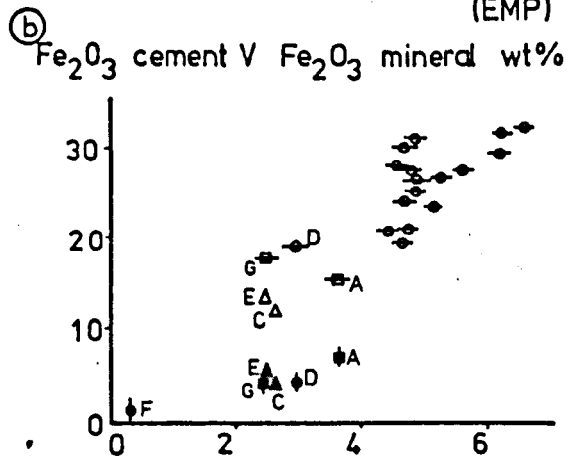
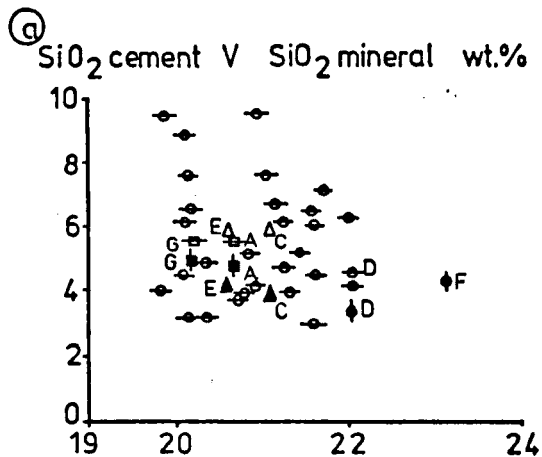
Hornain ( 1973 ) made a systematic study of ferrite composition from twenty-three different cement clinkers. Nine of the clinkers were synthetic mixes with additions of  $MgO$ ,  $TiO_2$  and  $Mn_3O_4$ . Four of the clinkers were laboratory prepared with measured amounts of  $TiO_2$  addition. The final ten samples were industrial cement clinkers. Hornain found

KEY

XRF analyses from pages 24,25,26

EMP analyses for Ferrite and Aluminate from pages 153, 154.

(Fig.8.6 ) CLINKER ANALYSIS (XRF) V ALUMINATE AND FERRITE ANALYSIS (EMP)

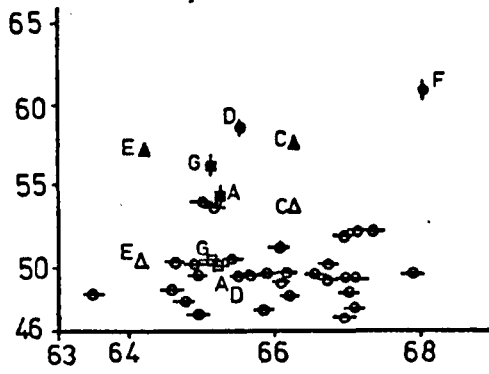


	KEY	
	ALUMINATE	FERRITE
WET PROCESS	◆	◐
SEMI-DRY PROCESS	◑	◒
DRY PROCESS	▲	△

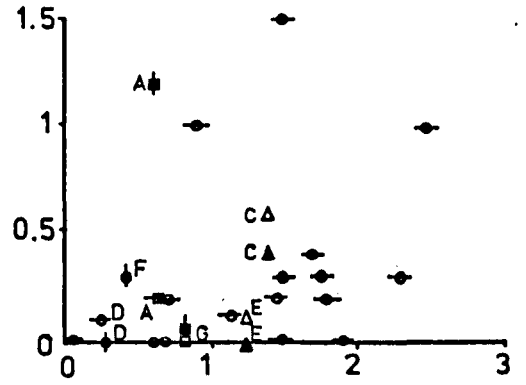
( Fig. 8.6 continued)

ALUMINATE AND FERRITE

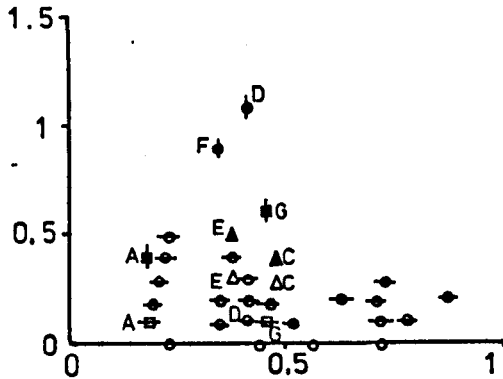
(f) CaO cement V CaO mineral wt.%



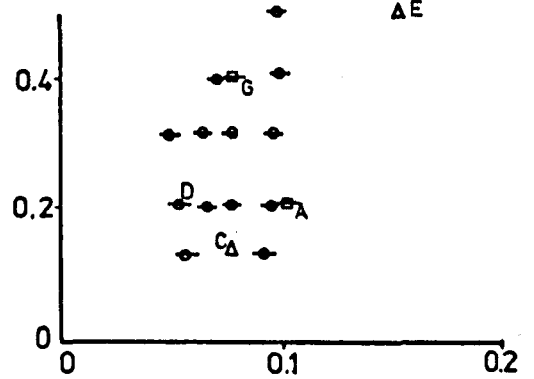
(g) SO<sub>3</sub> cement V SO<sub>3</sub> mineral wt.%



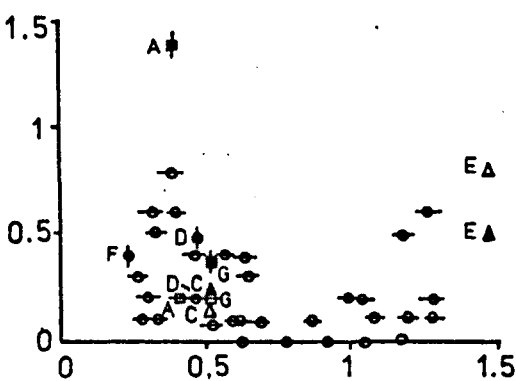
(h) Na<sub>2</sub>O cement V Na<sub>2</sub>O mineral wt%



(i) MnO cement V MnO mineral wt%



(j) K<sub>2</sub>O cement V K<sub>2</sub>O mineral wt.%



(k) Al<sub>2</sub>O<sub>3</sub>/Fe<sub>2</sub>O<sub>3</sub> V Al<sub>2</sub>O<sub>3</sub>/Fe<sub>2</sub>O<sub>3</sub> wt%

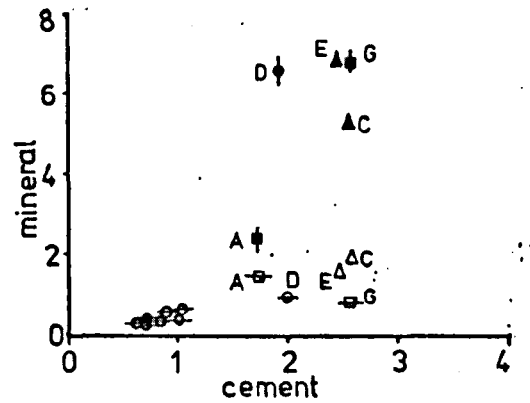


(Table 8.9 ). Electron microprobe analyses (mean value) of Ferrite from SRC clinker (K1,K3), SRC with PFA kiln addition clinker (PF) and L H trial mix (LH) .

Sample	K30530	PF0730	PF1130	PF1330	PF1530	PF1730	PF1930
SiO2	3.3	10.2	4.1	3.9	6.7	6.2	9.5
Al2O3	15.7	13.2	17.2	17.2	16.5	17.3	13.7
TiO2	0.8	0.2	0.7	0.8	0.6	0.5	0.5
Fe2O3	30.5	20.0	27.6	27.1	23.9	24.0	21.0
MnO	0.5	0.1	0.3	0.3	0.1	0.1	0.2
MgO	1.4	1.1	1.5	1.5	1.3	1.4	1.3
CaO	46.9	53.8	48.5	48.4	50.1	50.1	50.1
Na2O	0.1	0.2	0.1	0.1	n.d	n.d	0.2
K2O	n.d	0.5	0.1	0.1	n.d	0.2	0.1
P2O5	n.d						
SO3	n.d	1.0	n.d	n.d	0.3	0.1	0.3
TOTAL	99.2	100.3	100.1	99.4	99.5	99.9	96.9

Sample	PF2030	LH0900	LH1200	LH1300	LH1400	LH1500	LH1600
SiO2	9.5	8.0	7.6	3.9	3.1	3.7	6.1
Al2O3	13.7	15.9	14.0	15.5	14.0	13.8	11.9
TiO2	0.5	0.7	0.6	0.6	0.6	0.7	0.7
Fe2O3	20.9	25.6	27.8	29.0	32.0	32.1	29.0
MnO	0.1	0.4	n.d	0.2	0.3	0.6	0.6
MgO	1.2	1.1	1.1	1.2	1.1	1.1	1.1
CaO	53.7	49.7	49.7	48.0	47.8	47.3	50.2
Na2O	0.2	0.1	0.3	0.4	n.d	n.d	n.d
K2O	0.2	0.1	0.4	0.4	0.1	n.d	0.1
P2O5	n.d						
SO3	0.3	n.d	n.d	n.d	0.2	n.d	n.d
TOTAL	100.3	101.6	101.5	99.2	99.2	99.3	99.7

The last four digits after each sample identifier is the time of collection of the clinker.

(Table 8.10). Electron microprobe analyses (mean value) of Ferrite from SRC clinker (K1,K3)

Sample	K11930	K12030	K12130	K12230	K12330	K10030	K10130
SiO <sub>2</sub>	4.8	4.2	5.2	3.0	6.2	4.2	6.5
Al <sub>2</sub> O <sub>3</sub>	16.8	17.3	16.1	15.6	14.5	16.2	14.1
TiO <sub>2</sub>	0.7	0.1	0.5	0.8	0.7	0.5	0.6
Fe <sub>2</sub> O <sub>3</sub>	27.0	26.3	26.3	31.3	26.4	27.3	25.8
MnO	0.2	0.2	0.3	0.2	0.4	0.2	0.2
MgO	1.4	1.2	1.4	1.3	1.3	1.0	1.3
CaO	48.5	49.1	49.3	47.7	49.7	49.5	51.2
Na <sub>2</sub> O	0.3	0.5	0.4	n.d	0.2	0.2	0.1
K <sub>2</sub> O	0.2	0.8	0.6	0.3	0.3	0.1	0.1
P <sub>2</sub> O <sub>5</sub>	n.d						
SO <sub>3</sub>	n.d						
TOTAL	99.9	99.7	100.1	100.2	99.7	99.2	99.9

Sample	K10230	K10330	K10430	K10530	K31930	K32030	K32130
SiO <sub>2</sub>	6.3	4.5	7.2	4.5	4.5	4.1	4.8
Al <sub>2</sub> O <sub>3</sub>	16.1	17.3	14.9	15.8	13.1	15.9	17.8
TiO <sub>2</sub>	0.6	0.6	0.5	0.6	0.9	0.5	0.5
Fe <sub>2</sub> O <sub>3</sub>	25.5	26.6	23.7	27.8	31.6	28.5	26.8
MnO	0.1	0.2	n.d	0.3	0.7	0.2	0.2
MgO	1.1	1.4	1.1	1.4	1.0	1.3	1.4
CaO	49.5	49.1	51.9	48.2	47.5	47.2	49.4
Na <sub>2</sub> O	0.1	0.4	0.4	0.3	n.d	0.3	n.d
K <sub>2</sub> O	0.3	0.5	0.6	n.d	0.1	1.0	0.6
P <sub>2</sub> O <sub>5</sub>	n.d						
SO <sub>3</sub>	n.d	n.d	n.d	n.d	0.2	1.5	n.d
TOTAL	99.6	100.6	100.3	98.9	99.6	100.5	101.5

Sample	K32230	K32330	K30030	K30130	K30230	K30330	K30430
SiO <sub>2</sub>	6.1	4.6	6.6	7.7	4.3	8.9	4.0
Al <sub>2</sub> O <sub>3</sub>	17.7	15.6	16.8	13.0	16.0	12.2	17.1
TiO <sub>2</sub>	0.1	0.5	0.4	0.5	0.4	n.d	0.6
Fe <sub>2</sub> O <sub>3</sub>	21.2	25.7	25.7	24.2	28.3	25.5	28.8
MnO	n.d	0.2	0.2	0.4	0.3	0.4	0.3
MgO	1.1	1.2	0.9	1.3	1.3	1.3	1.4
CaO	52.3	49.5	50.3	52.3	49.2	49.8	48.7
Na <sub>2</sub> O	n.d	0.2	0.1	0.2	n.d	n.d	0.2
K <sub>2</sub> O	0.2	0.4	n.d	0.1	n.d	0.2	0.1
P <sub>2</sub> O <sub>5</sub>	n.d						
SO <sub>3</sub>	0.4	1.0	n.d	n.d	n.d	0.3	n.d
TOTAL	99.1	98.9	101.0	99.7	99.8	98.6	101.2

(Table 8-11 ). Electron microprobe analyses (mean values)

of Ferrite from works A,B,C,D,E,F and G .

Works Cement	WKS.B SRC	WKS.B PFB	WKS.B PFC	WKS.B PFD	WKS.B LHA	WKS.B LHB	WKS.B LHC
SiO <sub>2</sub>	5.1	4.1	6.7	9.5	4.9	7.6	3.9
Al <sub>2</sub> O <sub>3</sub>	15.8	17.0	16.5	13.7	15.8	14.1	15.5
TiO <sub>2</sub>	0.6	0.7	0.5	0.5	0.7	0.6	0.6
Fe <sub>2</sub> O <sub>3</sub>	26.7	27.6	24.0	20.9	26.8	27.8	29.3
MnO	0.3	0.3	0.1	0.2	0.4	0.2	0.3
MgO	1.3	1.5	1.4	1.3	1.1	1.1	1.2
CaO	49.7	48.5	50.5	53.7	49.7	49.7	48.0
Na <sub>2</sub> O	0.2	0.1	0.0	0.2	0.1	0.1	0.4
K <sub>2</sub> O	0.3	0.1	0.1	0.1	0.1	0.4	0.4
P <sub>2</sub> O <sub>5</sub>	0.0	0.0	0.0	0.0	0.0	0.0	0.0
SO <sub>3</sub>	0.2	0.0	0.2	0.3	0.0	0.0	0.0
TOTAL	100.2	99.9	100.0	100.4	99.6	101.6	99.6

Works Cement	WKS.B LHD	WKS.A OPC	WKS.E OPC	WKS.C OPC	WKS.D OPC	WKS.G OPC
SiO <sub>2</sub>	3.7	5.5	5.8	5.9	4.6	5.5
Al <sub>2</sub> O <sub>3</sub>	13.8	22.0	23.1	23.4	20.2	17.0
TiO <sub>2</sub>	0.7	0.8	0.7	1.0	1.6	1.8
Fe <sub>2</sub> O <sub>3</sub>	32.1	15.6	13.3	12.1	19.2	17.9
MnO	0.5	0.2	0.5	0.1	0.2	0.4
MgO	1.1	4.6	4.3	1.9	2.8	3.8
CaO	47.3	50.4	50.6	53.9	49.8	50.7
Na <sub>2</sub> O	0.1	0.1	0.3	0.3	0.1	0.2
K <sub>2</sub> O	0.1	0.2	0.8	0.2	0.2	0.2
P <sub>2</sub> O <sub>5</sub>	0.0	0.0	0.0	0.0	0.0	0.0
SO <sub>3</sub>	0.0	0.2	0.1	0.6	0.1	0.0
TOTAL	99.4	99.6	99.5	99.4	98.8	97.5

(Table 8-12 ). Electron microprobe analyses (mean values)

of Aluminate from works A,C,D,E,F and G .

Works Cement	WKS.A OPC	WKS.E OPC	WKS.C OPC	WKS.F WPC	WKS.D OPC	WKS.G OPC
SiO <sub>2</sub>	4.9	4.1	3.9	4.3	3.4	4.7
Al <sub>2</sub> O <sub>3</sub>	26.7	28.9	29.8	31.5	30.6	29.3
TiO <sub>2</sub>	0.2	0.0	0.5	0.0	0.3	0.0
Fe <sub>2</sub> O <sub>3</sub>	9.0	4.2	5.6	1.2	4.6	4.3
MnO	0.0	0.0	0.0	0.0	0.0	0.0
MgO	3.5	2.5	1.2	0.3	0.6	1.4
CaO	53.2	57.5	57.6	60.9	58.9	56.2
Na <sub>2</sub> O	0.4	0.5	0.4	0.6	0.9	1.1
K <sub>2</sub> O	1.4	0.5	0.2	0.4	0.5	0.9
P <sub>2</sub> O <sub>5</sub>	0.0	0.0	0.0	0.0	0.0	0.0
SO <sub>3</sub>	1.2	0.0	0.4	0.3	0.0	0.0
TOTAL	100.5	98.2	99.6	99.5	99.8	97.9

( Table 813) The variation in the levels of element substitution in Tricalcium aluminate and Ferrite , determined by electron microprobe analysis. ( in wt.% oxide )

Phase	Tricalcium aluminate	Tricalcium aluminate	Ferrite	Ferrite	Ferrite
Author	Fletcher	Hornain	Hornain	min. Kristmann	max. Kristmann
Year	1969	1971	1971	1977	1977
SiO <sub>2</sub>	4.0			1.8	3.1
TiO <sub>2</sub>	0.5	0.48			
Fe <sub>2</sub> O <sub>3</sub>	6.0				
MnO		0.04	5.8		
MgO	0.5			1.9	3.2
Na <sub>2</sub> O	1.0			0.1	0.3
K <sub>2</sub> O	1.0			0.1	0.2
CuO		0.38	1.45		
V <sub>2</sub> O <sub>5</sub>		0.05	0.1		
ZnO		0.39	1.5		
NiO		0.33	3.6		
Cr <sub>2</sub> O <sub>3</sub>		0.06	3.6		
CoO		0.58	5.0		

(Figure 8-7). Number of ions substituted versus number of ions substituted in ferrite calculated on 10 oxygens .

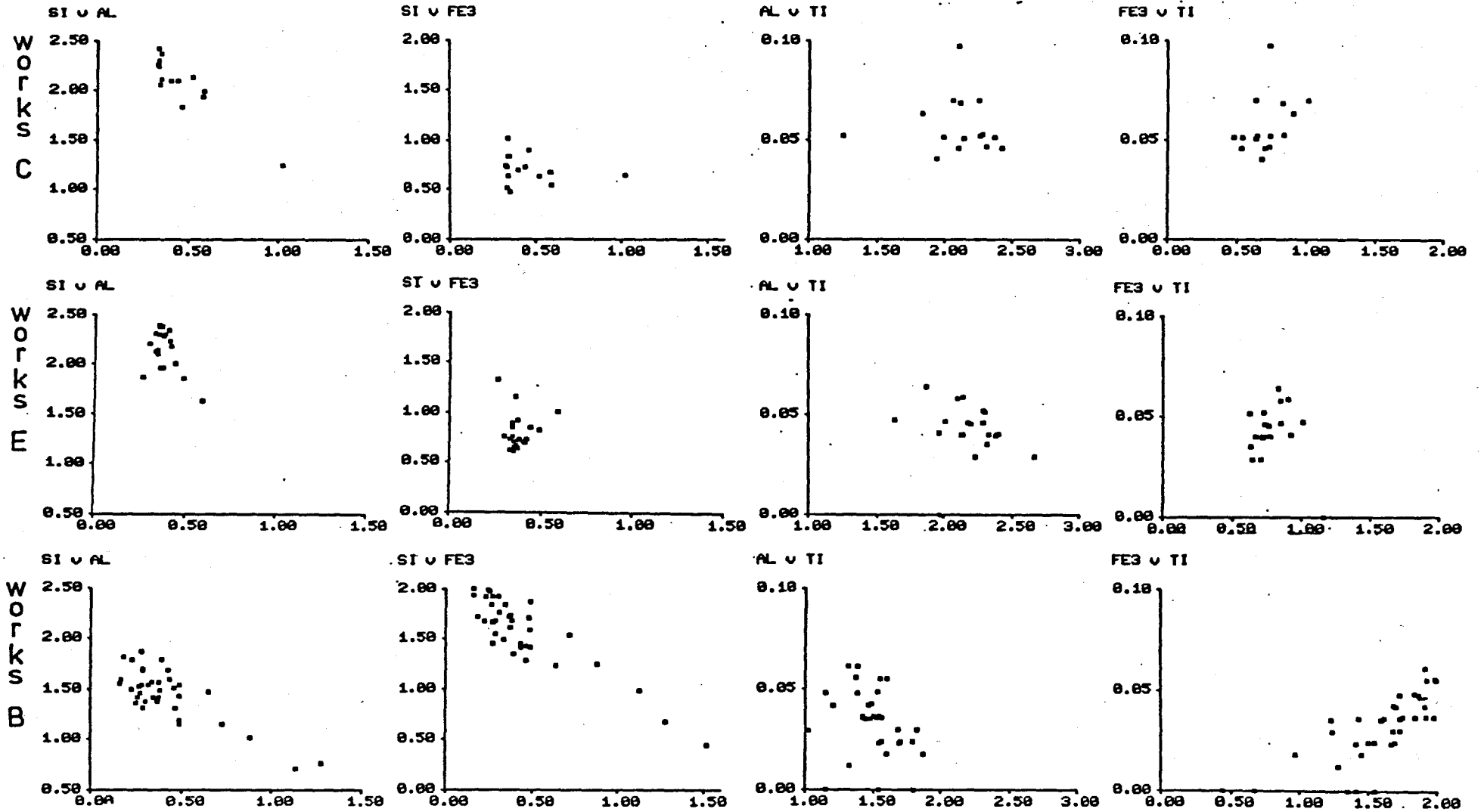
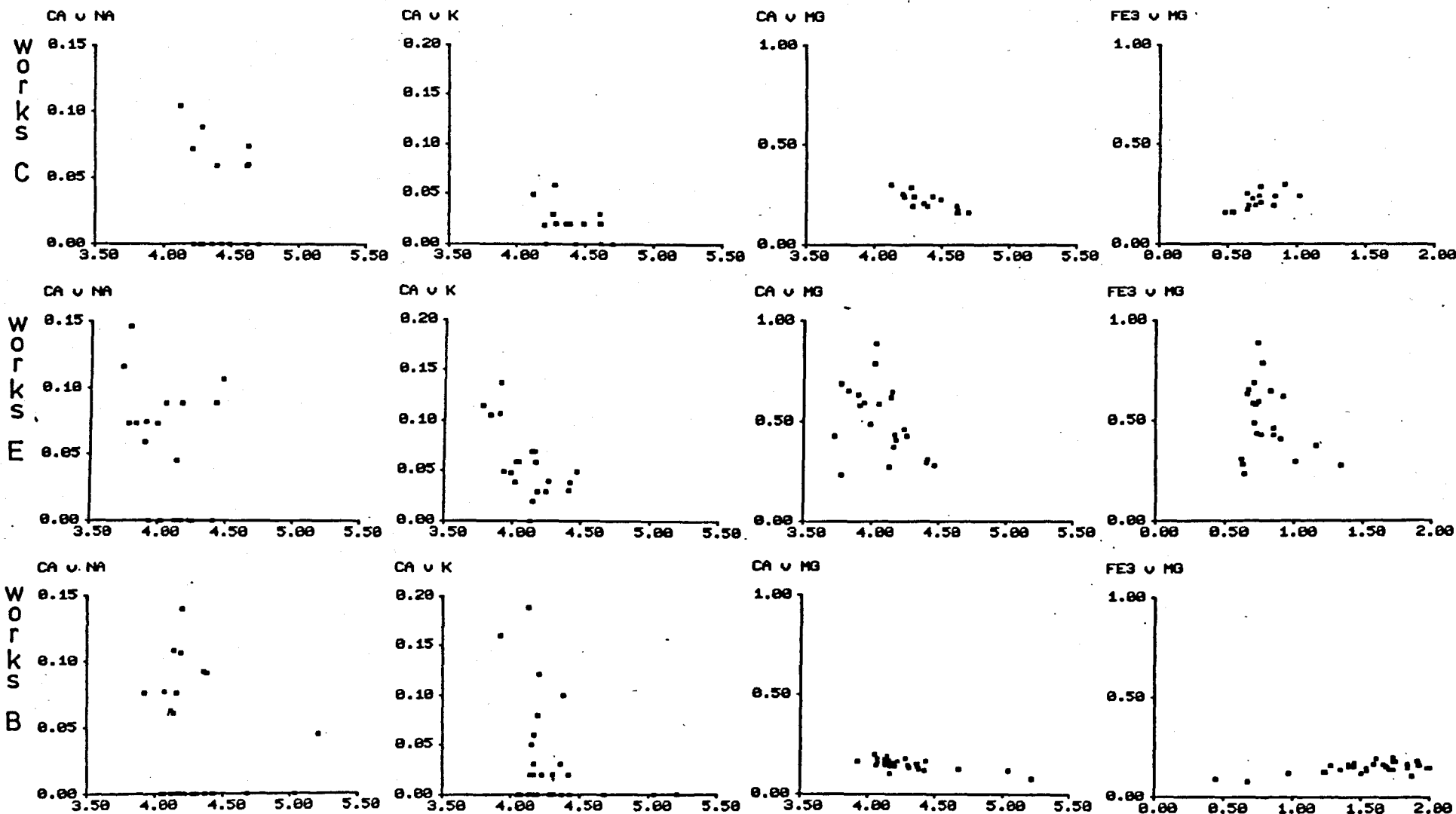


(Figure 8-8). Number of ions substituted versus number of ions substituted in ferrite calculated on 10 oxygens .



that the ferrite phase had different crystalline forms , from fibrous structures to large plate like forms . The ferrite crystals were always closely associated with aluminate crystals .

Hornain found that the  $\text{Al}_2\text{O}_3/\text{Fe}_2\text{O}_3$  molecular ratio of the ferrite increased linearly with the increase of the  $\text{Al}_2\text{O}_3/\text{Fe}_2\text{O}_3$  molecular ratios of the clinker until the clinker  $\text{Al}_2\text{O}_3/\text{Fe}_2\text{O}_3$  ratio was about 3 . The  $\text{Al}_2\text{O}_3/\text{Fe}_2\text{O}_3$  ratio in the ferrite was about 1.5 and remained at this level despite increases in the  $\text{Al}_2\text{O}_3/\text{Fe}_2\text{O}_3$  clinker ratio .

In the samples studied by the author, the range of  $\text{Al}_2\text{O}_3/\text{Fe}_2\text{O}_3$  ratios of the ferrite (Figure 8.6,k) was greater than the range proposed by Hornain.

The mineral compositions of the ferrite phases in the cement clinkers from works A, B, C, D, E and G , investigated by the author are shown in Tables 8.9, 8.10 and 8.11.

#### Substitution of $\text{SiO}_2$ and MgO in ferrite.

The  $\text{SiO}_2$  content of the cement did not directly influence the level of  $\text{SiO}_2$  substitution in the ferrite. (Figure 8.6,a). This was because the Si ions had a linked substitution with the Mg ions in the Al and Fe sites.

Hornain (1973) noted that the  $\text{SiO}_2$  content the ferrite was dependent on the MgO content . This was because there was a linked replacement . The small  $\text{Si}^{4+}$  ions ( 0.39Å ionic radius. ) replaced the large  $\text{Al}^{3+}$  ions (0.57Å ) and the large  $\text{Fe}^{3+}$  ions ( 0.68Å ). This created a vacant site and allowed the Mg ions ( 0.78Å ) to enter the lattice. The maximum MgO content of the ferrite was about 3%. The Mg ion replaced Ca and to a certain extent Fe by the following system.

An  $\text{Mg}^{2+}$  ion replaced a  $\text{Ca}^{2+}$  ion  
Three  $\text{Mg}^{2+}$  ions replaced two  $\text{Fe}^{3+}$  ions  
Plus one  $\text{Mg}^{2+}$  ion in an interstitial site.

Hornain found that the variation between the MgO content of the ferrite and the MgO content of the clinker, was caused the different thermal histories of the clinkers. If the clinker had been rapidly cooled, the MgO in the ferrite was approximately twice the MgO content of the clinker. If the clinker was cooled slowly, a greater proportion of the clinker MgO could crystallise as periclase. In industrial cement clinker this characteristic is important. This is because in normally cooled clinker, less periclase would form. This reduced the susceptibility to 'unsoundness' in the cement caused by the inversion of periclase to brucite.

In the production cement clinkers investigated by the author, the MgO in the ferrite increased generally with increased MgO in the clinker. (Figure 8.6,d). The linked substitutions of Si for Fe and Al, with Mg for Ca and Fe are shown in Figure 8.7 and figure 8.8. When the level of Mg substitution was low, the Mg ions replaced the Ca ions and the Si ions replaced Al and Fe, as shown in Figures 8.7 and 8.8 for Works B. When the level of Mg substitution increased, the Mg ions also replaced the Fe ions. This caused the variation between the Ca v Mg and the Fe v Mg substitution systems (Figure 8.8) for works B and works C ferrite with low MgO and the Fe v Mg (Figure 8.8) substitution for Works E ferrite with high MgO levels.

The ferrite with the highest MgO level of 4.5% (Figure 8.6,d) exceeded the 3% limit of substitution proposed by Hornain.

#### Substitution of Na<sub>2</sub>O in ferrite.

The Na<sub>2</sub>O level in ferrite was usually low, less than 0.5%, (Figure 8.6,k) and the Na substituted for Ca. ( Figure 8.8, Ca v Na ). The Na<sub>2</sub>O substitution in the ferrite was controlled by the tricalcium aluminate polymorph present in each of the individual clinkers. If the Na<sub>2</sub>O stabilised the orthorhombic form, there was less Na<sub>2</sub>O to substitute in the

other phases. If the cubic polymorph of aluminate was stabilised, less Na was substituted in the aluminate and the balance would substitute into the other phases.

#### Substitution of K<sub>2</sub>O in ferrite.

The K<sub>2</sub>O content in the ferrite was not directly controlled by the K<sub>2</sub>O in the clinker. (Figure 8.6,j) The K<sub>2</sub>O substitution was influenced by the aluminate polymorph in a similar manner to that of Na. The K ions substituted for the Ca ions, ( Figure 8.8, Ca v K).

#### Substitution of transition elements in ferrite.

Hornain (1971) used EMPA to investigate the proportioning of the transition elements between the different cement phases . The elements were added seperately to individual samples of the cement. The results are shown in Table 8.13. Hornain found that the Mn , Co , Ni , Cu , Ti and Zn were preferentially concentrated in the ferrite . The majority of the elements Mo , Co and Ni replaced Fe . The Ti ion replaced Fe primarily, but it also replaced Al to a limited extent . With Ni substitution there was an overall increase in the Al content of the ferrite at the expense of Fe . When the analyses were recalculated to 15 oxygens from the general formula  $Ca_6 ( Al,Fe_2 ) O_{15}$  there was a constant excess of calcium as well as a deficiency of alumina and iron . This was caused by the unavoidable analysis of many small inclusions of aluminate and calcium silicates within the ferrite. Hornain found that the TiO<sub>2</sub> content of the ferrite was always about six times greater than the TiO<sub>2</sub> level in the clinker.

The only transition elements that occurred at detectable levels in the production cements investigated by the author were Ti and Mn. There was a linear increase in the TiO<sub>2</sub> in the ferrite , as the TiO<sub>2</sub> in the clinker increased ( Figure 8.6,e). However the level of substitution was substantially less than six times the level of TiO<sub>2</sub> in the clinker

proposed by Hornain. For the cement clinkers with a low titanium content ( Works B and E ), the Ti substituted for Al, ( Figure 8.7, Al v Ti). In clinker with a higher TiO<sub>2</sub> content, (Works C ), the Ti substituted for Al and Fe. ( Figure 8.7 Al v Ti and Fe v Ti ).

#### Substitution of MnO in ferrite.

Hornain found that the MnO content of normal clinker was generally low, about 0.1%. The Mn was preferentially substituted in the ferrite phase and replaced the Fe ions. The MnO level in the ferrite was about twelve times more than the MnO level in the clinker.

The MnO content in the ferrite from the works investigated by the author was considerably higher than the 0.1% found by Hornain. The level of MnO in the ferrite was directly related to the MnO in the clinker. The presence or absence of MnO and the level of TiO<sub>2</sub> in analyses of the matrix, were good indicators to whether the phase was low iron ferrite or high iron aluminate. The tricalcium aluminate had no MnO and very low TiO<sub>2</sub>, usually less than 0.5%. The ferrite had some MnO and a TiO<sub>2</sub> level greater than 0.5%. This criteria provides a better method for separating the ferrite and aluminate analyses, than the method proposed by Kristmann (1977). He found that by utilising the differences in Al and Fe count ratios it was possible to distinguish between aluminate and ferrite electron microprobe analyses.

Kristmann found that the compositions of the ferrites varied, ( Table 12.1) . His analyses were plotted on a ternary phase diagram of CaO, Al<sub>2</sub>O<sub>3</sub> and Fe<sub>2</sub>O<sub>3</sub>. The composition of the ferrite from the OPC clinker was between C<sub>6</sub>A<sub>2</sub>F and C<sub>4</sub>AF. This contradicted the compositions which had been calculated from X-ray diffraction data. This indicated that the composition was between C<sub>4</sub>AF and C<sub>6</sub>AF<sub>2</sub>.

Woermann et al (1968) proposed that the ferrites were in the solid solution series Ca<sub>2</sub>(Fe<sub>1-p</sub>Alp)<sub>2</sub>O<sub>5</sub>. The value of p could be any value between 0 and 0.7. In the majority of industrial cement clinkers the

values were between 0.4 and 0.6.

### The mineral chemistry of tricalcium aluminate.

The major aluminate phase in Portland cement is tricalcium aluminate ( $C_3A$ ).

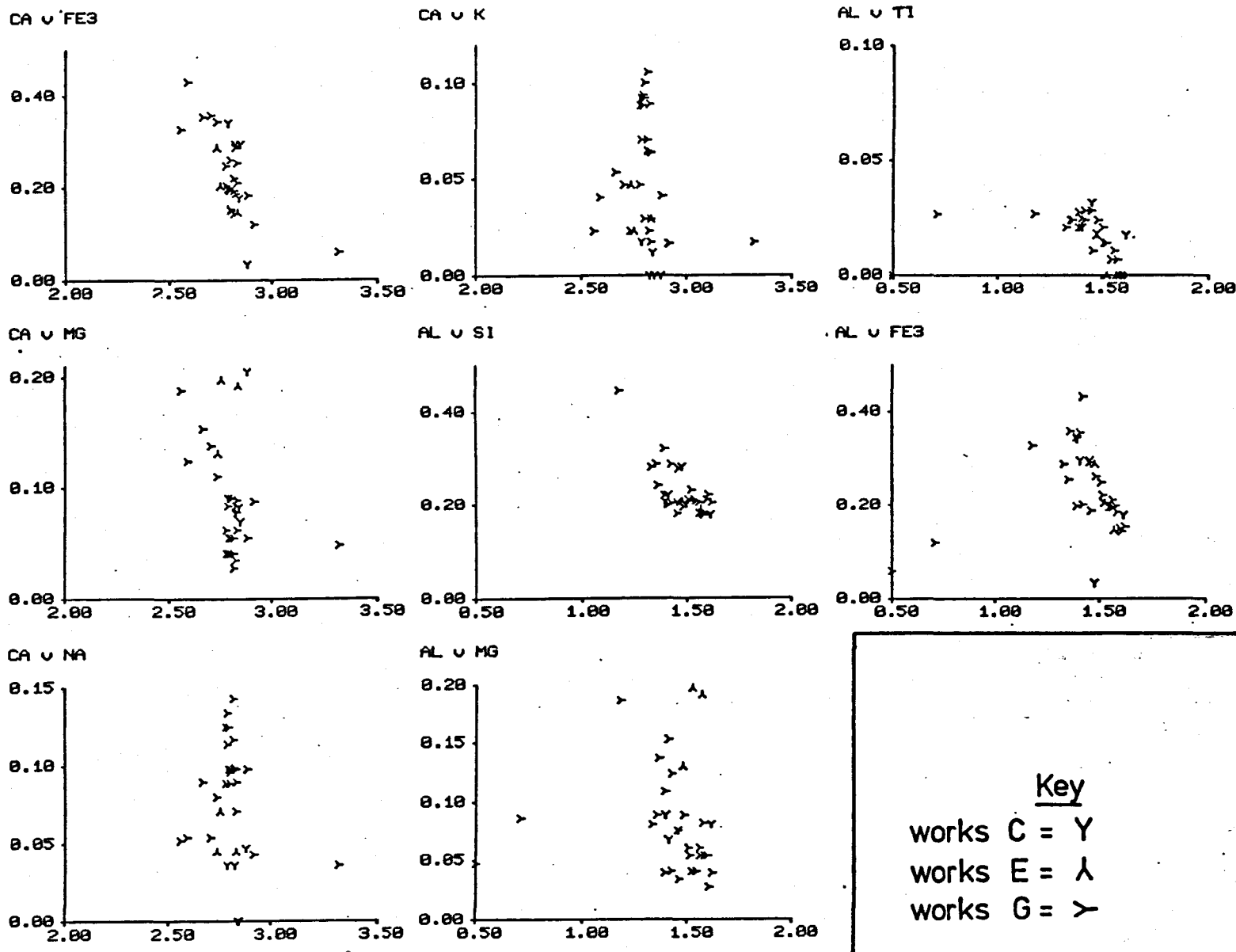
The presence or absence of it in cement is of major significance because of its rapid hydration characteristics and susceptibility to sulphate attack. The  $C_3A$  level in portland cement ranges from nil to about 15%. The size of the crystals varied from 5 $\mu$ m. to 30 $\mu$ m. The small crystals were difficult to analyse using EMPA without inadvertently sampling the adjacent phases, usually ferrite. The behaviour of  $C_3A$  in solid solutions was complex and was related to the crystal form, either cubic, orthorhombic or monoclinic. Muller-Hesse and Schwiete (1956) established that a level of 3%  $Na_2O$  substitution would stabilize the orthorhombic form. Fletcher (1969) used EMPA to analyse  $C_3A$  from an industrial cement clinker (Table 12.1). Fletcher found that alkalis substituted for Ca, the other minor elements substituted for Al.

The mineral compositions of the tricalcium aluminate phases in the cement clinkers from works A, C, D, E, F and G investigated by the author are shown in Table 8.12.

### Substitution of $SiO_2$ in tricalcium aluminate.

The level of substitution of Si into the aluminate was not directly controlled by the  $SiO_2$  content of the clinker. (Figure 8.6,a). This was because of the variable substitution of Fe ions for Al. These were in the same sites as the substituting Si ions occupied. The level of Fe substitution was dependant on the  $Al_2O_3/Fe_2O_3$  ratio of the clinker. (Figure 8.6,k)

(Figure 8-9). Number of ions substituted versus number of ions substituted in aluminate calculated on 6 oxygens .



Substitution of  $\text{Fe}_2\text{O}_3$  in tricalcium aluminate.

The  $\text{Fe}^{3+}$  substitution into the aluminate increased linearly as the  $\text{Fe}_2\text{O}_3$  content in the clinker increased. (Figure 8.6,b). The  $\text{Fe}^{3+}$  ions replaced the Al ions. (Figure 8.9 Al v  $\text{Fe}_3$ ). There was not a solid solution between  $\text{C}_3\text{A}$  and the ferrite solid solution series.

The stoichiometry of  $\text{Al}_2\text{O}_3$  in tricalcium aluminate.

The variation of  $\text{Al}_2\text{O}_3$  in the  $\text{C}_3\text{A}$  of the different clinkers (Figure 8.6,c), was primarily due to the substitution of Al by the other elements. This was controlled by the  $\text{Fe}_2\text{O}_3/\text{Al}_2\text{O}_3$  ratio of the clinker and the amount of alkalis in the clinker. The  $\text{Al}_2\text{O}_3/\text{Fe}_2\text{O}_3$  ratio of the tricalcium aluminate was substantially higher than the  $\text{Al}_2\text{O}_3/\text{Fe}_2\text{O}_3$  ratio of the clinker (Figure 8.6,k). This was because the liquid fraction which was produced in the burning process and from which the  $\text{C}_3\text{A}$  crystallized, had been depleted in iron. This was because the ferrite phases crystallized before the formation of the aluminate phase.

Substitution of MgO in tricalcium aluminate.

The level of Mg replacement in the  $\text{C}_3\text{A}$  increased generally with increased MgO in the clinker. (Figure 8.6,d) However if there was a substantial amount of periclase formed in the clinker, for example in the clinker from Works G, the amount of Mg substituted was lower than expected. The formation of the periclase was usually controlled by the cooling of the clinker as described previously for MgO substitution in the ferrite. The Mg appears to substitute for the Ca ions (Figure 8.9, Ca v Mg) and not for the Al ions, which was proposed by Hornian (1971).

The stoichiometry of CaO in tricalcium aluminate.

The CaO content of the tricalcium aluminate was not directly controlled

by the CaO levels in the clinker. (Figure 8.6,f). This was because the alkali elements substituted for the Ca ions . The level of alkali substitution into the aluminate determined which polymorphic form of aluminate was stabilized.

#### Substitution of Na<sub>2</sub>O and K<sub>2</sub>O in tricalcium aluminate.

The alkalis substituted for Ca, (Figure 8.9, Ca v K and Ca v Na ). If there was a high level of potassium and a low level of sodium available for substitution, the cubic polymorph was stabilized. If the potassium was low and the sodium was high the orthorhombic polymorph was stabilized. The availability of the alkalis for substitution was dependent, on the actual levels of alkali in the cement clinker and whether or not there was extensive development of alkali sulphate phases.

#### Substitution of SO<sub>3</sub> in tricalcium aluminate.

The levels of SO<sub>3</sub> in the aluminate and ferrite were extremely variable (Figure 8.6,g ) . This was thought by the author, to be due to the presence of small crystals of calcium sulphate in the matrix. These were unintentionally analysed because the electron micro probe beam interaction zone was often larger , 10 μm , than the size of the crystals of the matrix phases, 5 to 15 μm .

#### Substitution of transition elements in tricalcium aluminate.

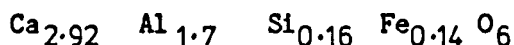
Hornain (1971) used EMPA to investigate the substitution of transition elements in C<sub>3</sub>A ( Table 8.13). None of the transition elements were preferentially partitioned into the C<sub>3</sub>A. The proportions of V,Cr and Mn substituted were extremely small. The other elements Co,Ni,Cu and Zn all substituted for the Fe or Si ions, which were themselves substituted elements, in the aluminate.

The overall level of TiO<sub>2</sub> substitution in the C<sub>3</sub>A was low , generally less than 0.5% (Figure 8.6, e). This level was not usually exceeded

even if the  $TiO_2$  content of the clinker was high. The Ti substituted for the Al (Figure 8.9, Al v Ti) This feature of low values, was useful to distinguish between analyses of tricalcium aluminates with a high level of Fe substitution and ferrites with a low iron content.

Compositional formula of tricalcium aluminate in cement.

Terrier and Hornain (1977) investigated the composition of aluminate from twenty-six cement clinkers. (Table 12.1) Some were from production kilns, the majority were laboratory prepared samples. Terrier and Hornain proposed that Si and Fe substituted for Al, atom for atom. On a basis of 6 oxygens the compositional formula of  $C_3A$  in cement was :-



They proposed that Mg and Ti substituted for Al and that Na and K substituted for Ca. This partly disagreed with Fletcher (1969), who had proposed that Mg substituted for Ca.

The author supports the latter proposal that Mg substituted for Ca. (Figure 8.9, Ca v Mg).

Kristmann (1977) used EMPA to study the composition of  $C_3A$  from many industrial cement clinkers. (Tables 8.13 and 12.1). He proposed that since in all the tricalcium aluminates some of the Al was replaced by Fe, the mineral formula was  $(Ca_3 (Fe_{1-p} Al_p)_2 O_6)$ . The values for p were between 0.80 and 0.90.

Preferred substitutions.

The preferential partitioning of the major and minor elements into the principal cement clinker phases is summarised in Table 8.14.

TABLE { 8.14 } Preferences of cement clinker minerals for major and minor oxides.

	SiO <sub>2</sub>	Al <sub>2</sub> O <sub>3</sub>	TiO <sub>2</sub>	Fe <sub>2</sub> O <sub>3</sub>	MnO	MgO	CaO	Na <sub>2</sub> O	K <sub>2</sub> O	SO <sub>3</sub>
Alite (rhomb)	3	1	1	1	2	1	4	1	1	1
Alite (mono 3)	3	1	1	1	2	2	4	1	1	1
Alite (mono 1)	3	1	1	1	2	2	4	1	1	1
Belite (alpha')	4	2	3	2	3	1	3	2	3	4
Belite (alpha)	4	2	3	2	3	1	3	2	3	4
Belite (beta)	4	2	3	2	3	1	3	2	2	4
Alu C3A (cubic)	1	4	2	3	1	3	2	3	4	3
Alu C3A (ortho)	1	4	2	3	1	3	2	4	3	3
Ferrite	2	3	4	4	4	4	1	3	2	2

Highest preference is 4 , lowest preference is 1

Mineral chemistry of the alkali sulphate phases.

Introduction

The presence of alkali sulphates in cement clinker is of more significance than the actual percentage content would indicate. The occurrence of alkali sulphates can effect the workability, setting and compressive strength of the cement. Cements with high alkali levels can also suffer from low durability due to alkali-aggregate reactions.

The alkali sulphate phases are soluble in water and some of the minerals will dissolve rapidly on contact with water. Others react with water and form a hydrated compound. These are the alkalis that have most direct effect on the quality of the cement in the early stages, the workability and the setting. The effects on the compressive strength is related to the alkali elements substituted in the calcium silicates and matrix phases. Indirectly the presence of alkali sulphates influences the strength of the cement because the composition of the alkali sulphate determines the availability of the alkali elements, which substitute in the major cement clinker phases.

The alkali sulphates in cement clinker.

Composition of alkali sulphate phases.

The alkali elements in clinker originate from two sources, the raw materials and the fuel. Pollitt and Brown (1968) found that if there was sufficient  $\text{SO}_3$  available, the alkalis  $\text{K}_2\text{O}$  and  $\text{Na}_2\text{O}$  occurred as sulphates. The quantity of alkali sulphate was determined by the ratio of total clinker sulphate to total alkali content. Pollitt and Brown proposed that potassium was likely to occur as potassium sulphate or by preference as one of two other sulphate forms depending on the amount of available sodium

(Table 8.15). Electron probe micro analysis of alkali sulphates present in cement clinker

Phase Analysis	CKS 32	CKS 33	KS 86	ASO 22	ASO 4	NKS 12
SiO2	1.0	2.7	0.4	2.6	2.2	0.9
Al2O3	n.d	n.d	n.d	0.3	0.4	0.9
TiO2	1.4	0.5	0.3	0.4	n.d	n.d
Fe2O3	n.d	n.d	n.d	0.4	0.6	0.3
MgO	n.d	n.d	n.d	n.d	n.d	n.d
CaO	35.0	32.6	2.2	12.9	14.5	4.2
Na2O	0.3	2.7	3.0	6.6	4.1	7.8
K2O	10.9	12.2	48.9	33.0	32.6	40.9
P2O5	n.d	n.d	n.d	n.d	n.d	n.d
SO3	50.6	45.3	44.2	42.1	42.7	37.6
TOTAL	99.2	96.1	98.9	98.4	97.3	92.5

Phase Analysis	ASO 13	NKS 14	KS= 1	NK= 1	CK= 1
SiO2	2.4	1.4	n.d	n.d	n.d
Al2O3	5.7	n.d	n.d	n.d	n.d
TiO2	n.d	n.d	n.d	n.d	n.d
Fe2O3	2.6	n.d	n.d	n.d	n.d
MgO	n.d	n.d	n.d	n.d	n.d
CaO	16.7	1.9	n.d	n.d	25.2
Na2O	5.6	7.5	n.d	9.3	n.d
K2O	29.8	44.0	54.0	42.5	21.1
P2O5	n.d	n.d	n.d	n.d	n.d
SO3	30.0	43.2	46.0	48.2	53.7
TOTAL	92.7	98.0	100.0	100.0	100.0

Stoichiometric compositions of alkali sulphates.

KS= is potassium sulphate  $K_2SO_4$

NK= is sodium potassium sulphate  $Na_2SO_4 \cdot 3K_2SO_4$

CK= is calcium potassium sulphate  $2CaSO_4 \cdot K_2SO_4$

NOTE.

ASO is a mixture of two or more alkali sulphates.

sulphate and calcium sulphate . The sodium sulphate might occur alone , but more likely it would combine with potassium and form a double alkali sulphate. The calcium could form calcium sulphate or as a calcium potassium sulphate , subject to the potassium sodium sulphate having formed previously. Overall the potassium sulphate was more likely to occur than the sodium sulphate.

Jawed and Skalny (1977) proposed that the compositions of the alkali sulphates which could occur in cement clinkers were;

Potassium sulphate (Arcanite)  $K_2SO_4$  .

Sodium potassium sulphate (Aphtitalite)  $Na_2SO_4 \cdot 3K_2SO_4$  or similar solid solution

Calcium potassium sulphate ( Calcium langbeinite )  $2CaSO_4 \cdot K_2SO_4$  or similar solid solution.

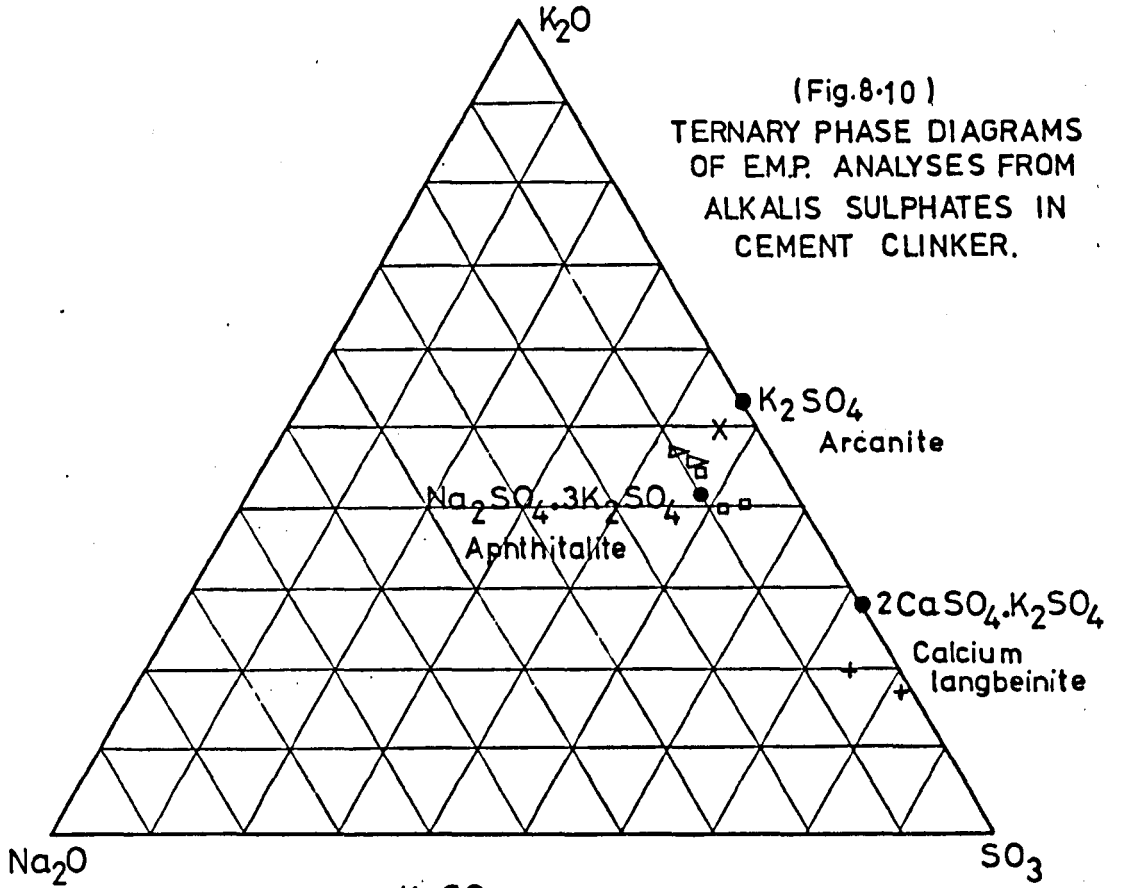
Mander (1977) reported that the burning zone atmosphere influenced the alkali sulphate phase formation . The calcium potassium sulphate was produced in an oxidising environment . The sodium potassium sulphate was formed in reducing conditions.

#### Mineral chemistry of the alkali sulphates.

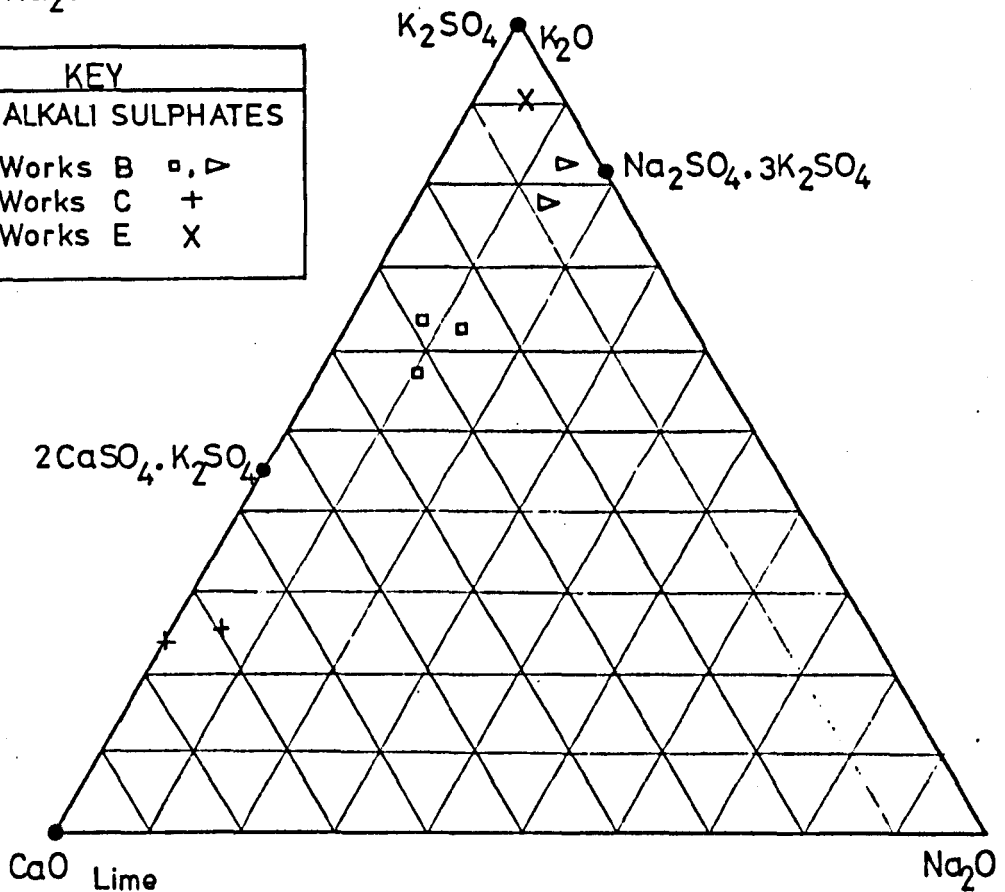
The chemical composition of the alkali sulphates found in the cement clinkers from the different cement works is shown in Table 8.15. The minerals are in solid solution series so the composition varies considerably. When the mineral analyses of the alkali sulphates was plotted on the ternary phase diagram  $CaO - K_2O - Na_2O$  and  $K_2O - Na_2O - SO_3$ , the variation is clearly shown. (Figure 8.10). Some of the compositions appear to be between two different phases. These analyses are probably the result of analysing fragments of several different crystals together.

The alkali sulphates from works C were the calcium potassium sulphate. The sulphates from works E were the potassium sulphate. The alkali

(Fig.8.10)  
 TERNARY PHASE DIAGRAMS  
 OF E.M.P. ANALYSES FROM  
 ALKALIS SULPHATES IN  
 CEMENT CLINKER.



KEY	
ALKALI SULPHATES	
Works B	□, ▷
Works C	+
Works E	X



sulphates from works B were the sodium potassium sulphates. There was sodium available because it had not been preferentially substituted into the tricalcium aluminate phase. The level of tricalcium aluminate in the clinker from works B was very low since the types of cement manufactured were sulphate resisting or low heat cement.

The occurrence of the alkali sulphates is extremely important because of their influence on the formation and stabilisation of the belite and tricalcium aluminate phases. The potassium based sulphates were the most likely alkali sulphate phases to form. This reduced the availability of the potassium to substitute in the tricalcium aluminate and stabilize the cubic form.

The mineral assemblages in cement clinker from the quaternary system CaO - SiO<sub>2</sub> - Al<sub>2</sub>O<sub>3</sub> - Fe<sub>2</sub>O<sub>3</sub>.

Introduction.

The mineral compositions of the calcium silicates, ferrites and aluminate phases from the cement clinkers studied by the author, have been plotted onto ternary phase diagrams, CaO - SiO<sub>2</sub> - Al<sub>2</sub>O<sub>3</sub> and CaO - Al<sub>2</sub>O<sub>3</sub> - Fe<sub>2</sub>O<sub>3</sub>. ( The figures 8.11 to 8.22 show subsystems of the main system. This is to enlarge the relevant section of the system to aid interpretation.) The phase boundaries, mineral compositions, temperatures of phase boundary intersections and compositional triangles are shown on Figure 8.11.

The compositions of the mineral phases in weight percent element, from each cement clinker of a different works or process has been plotted on an individual diagram. For several clinkers the analyses have been subdivided by symbols to show differences between compositions in the reduced and normal clinker. The analyses of the PFA addition clinker and the trial Low Heat Cement clinker from works B have been subdivided into timed samples. These were collected at different stages throughout the production trials.

Comparison of the mineral assemblages of ordinary portland cement clinker from dry process cement kilns.

Works C and E (Figures 8.12 and 8.13).

The calcium silicate phases in the clinkers from works C and E had slight variations in composition. There was a higher calcium to silica ratio in the alite from works C. The calcium to silica ratio in the belite from works C was lower than works E. This was due to the different polymorphic form of the alite in the two clinkers. The alite from Works C

(Fig. 8-11a)

PHASE EQUILIBRIUM DIAGRAM

CaO-Al<sub>2</sub>O<sub>3</sub>/60-SiO<sub>2</sub>/60

From OSBORN and MAUN (1960)

(temps. in °C)

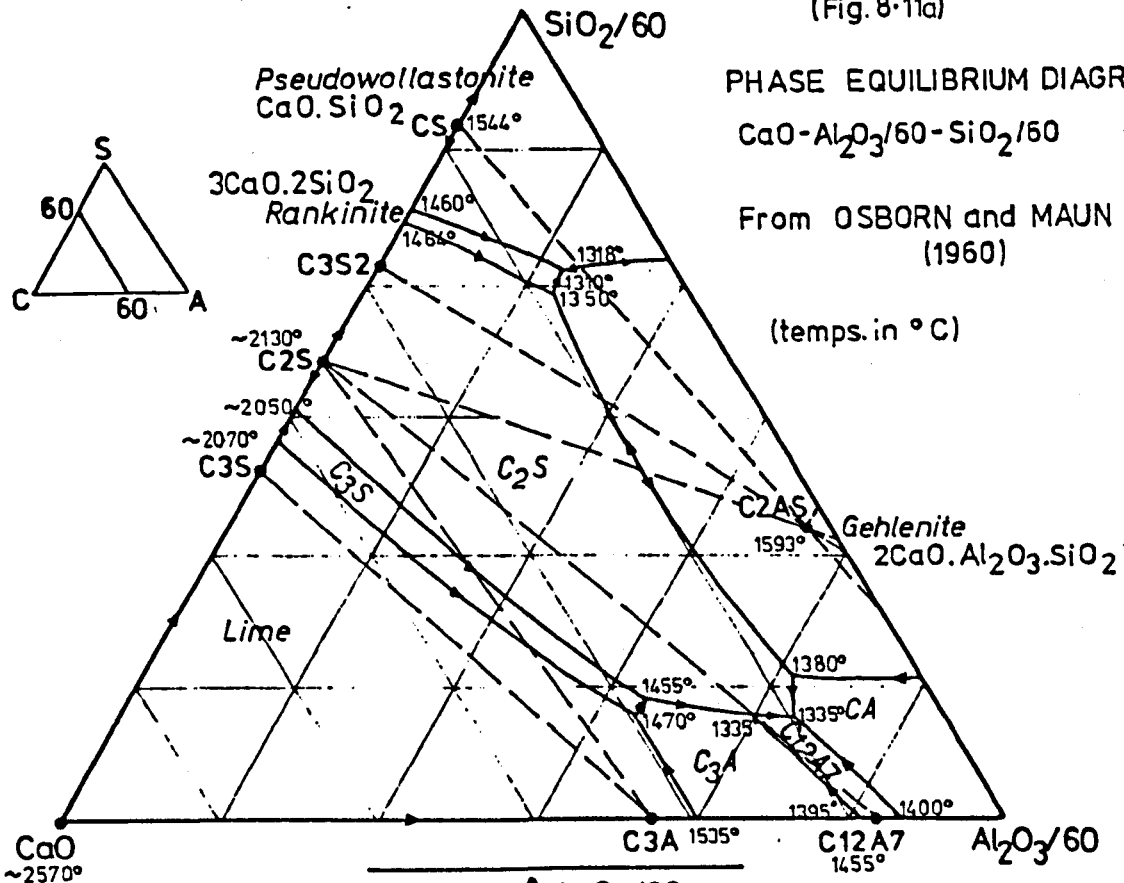
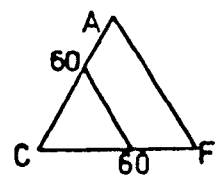


(Fig. 8-11b)

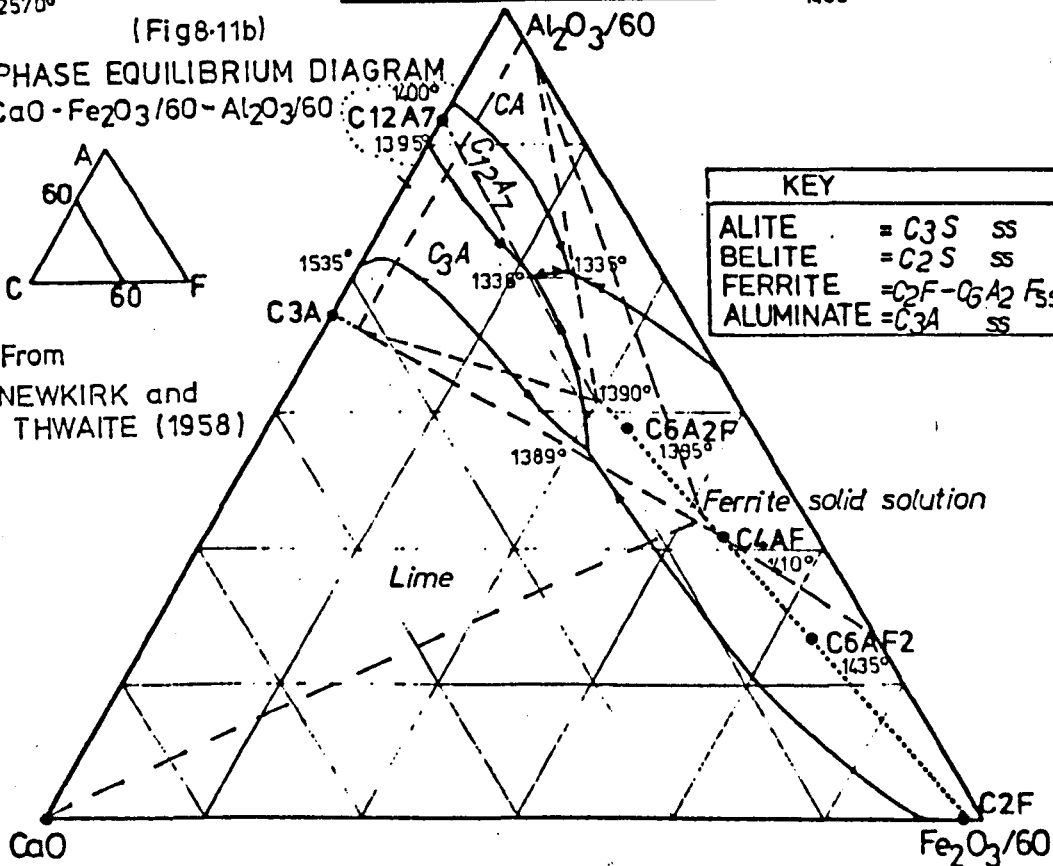
PHASE EQUILIBRIUM DIAGRAM

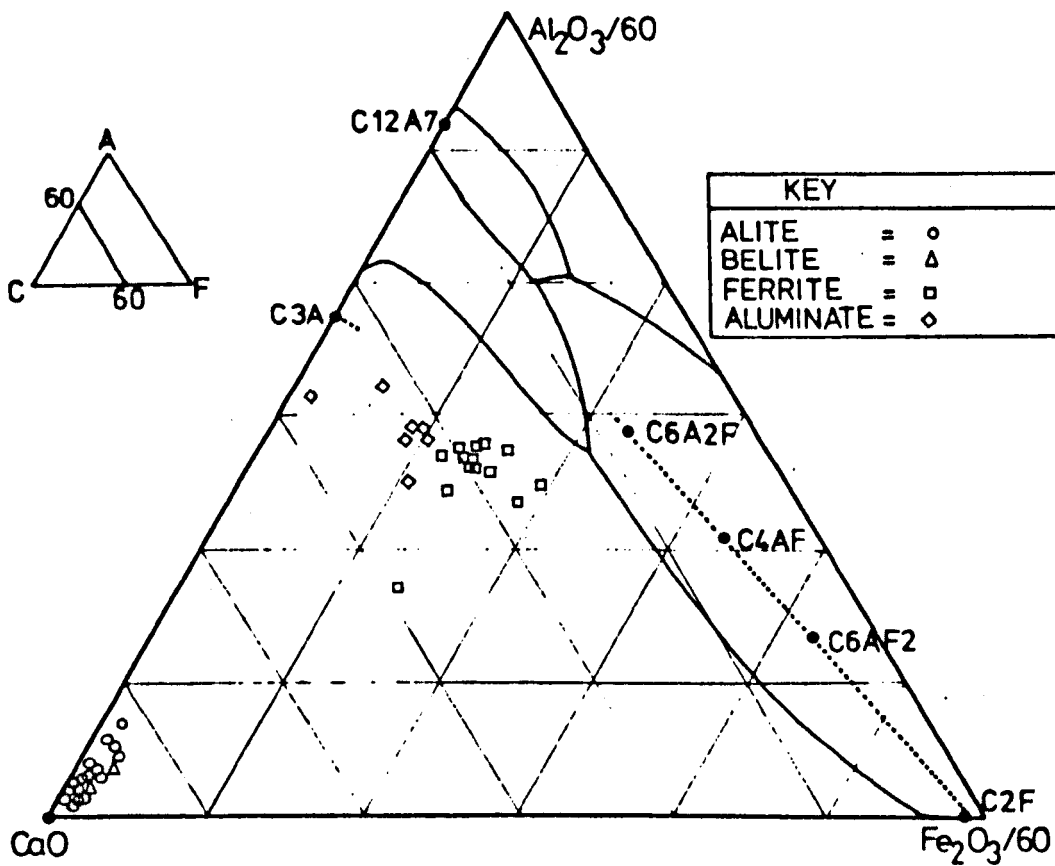
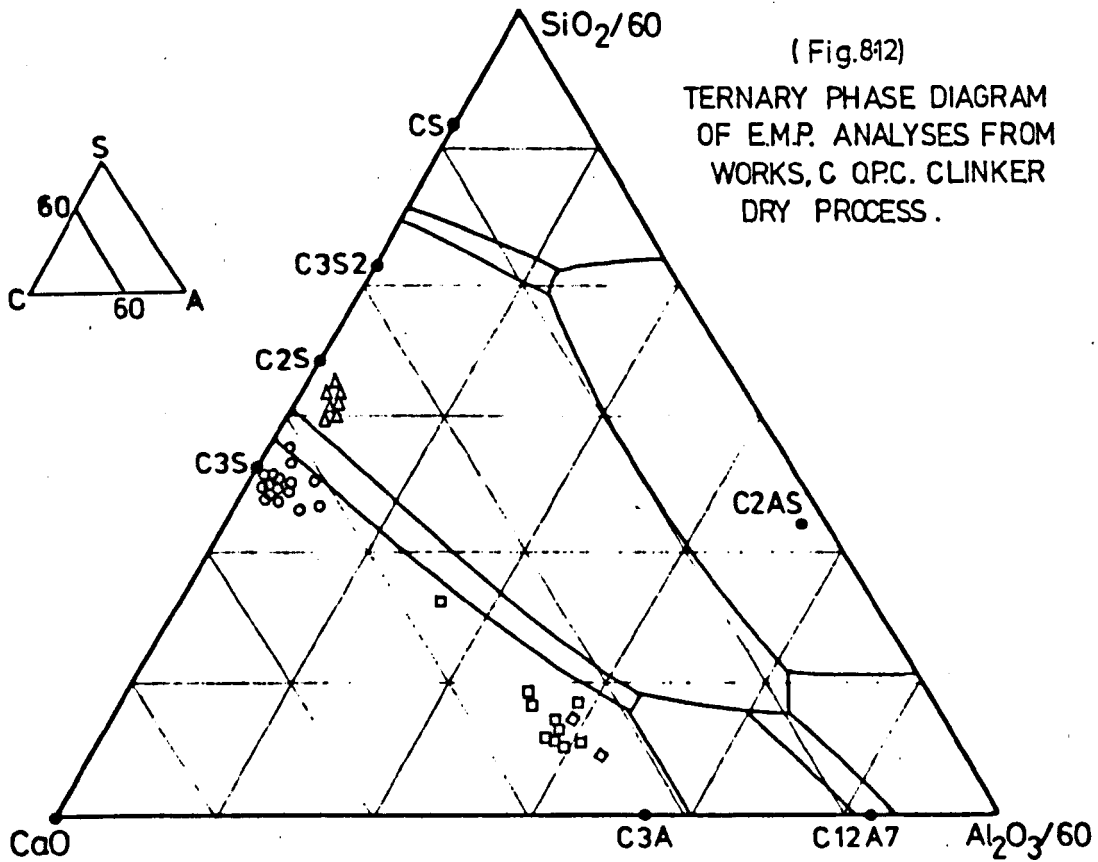
CaO-Fe<sub>2</sub>O<sub>3</sub>/60-Al<sub>2</sub>O<sub>3</sub>/60

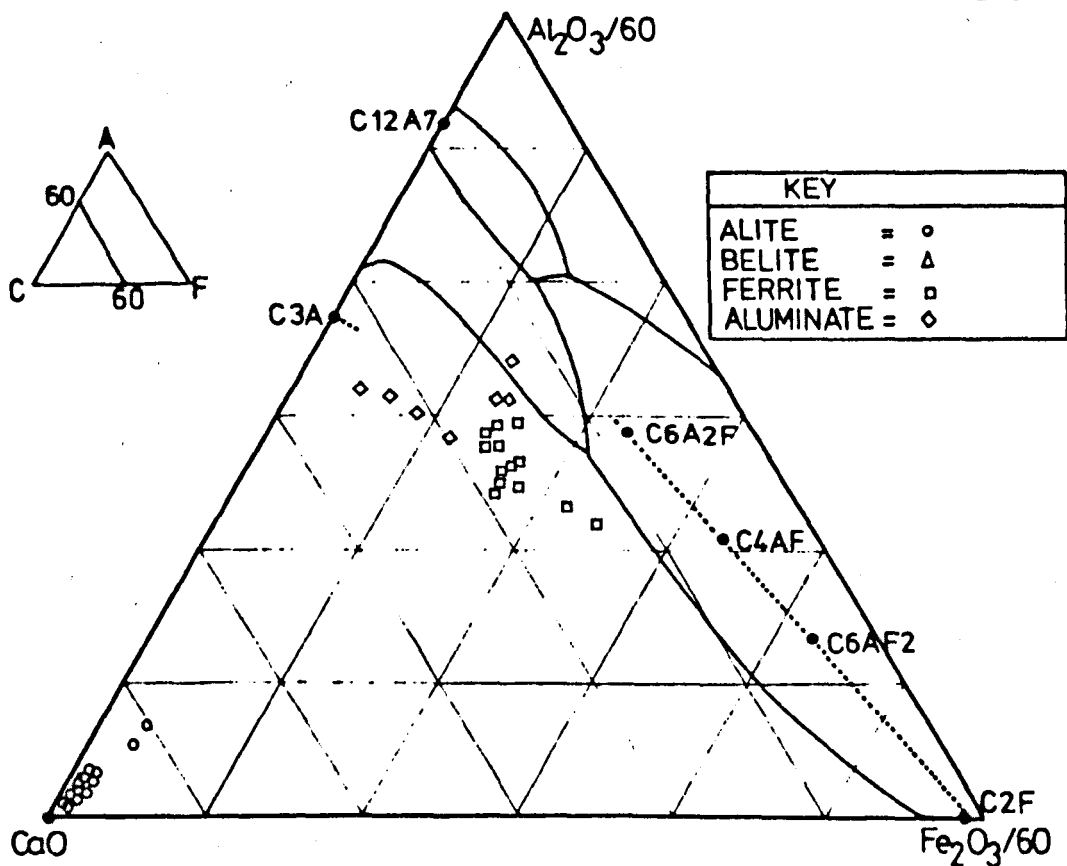
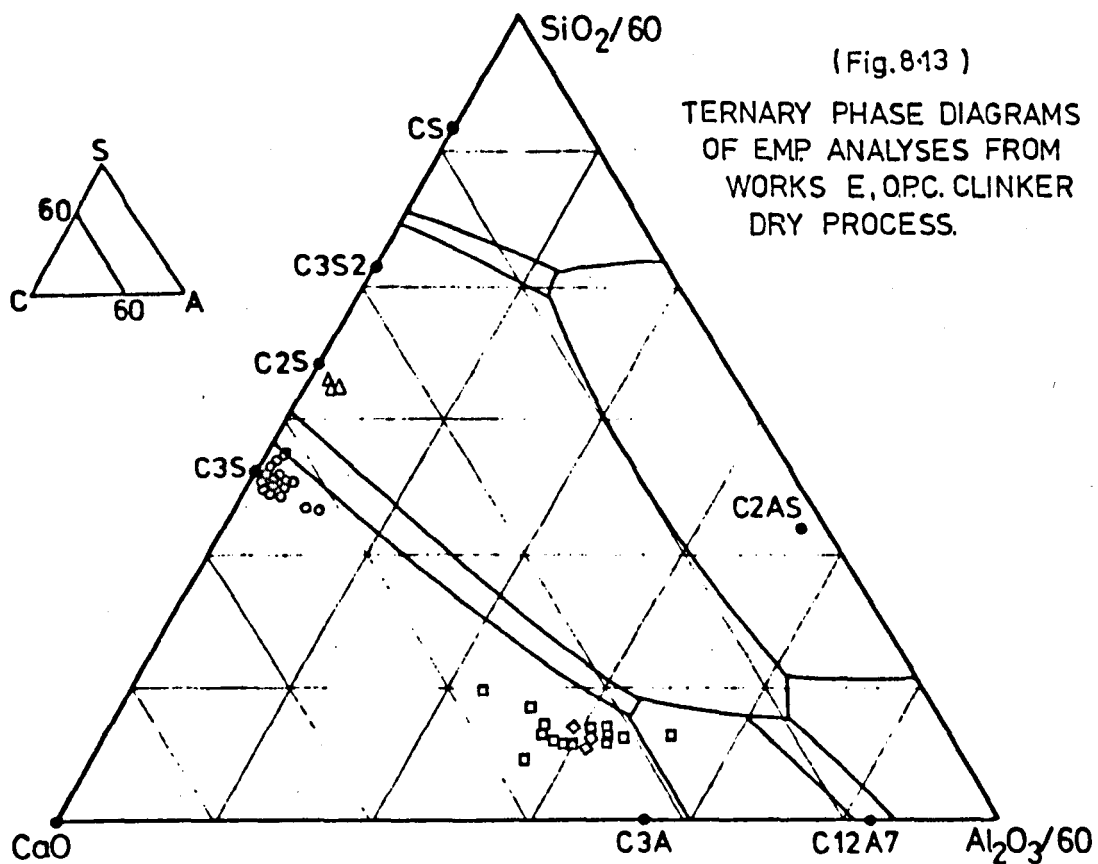


From NEWKIRK and THWAITE (1958)

KEY		
ALITE	= C <sub>3</sub> S	SS
BELITE	= C <sub>2</sub> S	SS
FERRITE	= C <sub>2</sub> F - C <sub>6</sub> A <sub>2</sub> F <sub>5</sub>	SS
ALUMINATE	= C <sub>3</sub> A	SS







clinker was predominantly rhombohedral, whilst the alite from works E was mostly in the monoclinic form. The aluminate and ferrite phases showed more variation in their compositions. The difference between the alumina iron ratio of the two clinkers was small ( works C = 2.58 , works E = 2.52).

However the differences between the composition of the aluminate phases present in the clinker was significant. The mineral assemblage of the aluminate phases from Works E showed two distinct trends. This indicated that there was two aluminate phases present. The trend of the analyses leading towards the stoichiometric composition of  $C_3A$  indicated that tricalcium aluminate was one of the aluminate phases. The other trend of the aluminate analyses indicates that there was an alumina rich phase. This mineral was calcium aluminate,  $CaO \cdot Al_2O_3$ .

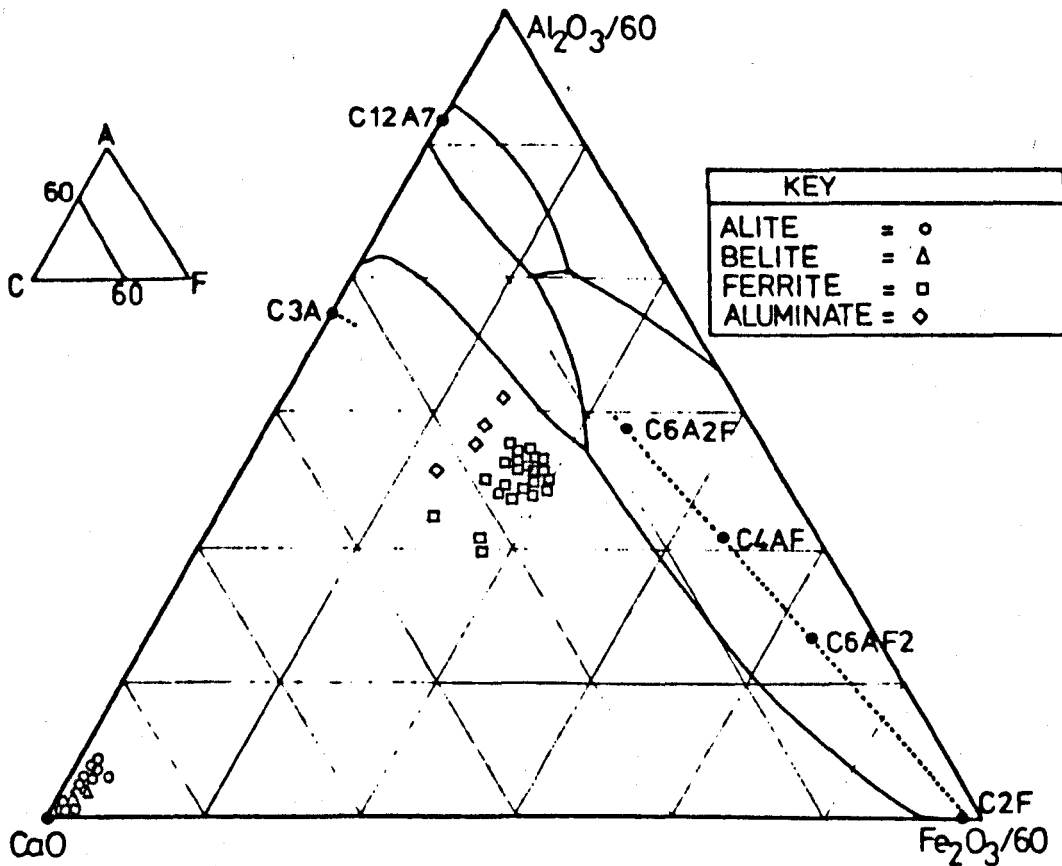
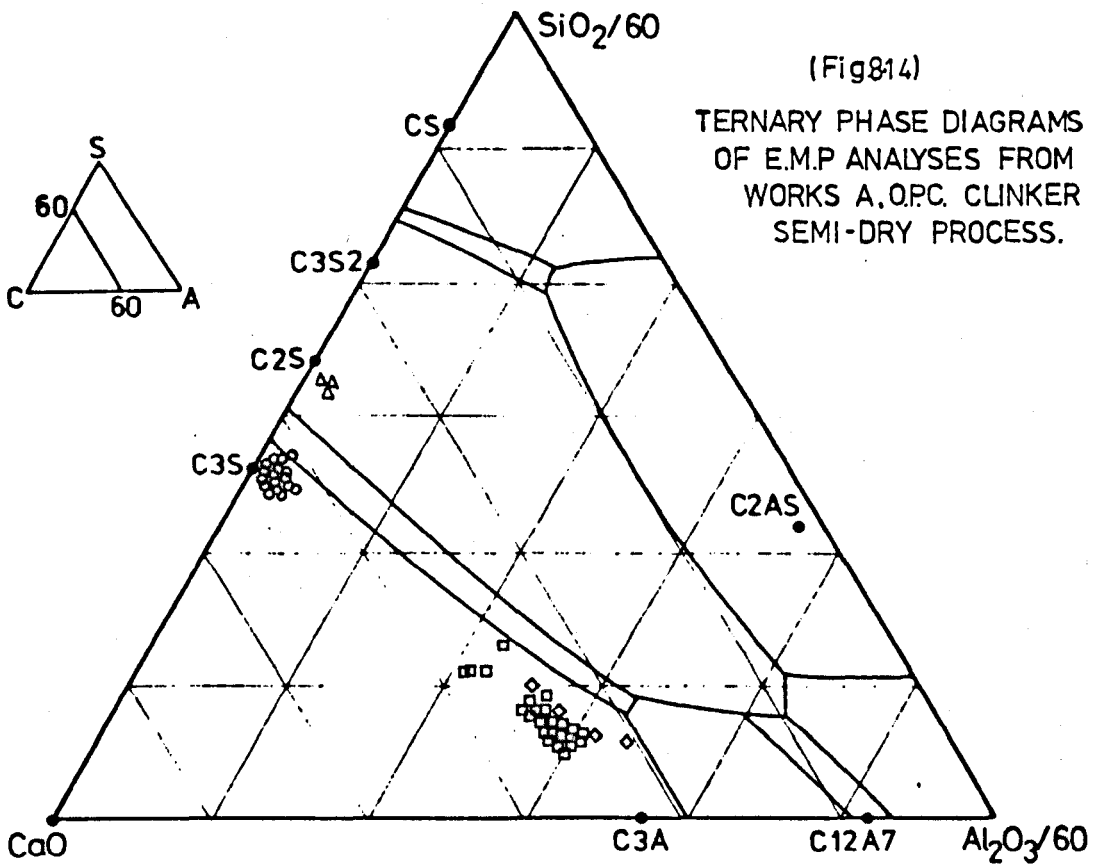
The calcium aluminate phase was not detected in the clinker from works C.

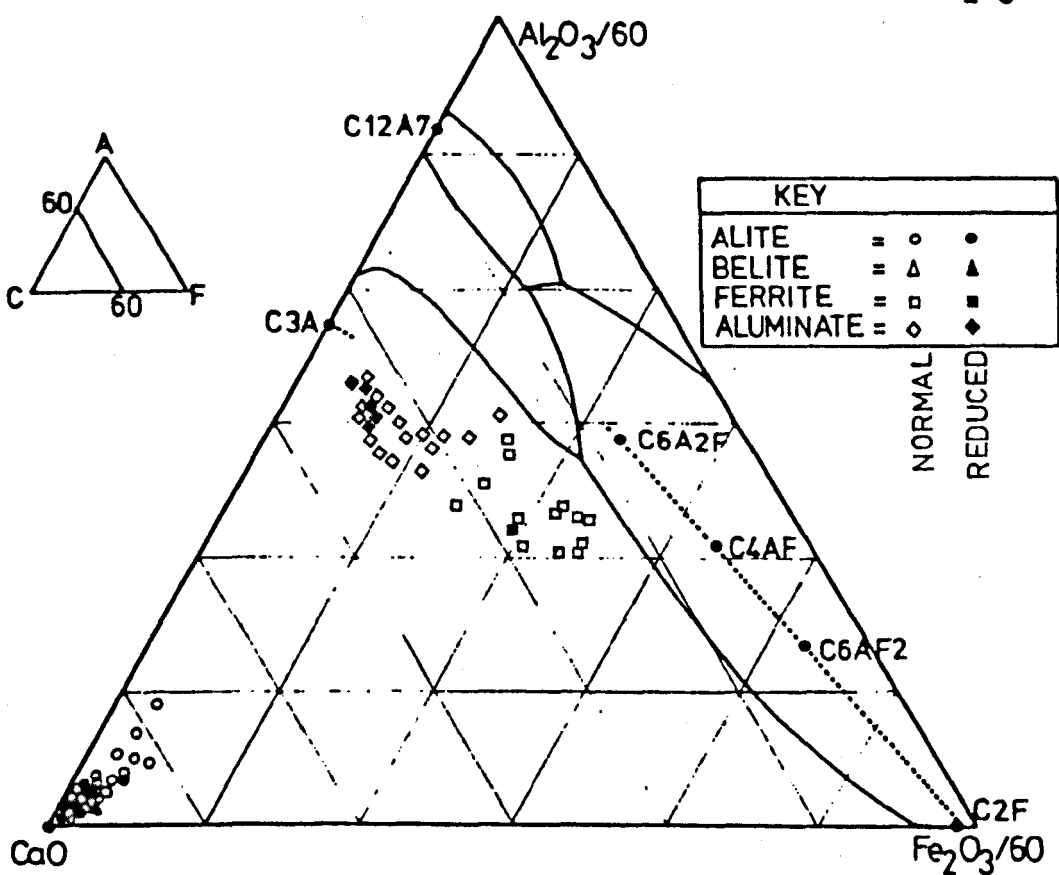
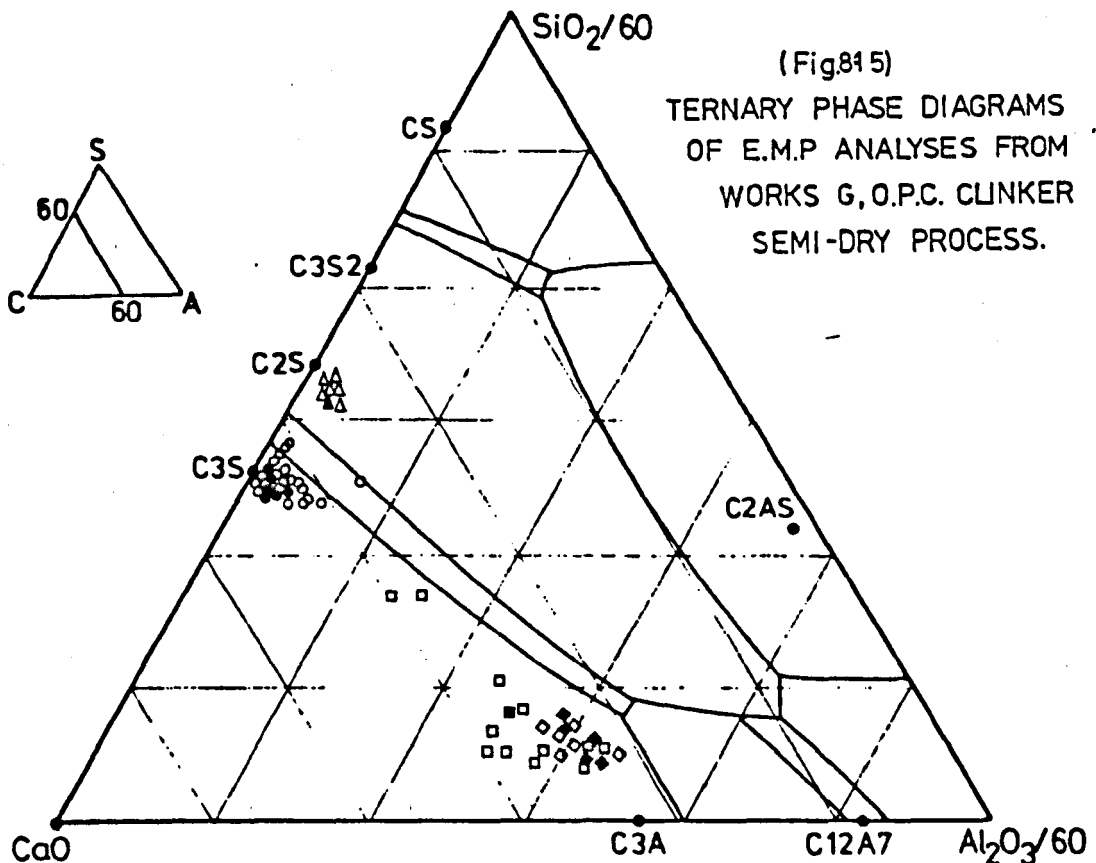
The ferrite from works C was predominantly of composition  $C_6A_2F$  . The ferrite from works E contained more iron, the composition was between  $C_6A_2F$  and  $C_4AF$ . The higher iron level in the ferrite from works E was due to the enrichment of iron in the liquid fraction of the clinker. This was caused by the early crystallization of the calcium aluminate.

Comparison of the mineral assemblages in ordinary portland cement clinker from semi-dry process kilns.

Works A and G (Figures 8.14 and 8.15).

The alite from works A and works G had very similar compositions. The compositions of the belite phases in the two different clinkers were also similar. The compositions of the ferrites and aluminates between the two clinkers showed significant variation. The composition of the ferrite from works A was close to the  $C_6A_2F$  composition except for a shift towards the  $CaO$  and  $Al_2O_3$  end positions. This is a combination of two factors , one is a feature of the graphical representation of a three phase





assemblage in a quaternary system. The ternary diagram is a single side of a three dimensional structure. If the actual compositions of the minerals is inside the structure i.e. it has a composition which contains the four component elements, then the translation of this data to a three component diagram will cause a shift in the apparent composition of the phase. This factor is the same for all the analyses plotted on all of the diagrams. Figure 8.16 shows a three dimensional representation of the quaternary subsystem  $\text{CaO} - \text{C}_{12}\text{A}_7 - \text{C}_2\text{S} - \text{C}_2\text{F}$ .

The second factor is due to mineralogical and instrumental features. The shift towards the  $\text{CaO}$  and  $\text{Al}_2\text{O}_3$  apices is caused by the unintentional sampling of the calcium silicate and the aluminate phases during the analysis of the ferrite crystals. This is due to the size of the electron microprobe beam interaction zone, about  $10 \mu\text{m}$ , and the size of the ferrite crystals from  $5$  to  $15 \mu\text{m}$ .

This sampling effect was also shown by the apparent composition of the aluminate phase in the clinker from works A. The tricalcium aluminate crystals were in the cubic modification and were small, about  $5 \mu\text{m}$  in size. Thus small areas of ferrite and the calcium silicate phases were unintentionally included in the zone of analysis.

The aluminate and ferrite phases from works G had a more distinct separation. This was because the tricalcium aluminate had crystallised in the orthorhombic form as lath shaped crystals. These were larger than the cubic form. Since they were larger than the beam interaction zone, there was less sampling of the adjacent phases. The ferrite phase was richer in iron and had a composition between  $\text{C}_6\text{A}_2\text{F}$  and  $\text{C}_4\text{AF}$ . In the reduced clinker, the ferrite content was less than in the normal clinker. The tricalcium silicate contained less iron in solid solution. Thus the occurrence of reducing conditions in the kiln has most effect on the distribution of iron in the cement clinker phases.

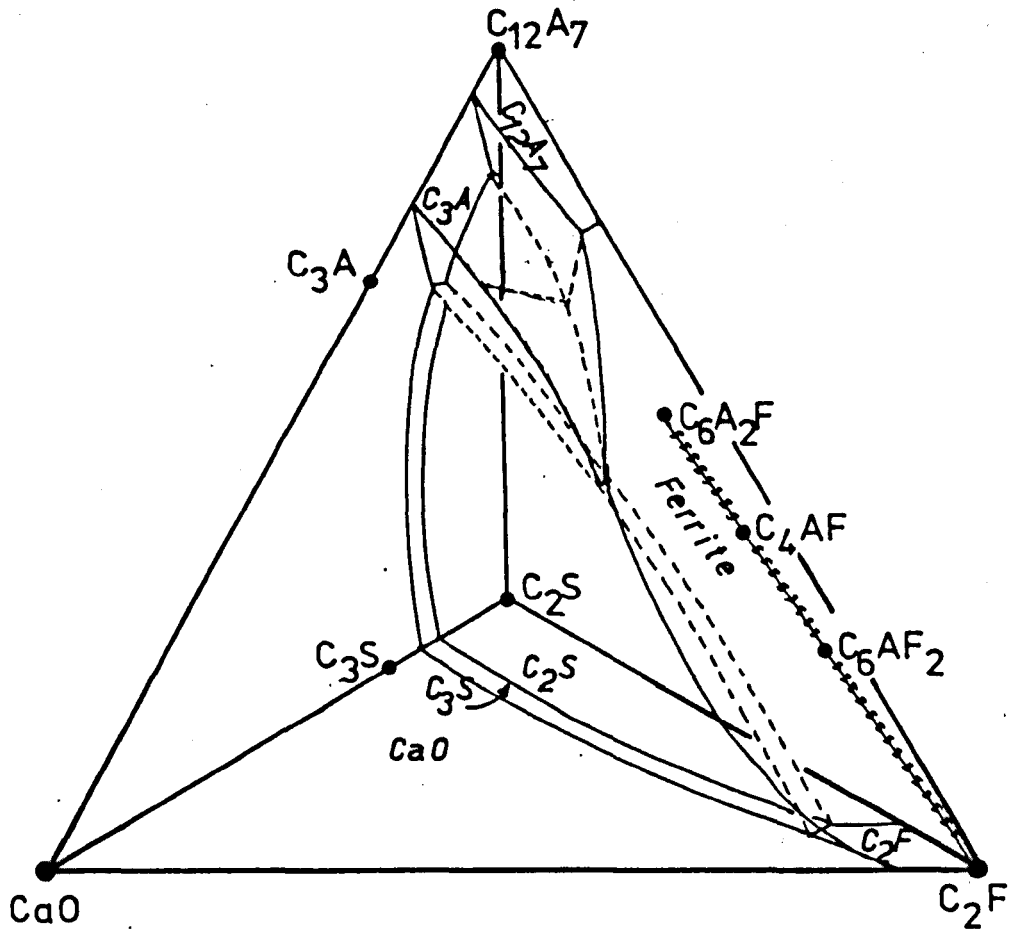


(Figure 8-16) THE QUATERNARY SUB SYSTEM  
CaO - C<sub>2</sub>S - C<sub>12</sub>A<sub>7</sub> - C<sub>2</sub>F SHOWING  
PHASE VOLUMES OF PRINCIPLE  
CEMENT CLINKER MINERALS.  
(C<sub>2</sub>S volume after Lea and Parker, 1934)

The mineral assemblages in ordinary portland cement clinker from wet process kilns.

Works D (Figure 8.17).

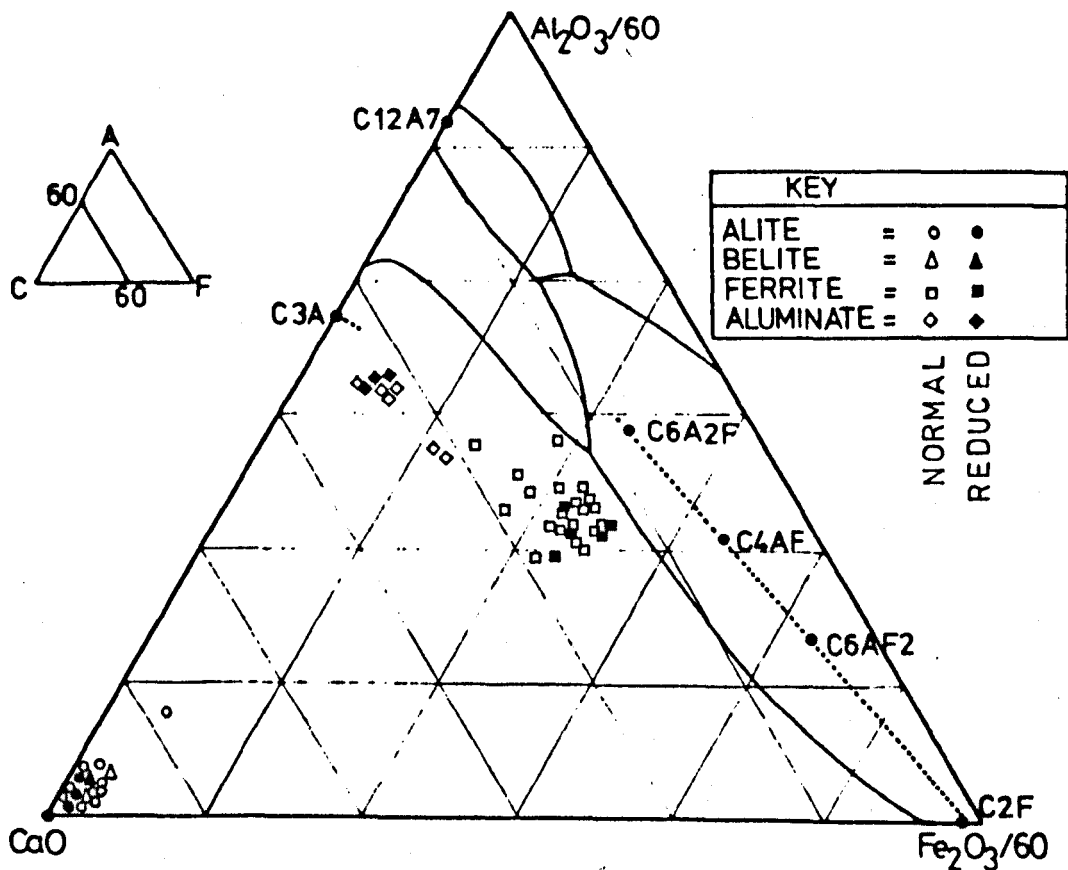
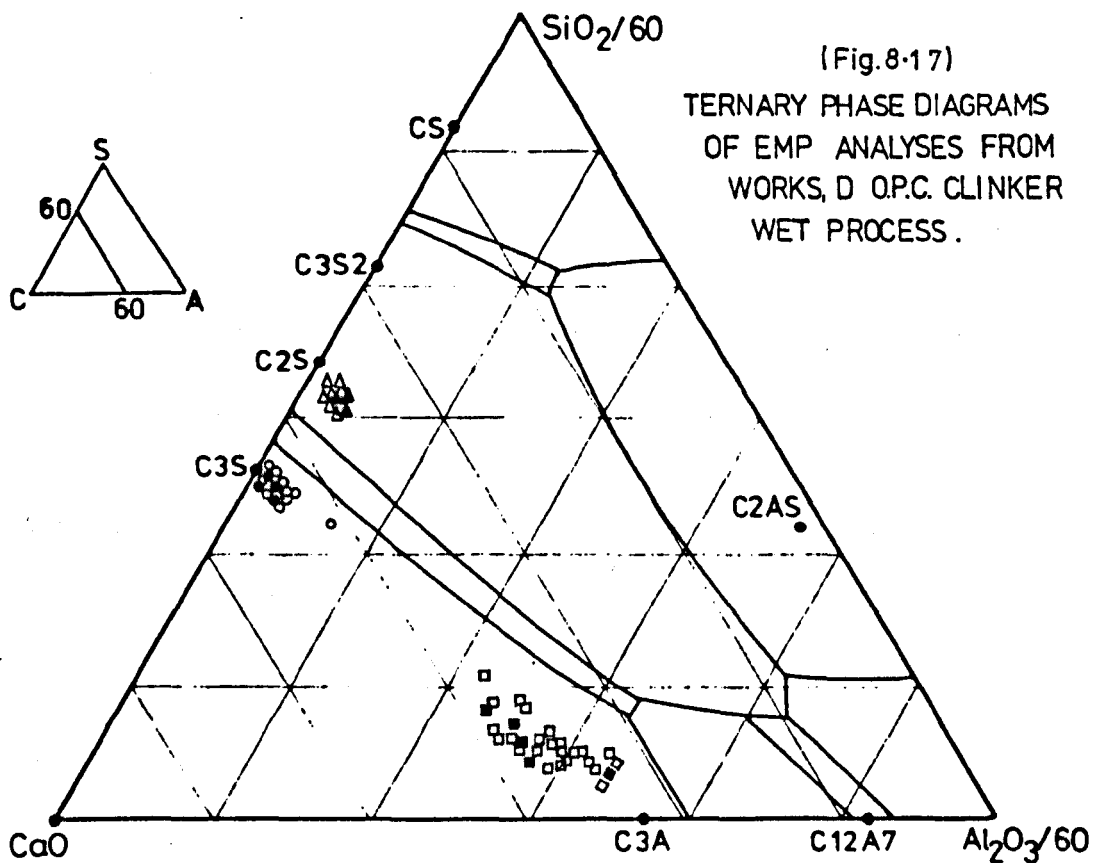
The alite and belite phases from works D have a similar calcium to silica ratio as the calcium silicate phases from the other types of process. The aluminate phase was predominantly in the orthorhombic form. Therefore the interference effects from the adjacent phases was lessened. The composition of the ferrite phase was between  $C_6A_2F$  and  $C_4AF$ . The reduced clinker had a greater separation between the ferrite phase and the tricalcium aluminate. This was due to the better crystallisation of the tricalcium aluminate in the reduced clinker.

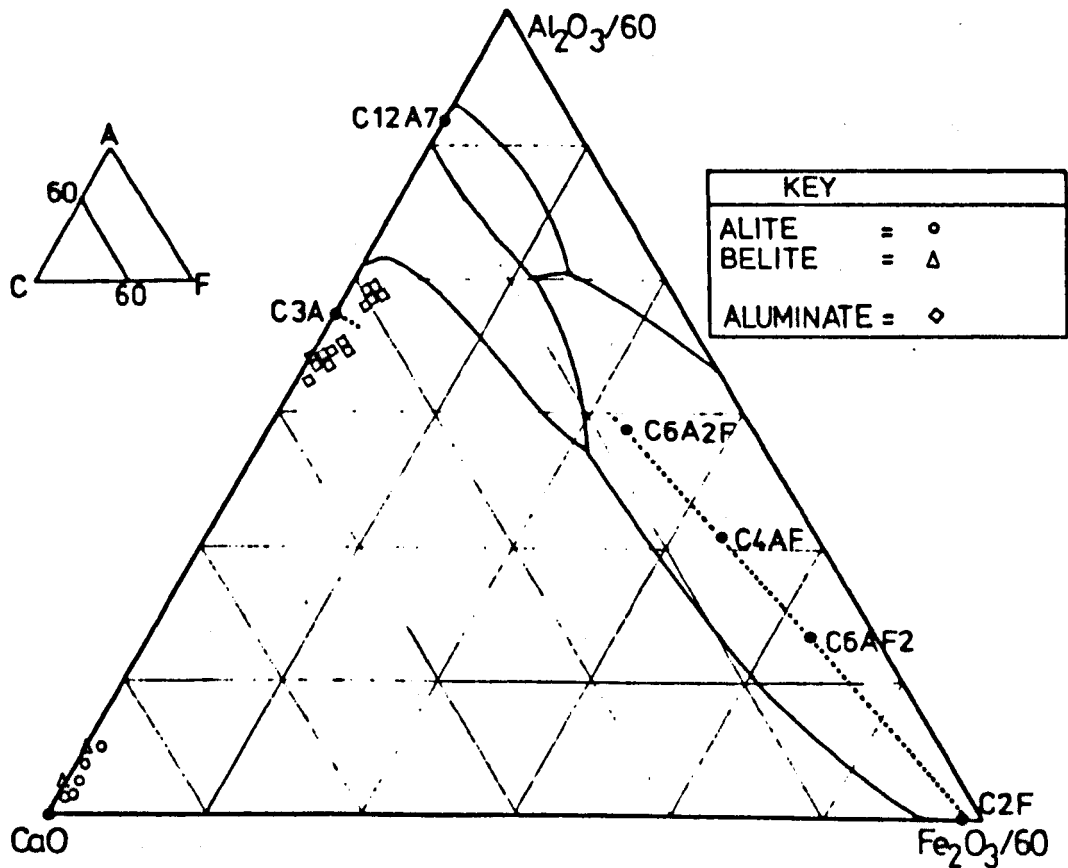
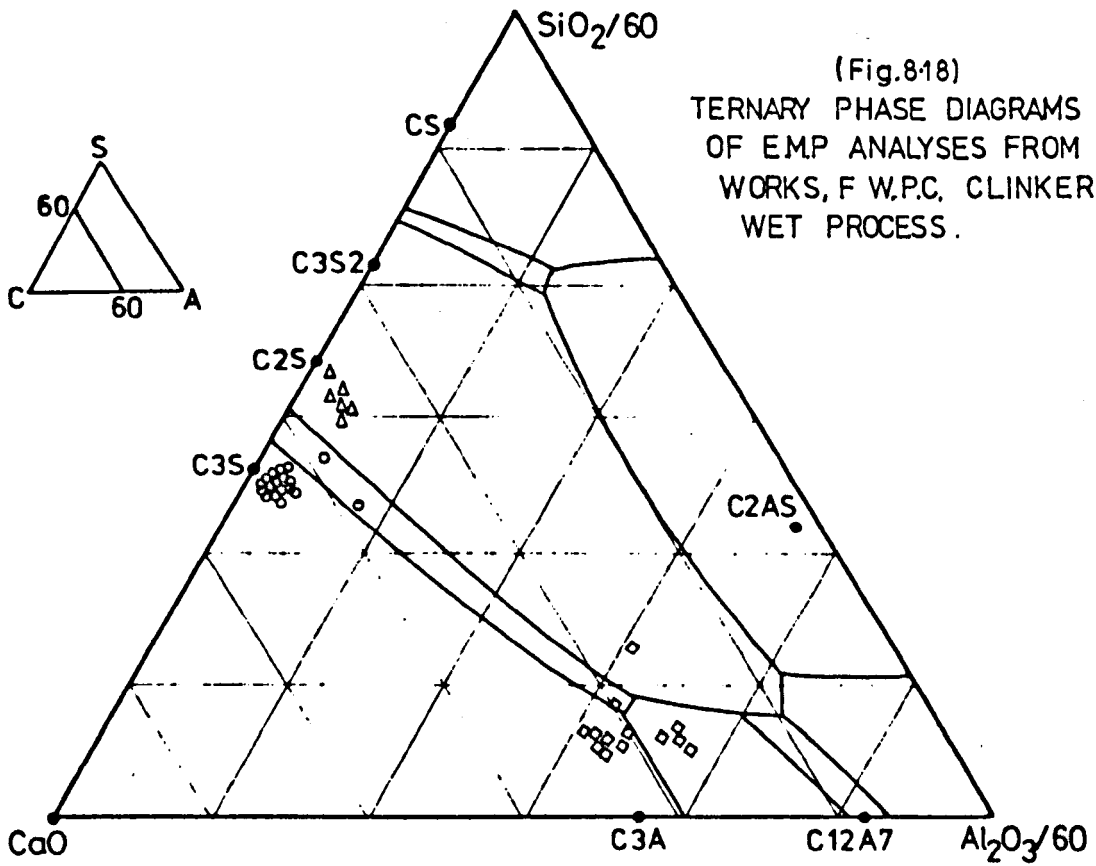
The mineral assemblage in white portland cement clinker from a wet process kiln.

Works F (Figure 8.18).

The clinker from this works was produced in reducing conditions by an oilfired kiln.

The alite and belite phases had a slightly higher level of  $Al_2O_3$  when compared with the OPC calcium silicate phases. The level of iron in all the phases was very low because the iron content of the kiln feed was low and the burning in reducing conditions kept the iron in a reduced state. The aluminate analyses show two distinct groups. The cluster between the CaO point and the  $C_3A$  point was from analyses of tricalcium aluminate. The cluster of analyses between the  $C_3A$  point and the  $C_{12}A_7$  point was from another aluminate phase of composition  $C_{12}A_7$ . This phase had formed because of the absence of iron in the system.





The mineral assemblage in low heat cement clinker from a wet process kiln, Works B ( Figure 8.19).

In the manufacture of this cement, a high iron content feed is used to prevent the formation of tricalcium aluminate. The early clinker samples that were collected before the iron was added, had alite with a higher alumina content than the later samples. The belites had a less distinctive division. In the early samples of the production trial, the composition of the ferrite was near  $C_4AF$ . As the trial proceeded and the kiln conditions settled, the ferrite composition moved towards the iron rich end of the ferrite series, to  $C_6AF_2$ .

The mineral assemblage in sulphate resisting cement clinker from wet process kilns.

Works B (Figure 8.20), Production SRC clinker.

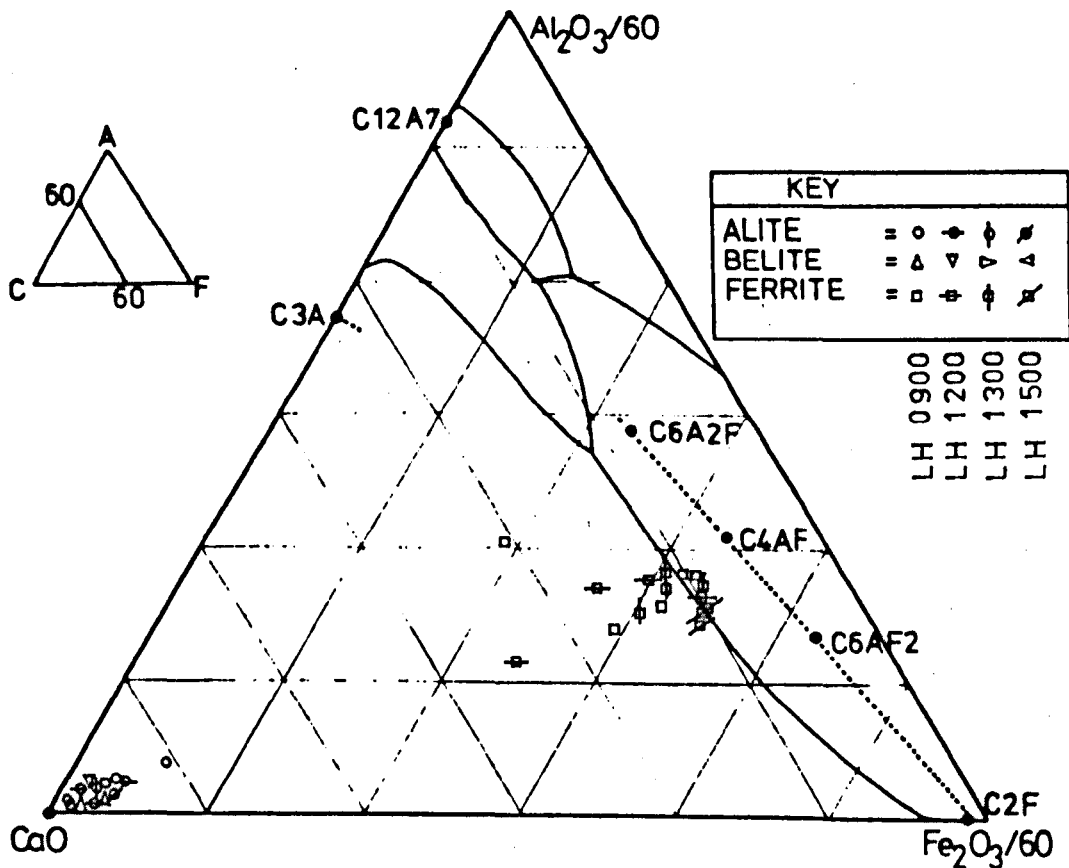
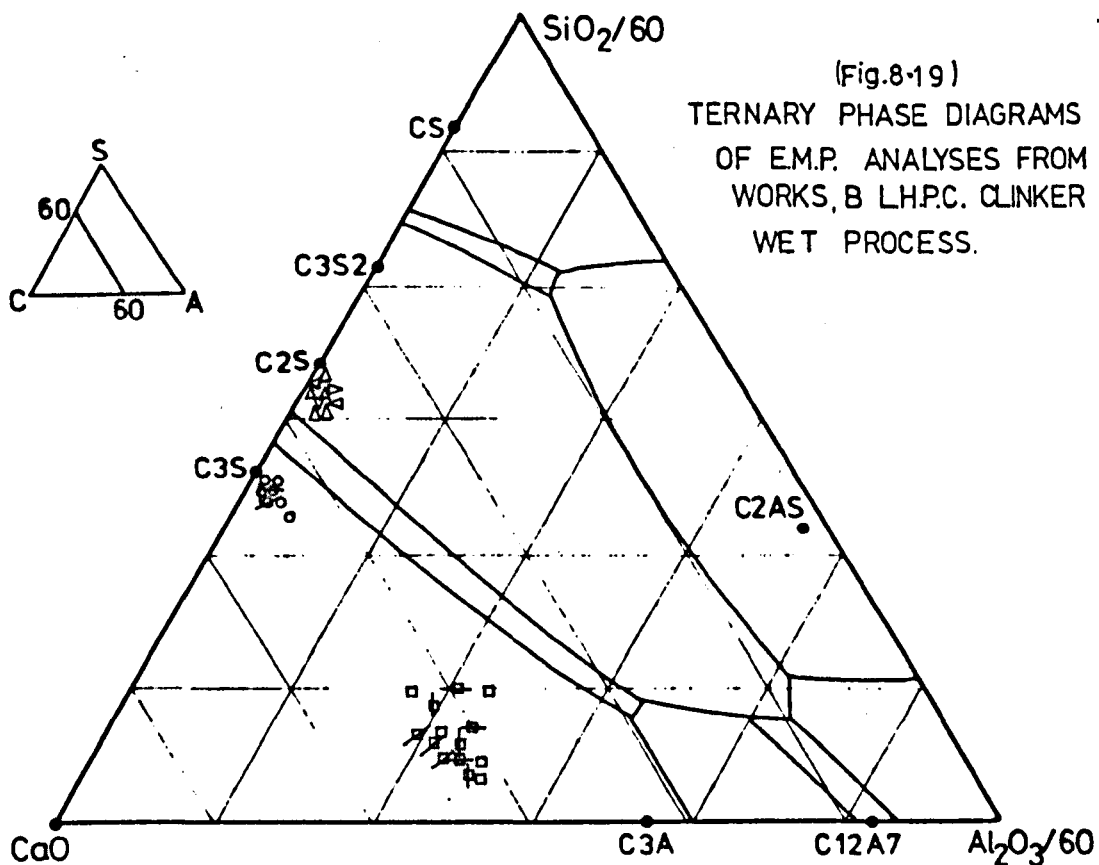
The cement clinker was collected individually from the two kilns. The calcium silicates had no overall differences between the two kilns. The ranges of composition of the belite from the kilns is wider than the compositions of the belites from the OPC clinkers. This was due to the higher levels of minor element substitution, especially sodium and potassium, in the belite. This was caused by the absence of any substantial amount of tricalcium aluminate, in which these elements might preferentially substitute. The analyses between the cluster of ferrite symbols and the cluster of alite analyses, were caused by the microprobe beam striking sections of the two phases simultaneously.

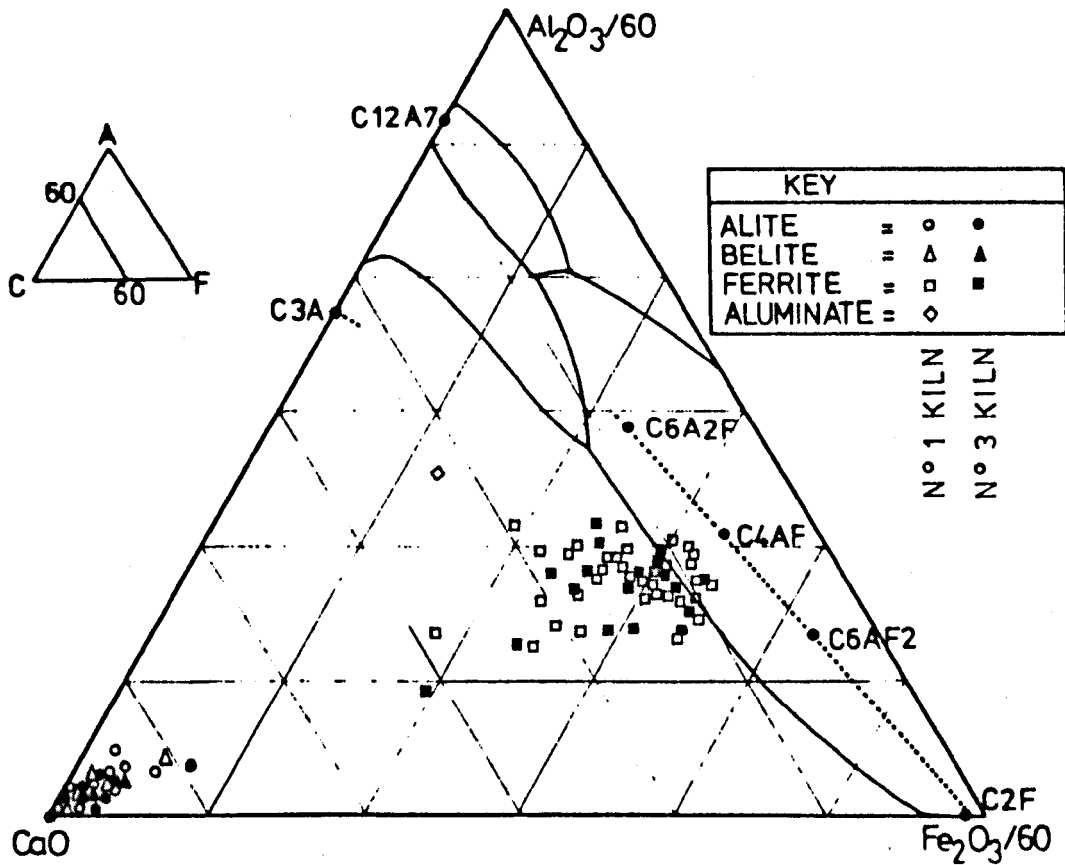
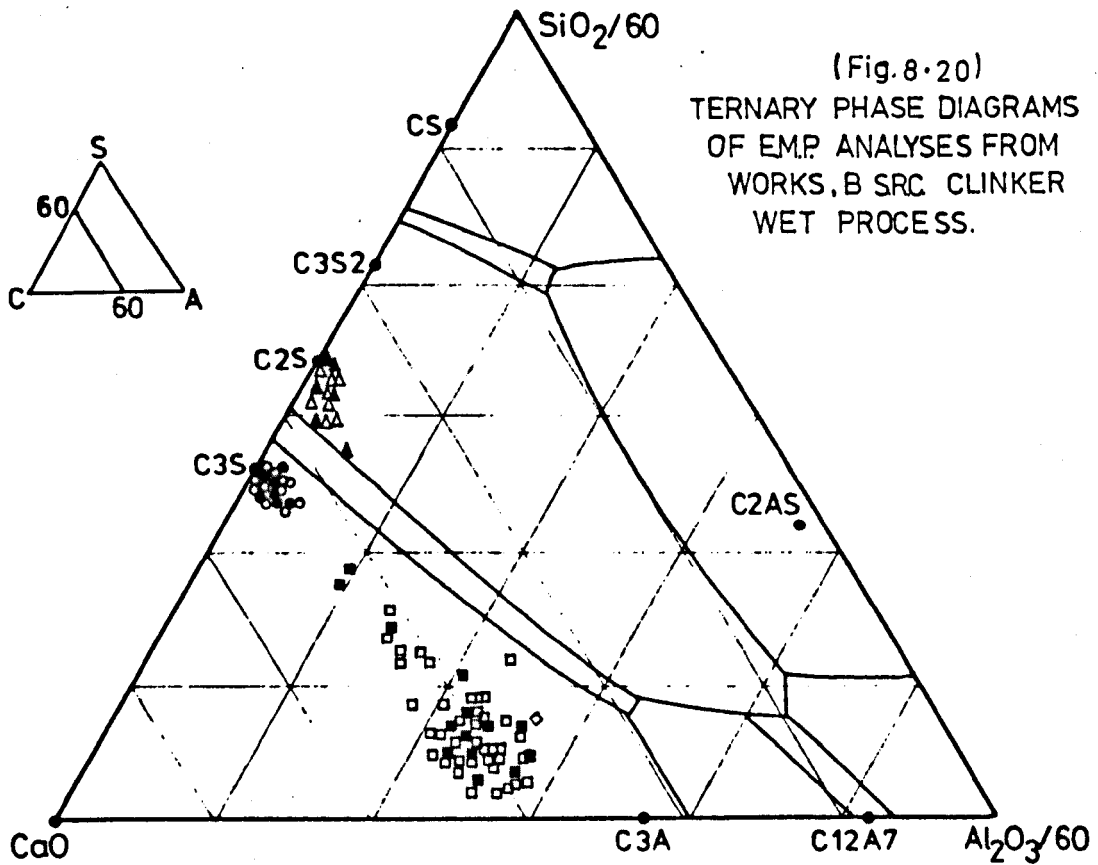
The ferrite analyses show no difference between the two kilns. The overall composition of the ferrite was between  $C_4AF$  and  $C_6AF_2$ . A higher iron content than the ferrite in the OPC clinker.

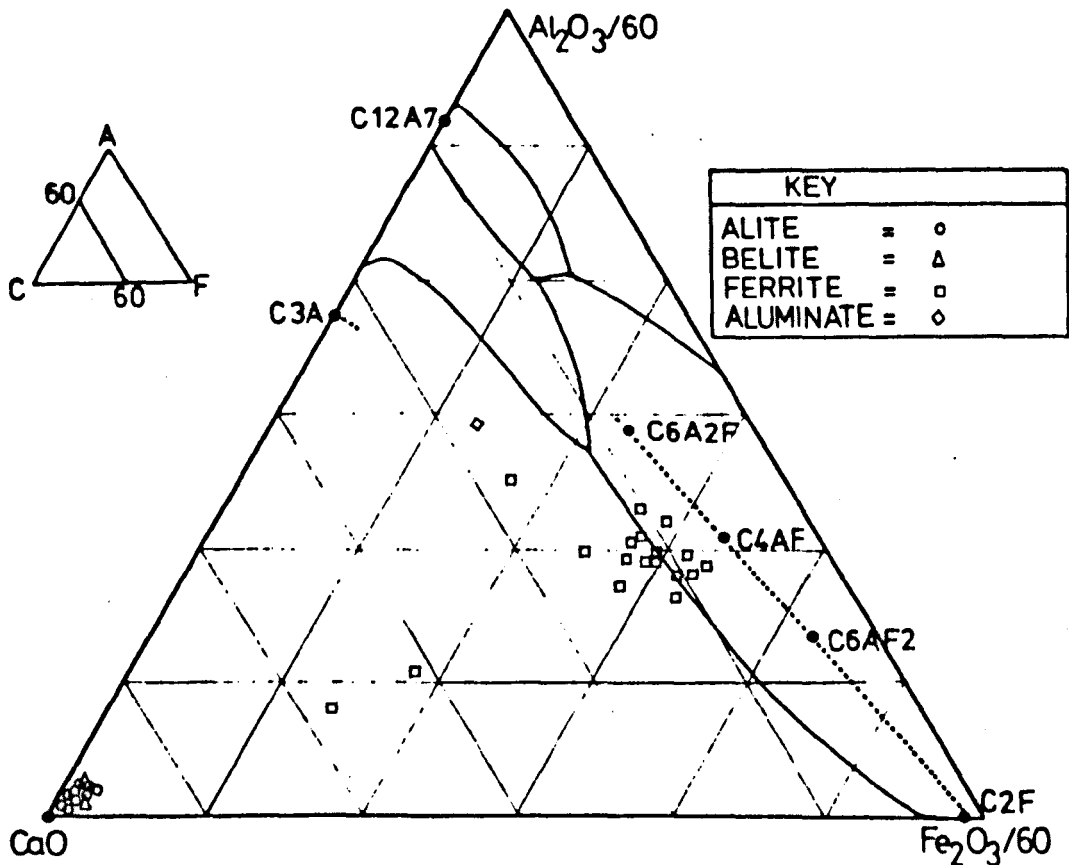
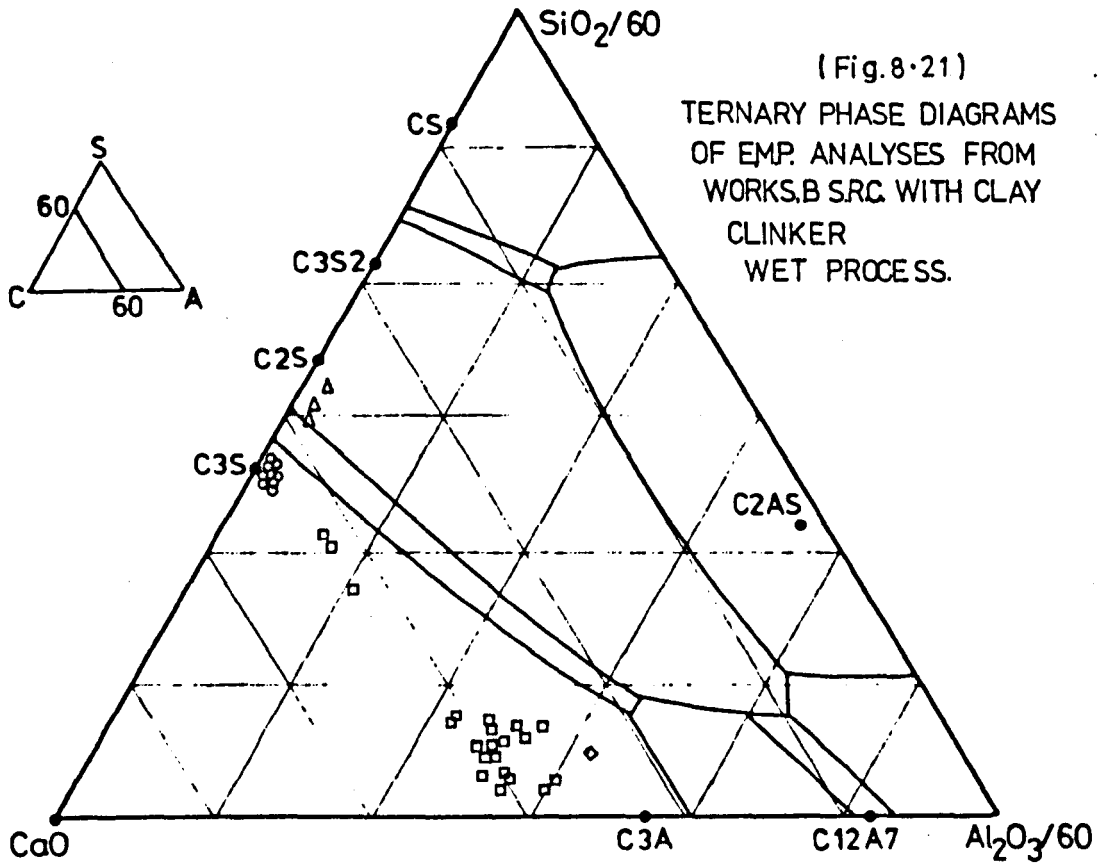
The mineral assemblage in sulphate resisting cement clinker made from chalk and clay.

Works B (Figure 8.21)

Prior to the use of PFA in the manufacture of SRC clinker, works B







used clay. The overall mineral assemblage was similar to the SRC clinker from PFA. There were some minor variations in the compositions of the phases. The belite and ferrite had a higher level of CaO. This was due to the higher level of frelime in the clinker. In the SRC clinker from PFA, the ash was lime deficient and reduced the overall frelime by reacting with it to produce belite. The amount of iron in the ferrite from the clinker with clay was slightly lower, with the composition near to  $C_4AF$ . This was because the iron in the PFA was predominantly in the form of magnetite and hematite. Thus it was more readily available for the formation of ferrite from the liquid fraction. Rather than being bound in some of the clay minerals which are usually more refractory in nature.

The mineral assemblage in the sulphate resisting cement clinker with PFA addition.

Works B, (Figure 8.22).

In the production cycle at works B the dust from the exhaust gases from all the kilns was recycled back into kiln 3. This caused the clinker from this kiln to have a high frelime level. To reduce this excess frelime, PFA was added to the feed to combine with frelime and form belite. The analyses from the first clinker show an overall decrease in the CaO content of the all the phases, when compared with the normal SRC clinker (Figure 8.20). During the middle period of the test the frelime level remained low. The last sample was collected when the PFA addition had ceased. The frelime level in the clinker increased dramatically. The ferrite phase showed the greatest variation in the content of CaO throughout the trial. However the iron content of the ferrite was relatively static. The composition of the ferrite was close to  $C_4AF$ .

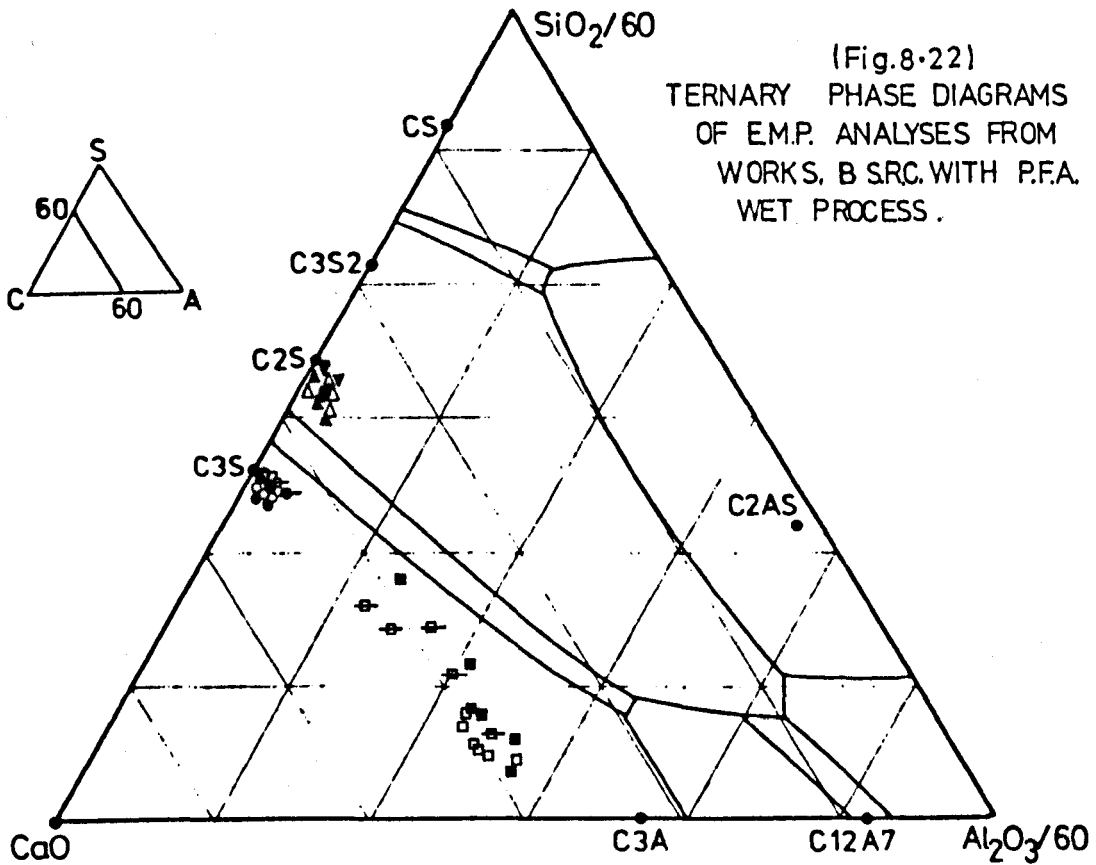
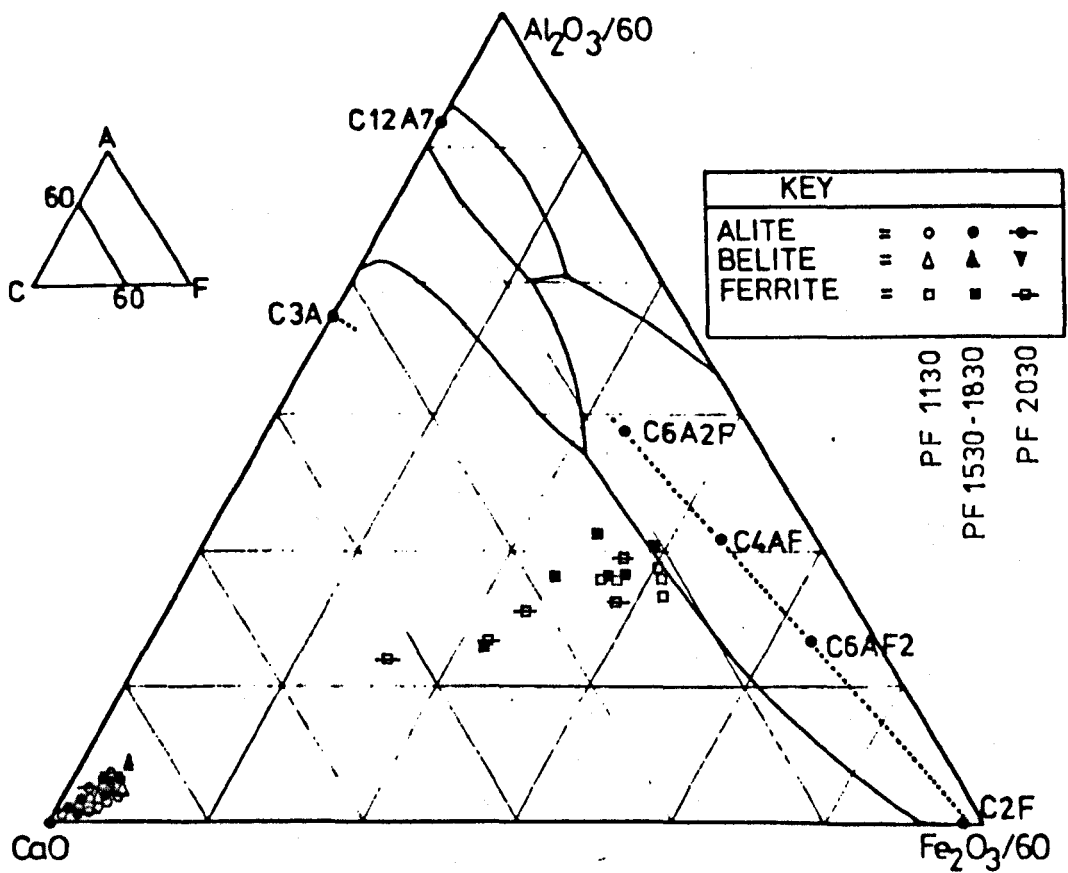
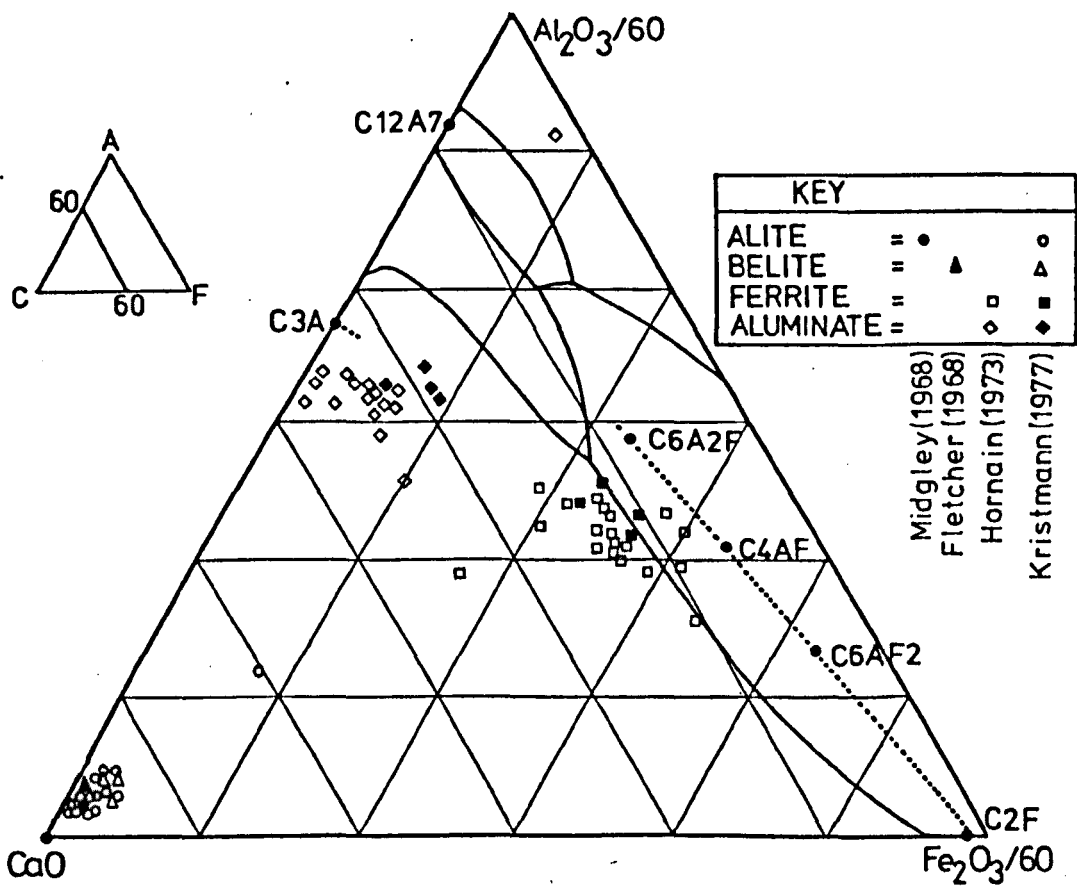
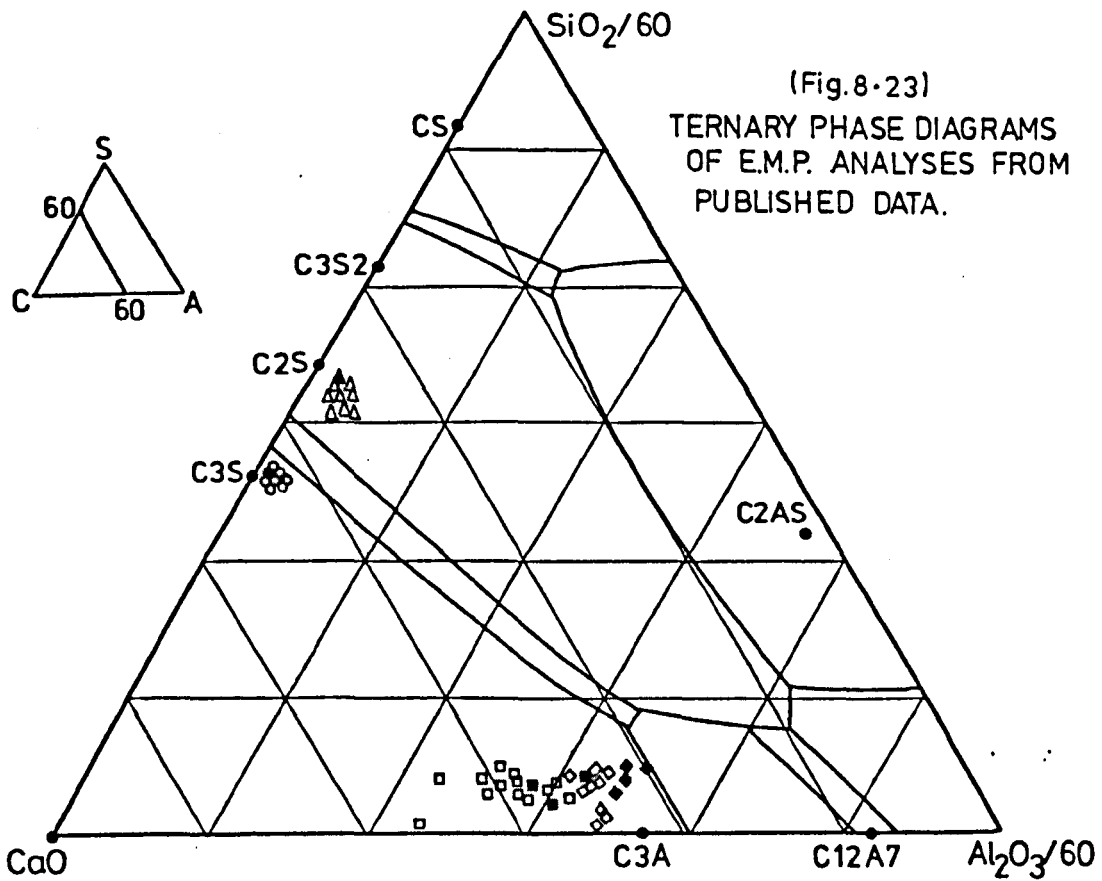


(Fig.8-22)  
 TERNARY PHASE DIAGRAMS  
 OF E.M.P. ANALYSES FROM  
 WORKS, B.S.R.C. WITH P.F.A.  
 WET PROCESS.



KEY	
ALITE	= ○ ● ↖
BELITE	= △ ▲ ▼
FERRITE	= □ ■ ⊕

PF 1130  
 PF 1530-1830  
 PF 2030



Ternary phase diagram plots of published analyses of cement clinker phases.

For comparison purposes the analyses of cement clinker minerals which have been given in publications are plotted on identical phase diagrams. (Figure 8.23). The analyses are not all from one type of cement or process and do not represent a mineral assemblage from a cement clinker.

Future development.

The use precise mineral analyses for production control of cement would be complex and expensive. However in the analysis of potential cement quality and performance, the mineral analyses provide very useful data, for the future developments of cement, which may be to improve the performance, or to utilise waste and byproducts in the manufacture of the cement clinker. The use of mineral analyses will be crucial in the development process.

## Chapter nine

The compressive strength and quality of portland cement and concrete.

### Introduction.

The major use of a cement is as a binder material in concrete . The relationship between the chemical , mineralogical and petrological characteristics of the clinker, and the physical properties of the cement is of great interest to the producers and users . One of the most important physical properties of cement and hence concrete is the strength.

### Factors influencing the strength of cement.

Chatterjee (1979) proposed that the effects of composition, mineral structure and petrological characteristics on the quality of cement clinker were related phenomenologically. Individually the effects due to the various characteristics were difficult to assess. If they were considered in combination the interrelationships were extremely complex.

Thus the correlations between clinker characteristics and cement quality are best examined individually before attempting to assess composite models.

The strength of the concrete must be related to the phase content of the cement . The compressive strength of the different cement minerals is shown in Figure 9.1. These minerals react with the water at different rates and form the hydrated minerals which bind the aggregate together .

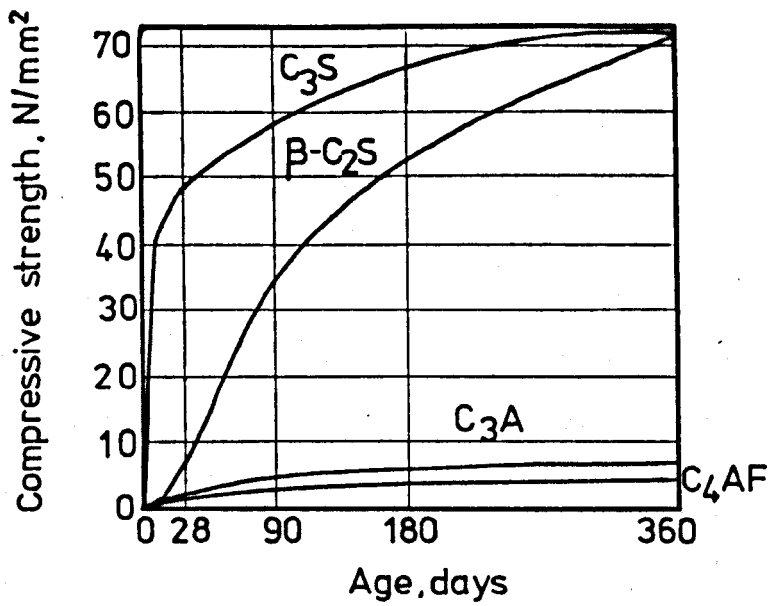


(Fig.9-1) COMPRESSIVE STRENGTH OF THE MAJOR CONSTITUENTS OF PORTLAND CEMENT (after Bogue and Lerch, 1934)

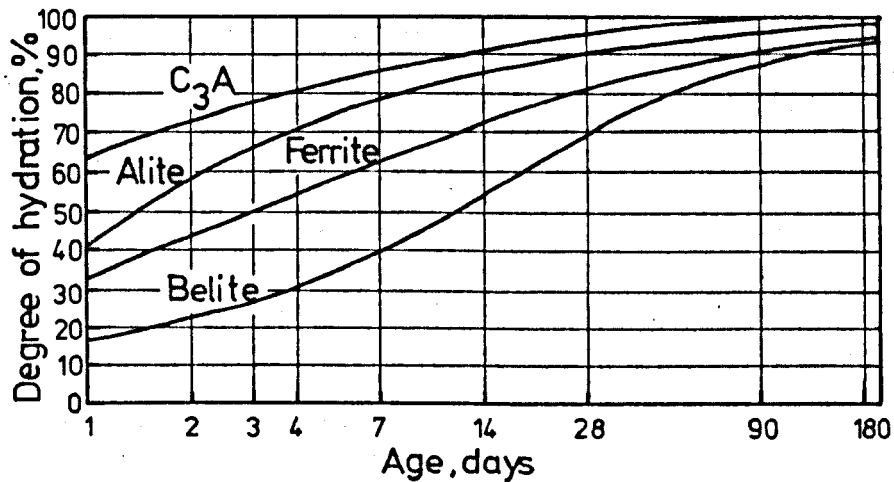


(Fig.9-2) RATES OF HYDRATION OF THE VARIOUS COMPOUNDS IN PORTLAND CEMENT (after Copeland and Kantro, 1960)

The rate of hydration of each specific mineral is dependant on the precise mineral composition , especially the minor elements which substitute into the mineral structure.

By comparing Figure 9.1 and Figure 9.2, it is apparent that the rate of hydration does not directly relate to the 28 days compressive strength of the phases . The actual strength development in concrete is influenced by the interaction of the different phases as they hydrate. The rate of hydration of the compounds in the cement, in the early stages is similar to the rate of hydration of the individual phases. The percentage of hydration against time for the major cement phases is shown in Figure 9.2. During this stage the hydration is selective. The degree of hydration in the cement and thus its early strength, is determined by the hydration rate of the individual phases. The hydration proceeds and a layer of calcium silicate hydrate gel ( CSH ) forms around each cement grain. As this layer thickens the rate of hydration becomes more dependent on the rate of water diffusion through the layer .

Birchall et al (1980) have proposed an osmotic membrane model . In this process the water is preferentially drawn in through the gel coating which eventually ruptures under the osmotic pressure. This allows renewed hydration and the growth of secondary hydration products. This occurs after the dormant period in the cement following the early hydration reactions. Thus they conclude that the later and final strengths are more dependent on the characteristics of the CSH layer, than the reactivity of each of the cement minerals.

#### Phase composition.

There have been many attempts to find relationships between the strength of cement and the chemical phase content of the clinker . Butt and Timashev ( 1962 ) investigated a large number of samples of clinker from production kilns . Their conclusions were that, the optimum  $C_3A$  content for cement was between 8 to 12 % . Above this level the strength

was reduced . The optimum  $C_4AF$  content was between 12 to 13 %. Excess  $C_4AF$  caused a reduction in strength . The optimum content of  $C_3S$  was 50 to 55%. An increase above this figure did not cause any significant increase in strength and occasionally caused a reduction .

A method proposed by Alexander ( 1972 ) related the compressive strength of a cement to the specific surface area and the Bogue proportion of alite and aluminate . This equation gave a good correlation for 3 and 7 day compressive strengths but was very inaccurate for 28 day strengths.

The use of the Bogue calculation for the estimation of alite and aluminate contents introduced errors due to the inaccuracy of the Bogue calculation especially for aluminate .

#### Phase composition and physical properties.

Popovics (1967) proposed an exponential equation to model the strength developing capacity of Portland Cement. Following extensive research , Popovics introduced a modified version of of the 1967 equation. This later version included the influence of the cement fineness on the compressive strength development . The results were also expressed in conventional units of lb./in.<sup>2</sup>. Three assumptions were used in the modified equation.

1. After 90 days the strength of the pastes, mortars and concrete made with Portland Cement were independent of the compound composition of the cements.
2. The rate of hardening parameters were proportional to the specific surface of the cement.
3. The compressive strengths of the standard Portland Cement mortars at the age of 90 days was proportional to the specific surface of the cement.

The modified equation had the following form.-

$$F = F_{90} \frac{1 - C_3 e^{-b_1 t} - (1 - C_3) e^{-b_2 t}}{1 - C_3 e^{-90 b_1} - (1 - C_3) e^{-90 b_2}}$$

F = estimated mortar strength at age of t days.

F<sub>90</sub> = strength parameters representing mortar at age of 90 days

For compressive strength

Cement cured in water F<sub>90</sub> = 5500 S<sub>s</sub>/S<sub>o</sub> ( in pounds per square inch )

Cement cured in moist air F<sub>90</sub> = 5900 S<sub>s</sub>/S<sub>o</sub> ( in pounds per square inch )

S<sub>s</sub> = specific surface of cement under consideration ( in cm<sup>2</sup>/g )

S<sub>o</sub> = specific surface of typical OP cement.

t = age of specimen at testing ( in days )

C<sub>3</sub> = computed C<sub>3</sub>S content of the cement ( in % )

b<sub>1</sub> and b<sub>2</sub> = rate hardening parameters independent of C<sub>3</sub>S content, strength and age but may be a function of C<sub>3</sub>A content, fineness, curing temperature and other factors which influence hydration, for example gypsum content, minor constituents, admixtures and the water cement ratio.

Popovics has calculated several values for b<sub>1</sub> and b<sub>2</sub> which may be substituted into the modified equation.

For compressive strengths of mortar.

$$b_1 = 0.20 (S_s/S_o)$$

$$b_2 = 0.005 C_3 A (S_s/S_o)$$

(The conversion factor for lb./in<sup>2</sup> to N/mm<sup>2</sup> is 0.0069).

When Popovics compared the results of the compressive strengths of three cements studied by Klieger (1957), with values that were calculated

from his modified equation there was a reasonable correlation.

Egorov et al ( 1975 ) prepared a series of pilot plant cement clinkers with varying phase compositions and moduli values . The clinker was ground to produce cement with identical fineness and  $SO_3$  contents ,and it was then tested under standard conditions . From these tests a strength/mineral correlation model was made . However the model did not take into account the effect of compositional modifications , size ,morphology of grain and structural differences . The variation in these factors reduced the accuracy of this model .

Popovics ( 1976 ) investigated the role of  $C_3A$  on the hardening of cement. He found that  $C_3A$  influenced the strength development proportionally more than the quantity present . The  $C_3A$  acted partially as a catalyst . The effect of the  $C_3A$  on the strength development depended on the quantity of  $C_3S$  present . A very high  $C_3S$  content had a detrimental effect on the ultimate compressive strength of Portland concrete.

Knofel ( 1979 ) made a series of Portland cements, from chemically pure materials, using a laboratory kiln . The LSF , Silica Ratio and Alumina Ratio were varied for different samples . The actual phase content of the clinker was measured by a microscopical point counting technique . The clinker was ground with 6 % gypsum to produce cement and used to make test specimens for compressive strength measurements . From this study Knofel established an empirical relationship between the phase content and the 28 day compressive strength . This was represented by the following equation .

$$28 \text{ day compress. strength} = (3 \times \text{Alite}) + (2 \times \text{Belite}) + (\text{Aluminate} - \text{Ferrite})$$

When Knofel investigated cement from production kilns, he found that the incorporation of minor elements and the differences in burning , cooling and grinding greatly reduced the accuracy of the relationship .

A further investigation of cement from a specific works showed that a

similar equation could be used to predict the strength for cement from a single works but this was only accurate if the production conditions remained the same.

#### Phase composition and chemical properties.

In an attempt to study the influence of phase composition and hydration rates on cement. Abdul-Maula and Odler ( 1982 ) used pure chemical reagents to make cement in a laboratory . The phase content of each clinker was controlled by adjusting the composition of the raw meal . The compressive strength of these cements was tested using small specimens in a micro compression test. The replacement of  $C_3S$  by  $C_2S$  and the replacement of  $C_3S$  by  $C_3A$  produced an overall decrease in 28 day strength in each case . The replacement of  $C_3S$  by  $C_4AF$  produced an overall increase in 28 day strength . The replacement of  $C_3S$  by  $C_3A$  and  $C_4AF$  produced an increase in the early strengths, then a decrease in compressive strength at 28 days.

From this investigation the significance of  $C_3S$  for high final strengths was apparent . The effect of the  $C_3A$  and  $C_4AF$  phases was variable and influenced the cement to a greater degree than their percentage presence would signify .

To study the influence of minor oxides , measured amounts were added to the raw cement feed before firing . The addition of these oxides caused a significant variation in the phase composition . The free lime content was higher following the addition of  $MgO$ ,  $Na_2O$  or  $K_2O$  additions. This was due to the substitution of calcium by these elements. The addition of  $MgO$  to a level of 5 % produced a moderate decline in 28 day strength . Abdul and Odler found that the percentage of hydrated  $C_3S$  was also reduced and the reduction in strength was probably related to the slower hydration rate of the high  $MgO$  cement . The addition of  $Na_2O$  or  $K_2O$  up to a level of 1% produced a slight decrease in the later compressive strengths. The addition of 1%  $Na_2O$  reduced the fraction of  $C_3S$  that was hydrated after 28 days from 85% to 78%. Abdul and Oder

concluded that the incorporation of the minor oxides into the lattice of the four major cement phases was only of minor significance.

The second part of Abdul and Odler's investigation only studied the effect of one minor oxide in cement at a time. Scant consideration was given to the interdependent effects of the multiple minor oxides substitutions in the cement phases. Due to this, the author believes that Abdul and Odler's conclusions are oversimplified.

Odler and Wonnemann (1983) investigated the effects of alkalis on the hydration of portland cement. They prepared mixes of cement and added small amounts of potassium and sodium. They found that the  $K_2O$  and  $Na_2O$  were preferentially incorporated in the  $C_3A$  phase. The rate of  $C_3A$  hydration was slowed in cements with  $Na_2O$  and accelerated in cements with  $K_2O$  added. They noted that the  $C_3S$  hydration rate was not altered significantly. Overall they concluded that the development of strength was not unduly altered by the presence of the alkalis in the clinker.

Odler and Wonnemann used pure chemicals to make their trial cements and added either potassium or sodium. This simulation of alkalis in cement clinker is not an accurate representation of the actual multiple interdependent substitutions that occur in production cement clinker manufactured from natural raw materials. Thus their overall conclusions can only be valid for the experimental cements they produced.

None of the methods proposed for estimating compressive strength were accurate or realistic when using phase contents. Therefore other factors must influence the cement strength.

#### Microstructure of cement clinker.

Several researchers have investigated the effect of clinker microstructure on the cement quality.

Grzymek (1959) found that increased 1 day and 28 day compressive strengths were almost proportional to decreased alite grain size. Butt and Timashev (1962) found that the size of alite did influence the strength of cement but its role depended on other factors. They observed that clinker with alite grains between 35 $\mu$ m and 40  $\mu$ m. had a greater strength than clinker with extremely fine or very coarse crystals of alite. Okorokov and Volkonskii (1975) categorised clinker into five groups based on the dimensions of the alite crystals. From this they found that the strength was increased with a higher content of alite. The strength was also related to the size of the alite. If the size exceeded 100 $\mu$ m. the compressive strength of the cement was reduced.

The combined effects of size and shape of both alite and belite have been investigated by Sudukas et al (1975). They established a classification system for the differences in clinker microstructure. They found that for cement with the same silica ratio, alumina ratio and phase composition, the 28 day strength could vary by 25%. Examples of the clinker microstructure are shown in Figure 9.3 . The clinker microstructure that produced the highest 28 day strength with all moduli and phase compositions being equal , was that shown as TYPE 1 in Figure 9.1.

The differences in microstructure and the variations in phase composition influence the strength and quality of the cement . However none of the models work consistently for all cements. This is because the composition and reactivity of the cement minerals must be considered when developing a model for cement quality.

#### Multistatistical methods.

A major statistical study was carried out on 199 commercial cements by Blaine et al. (1965). the properties of cement were correlated with compositional parameters of the clinker . These results indicated that

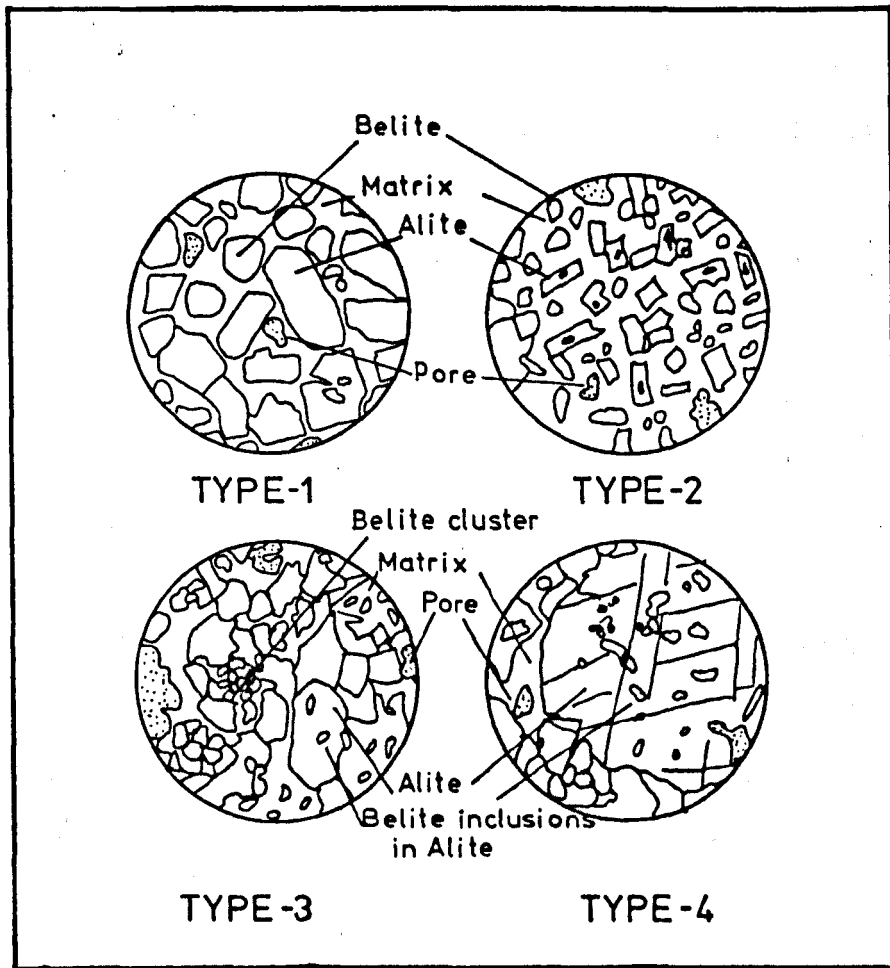


(Fig. 9.3)

ILLUSTRATIVE SKETCHES OF THE DIFFERENT TYPES OF CLINKER MICROSTRUCTURE. (After Sudakas et al. 1975 )

an increased  $C_3S$  content led to an increase in compressive strength at all ages, but especially 28 day. The presence of  $C_3A$  had a positive influence on early strength values, but a negative effect on the later strengths. The  $K_2O$  level in the clinker had similar correlations. Blaine found that the percentage gain in strength from early to late strengths decreased in step with increased alkalis level.

Influences of minor phases in cement clinker on the compressive strength development.

The alkali sulphate phases.

The alkalis in cement originate from the raw material used to make the kiln feed. Most of the alkali elements are in the clay or shale fraction. The use of coal in burning the feed introduces more alkalis and sulphur. Approximately 50% of the alkalis in the raw feed are volatilised in the kiln between  $800^{\circ}C$  and  $1000^{\circ}C$ . These gases condense on cooler sections of the kiln, some are discharged from the kiln via the exhaust gases. Frequently to reduce pollution, these gases and high alkali dusts are recycled back into the kiln. The use of energy efficient dry process kilns with the incoming feed being preheated by the alkali rich exhaust gases increases the overall alkali content of the cement.

Jawed and Skalny (1977) reviewed research that had been made on alkalis in cement and the effects on clinker formation, hydration and quality of cement. A detailed investigation on the influence of alkalis was carried out by Osbaeck (1979). He used the Bogue formula to calculate phase compositions from his chemical analyses. With this data, Osbaeck studied the effects of  $Na_2O$  and  $K_2O$  on the strength of mortars. He found the best correlation was between 28 day compressive strength and the soluble alkali-content. The total alkali content had a poorer negative correlation. As an experiment, Osbaeck prepared mortar test pieces with mixing water which contained varying amounts of potassium sulphate ( $K_2SO_4$ ).

The 1 day and 3 day compressive strengths showed an overall increase. There was no effect on the 7 day sample, but the 28 day strength was reduced by 18 %.

In the authors opinion the additon of  $K_2SO_4$  to the mixing water was not an accurate model of the influence of alkalis on the quality of cement. A substantial proportion of the alkali elements in cement clinker are as substituted ions in the major clinker phases. More alkalis are in the form of alkali sulphates. This is not simulated by the addition of alkali sulphates to the mixing water. When cement is hydrated the alkalis are released from the clinker minerals at different rates and stages in the hydration process. Differences in the composition of the individual clinker phases are responsible for altering the reactivity and hydraulicity of the minerals in the cement clinker.

Gebauer and Kristmann (1979) investigated on cement clinker from both wet and dry production kilns. They studied the clinker with conventional chemical and mineralogical techniques. The chemical analysis indicated that the average quantities of alkalis and sulphates in dry process kilns was only fractionally higher than the level for wet process kilns. This contradicted a commonly held belief that the low 28 day compressive strength of cement from energy saving dry process kilns, was due to the increased alkali and sulphate levels in the kiln and the clinker. They found that the alkali sulphate occurred in two forms; potassium sulphate with some replacement of  $K_2O$  by  $Na_2O$  or  $CaO$  and calcium potassium sulphate with some  $Na_2O$ .

After analysis the clinkers were then ground in the laboratory to produce cement and tested for compressive strength. The properties of the clinker and cement were correlated against each other. The factor that was predominantly highly correlated with strength in cement mortar samples was potassium oxide, especially the water soluble potassium sulphate. The potassium increased the early strength and decreased the 28 day and 275 day compressive strength of the mortar. However no

correlation was found between potassium oxide in commercial cement and concrete strength. Gebauer and Kristmann thought that factors such as the fineness of the cement, quality of the gypsum, and interactions between the cement and the aggregate of the commercial cement masked the effects of the potassium oxide.

They found that the presence of alkalis sulphate increased the reactivity of the cement minerals in the commercial cement. This influenced the storage stability of the cement. The reactive cement with a high potassium content was covered in crystals of ettringite and syngenite after a few hours exposure to humid air. The cement had poor flow characteristics and tended to form lumps in bags or silos. A similar effect was observed when the cements were hydrated. The reactive cement was covered with large needle-like crystals of syngenite and ettringite after a few minutes. The low reactivity cement with a low potassium content, had only a few small hydrate crystals. After 24 hours the large crystals from the reactive cement had recrystallised to small crystals, similar to the crystals on the cement with low reactivity. Johansen (1977) investigated the effect on compressive strengths of adding  $K_2SO_4$  to commercial OP cement and SR cement. He thought that this was similar to the change from a wet process kiln to a dry kiln with a suspension preheater. The compressive strengths increased for the early strengths and decreased for the 28 day test. When he tried a correlation between the quantity of chemically combined water in the mortar after 3 minutes and the 28 day compressive strength. A negative correlation value was obtained. Johansen concluded that the reactions taking place immediately after addition of the water were crucial in the development of strength.

The effects of the increased alkalis level on the ultimate strength of cement from production dry process kilns was minimal. The dry kilns usually produced a clinker with a higher  $C_3S$  level than wet process kilns. This caused an increased 28 day strength and offset the reduction in strength caused by the presence of  $K_2SO_4$ . If the alkalis level was very

high , the effects could be reduced further by the addition of gypsum into the raw kiln feed. Butt et al (1971) proposed that the addition of extra gypsum also lowered the amount of alkali substitution into the clinker minerals. The alkali substitutions produced minerals with slower hydration rates and lower strengths.

Effects of gypsum on the 28 day compressive strength of cement.

From these different investigations it is apparent that the optimum amount of gypsum required to give the best performance from cement varies considerably. Sprung and Rechenberg (1977) found that in high alkali cements, the alkalis suppressed the solubility of  $\text{Ca(OH)}_2$  and promoted the dissolution of  $\text{C}_3\text{A}$ . If the quantity of gypsum added was too small, quick setting of the cement occurred. This was due to the formation of aluminate hydrate. If the gypsum addition was too much, quick setting occurred because of the formation of ettringite.

Jawed and Skalny (1977) in their review of alkalis in cement , reported that the optimum  $\text{SO}_3$  content was dependent on the level of alkalis and  $\text{C}_3\text{A}$  as follows.-

Alkali	$\text{C}_3\text{A}$	Optimum $\text{SO}_3$
Low <0.5%	Low < 6%	2%
Mid =1.0%	Low < 6%	3% to 4%
High >2.0%	High >10%	3.5% to 4%
Low <0.5%	High >10%	2.5% to 4%

The optimum  $\text{SO}_3$  content is achieved by adding  $\text{SO}_3$  in the form of gypsum ( $\text{SO}_3$  content = gypsum % x .476 ) to the existing  $\text{SO}_3$  in the clinker before grinding the mixture to produce the cement.

The small changes required to produce a good quality cement from a dry process kiln are substantially less expensive than the high energy costs of operating a wet process kiln.

The influence of alite polymorph on the compressive strength of cement.

The major component of portland cement is alite, it may occur in several polymorphic forms. The triclinic form is the lowest temperature phase. It is followed by the monoclinic form and finally the highest temperature phase, the rhombohedral or trigonal form. The presence of impurities in alite can stabilize the monoclinic and rhombohedral forms at room temperature. In most cements the monoclinic form is stabilized, however in some cements the rhombohedral form can occur. Gourdin et al. (1980) found that there was a strong correlation between the presence of rhombohedral alite in commercial cements and high compressive strengths. Several researchers have prepared rhombohedral alite ( Ono et al., 1965, Nurse et al., 1966 ), but they used large amounts of additives such as  $Mn_2O_3$  to stabilize the alite.

These elements do not occur in commercial cement raw feed at the required level. In many cases the stabilizing element used would preferentially partition into the other phases in the clinker. The manganese would preferentially substitute in the ferrite. This would change the hydraulicity of the other phases and require large amounts of the additive to reach the level required to stabilize the alite. Aldous (1983) tried variable amounts of  $Al_2O_3$ ,  $Fe_2O_3$ , F,  $TiO_2$ ,  $Mn_2O_3$ , and MgO in different combinations to stabilise rhombohedral alite. The presence of MgO,  $Fe_2O_3$  and  $Al_2O_3$  stabilized the monoclinic form. The addition of the following elements stabilised the rhombhedral form.-

$Al_2O_3$	$Fe_2O_3$	F	$Mn_2O_3$	$TiO_2$	
1.6%		0.4%			= R
0.6%	0.5%	0.5%			= R
0.7%	1.0%			0.9%	= R
1.1%		1.1%	2.4%		= R

To test the compressive strengths of the rhombohedral and triclinic alites, the samples were ground and mixed with sand and grit to make micro-concrete cubes (25mm) of each polymorph. These cubes were tested for

compressive strength at 1, 7 and 28 day intervals. Cubes made with Ordinary portland cement were used as a reference. The rhombohedral alites with fluorine and alumina had the highest 28 day strengths of 56 N/mm<sup>2</sup>. The cubes with fluorine, iron and alumina addition had very low strengths at 1 day but were only slight lower after 28 days, about 55 N/mm<sup>2</sup>. Both samples were above the 28 day strength of the reference OPC, which was 40 N/mm<sup>2</sup>.

As an experiment to simulate the hydration conditions of a cement, Aldous mixed C<sub>3</sub>A and hemihydrate with the rhombohedral alite. This mixture produced a cement with a 28 day strength of 64 N/mm<sup>2</sup>. A similar mixture with triclinic alite had a 28 day strength of 45 N/mm<sup>2</sup>. Aldous concluded that after an extended dormant period, the rhombohedral alite reacted faster than the monoclinic or triclinic alites. This produced the enhanced later compressive strengths. Harada et al. (1978) noticed that hydrated rhombohedral alite had a different morphology to those formed from monoclinic or triclinic alite pastes. The pastes had a different pore size distribution. Harada did not make any strength determinations.

The author has found that production Ordinary portland cement from Works C, had a substantial quantity of rhombohedral alite. This cement contained 0.27 wt.% fluorine and had a high alumina content. The fluorine was preferentially substituted in the belite phase, about 1.1 wt% element. The alite phase in the clinker contained between 0.4 and 0.6 wt.% fluorine. This cement had a relatively high 28 day compressive strength of 51 N/mm<sup>2</sup>, when compared with other OP cements which do not have rhombohedral alite.

The author proposes that the composition and morphology of the four major cement phases and the quantities at which they are present, can be beneficial or detrimental to the ultimate compressive strength of the cement. The mechanisms of minor element substitution are closely interrelated, therefore the effects of the substitutions on the strength

of the cement are interdependent. The investigation of the effect of one or two of the minor elements in isolation will produce results of limited application. The contribution of an individual cement phase to the actual cement strength is not directly related to the amount of the mineral present. Thus the use of linear regression analysis, or other statistical methods that operate on the basis of a linear relationships, to establish the contribution of different parameters, can lead to erroneous results. Any technique used to relate the mineralogical, chemical and physical properties of cement clinker to the quality of the cement must overcome these limitations, to produce accurate correlations.

Chapter ten

ANALYSIS OF THE MINERALOGICAL, CHEMICAL AND PETROLOGICAL CHARACTERISTICS  
INFLUENCING THE QUALITY OF CEMENT CLINKER.

The factors influencing the quality of cement clinker.

Introduction.

The numerical results of the analyses and tests made on the cement clinkers were stored in a database system on an Apple II micro computer. The results from each cement clinker were divided into the following groups.

1. Chemical analyses of cement clinkers and kiln feeds, determined by X-ray fluorescence, Atomic Absorption Spectrometer, or titrimetric methods. From these results the LSF, free lime, Alumina and Silica Ratios were calculated. (Chapter 3)
2. Mineral analyses of the alite, belite, ferrite, tricalcium aluminate, calcium aluminate and alkali sulphates, were determined by electron microprobe analysis. From this data the mineral formula was recalculated to give the composition of the actual minerals. (Chapter 8)
3. Petrological and mineralogical characteristics, such as size and range of calcium silicates, polymorphs of belite and tricalcium aluminate, percentages of phases present, porosity and reduction in the clinker nodules. (Chapters 5 and 6)
4. Potential phase composition of the clinker by Bogue calculation, matrix calculation and microscopical point counting. (Chapter 7)
5. The quality of the clinker was measured by British Standard tests. (Chapter 3)

To assess the influence of these clinker characteristics on the quality of cement, several techniques were tried.

### Correlation coefficients.

All the data values were correlated on a one to one basis to identify the linear relationships between the clinker characteristics. This produced a correlation matrix of 132 by 132 parameters.

However after plotting the graphs of the correlation pairs, it was apparent that many of the relationships were not linear. For example, the level of element substitution in a clinker phase was controlled by the polymorphic form of the mineral and the type of production process, as well as the amount of element present in the cement. Thus the use of this statistical method was not suitable.

To overcome problems due to the non linear relationships and skewed distributions, a type of Trend analysis was devised to compare the different properties of the cement simultaneously.

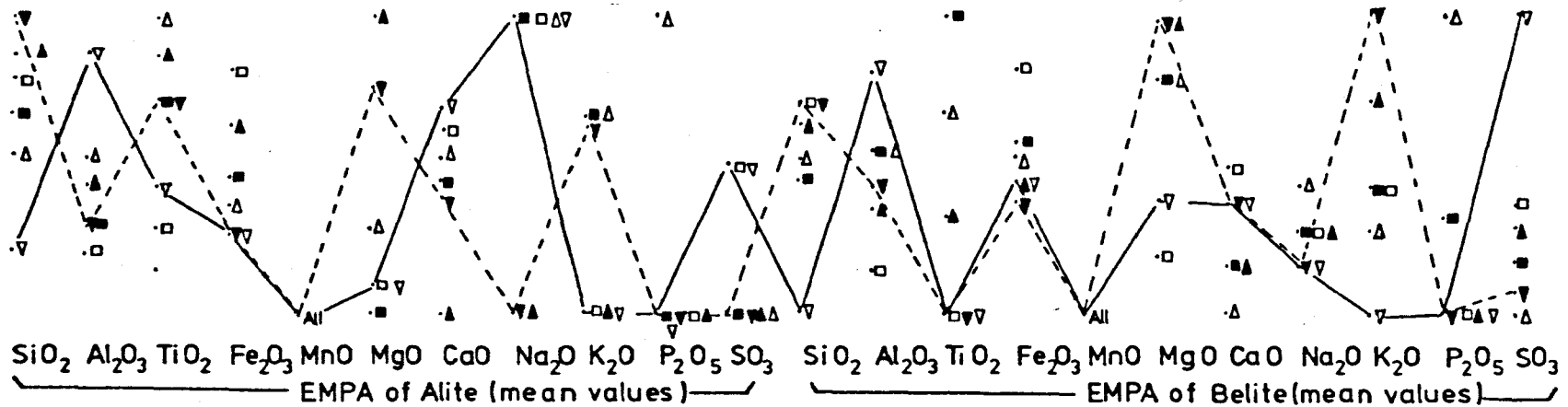
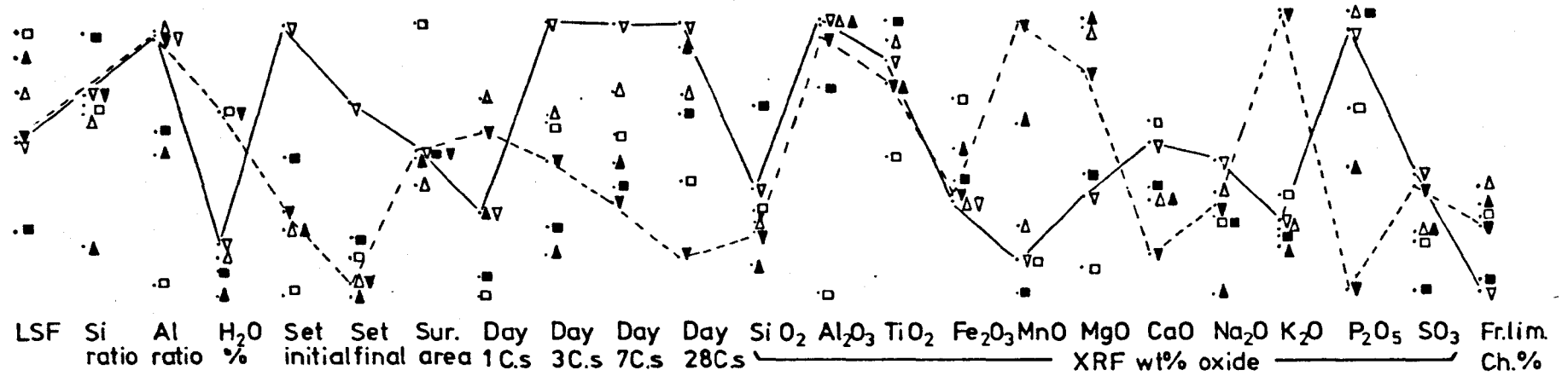
### Trend analysis of the cement clinker from works A,B,C,D,E,F and G.

In this analysis technique the values for each of the parameters ( Eg.  $\text{SiO}_2$  in alite ) for each of the different cement clinkers was normalised and plotted on a set scale. The highest value was at the top and the lowest value was at the base. The other values were plotted between the two extreme values. This normalisation process was used to overcome the variation in the ranges of the different parameters. The normalised plots are shown in Figure (10.1).

There is no implied relationship between each of the parameters and its neighbour.

The results for all the cement clinkers were compiled . In the Trend analysis the cement clinkers from Works A,B,C,D,E and G were assigned a symbol. The symbols were paired as follows.

(Figure 10.1) TREND ANALYSIS OF THE CEMENT CLINKERS FROM WORKS A,B,C,D,E AND G.



**KEY**

Works.	Type.	Process	Works.	Type.	Process
A	△	OPC semi-dry	D	■	OPC wet
B	□	SRC wet	E	▽	OPC dry---- (low strength)
G	∇	OPC dry ← (high strength)	G	▲	OPC semi-dry

(Figure 10-1.continued) TREND ANALYSIS.

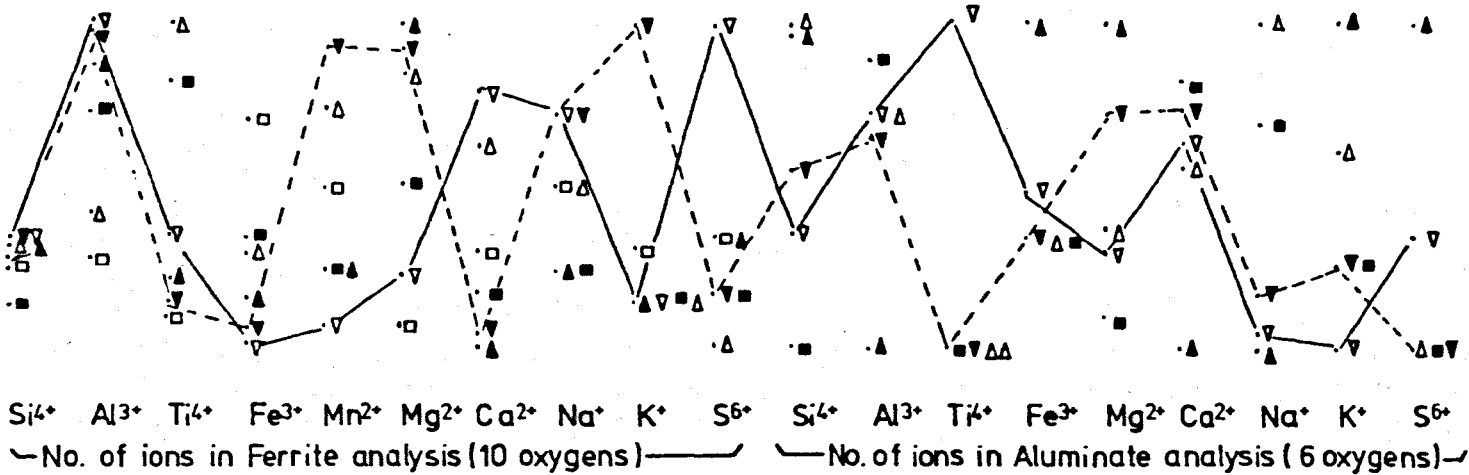
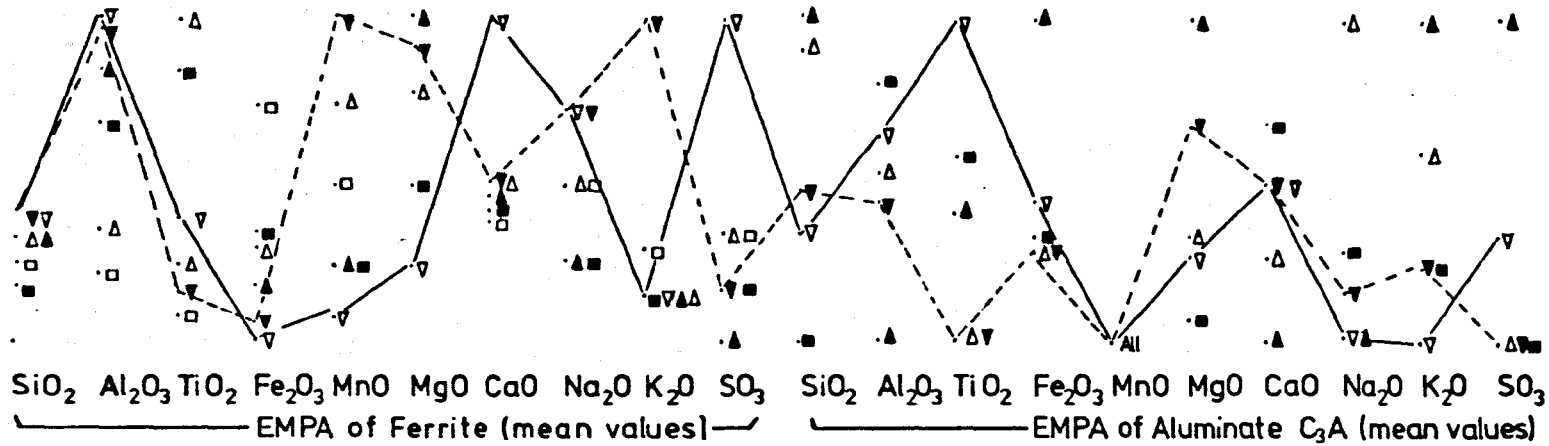
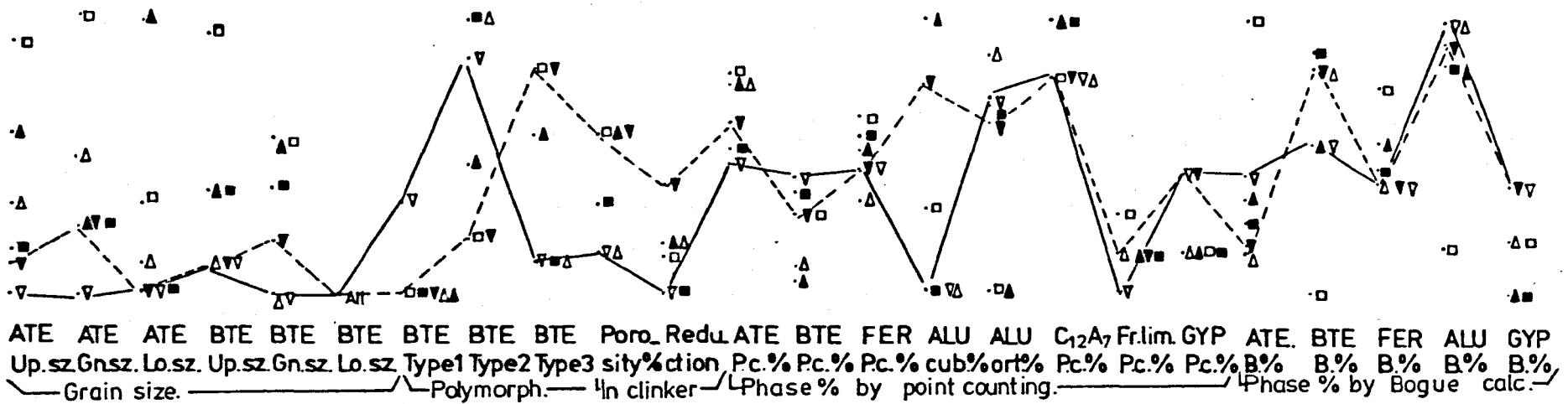
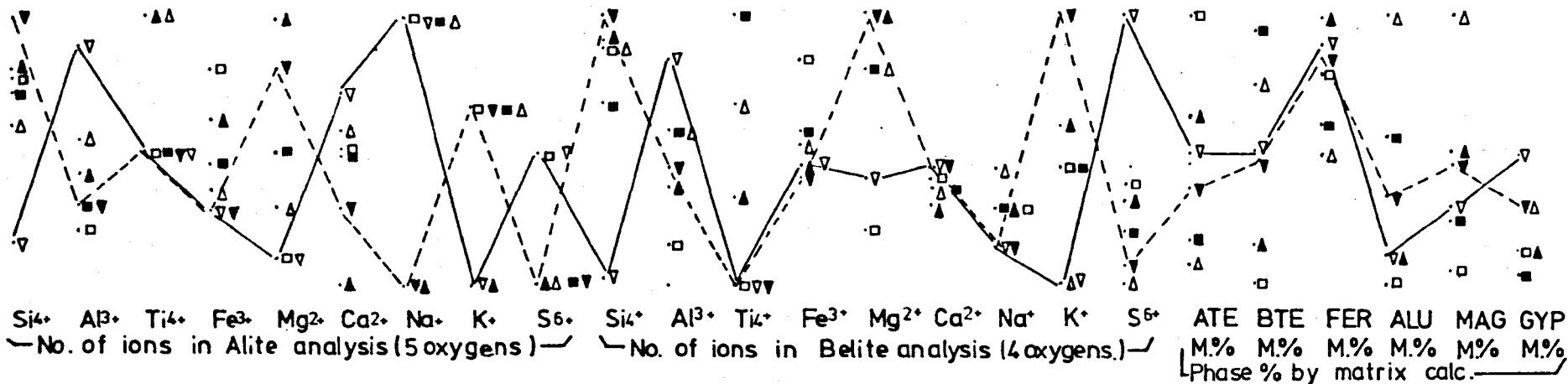


(Figure 10.1. continued) TREND ANALYSIS



Works C = ▽ Dry process  
Works E = ▼ Dry process  
  
Works A = ▲ Semi-dry process  
Works G = △ Semi-dry process  
  
Works B = □ Wet process  
Works D = ■ Wet process

To aid the interpretation of the trend analysis the cements with the highest and lowest 28 day compressive strengths have been identified by joining the locations of each of the symbols representing the cements.

After examining the trend analysis figures and recording the parameters where there was substantial divergence, two lists were compiled. One in which high values of the parameter were apparently beneficial to high 28 day compressive strength. The other list was of parameters where a high value seemed detrimental to a high 28 day strength.

To select the parameters in the two lists which had the most consistent effect on the compressive strength of all the cement clinkers, the sequence of the symbols from the 28 day strength plot was compared along side all the other selected parameters. From this a set of parameters which had a similar sequence was defined.

These parameters were -

H<sub>2</sub>O%  
K<sub>2</sub>O XRF  
MgO alite  
K<sub>2</sub>O belite  
K<sup>+</sup> belite  
MnO ferrite

These parameters were all from the detrimental list. Thus a high value of these parameters is associated with a low 28 day compressive strength.

### Analysis of Trend results.

The reasons why the parameters selected by the trend analysis are responsible for low strength cement can be deduced from the behaviour and properties of the cement clinker minerals. These characteristics have been established from the overall investigation of the cement clinkers from the different works and processes.

#### The water - cement ratio ( $H_2O$ %).

The quantity of water used to mix a mortar or concrete is critical. Extensive research has shown that excess mixing water produces a weak concrete. The water cement ratio is the amount of water per unit weight of the cement in the concrete. The ratios are usually expressed as a decimal fraction. (ie. A concrete with a water cement ratio of 0.5 would require 0.5 Kg. of water per 1 Kg. of cement.) Most concretes have a water cement ratio between 0.4 and 0.7. The ratio used depends on the strength requirements of the concrete. Lower ratios can be used but the concrete has low workability unless water reducing admixtures or superplasticizers are added.

#### The level of magnesium substitution in alite ( MgO alite ).

The amount of MgO substituted in the alite structure is important because it stabilises the monoclinic polymorph of alite. Aldous ( 1983 ) has shown that if the rhombohedral polymorph is stabilised in the clinker. It produces a higher strength cement than the cement with the monoclinic alite.

#### The level of manganese substitution in ferrite ( MnO ferrite ).

The level of MnO substituted in ferrite is significant because it acts in a manner similar to iron. It is preferentially substituted in ferrite,

therefore the amount of ferrite in the clinker would be higher than expected. The additional ferrite required more calcium, this changed the calcium/silica ratio in favour of the lime deficient phase, which is belite. The belite has a lower 28 day compressive strength than alite. (see Figure 9.1 chapter 9). Thus a cement which has a high level of manganese substitution in the ferrite will have a lower compressive strength.

#### The influence of potassium on the compressive strength of cement.

The parameters which have a major influence on the strength are the potassium levels in the cement ( $K_2O$  XRF) and the potassium substitution in the belite. ( $K_2O$  belite and  $K^+$  belite). The potassium in the cement clinker has a primary effect on the formation and stabilisation of the tricalcium aluminate, the belite, the alite phase and the alkali sulphates. The partitioning of the potassium between the phases is complex. It is partially influenced by the production process and the kiln operating conditions.

#### The influence on alkali sulphates.

Pollit and Brown (1968) found that the quantity of alkali sulphates, such as sodium potassium sulphate, calcium potassium sulphate and potassium sulphate, was determined by the ratio of the total clinker sulphate to the total alkali content.

An increased level of alkali sulphates tends to form in dry process kilns with preheaters. This is because of the recycling of the alkali rich exhaust gases when they condense on the incoming feed.

#### The influence on tricalcium aluminate.

If there is a high potassium level and a low sodium level, the cubic polymorph of tricalcium aluminate is stabilised and it can accommodate a substantial amount of potassium substitution. If there is a higher sodium level, the orthorhombic polymorph of tricalcium aluminate is stabilised

preferentially. This has a low limit of potassium substitution. Thus there is more potassium available to substitute into the other clinker phases, principally belite and to a very small extent, into the alite phase.

#### The influence on alite.

If there is an excess of potassium to substitute into the alite, it will accept up to 0.1 wt%.oxide. Any higher amounts will disrupt the crystal lattice and the alite will dissociate to CaO and SiO<sub>2</sub>. This reduces the quantity of alite in the cement clinker. Thus because the alite phase contributes the most to the strength of a cement, this concrete will have a low compressive strength.

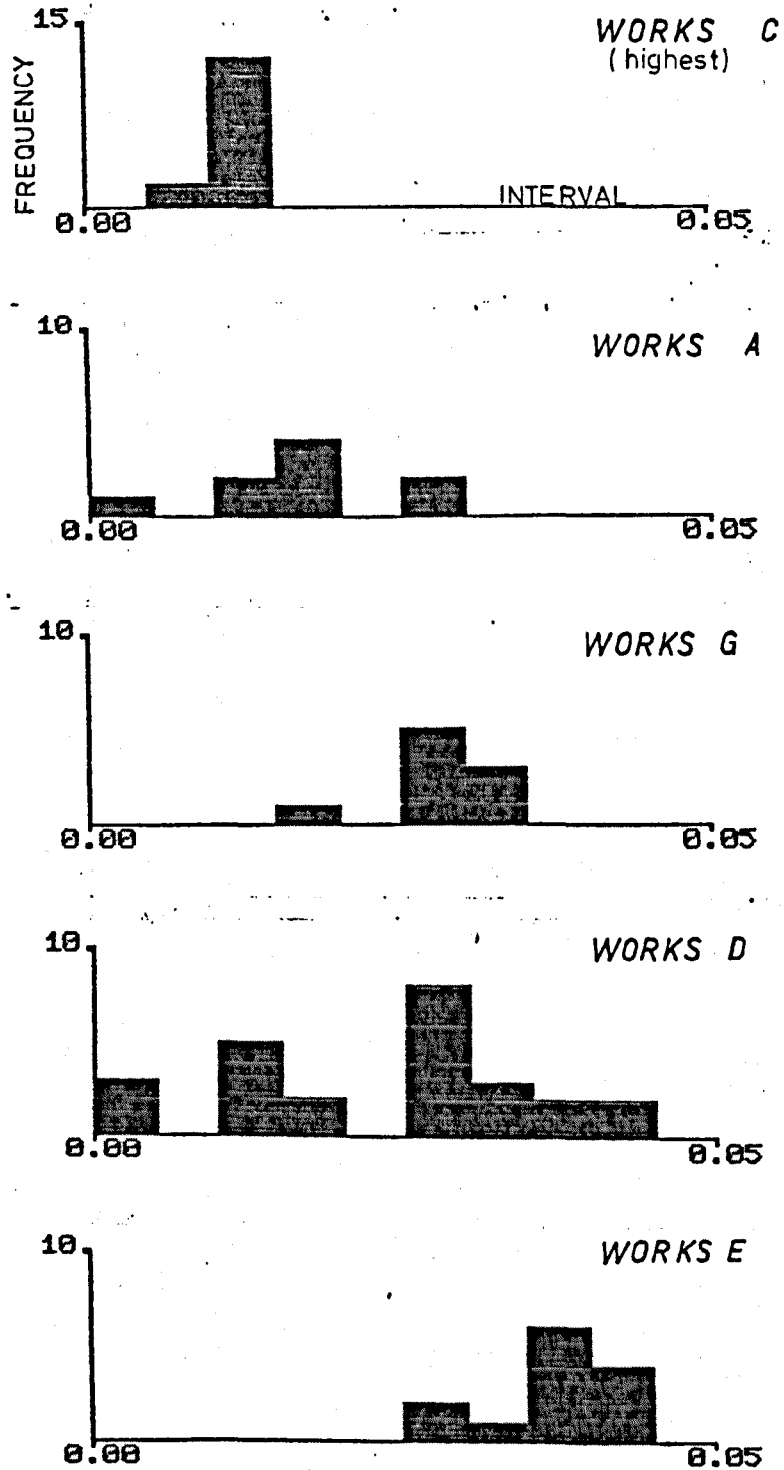
#### The influence on belite.

Regourd and Guinier (1974) and Hjorth (1971) both found that the alpha dash ( $\alpha'$ ) polymorph of belite had a higher level of potassium than the beta ( $\beta$ ) form of belite. Jawed and Skalny (1977) in their review on alkalis in cement noted that  $\beta$  belite could convert to  $\alpha'$  belite by the substitution of potassium.

The beta polymorph has the best reactivity with water and contributes the greatest amount to the strength development in the cement, of any of the belite polymorphs. Thus if there is less beta belite present in the clinker, the contribution to the overall strength of the cement will be reduced.

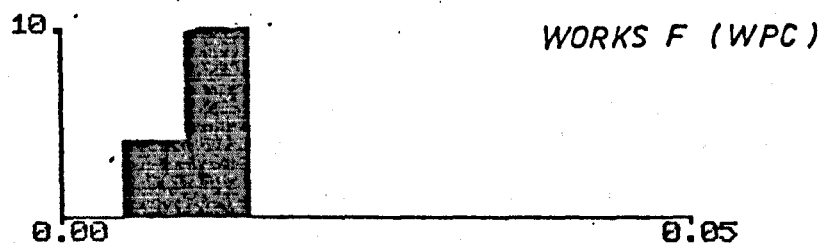
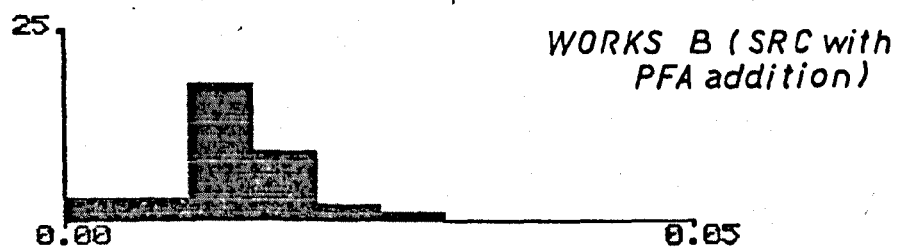
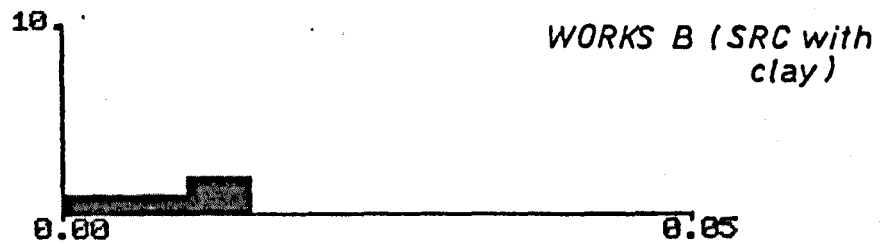
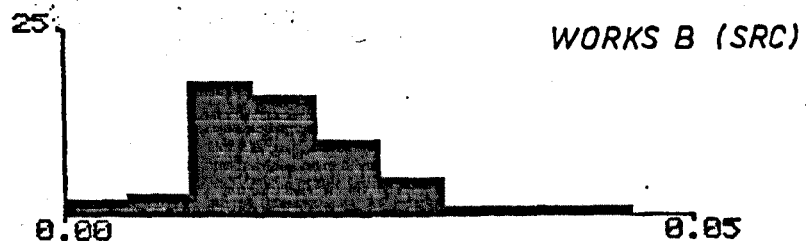
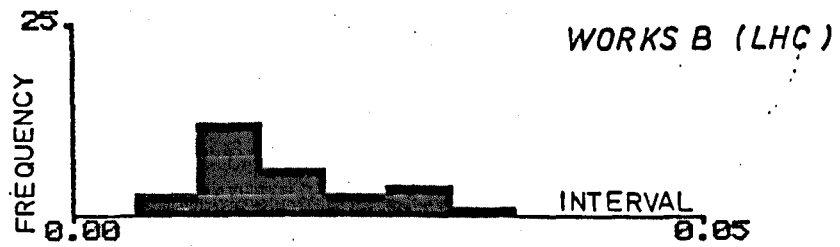
The distribution of the number of K<sup>+</sup> ions substituted in the belite from the cement clinkers from all the works is shown in Figures 10.2 and 10.3. The distribution histogram shows the number of belite analyses with the amount of K<sup>+</sup> ions substituted at each 0.005 interval. ( Calculated on the basis of 4 oxygens in the mineral formula.). From these distributions the median point has been plotted on Figure 10.4. This shows the precise

(Figure 10-2). The distribution of the levels of potassium substitution in belite ( after recalculation on the basis of 4 oxygens ) , from ordinary portland cement..



The histograms are arranged in order of increased 28 day compressive strengths.

(Figure 10.3). The distribution of the levels of potassium substitution in belite from sulphate resisting, low heat and white portland cement (after recalculation on the basis of 4 oxygens).



KEY

A = OPC clinker from Works A

B = SRC or LHC clinker from Works B

C = OPC clinker from Works C

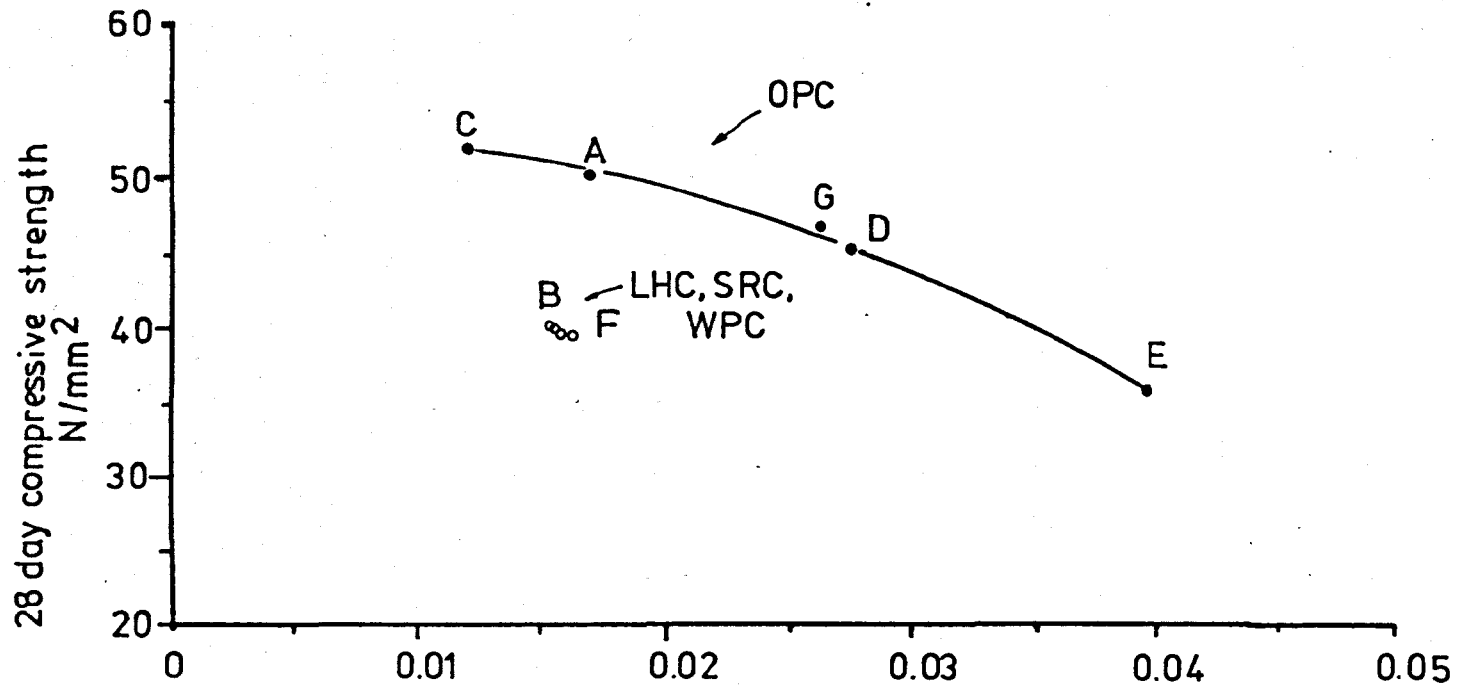
D = OPC clinker from Works D

E = OPC clinker from Works E

F = WPC clinker from Works F

G = OPC clinker from Works G

(Fig.10·4) RELATIONSHIP BETWEEN 28 DAY COMPRESSIVE STRENGTH AND LEVELS OF POTASSIUM SUBSTITUTION IN BELITE.



Mid point of distribution of potassium levels in belite from cement clinker. (derived from Figs 10·2 & 10·3)

relationship between the level of potassium substitution in the belite from the cement clinkers and the 28 day compressive strength of the cement. There is a difference in the positions of the curves for the various types of cement. This is due to the presence of tricalcium aluminate in the Ordinary Portland and White Portland Cements. The interrelationship with the belite on the partitioning of the potassium is extremely important. The other cements, sulphate resisting and low heat contain little or no tricalcium aluminate. Therefore the partitioning of the potassium is influenced more by the other phases.

Thus the role of potassium and potassium substitution in the cement clinker is crucial to the potential compressive strength of the portland cement.

#### Conclusions and recommendations.

The level of potassium in cement should be kept as low as possible. The presence of potassium in the cement feed need not be detrimental to the compressive strength of the cement, if the destination of the potassium can be controlled. Alkali sulphates in the form of calcium potassium sulphate are less deleterious than potassium sulphate.

Potassium substituted in the tricalcium aluminate phase does not have any significant effect on the strength of the cement. However potassium substitution in belite significantly affects the strength of cement.

Potential losses in strength due to the stabilisation of an unreactive polymorph, can be overcome by the stabilisation of the rhombohedral alite polymorph. This contributes greater strength to the cement and offsets the reduced contribution from the other phases.

## Summary of the results and suggestions for further research.

### Sample Selection.

The samples of cement clinker were supplied by Blue Circle and were collected from different cement works in the United Kingdom. A variety of types of cement clinker and methods of production were chosen to reflect the range of mineralogy and chemistry present in normal production Portland cement clinker.

### Analysis

All the samples supplied were examined mineralogically, petrologically and chemically. The analyses of the compositions of the cement clinker were used in an attempt to determine the actual phase composition of the individual cement clinkers. The recalculation method used the features of matrix mathematics for solving several simultaneous equations. However the potential accuracy of this method was reduced because it was not possible to obtain totally uncontaminated analyses of the clinker matrix phases. This was due to their small grain size.

The data on mineral compositions was used to investigate the effects of minor elements on the stoichiometry of the cement clinker phases. From this study it was possible to investigate the partitioning of the minor elements in the different mineralogical assemblages.

## Physical properties.

Tests on the quality of the cement, to BS 4550, were made by Blue Circle on all the different types of cement, but not on all of the samples. These results were combined with the data from the mineralogical and chemical analyses carried out by the author. This combination was used to identify which mineralogical, chemical and physical properties of the cement clinker had the most influence on the compressional strength of the cement when used in concrete.

## Conclusions

The combination of the mineralogical properties and the quality data in the Trend analysis ( Chapter 10 ) identified several parameters which had a significant effect on the compressive strength of the concrete.

These were -

The water-cement ratio

The level of magnesium substitution in the alite phase.

The level of manganese substitution in the ferrite phase.

The overall amount of potassium in the cement.

The level of potassium substitution in the belite phase.

The mineralogical parameter which had the most dramatic effect on the concrete strength was the amount of potassium substituted into belite, the dicalcium silicate phase in the cement clinker. A high level of potassium in the belite, produced a concrete with a low 28 day compressive strength.

The potential level of potassium in the belite could not be predicted by the overall amount of potassium in the cement clinker. The presence or absence of other clinker mineral phases was crucial to

the partitioning behaviour of the potassium. The phase which had the most influence was tricalcium aluminate ( C3A ). The aluminate usually forms in the cement clinker as either cubic or orthorhombic crystals.

If the C3A was stabilised in the orthorhombic form, some potassium could substitute into the crystal lattice. However if the cubic form of C3A was present in the clinker , a higher level of potassium substitution was possible. Thus less potassium was available to substitute into the belite phase, which would lower the potential strength of the concrete.

#### Further Research.

The effect of minor element partitioning within the cement clinker is extremely important. Future research should concentrate on the preferential partitioning of these elements and controlling their destination. This could be achieved by investigating the effectiveness of various stabilizing elements on the different cement clinker mineral phases.

If the belite phase could be stabilized so that little or no potassium could substitute into the structure, the influence the polymorphic form of tricalcium aluminate has on the preferential partitioning of the potassium would be diminished. Alternatively , the cubic form of C3A could be stabilized so that potassium would preferentially substitute into the aluminate phase.

This investigation should be repeated on the other clinker mineral phases to stabilize the optimum polymorphic form and enhance the strength characteristics of the cement.

The effects of each of the stabilizing elements on the all the clinker phases would have to be investigated to prevent the

stabilization of undesired polymorphic forms.

Ideally the research would commence with laboratory prepared raw materials. To this would be added small quantities of material containing possible stabilizing elements. The sintering conditions and the thermal history could be accurately controlled and monitored.

When suitable additives had been selected. The experimental mixes should be made from raw materials which would be used in the economic production of cement clinker. Finally the trials could be scaled up to use a pilot plant kiln. This would produce results which could be used to predict partition preferences in a full size production cement kiln.

Appendix two.

PULVERISED FUEL ASH.

Introduction.

Pulverised fuel ash ( P. F. A.). The ash is produced by the burning of crushed coal in the steam generation furnaces at power stations. The chemical composition of P. F. A. varies slightly depending on individual collieries supplying the power stations.

INVESTIGATION OF P. F. A. FROM DRAX POWER STATION ( U. K.)

OPTICAL EXAMINATION IN OIL AND SCANNING ELECTRON MICROSCOPE INVESTIGATION .

The particles were predominantly spherical and some were hollow (cenospheres ). The hollow spheres frequently contained many smaller spheres inside .( Plate 1b. ) Other fragments were of irregular shape, or were pieces of larger cenospheres which had broken. The spheres were of three distinct types ; smooth surfaced and transparent ( Plate 1d. ), rough surfaced and opaque .(Plate 1g.) or smooth surfaced and opaque. The transparent spheres were glasslike , with a size range from 1 mm.(rare) to 0.5 um (Plate 1b.) The rough surfaced opaque spheres were attracted and repelled by magnetic fields and were thus identified as magnetite ( $Fe_2Fe_3O_4$  ) , the size varied from 0.5 mm. to 0.5 um . The smooth surfaced opaque spheres were glass with inclusions of magnetite which made them slightly susceptible to magnetic influence. The irregular fragments were dominantly glass or glass with magnetite spheres which had broken . Occasionally there were particles with a honeycombed appearance , these were probably residual unburnt coal (coke) (Plate 1a.). In the S E M. investigation several long lath shaped crystals were observed, these had the characteristics of mullite ( $2SiO_2.3Al_2O_3$ ) .(Plates 1c. and 1e.). Occasionally there were small quartz (  $SiO_2$  ) grains with fused edges . (Plate 1f. ) In all of the samples there were many small well formed rhombohedral gypsum crystals ( $CaSO_4.2H_2O$  ) .(Plate 1d.)

X-RAY DIFFRACTION.

An X-ray diffractometer trace of P.F.A. is shown in Figure 11.1 The major constituent was a glass phase ( 70 % ). This was indicated by a hump in the diffractometer trace . The other phases detectable were:-

Magnetite ( 9 % )  
Haematite ( 5% )  
Quartz ( 5% )                      Semi quantitative  
Mullite ( 3% )  
Carbon ( 3% )  
Gypsum ( 3% )  
Freelime ( CaO ) ( 2 % )  
and some sulphur and potassium alum.

The percentage in brackets is the approximate amount of the phase present in the PFA investigated.

RADIOACTIVITY.

The radioactivity of the P.F.A. samples was tested and on average had a low level of activity. Approximately 40 counts per minute compared with a background of 20 counts per minute .

PLATE.1

Scanning electron microscope photo-micrographs.

Plate 1a. Pulverised fuel ash, PFA.

The irregular shaped honeycombed particle in the centre, is a fragment of unburnt coke.

Plate 1b. PFA

Many of the spheres are hollow ( cenospheres ) and contain several smaller spheres inside. The surface of these spheres is very smooth, even at high magnification.

Plate 1c. PFA

The long accicular crystals are Mullite ( $3Al_2O_3 \cdot 2SiO_2$  ), which is a minor constituent of PFA. They are derived from the non carbonaceous material in the coal.

Plate 1d. PFA

The rhombohedral crystal in the centre is calcium sulphate, a minor constituent of PFA. The spheres in the ash have a very large size range. This is demonstrated by the very small spheres in the bottom left resting on the surface of a very large sphere.

Plate 1e. PFA

The long crystals on the left are Mullite. Amongst the mullite laths are small glassy spheres. There is an irregular sphere of magnetite in the background.

Plate 1f. PFA

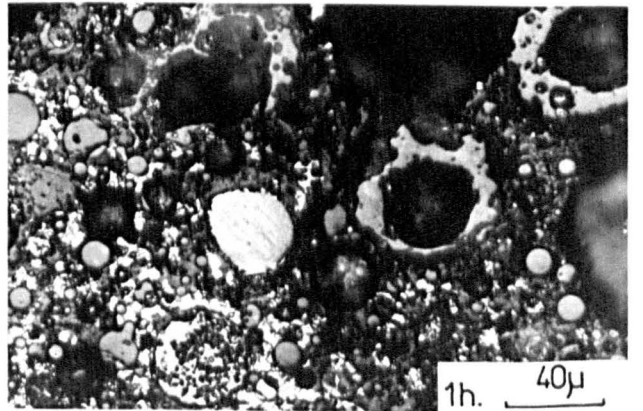
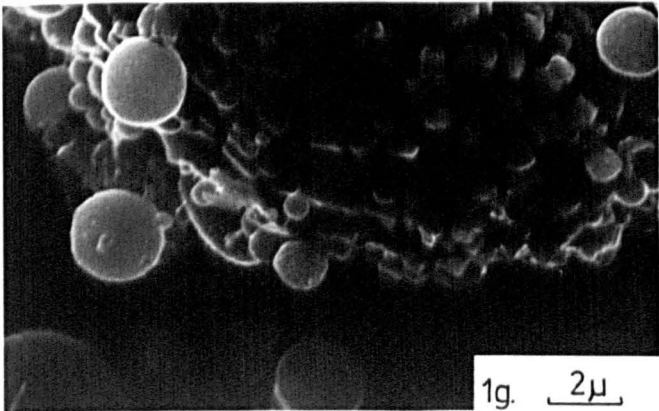
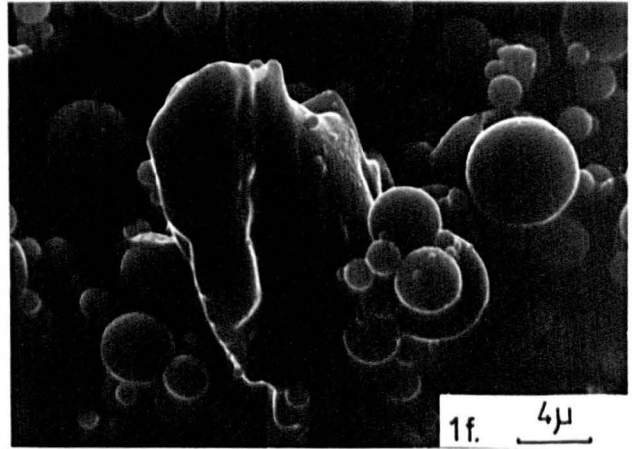
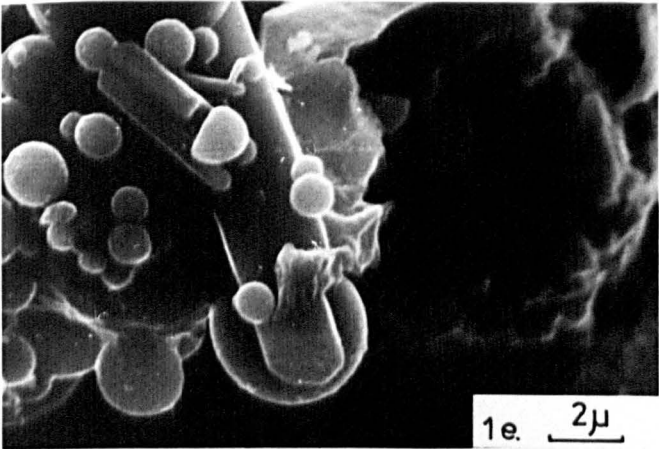
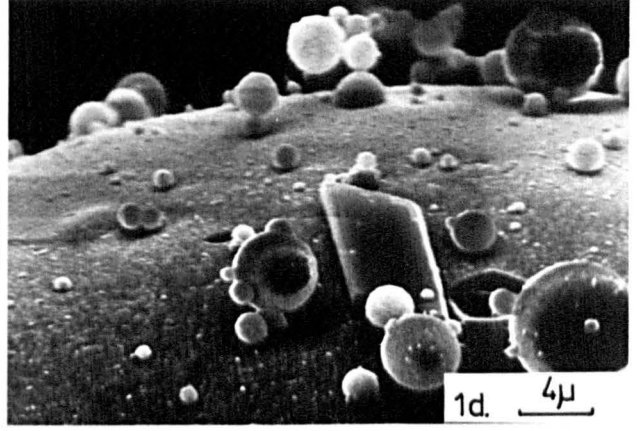
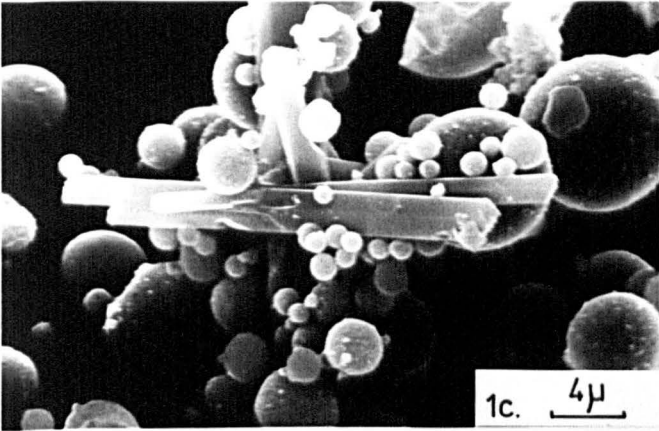
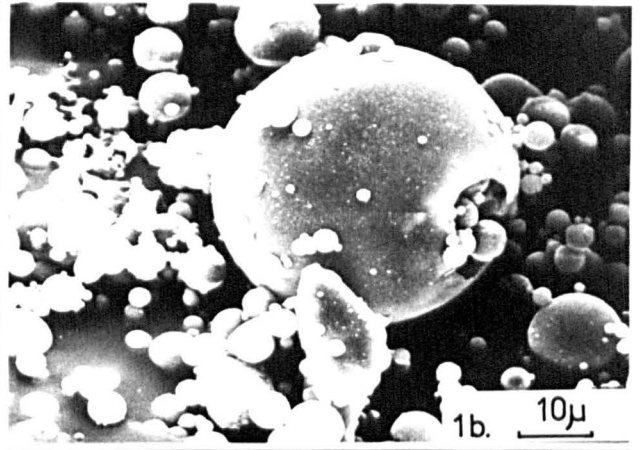
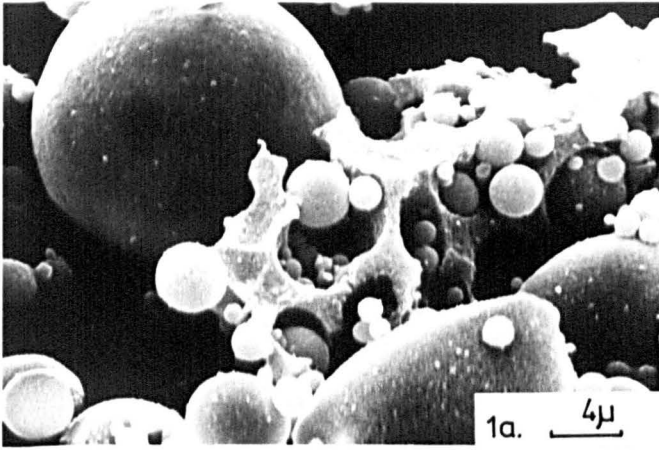
The grain in the centre is a quartz crystal with fused edges. It occurs as a very minor constituent in PFA.

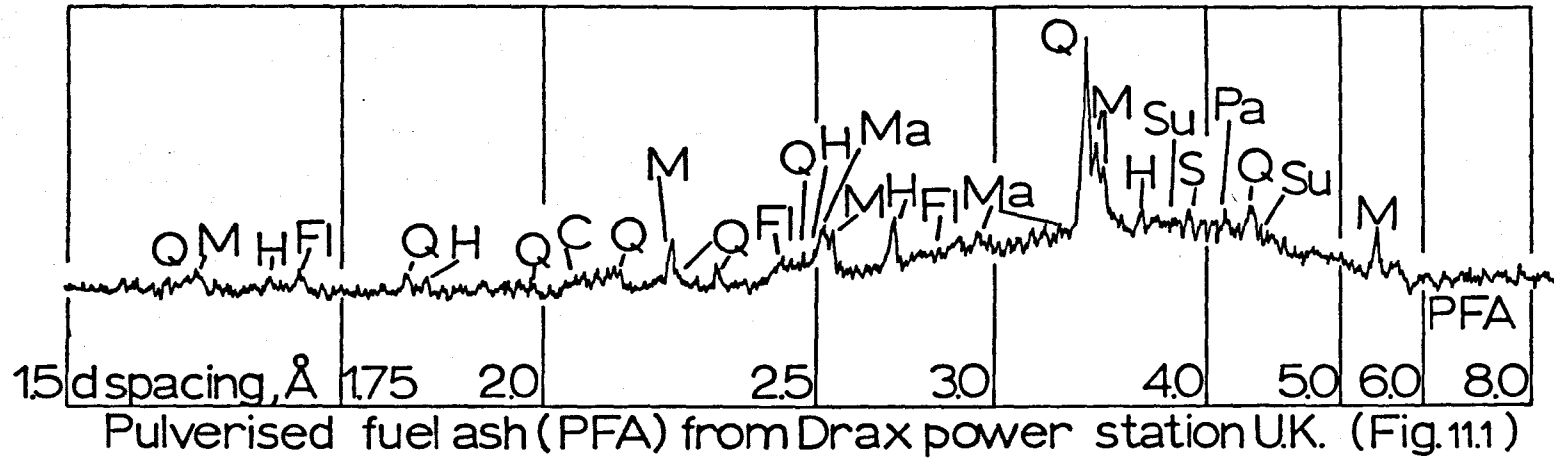
Plate 1g. PFA

The agglomeration of angular crystals in the upper part of the Plate is one of the rough surfaced, opaque spheres which are a major constituent of PFA. These spheres are predominantly magnetite with some hematite.

Plate 1h. Reflected light photo-micrograph of PFA.

The grain in the centre, showing the intergrowth texture is magnetite with an intergrowth of hematite. The other spherical grains of differing sizes are either glass or glass with magnetite inclusions.





KEY for X-ray diffractogram of Pulverised fuel ash (PFA).

C = Carbon ( residual coal )

Fl = Freelite

H = Haematite

M = Mullite

Ma = Magnetite

Pa = Potassium alum

Q = Quartz

S = Sulphur

Su = Gypsum

ELECTRON MICROPROBE ANALYSIS.

Experimental technique.

A sample for analysis was prepared by mixing the P.F.A. with a small quantity of " Araldite " adhesive to a thick paste, and curing to a set . The pellet of P.F.A. was then prepared for microprobe analysis. Plate 1h. shows a polished surface specimen , a sphere with magnetite and haematite is centre right. The other constituents are glass and magnetite spheres and glassy spheres.

Results of electron microprobe analysis of P.F.A.

	Magnetite spheres	Glass spheres	Combined glass and Magnetite spheres.
Number of analyses .	6	10	15
SiO <sub>2</sub>	3.6	52.7	42.2
Al <sub>2</sub> O <sub>3</sub>	4.3	33.0	30.7
TiO <sub>2</sub>	trace	1.2	1.4
Fe <sub>2</sub> O <sub>3</sub>	84.64	4.5	17.8
MgO	0.8	1.5	1.5
CaO	0.5	0.3	1.0
Na <sub>2</sub> O	0.6	0.7	0.9
K <sub>2</sub> O	0.2	5.8	3.0
Total	99.6	99.7	98.5

The compositions shown are averages of the number of analyses quoted.

X-RAY FLUORESCENCE.

The dried P.F.A. was prepared as a glass disc for X.R.F. analysis. A chromium x-ray tube was used to irradiate the discs. The instrumental conditions are given in Appendix 4 .

CHEMICAL COMPOSITION .

SiO <sub>2</sub>	51.50
Al <sub>2</sub> O <sub>3</sub>	26.27
TiO <sub>2</sub>	0.96
Fe <sub>2</sub> O <sub>3</sub>	10.07
MnO	0.64
MgO	1.27
CaO	1.77
Na <sub>2</sub> O	0.90
K <sub>2</sub> O	3.54
P <sub>2</sub> O <sub>5</sub>	0.20
SO <sub>3</sub>	0.25
LOI	3.16

Total 100.53

The L.O.I. represents the percentage of unburnt fuel in the ash.

Appendix three, a.

SAMPLE PREPARATION FOR MAJOR ELEMENT DETERMINATION BY X-RAY FLUORESENCE USING GLASS DISCS.

A 0.270g. sample of the milled cement clinker was accurately weighed into a platinum crucible. 0.3730g. of Na<sub>2</sub>O<sub>3</sub> and 2.00g. of 'Spectroflux 109' ( made by Johnson Matthey ) was added and gently mixed together.

The sample in the crucible was heated over a microburner until it had fused together. The crucible and sample was allowed to cool and weighed . The weight difference was the loss on ignition ( LOI ) . The sample was reheated and transferred to a blast burner for final heating before being cast as a glass disc on a pre polished graphite dish. The disc was transferred to a hot plate to anneal for at least 2 hours. All the samples were made in duplicate.

Sample preparation for sodium determination using powder pellets.

About 20g. of the milled cement clinker was ground in a small agate pestle and mortar until the sample was smooth. The powder press was filled with approximately 20g. of boric acid and tapped flat. The cement sample was poured onto the boric acid to make a thick layer. A polished tungsten platten was placed on top in the press. The press was evacuated with a vacuum pump. The entire assembly was then pressed at 15 tonnes. This was maintained for 5 seconds, the pressure was gradually released. The prepared pellets were kept in a dessicator to prevent hydration of the cement clinker phases.

SAMPLE PREPARATION FOR ATOMIC ABSORPTION SPECTROSCOPY.

To prepare a solution from the cement .500g. of the fine ground clinker was weighed into a conical beaker and mixed with 25ml. of distilled water. After a short stir, 5ml. of conc. HCl acid was added and the mixture was digested over a steam bath for 20 minutes until the cement had dissolved. The liquid was filtered through a medium textured filter paper into a 100ml. volumetric flask. The sample was washed through with 1% (v/v) HCl and hot water. The flask was cooled and diluted to volume with distilled water. From the 100 ml. flask a 25ml. aliquot was taken and diluted to 100 ml. From this dilution a 20 ml. sample was taken and mixed with 50 ml. of 5% (w/v) lanthanum solution , this was diluted with distilled water to 500 ml. Each of the samples was prepared in duplicate . The samples were analysed for magnesium using an air - acetylene flame. A set of standards within the correct range were used for calibration.

Appendix three b.

Chemical composition of SRC clinker with clay.

SiO <sub>2</sub>	20.58
Al <sub>2</sub> O <sub>3</sub>	4.27
TiO <sub>2</sub>	0.1
Fe <sub>2</sub> O <sub>3</sub>	4.8
MgO	1.5
CaO	67.13
Na <sub>2</sub> O	0.20
K <sub>2</sub> O	0.21
P <sub>2</sub> O <sub>5</sub>	0.16
SO <sub>3</sub>	0.2

LOI	0.8
<u>Total</u>	<u>99.85</u>

Appendix four.

INSTRUMENTS USED AND OPERATING CONDITIONS.

XRD

Philips PW 1050 diffraction set  
operating at 40 Kv, 25 mA.  
Cobalt target tube - cobalt K alpha radiation. attenuation 3  
time constant 4  
scan rate 1° of 2θ per minute.  
Samples- Dry cavity mounts ( unorientated ).

XRF

Philips PW 1212 fluorescence set  
operating at selectable conditions upto 60 Kv, 32 mA  
Chromium target tube.  
Samples- Glass discs and pressed powder pellets.

ELECTRON MICROPROBE

Cambridge Instruments Geoscan with Link system model 290 2Kv energy  
dispersive spectrometer.  
Beam conditions-  
Accelerating potential 15 Kv  
Specimen current 2.7 nA.  
Instrumental conditions  
Kelvex detector resolution c. 150 eV  
Take off angle - 75  
Live time - 100 live seconds.  
Standard - cobalt metal block  
Samples- carbon coated blocks and thin sections. ( Polished ).  
Data processing for analysis.  
Data collection processing program was stored on dual floppy disc system.  
The signal was processed by a Harwell processor model 2010 and converted to  
a digital format . The digitised information was stored in a 16K Nova 2-10  
computer. The software was from Link and was a ZAF 4 program.

ATOMIC ABSORPTION SPECTROSCOPY.

SP 1950 spectrometer.  
using magnesium lamp  
Lamp current 4mA wavelength 285.2 Nm  
Monochromator slit width 0.1mm.  
Burner 10 cm. slot  
Fuel Acetylene flow rate 1200 Ml/min. Oxidant air flow rate 5 l/min  
Burner height 0.6 cm.  
Integration time 4 seconds

Appendix five.

PREPARATION OF POLISHED SURFACE SPECIMENS SUSCEPTIBLE TO HYDRATION FOR REFLECTED LIGHT INVESTIGATION AND ELECTRON MICROPROBE ANALYSIS.

Impregnation to prevent disintergration of sample.

1. Select samples and size for block mould.
2. Mix suitable impregnation resin to manufacturer's instructions. The resin used by the author was 'PETROPOXY 154' because it had low viscosity when hot. This was ideal for specimen impregnation.
3. Impregnate the specimens with resin. With 'PETROPOXY' the samples were heated in an oven at 125°C, the resin was poured over the hot specimens and returned to the oven to cure. N.B. PETROPOXY is ideal for Electron microprobe specimens because it will not contaminate the instrument if the electron beam strikes the cured resin.

Blocking of the impregnated specimen.

1. Grease block mould with releasing agent and assemble mould.
2. Place impregnated specimens in moulds with surface selected for polishing face downwards.
3. Prepare blocking resin to the manufacturer's instructions. 'ARALDITE' is a suitable resin.
4. Pour mixed resin slowly into mould to avoid air bubbles. Leave to cure for 24 hours.

Grinding of block.

1. Release block from mould.
2. Label block with indelible pen or engraver.
3. Grind back of block flat on grinding wheel lubricated with OIL OR PARAFFIN. Do not use water.
4. Grind front surface of block to just expose sample. Bevel the front edge of the block to prevent buildup of polishing media.
5. Mix carborundum grit 400 to slurry with 2 to 1 mixture of paraffin and liquid paraffin on a glass plate. Grind front surface of block until reasonably smooth.
6. Place sample face downwards in beaker containing paraffin. Place beaker in ultrasonic bath until all the grit has been removed from the sample.
7. Repeat 5 and 6 using 600 grit on clean glass plate. Repeat for 800 and 1200 grit.  
After 1200 grit the surface should have a slight polish.
8. The block should be prepared to fit the mounting head on the polishing machine. This usually entails drilling a central hole in the back of the block.

Polishing blocks. ( Using Engis polisher).

1. Place 6 $\mu$ m. diamond paste on pellow lap.
2. Clean blocks with Inhibisol solvent and fit to polishing head using 5lb. polishing weight.
3. Spray Engis OIL based lubricant onto lap.
4. Run turntable at 67 revs per minute for 1 hour.
5. Clean polished block surface with Inhibisol and soft paper.
6. Repeat 1 to 5 using progressively finer diamond pastes and the following conditions.

Paste	Weight	Revs.	Duration
3 $\mu$ m.	4 lbs.	75	1/2 hour
1 $\mu$ m.	4 lbs.	90	1/2 hour
1/4 $\mu$ m.	1 lb.	100	1/2 hour

Examine specimen with reflecting light microscope to determine quality of polish and repeat cycles if necessary.

The specimen is suitable for examination with reflected light and EMP analysis.

To prepare a polished THIN section additional work is required.

1. Carefully remove the specimen from the resin block using a fine saw or cutter.
2. Mount sample polished face down on microscope slide with LAKESIDE 70 or similar medium.
3. Remove back of specimen with dry or paraffin lubricated grinding wheel, until the specimen slice is only 2mm thick.
4. Slowly remove layers of the specimen using 800 carborundum grit and paraffin liquid paraffin mixture. This process is continued until specimen is wafer thin and can be seen through . Monitor the process with a transmitting light microscope.
5. When the specimen is at the required thickness , mount the back of the sample onto a glass slide with Araldite. Press gently to remove any air bubbles between the slide and the sample. Put identification mark on the slide with scribe. Leave to cure .
6. Remove specimen from grinding slide by dissolving the Lakeside resin with alcohol. Wipe polished surface clean with soft cloth. This process should be carried out as rapidly as possible , because the alcohol can etch the belite crystals.

The specimen is suitable for examination by reflected or transmitted light. A coating of carbon is required before analysis by electron microprobe.

The polished blocks and sections MUST be kept in a dessicator, to prevent hydration and disintergration of the clinker samples.

Petropoxy , Araldite , Inhibisol , Engis and Lakeside are all trade marks.

Inhibisol is an industrial solvent based on trichloroethylene and was available from -  
Bestobell Chemical Products,  
Bassington Industrial Estate,  
Cramlington,  
NE23 8AL.

Petropoxy 154 is a plastic resin available from -  
Production Techniques Ltd.  
15, Kings Road,  
Fleet,  
Hampshire.

Araldite is a resin Manufactured by Ciba-Geigy. There are local suppliers throughout the country.

Lakeside 70 is a thermoplastic resin available from-  
Production Techniques Ltd,  
15. Kings Road,  
Fleet,  
Hampshire.

Appendix seven.

THE BOGUE CALCULATION.

The Bogue method assumes that the cement consists of C3S, C2S, C3A and C4AF. Since the actual composition varies from the stoichiometric formula, the calculation deviates from the true composition of the cement. Therefore the Bogue composition is often termed the 'potential' composition.

The Bogue method uses the oxide composition of the material to give the phase composition. The chemical composition is usually determined by X ray Fluorescence. The free lime content of the clinker is often determined by a titrimetric method. The following oxides totals are used in the Bogue calculation.- SiO<sub>2</sub>, Al<sub>2</sub>O<sub>3</sub>, Fe<sub>2</sub>O<sub>3</sub>, CaO, SO<sub>3</sub>.

The free lime value is subtracted from the CaO content and the corrected CaO content is used in the following equations with the other oxides.

$$C3S = 4.071 CaO - (7.6 SiO_2 + 6.718 Al_2O_3 + 1.43 Fe_2O_3 + 2.852 SO_3)$$

$$C2S = 2.867 SiO_2 - 0.7544 C3S$$

$$C3A = 2.65 Al_2O_3 - 1.692 Fe_2O_3$$

$$C4AF = 3.043 Fe_2O_3$$

$$\text{Gypsum} = 1.7 \times SO_3$$

( from Soroka 1979 )

These equations are applicable for most cements with an Al<sub>2</sub>O<sub>3</sub>/Fe<sub>2</sub>O<sub>3</sub> ratio equal to or greater than 0.64. If the cement is very low in alumina the equations are not valid. The matrix phases are assumed to be C4AF and C2F. There is no C3A.

In this case the following equations apply.

$$C3S = 4.071 CaO - (7.6 SiO_2 + 4.479 Al_2O_3 + 2.859 Fe_2O_3 + 2.852 SO_3)$$

$$C2S = 2.867 SiO_2 - 0.7544 C2S$$

$$C3A = 0$$

$$C4AF + C2F = 2.1 Al_2O_3 + 1.702 Fe_2O_3$$

## Matrix Recalculation

The chemical analysis ( XRF ) data used in this matrix method was from Table 3.1 page 24.

The mineral analyses used were from

Table 8.2 page 128 for alite compositions

Table 8.6 page 139 for belite compositions

Table 8.11 page 154 for ferrite compositions

Table 8.12 page 154 for aluminate compositions

The computer program uses a Gauss-Jordan discrimination method to calculate the unknown matrix.

The original subroutine was derived from " Statistics and Data analysis in Geology " by J.C Davis 1973. Pub. Wiley. The original program was written in FORTRAN.

Matrix calculation method.

The phase composition, mineral composition and the chemical composition of the cement clinker can be expressed as a series of simultaneous equations. Thus

(amount of oxide in phase) X (percentage of phase present) = (Total amount of each oxide in clinker).

eg.

(CaO ate)%ate + (CaO bte)%bte + (CaO fer)%fer + (CaO alu)%alu + (CaO gyp)%gyp + (CaO mag)%mag = Total CaO in clinker. This is repeated for each oxide. Since each oxide value is multiplied by percentage of phase present, the multiplier may be represented by a matrix.

$$\begin{bmatrix} \text{CaO ate} & \text{CaO bte} & \text{CaO fer} & \text{CaO alu} & \text{CaO gyp} & \text{CaO mag} \\ \text{SiO}_2 \text{ ate} & \text{SiO}_2 \text{ bte} & \text{SiO}_2 \text{ fer} & \text{SiO}_2 \text{ alu} & \text{SiO}_2 \text{ gyp} & \text{SiO}_2 \text{ mag} \\ \text{Fe}_2\text{O}_3 \text{ ate} & \text{Fe}_2\text{O}_3 \text{ bte} & \text{Fe}_2\text{O}_3 \text{ fer} & \text{Fe}_2\text{O}_3 \text{ alu} & \text{Fe}_2\text{O}_3 \text{ gyp} & \text{Fe}_2\text{O}_3 \text{ mag} \\ \text{Al}_2\text{O}_3 \text{ ate} & \text{Al}_2\text{O}_3 \text{ bte} & \text{Al}_2\text{O}_3 \text{ fer} & \text{Al}_2\text{O}_3 \text{ alu} & \text{Al}_2\text{O}_3 \text{ gyp} & \text{Al}_2\text{O}_3 \text{ mag} \\ \text{SO}_3 \text{ ate} & \text{SO}_3 \text{ bte} & \text{SO}_3 \text{ fer} & \text{SO}_3 \text{ alu} & \text{SO}_3 \text{ gyp} & \text{SO}_3 \text{ mag} \\ \text{MgO ate} & \text{MgO bte} & \text{MgO fer} & \text{MgO alu} & \text{MgO gyp} & \text{MgO mag} \end{bmatrix} \times \begin{bmatrix} \text{Ate\%} \\ \text{Bte\%} \\ \text{Fer\%} \\ \text{Alu\%} \\ \text{Gyp\%} \\ \text{Mag\%} \end{bmatrix} = \begin{bmatrix} \text{CaO} \\ \text{SiO}_2 \\ \text{Fe}_2\text{O}_3 \\ \text{Al}_2\text{O}_3 \\ \text{SO}_3 \\ \text{MgO} \end{bmatrix}$$

The % of phase matrix is the unknown, this may be made the subject of the equations by multiplying the first matrix by its inverse. This produces the following expression.

(% of phase present) = (amount of oxide in phase)<sup>-1</sup> X (total % of oxide in cement)

The expression may be evaluated by multiplying together the matrices on the right hand side of the equation (rows times columns). This produces the values for the unknown matrix, the % of phase present. Since matrix multiplication is repetitive, is an ideal task for a microcomputer. The following program performs the phase composition calculation. (This program is in Applesoft Basic and runs on a Apple II computer.)

The data statements 1020 to 1070 are the mineral compositions by EMPA of alite, belite, ferrite, aluminate, magnesite and gypsum respectively.

The values are in weight percent of the following oxides SiO<sub>2</sub>, Al<sub>2</sub>O<sub>3</sub>, Fe<sub>2</sub>O<sub>3</sub>, MgO, CaO and SO<sub>3</sub>. To run the program the amount of each oxide in the clinker as determined by XRF is input after each prompt. The computer then performs the matrix calculation and displays the percentage of each phase present in the cement clinker. To compensate for freelite, the percentage of freelite should be deducted from the CaO value before performing the calculation.

```

10 DIM A(6,6),B(6),M$(6),S$(6)
20 GOTO 300
100 FOR I = 1 TO 6
110 D = A(I,I)
120 FOR J = 1 TO 6
130 A(I,J) = A(I,J) / D
140 NEXT J
150 B(I) = B(I) / D
160 FOR J = 1 TO 6
170 IF I = J GOTO 230
180 R = A(J,I)
190 FOR K = 1 TO 6
200 A(J,K) = A(J,K) - R * A(I,K)
210 NEXT K
220 B(J) = B(J) - R * B(I)
230 NEXT J
240 NEXT I
250 RETURN
300 FOR I = 1 TO 6: READ M$(I): NEXT I
310 FOR I = 1 TO 6: READ S$(I): NEXT I
320 FOR I = 1 TO 6
330 FOR J = 1 TO 6
340 READ A(J,I)
350 NEXT J
360 PRINT S$(I),
370 INPUT B(I)
380 NEXT I
400 GOSUB 100
410 PRINT "MINERAL PERCENTAGES":
PRINT
420 FOR I = 1 TO 6
430 PRINT M$(I),B(I) * 100
440 NEXT I
500 END
1000 DATA ALITE,BELITE,FERRITE
,ALUMINATE,MAGNESITE,GYPSUM
1010 DATA SiO2,Al2O3,Fe2O3,MgO,
CaO,SO3
1020 DATA 24.6,1.2,.5,.6,72.1,0
1030 DATA 31.2,1.8,.9,.4,63.5,.
8
1035 DATA 5.5,17,18,3.8,50.7,0
1040 DATA 4.3,31.5,1.2,.3,60.9,
.3
1050 DATA .5,0,0,99.5,0,0,0
1070 DATA 0,0,0,0,41.2,58.8

```

## Appendix eight , a.

The operation of the Electron microprobe and aquisition of the mineral analyses.

### Instruments.

The electron microprobe used was a Cambridge Instruments 'GEOSCAN' with a Link Systems model 290 2Kv energy dispersive spectrometer attached. The data derived from the detector was processed by a Harwell processor on a Nova computer. The software used to process the spectra was from Link systems ( ZAF 4 using a least squares fitting method.)

### Standards.

The specimens used to provide the standard spectra for the different elements were either metals or silicates. The accuracy , precision and detection limits of energy dispersive electron microprobe analyses of the silicates has been investigated by Dunham and Wilkinson (1978).

### Analysis.

The analyses were made on carbon coated polished blocks or polished thin sections. The accelerating potential used was 15 Kv for all of the elements . The specimen current was about 3 nA. The spectra was counted for 100 live seconds. Before each days run of analyses a cobalt spectra was recorded to standardise the analyses.

Suitable areas for analysis were chosen avoiding pits, cracks, rough surfaces or surface contamination due to polishing grease. By using photomicrographs of the samples which had been made before the specimen was coated with carbon , it was possible to identify the different phases in the cement. This technique also enabled the author to avoid to some extent areas of the specimen , where two or more phases would be excited by the electron beam. When a suitable area was found by optical examination the analysis was made. The computer processed results were output to a printer.

### Processing of the data output.

The analysis of the sample was expressed in weight percent element, the oxygen content was determined by difference.

The analysis was also calculated in weight percent oxide. The total for the oxide content was checked , if the total was unusually low the analysis was discarded. For many of the minor elements the percentage of the element present was close to the detection limit of the energy dispersive analysis system. The computer calculated detection limits are shown in Fig. The actual detection limits calculated by the author ( shown in Figure 11.1) are lower in all but one element (Na), than the computer calculated limits.

The actual detection limits were calculated by plotting all the values obtained for an individual element. The mean and standard deviation were determined and the results plotted on Figure 11.1 as the mean plus two standard deviations.

If the amount of element shown in the analysis was below the detection limit the value for the individual element was recorded as 'not detected' in the results. ( Tables 12.2 to 12.12 ).

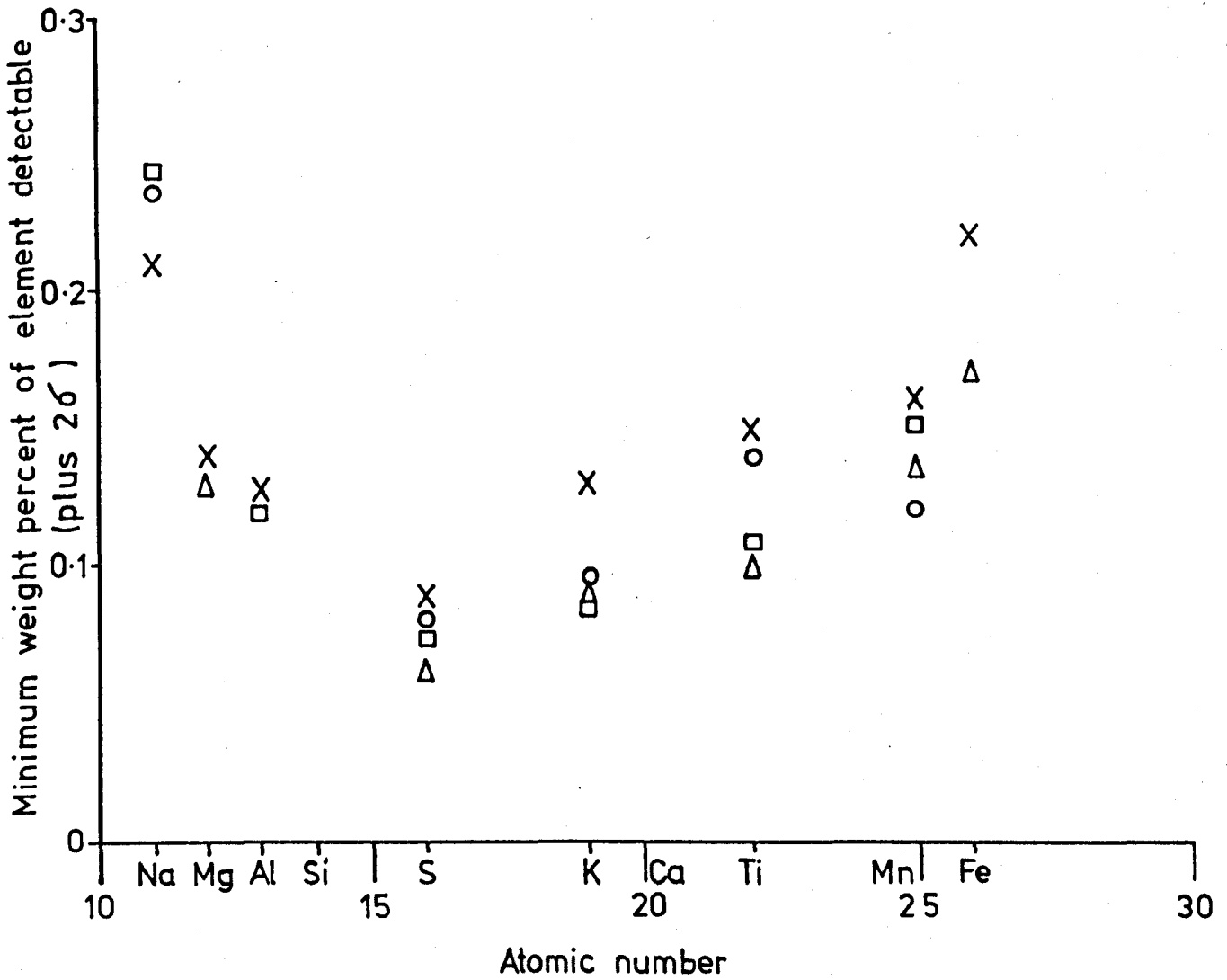


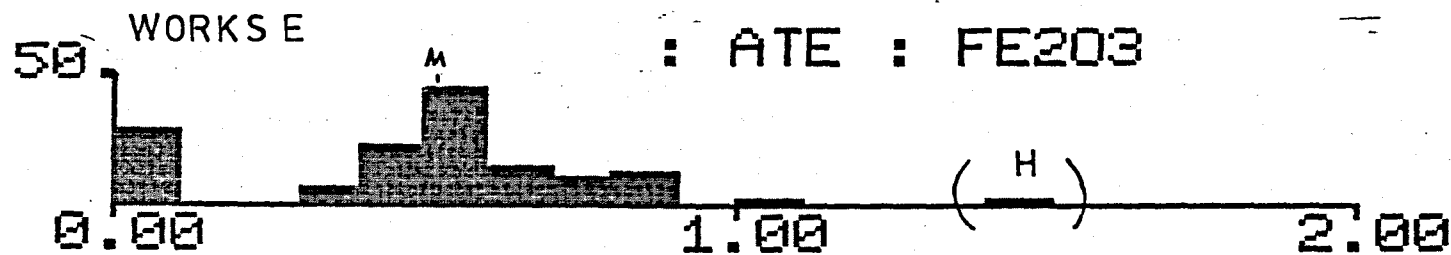
Fig.11.2

Detection limits of Electron microprobe analysis, using K lines.

(All determinations at 15 KeV. for 100 live seconds.)

KEY

- Calcium silicates                    o
- Labradorite                            Δ
- Olivine                                    □
- Computer calculated limits    X



Calculation of the mean composition of the major clinker minerals.

From the mineral analyses for each major phase in each clinker, the mean value of each oxide was obtained by: Individually plotting the distribution of the weight percentage oxide values in each phase analysed. (histogram distribution). Any high values ( H ) were removed before determining the mean value ( M ).

In the distribution above the high value of Fe<sub>2</sub>O<sub>3</sub> in the alite was the result of exciting a small portion of ferrite with the electron beam, whilst analysing an alite grain.

(Table 12.0) List of cement clinker specimens with their Electron microprobe analysis spot numbers.

WORKS A. OPC	WORKS B. SRC with clay	WORKS B. SRC with PFA kiln 1	WORKS B. SRC with PFA kiln 3	WORKS B. SRC with PFA + PFA
A1/2 1-26	BSCM 1-30	B1930 1-35	B1930 1-25	0730PF 1-26
A3/4 27-51	BSCM 40-66	B2030 1-26	B2030 1-29	1130PF 1-39
A5/6 61-87		B2130 1-26	B2130 1-30	1330PF 1-27
A7/8 88-112	WORKS B LHC	B2230 1-24	B2230 1-24	1530PF 1-27
A9/10 113-139	trial lowheat	B2330 1-26	B2330 1-31	1730PF 1-27
A16/17 141-165		B0030 1-64	B0030 1-26	1930PF 1-26
A20 170-192	LH0900 1-31	B0130 1-27	B0130 1-26	2030PF 1-26
A21 200-220	LH1200 1-25	B0230 1-36	B0230 1-27	
	LH1300 1-26	B0330 1-34	B0330 1-25	
	LH1400 1-26	B0430 1-26	B0430 1-28	
	LH1500 1-22	B0530 1-54	B0530 1-26	
	LH1600 1-26			

WORKS C OPC	WORKS D OPC	WORKS E OPC	WORKS F WPC	WORKS G OPC
C1/3 1-54	D1/2 1-26	E1 1-25	F1/2 1-39	G1 1-29
C9 55-88	D3/4 27-52	E3/4 26-52	F3 40-68	G2R 30-67
C10 89-114	D6 91-104	E5 53-83	F4 69-100	G4 78-102
C11 115-139	D8/9 110-136	E6/7 86-107		G5 103-127
C19 141-187	D10/11 137-165	E9/10 108-125		G6 128-151
CF 201-224	D12/13 176-200	E41 126-152		G7R 152-175
	D14 200-222	E14/15 180-196		G8 176-200
		E20 201-215		G9 201-221













(Table 12.4). Electron Microprobe analyses of cement clinker mineral phases from Works B of SRC from kiln No. 3.

Code	Spot	1	2	3	4	5	7	8	9	10	11	12	14	15	16	17	18	21	22	23	24	1	2	4	5	6	8	9	11	12									
S102		24.4	24.2	24.3	24.8	24.0	24.4	24.6	23.9	24.8	24.7	24.4	24.4	24.6	24.1	24.3	24.0	23.9	24.0	24.3	23.4	23.2	24.8	24.7	24.2	24.5	24.6	23.9	24.6	24.6	23.9	24.0							
AL2O3		0.9	0.8	0.8	0.8	0.8	0.7	0.8	0.9	1.0	0.8	0.8	0.9	0.9	0.9	0.9	0.9	1.1	1.3	1.3	1.8	2.4	2.4	0.9	0.9	1.0	1.4	0.8	1.8	0.9	1.2	1.2							
TiO2		n.d.	n.d.	n.d.	n.d.	n.d.	n.d.	n.d.	n.d.	n.d.	n.d.	n.d.	n.d.	n.d.	n.d.	n.d.	n.d.	n.d.	n.d.	n.d.	0.3	n.d.	n.d.	n.d.	n.d.	n.d.	n.d.	n.d.	n.d.	n.d.	n.d.	n.d.							
FE2O3		1.2	1.1	1.0	0.8	1.0	0.4	0.8	0.9	0.6	0.9	1.0	0.7	0.6	0.9	0.8	0.9	1.1	1.1	1.1	2.0	1.9	0.3	0.8	1.0	1.1	0.7	1.5	1.0	0.9	1.1								
MnO		n.d.	n.d.	n.d.	n.d.	n.d.	n.d.	n.d.	n.d.	n.d.	n.d.	n.d.	n.d.	n.d.	n.d.	n.d.	n.d.	n.d.	n.d.	n.d.	n.d.	n.d.	n.d.	n.d.	n.d.	n.d.	n.d.	n.d.	n.d.	n.d.	n.d.	n.d.							
MSO		0.4	0.5	0.4	0.3	0.3	0.4	0.4	0.4	0.3	0.4	0.3	0.6	0.3	0.4	0.3	0.4	0.4	0.4	0.4	0.3	0.3	0.4	0.4	0.3	0.5	0.5	0.6	0.4	0.6	0.6	n.d.							
CaO		72.3	72.9	72.6	72.0	73.0	73.1	72.9	72.5	72.3	72.6	72.5	72.2	72.2	72.1	72.9	72.6	71.3	70.8	69.6	68.7	72.8	72.6	72.0	72.3	72.1	71.6	71.8	71.9	72.9	72.9								
SiO2		n.d.	n.d.	n.d.	n.d.	n.d.	n.d.	n.d.	n.d.	n.d.	n.d.	n.d.	n.d.	n.d.	n.d.	n.d.	n.d.	n.d.	n.d.	n.d.	n.d.	n.d.	n.d.	n.d.	n.d.	n.d.	n.d.	n.d.	n.d.	n.d.	n.d.	n.d.							
K2O		n.d.	n.d.	n.d.	n.d.	n.d.	n.d.	n.d.	n.d.	n.d.	n.d.	n.d.	n.d.	n.d.	n.d.	n.d.	n.d.	n.d.	n.d.	n.d.	n.d.	n.d.	n.d.	n.d.	n.d.	n.d.	n.d.	n.d.	n.d.	n.d.	n.d.	n.d.	n.d.						
P2O5		n.d.	n.d.	n.d.	n.d.	n.d.	n.d.	n.d.	n.d.	n.d.	n.d.	n.d.	n.d.	n.d.	n.d.	n.d.	n.d.	n.d.	n.d.	n.d.	n.d.	n.d.	n.d.	n.d.	n.d.	n.d.	n.d.	n.d.	n.d.	n.d.	n.d.	n.d.	n.d.						
SO3		n.d.	n.d.	n.d.	n.d.	n.d.	n.d.	n.d.	n.d.	n.d.	n.d.	n.d.	n.d.	n.d.	n.d.	n.d.	n.d.	n.d.	n.d.	n.d.	n.d.	n.d.	n.d.	n.d.	n.d.	n.d.	n.d.	n.d.	n.d.	n.d.	n.d.	n.d.	n.d.						
TOTAL		99.2	99.5	99.1	98.9	99.1	98.9	99.0	99.0	99.0	99.0	99.1	98.8	99.5	98.6	99.0	99.4	99.3	99.7	99.6	99.6	100.1	99.7	99.7	98.9	100.1	99.5	100.0	98.9	98.9	100.4								
Code	Spot	24	25	1	8	9	10	13	14	15	16	17	23	26	29	2	3	4	7	Code	Spot	13	14	16	17	18	19	20	21	26	27	28	31	1	2	3	4	5	6
S102		24.5	23.8	24.0	23.8	24.3	24.3	24.6	24.5	24.1	24.6	24.5	24.2	24.7	24.4	25.1	25.5	25.6	25.0	24.0	24.4	24.6	24.7	24.2	25.0	25.0	25.2	24.7	24.9	24.7	24.6	24.6							
AL2O3		1.2	1.4	1.4	1.0	1.2	1.2	1.0	0.8	1.2	1.0	0.9	1.2	1.2	1.3	0.7	0.9	0.7	0.6	1.0	1.1	1.1	0.7	1.3	0.9	0.8	0.8	1.1	0.8	1.1	0.8	0.6	0.9	0.4					
TiO2		n.d.	n.d.	n.d.	n.d.	n.d.	n.d.	n.d.	n.d.	n.d.	n.d.	n.d.	n.d.	n.d.	n.d.	n.d.	n.d.	n.d.	n.d.	n.d.	n.d.	n.d.	n.d.	n.d.	n.d.	n.d.	n.d.	n.d.	n.d.	n.d.	n.d.	n.d.	n.d.	n.d.	n.d.				
FE2O3		1.0	1.3	1.5	1.0	1.3	0.9	1.0	1.0	0.9	1.0	0.8	1.2	1.2	1.3	1.0	1.1	0.8	0.7	0.6	0.6	0.7	0.7	0.9	1.0	0.8	0.8	0.9	0.9	0.9	0.8	0.8	0.8	0.3					
MnO		n.d.	n.d.	n.d.	n.d.	n.d.	n.d.	n.d.	n.d.	n.d.	n.d.	n.d.	n.d.	n.d.	n.d.	n.d.	n.d.	n.d.	n.d.	n.d.	n.d.	n.d.	n.d.	n.d.	n.d.	n.d.	n.d.	n.d.	n.d.	n.d.	n.d.	n.d.	n.d.	n.d.	n.d.				
MSO		0.3	0.5	0.5	0.4	0.4	0.5	0.3	0.3	0.5	0.4	0.4	0.6	0.5	0.5	0.4	0.5	0.5	0.2	0.2	0.3	0.4	0.5	0.3	0.3	0.5	0.4	0.3	0.4	0.2	0.4	0.3	0.4	0.3					
CaO		72.4	72.3	72.4	72.1	72.4	71.9	72.1	73.0	72.5	73.0	72.5	73.0	72.9	73.0	71.8	71.1	72.2	72.5	72.6	72.4	72.6	72.9	72.6	72.8	73.2	72.6	72.1	72.9	72.6	72.8	72.8	72.8	72.8					
SiO2		n.d.	n.d.	n.d.	n.d.	n.d.	n.d.	n.d.	n.d.	n.d.	n.d.	n.d.	n.d.	n.d.	n.d.	n.d.	n.d.	n.d.	n.d.	n.d.	n.d.	n.d.	n.d.	n.d.	n.d.	n.d.	n.d.	n.d.	n.d.	n.d.	n.d.	n.d.	n.d.	n.d.	n.d.				
K2O		n.d.	n.d.	n.d.	n.d.	n.d.	n.d.	n.d.	n.d.	n.d.	n.d.	n.d.	n.d.	n.d.	n.d.	n.d.	n.d.	n.d.	n.d.	n.d.	n.d.	n.d.	n.d.	n.d.	n.d.	n.d.	n.d.	n.d.	n.d.	n.d.	n.d.	n.d.	n.d.	n.d.	n.d.	n.d.			
P2O5		n.d.	n.d.	n.d.	n.d.	n.d.	n.d.	n.d.	n.d.	n.d.	n.d.	n.d.	n.d.	n.d.	n.d.	n.d.	n.d.	n.d.	n.d.	n.d.	n.d.	n.d.	n.d.	n.d.	n.d.	n.d.	n.d.	n.d.	n.d.	n.d.	n.d.	n.d.	n.d.	n.d.	n.d.	n.d.	n.d.		
SO3		n.d.	0.2	0.7	0.2	0.4	n.d.	n.d.	n.d.	n.d.	n.d.	n.d.	0.2	n.d.	n.d.	n.d.	n.d.	n.d.	n.d.	n.d.	n.d.	n.d.	n.d.	n.d.	n.d.	n.d.	n.d.	n.d.	n.d.	n.d.	n.d.	n.d.	n.d.	n.d.	n.d.	n.d.			
TOTAL		99.4	99.5	100.5	98.6	100.4	99.6	98.9	99.2	100.1	99.9	99.6	99.9	100.6	100.6	99.1	99.1	99.0	99.0	100.1	98.8	99.2	99.2	99.0	99.0	100.0	99.7	100.0	99.5	99.5	100.2	99.7	99.5	99.5	99.3	99.9			
Code	Spot	12	13	15	16	17	20	21	23	24	25	1	2	3	6	7	8	12	13	Code	Spot	7	9	11	12	13	16	17	18	20	21	24	25	26	1	2	3	4	5
S102		25.4	25.0	25.2	25.2	25.4	25.0	24.6	25.2	24.8	25.3	25.1	21.3	25.2	23.9	22.9	24.5	24.4	22.7	24.5	24.5	24.8	24.7	24.6	24.6	24.6	24.0	24.8	24.5	24.6	24.5	24.6	24.5	24.6	24.5	24.5			
AL2O3		1.2	0.8	0.9	0.7	0.7	1.0	1.0	0.6	0.9	0.7	2.1	2.9	1.0	1.1	2.9	0.9	1.1	1.7	1.4	0.9	0.9	0.7	0.7	0.8	0.8	1.1	0.7	0.9	0.9	0.9	0.9	1.0	1.0	1.0				
TiO2		n.d.	n.d.	n.d.	n.d.	n.d.	n.d.	n.d.	n.d.	n.d.	n.d.	n.d.	n.d.	n.d.	n.d.	n.d.	n.d.	n.d.	n.d.	n.d.	n.d.	n.d.	n.d.	n.d.	n.d.	n.d.	n.d.	n.d.	n.d.	n.d.	n.d.	n.d.	n.d.	n.d.	n.d.	n.d.	n.d.		
FE2O3		1.0	0.6	0.9	0.7	0.9	0.9	1.2	0.9	1.3	0.8	1.9	5.3	0.9	1.3	1.3	1.1	0.9	1.0	1.4	0.9	0.8	0.9	0.7	0.7	1.0	1.1	0.9	0.9	0.9	0.9	0.9	0.9	1.0	1.0	1.0			
MnO		n.d.	n.d.	n.d.	n.d.	n.d.	n.d.	n.d.	n.d.	n.d.	n.d.	n.d.	n.d.	n.d.	n.d.	n.d.	n.d.	n.d.	n.d.	n.d.	n.d.	n.d.	n.d.	n.d.	n.d.	n.d.	n.d.	n.d.	n.d.	n.d.	n.d.	n.d.	n.d.	n.d.	n.d.	n.d.	n.d.		
MSO		0.4	0.4	0.5	0.4	0.5	0.5	0.3	0.3	0.4	0.4	0.5	0.5	0.3	0.6	0.5	0.3	0.3	0.4	0.2	0.3	0.3	0.4	0.4	0.4	0.4	0.4	0.4	0.4	0.4	0.4	0.4	0.4	0.4	0.4	0.4	0.4		
CaO		71.1	72.2	72.1	72.8	72.0	73.0	71.7	72.4	72.4	73.1	69.9	68.4	71.6	72.2	71.7	73.1	71.7	71.6	72.3	72.4	71.2	72.6	72.6	73.0	72.7	72.5	72.7	73.3	72.1	72.4	72.4	72.4	72.4	72.4	72.4	72.4		
SiO2		n.d.	n.d.	n.d.	n.d.	n.d.	n.d.	n.d.	n.d.	n.d.	n.d.	n.d.	n.d.	n.d.	n.d.	n.d.	n.d.	n.d.	n.d.	n.d.	n.d.	n.d.	n.d.	n.d.	n.d.	n.d.	n.d.	n.d.	n.d.	n.d.	n.d.	n.d.	n.d.	n.d.	n.d.	n.d.	n.d.	n.d.	
K2O		n.d.	n.d.	n.d.	n.d.	n.d.	n.d.	n.d.	n.d.	n.d.	n.d.	n.d.	n.d.	n.d.	n.d.	n.d.	n.d.	n.d.	n.d.	n.d.	n.d.	n.d.	n.d.	n.d.	n.d.	n.d.	n.d.	n.d.	n.d.	n.d.	n.d.	n.d.	n.d.	n.d.	n.d.	n.d.	n.d.	n.d.	
P2O5		n.d.	n.d.	n.d.	n.d.	n.d.	n.d.	n.d.	n.d.	n.d.	n.d.	n.d.	n.d.	n.d.	n.d.	n.d.	n.d.	n.d.	n.d.	n.d.	n.d.	n.d.	n.d.	n.d.	n.d.	n.d.	n.d.	n.d.	n.d.	n.d.	n.d.	n.d.	n.d.	n.d.	n.d.	n.d.	n.d.	n.d.	n.d.
SO3		0.2	n.d.	n.d.	n.d.	n.d.	n.d.	n.d.	n.d.	n.d.	n.d.	n.d.	n.d.	n.d.	n.d.	n.d.	n.d.	n.d.	n.d.	n.d.	n.d.	n.d.	n.d.	n.d.	n.d.	n.d.	n.d.	n.d.	n.d.	n.d.	n.d.	n.d.	n.d.	n.d.	n.d.	n.d.	n.d.	n.d.	
TOTAL		99.3	99.0	99.6	99.8	99.4	99.8	99.4	99.4	99.8	100.3	99.0	99.7	99.6	99.9	100.1	100.5	98.8	99.7	100.0	99.0	98.0	99.3	99.0	99.3	100.0	99.0	99.0	98.0	99.1	99.5	100.0	99.1	99.5	100.0	99.1	99.5		



(Table 2.4 continued). Electron Microprobe analyses of cement clinker mineral phases from Works 3 of SRC from kiln No. 3.

Code Spot	BTE 17	BTE 19	BTE 20	BTE 22	BTE 4	BTE 8	BTE 9	BTE 10	BTE 17	BTE 18	BTE 19	BTE 22	BTE 11	BTE 13	BTE 23	BTE 28	BTE 5	BTE 6	Code Spot	FER 11	FER 49	FER 50	FER 51	ALU 16
S102	30.2	31.3	30.9	32.4	29.4	30.1	30.4	30.0	30.7	28.6	30.1	33.3	31.7	33.1	31.7	32.2	31.3	32.0	S102	4.3	2.0	1.9	3.7	6.0
AL203	1.7	1.0	1.3	0.3	1.4	1.7	1.6	1.4	1.6	1.5	1.6	0.5	1.1	0.8	1.2	1.1	1.5	1.4	AL203	14.9	16.6	16.0	14.3	19.0
T102	n.d	n.d	n.d	n.d	n.d	n.d	n.d	n.d	n.d	n.d	n.d	n.d	n.d	n.d	n.d	n.d	n.d	n.d	T102	0.6	0.9	0.9	1.0	0.3
FE203	1.8	1.4	1.9	0.7	1.6	1.7	2.1	2.0	1.7	1.8	1.5	1.1	1.4	1.1	1.7	1.2	2.0	1.7	FE203	30.2	31.4	32.3	31.2	18.3
MNO	n.d	n.d	n.d	n.d	n.d	n.d	n.d	n.d	n.d	n.d	n.d	n.d	n.d	n.d	n.d	n.d	n.d	n.d	MNO	0.5	0.5	0.6	0.4	n.d
NSO	0.2	n.d	n.d	n.d	0.3	0.4	0.2	0.2	0.3	0.2	0.3	n.d	n.d	0.3	n.d	0.2	0.4	n.d	NSO	1.4	1.3	1.2	1.3	0.8
CAO	63.2	63.9	64.8	64.5	65.0	63.6	63.7	64.2	64.9	67.1	65.1	64.4	63.7	64.3	64.2	64.7	63.6	63.7	CAO	47.9	46.5	46.1	47.1	53.3
NA2O	0.4	0.4	n.d	0.4	n.d	0.4	0.6	n.d	0.4	n.d	0.5	n.d	0.4	0.3	n.d	0.3	0.6	0.5	NA2O	n.d	n.d	n.d	n.d	n.d
K2O	0.6	0.6	0.4	0.5	0.5	0.5	0.5	0.5	0.5	0.3	n.d	n.d	0.6	0.4	0.5	0.5	0.5	0.4	K2O	n.d	n.d	n.d	n.d	0.3
P205	n.d	n.d	n.d	n.d	n.d	n.d	n.d	n.d	n.d	n.d	n.d	1.0	n.d	n.d	n.d	n.d	n.d	n.d	P205	n.d	n.d	n.d	n.d	n.d
SO3	1.0	0.7	0.2	0.2	1.1	1.1	0.7	0.7	0.8	0.7	n.d	0.3	0.3	n.d	0.2	n.d	0.2	0.4	SO3	n.d	n.d	n.d	n.d	0.7
TOTAL	99.1	99.3	99.5	99.0	99.3	99.5	99.8	99.0	100.9	100.2	100.1	99.6	99.2	100.3	99.5	100.2	100.1	100.1	TOTAL	99.8	99.2	99.0	99.0	98.7

Code Spot	BTE 7	BTE 9	BTE 45	FER 19	FER 20	FER 18	FER 21	FER 5	FER 6	FER 18	FER 19	FER 22	FER 26	FER 27	FER 19	FER 7	FER 15	FER 22
S102	33.9	34.1	31.1	3.0	6.1	4.7	3.5	4.9	8.2	4.7	5.5	2.3	3.5	4.6	6.1	3.3	6.0	3.6
AL203	0.7	0.3	1.5	14.1	12.2	15.1	16.6	19.2	15.9	16.6	18.3	19.5	20.2	14.7	16.3	16.1	14.4	18.1
T102	n.d	n.d	n.d	0.9	0.8	0.6	0.4	n.d	0.6	0.6	0.4	0.5	0.3	0.8	n.d	0.8	0.2	0.4
FE203	1.1	0.8	1.4	32.2	31.0	28.8	28.1	22.6	20.8	26.8	24.0	28.9	24.5	28.7	23.5	30.4	21.9	25.7
MNO	n.d	n.d	n.d	0.7	0.4	n.d	0.3	n.d	0.3	n.d	n.d	0.3	0.7	n.d	0.6	n.d	n.d	n.d
NSO	n.d	0.3	n.d	1.2	0.9	1.2	1.4	1.2	1.1	1.6	1.3	1.7	1.5	1.4	1.2	1.4	1.4	1.1
CAO	64.0	64.5	64.3	47.2	48.5	48.6	46.6	49.3	52.1	48.4	49.9	47.6	49.3	50.0	51.7	47.9	49.5	50.5
NA2O	n.d	n.d	0.3	n.d	n.d	0.3	0.5	0.9	0.6	0.7	0.7	n.d	0.5	n.d	n.d	n.d	1.0	n.d
K2O	0.4	0.4	0.4	n.d	0.2	0.3	1.6	1.2	1.0	0.5	0.8	n.d	0.6	n.d	n.d	0.2	1.9	n.d
P205	n.d	n.d	n.d	n.d	n.d	n.d	n.d	n.d	n.d	n.d	n.d	n.d	n.d	n.d	n.d	n.d	n.d	n.d
SO3	n.d	n.d	0.4	n.d	0.4	0.6	2.3	n.d	n.d	n.d	n.d	n.d	n.d	n.d	n.d	n.d	4.0	0.4
TOTAL	100.1	100.4	99.4	99.3	100.8	100.3	101.0	99.6	100.3	100.2	100.9	100.5	100.7	101.0	99.0	100.5	100.3	99.8

Code Spot	FER 23	FER 24	FER 30	FER 10	FER 14	FER 15	FER 23	FER 17	FER 18	FER 25	FER 9	FER 11	FER 14	FER 4	FER 12	FER 25	FER 26	FER 10
S102	4.2	4.7	6.1	19.7	11.2	16.6	3.5	14.4	5.8	2.8	3.1	5.5	8.9	3.4	6.2	2.8	3.6	3.9
AL203	16.6	15.5	12.8	5.1	11.0	8.4	13.7	7.7	16.2	15.6	14.8	17.1	12.1	15.5	15.5	19.2	18.0	16.2
T102	0.4	0.7	0.7	n.d	0.5	n.d	1.0	0.3	0.6	0.6	0.6	0.3	n.d	0.7	0.6	0.4	0.5	0.6
FE203	24.9	27.6	28.5	7.6	21.0	11.5	32.8	16.5	23.9	31.3	32.2	24.3	25.4	31.9	26.8	28.3	28.2	28.9
MNO	n.d	0.3	0.6	n.d	n.d	n.d	0.6	0.3	0.3	0.5	0.6	n.d	0.4	0.4	0.3	0.3	n.d	0.3
NSO	1.0	1.3	1.2	0.8	1.1	0.7	1.3	1.0	1.3	1.4	1.2	1.3	1.2	1.5	1.4	1.3	1.3	1.5
CAO	51.7	48.2	51.4	66.6	55.7	63.2	47.4	58.9	51.2	47.2	47.2	51.5	49.9	47.7	50.1	48.6	48.8	47.7
NA2O	n.d	n.d	n.d	n.d	n.d	0.3	n.d	n.d	0.6	n.d	n.d	n.d	n.d	0.5	n.d	n.d	0.4	0.4
K2O	0.2	n.d	0.3	n.d	n.d	n.d	n.d	0.2	n.d	0.2	n.d	n.d						
P205	n.d	n.d	n.d	n.d	n.d	n.d	n.d	n.d	n.d									
SO3	0.8	0.2	0.3	n.d	n.d	n.d	0.3	n.d	n.d	n.d	n.d	n.d						
TOTAL	99.8	98.5	101.6	99.8	100.5	100.7	100.3	100.1	100.2	99.4	99.7	100.0	98.4	101.6	101.1	100.9	100.8	99.5



(Table 2.6). Electron Microprobe analyses of cement clinker mineral phases from Works B of SRC with PFA addition .

Code Spot	ATE 1	ATE 2	ATE 3	ATE 4	ATE 5	ATE 6	ATE 8	ATE 9	ATE 10	ATE 11	ATE 15	ATE 16	ATE 17	ATE 18	ATE 20	ATE 25	ATE 26	ATE 1	Code Spot	ATE 5	ATE 6	ATE 8	ATE 9	ATE 10	ATE 11	ATE 13	ATE 14	ATE 15	ATE 19	ATE 25	ATE 26	ATE 27	ATE 1	ATE 3	ATE 6	ATE 7	ATE 14		
S102	24.1	24.4	24.6	24.8	24.2	24.1	24.1	24.9	25.1	24.7	24.1	24.5	24.1	24.8	22.3	24.4	24.0	24.6	S102	25.0	25.0	24.9	24.8	25.2	25.0	24.5	24.3	24.9	24.9	24.8	24.9	25.0	24.1	24.6	24.2	24.6	24.4		
AL203	1.6	0.8	0.8	0.8	1.0	1.2	1.1	0.9	0.8	0.8	1.3	0.8	1.2	1.1	2.8	0.8	0.9	0.8	AL203	0.8	0.7	1.0	0.7	0.8	0.8	0.7	1.2	0.6	1.0	0.8	1.0	0.7	1.2	1.0	1.1	1.1	1.1		
T102	n.d	n.d	n.d	n.d	n.d	n.d	n.d	n.d	n.d	n.d	0.3	n.d	n.d	n.d	0.2	n.d	n.d	n.d	T102	n.d	0.2	n.d																	
FE203	1.6	0.8	0.8	1.0	1.0	1.1	1.3	0.9	0.9	0.9	1.6	1.0	0.9	1.0	3.2	0.9	1.0	0.9	FE203	0.9	0.7	0.9	0.9	0.9	1.0	0.9	1.4	0.9	1.0	0.8	1.1	0.8	0.7	0.7	0.7	0.7	1.1		
NMO	n.d	n.d	n.d	n.d	n.d	n.d	n.d	n.d	n.d	n.d	n.d	n.d	n.d	n.d	n.d	n.d	n.d	n.d	NMO	n.d																			
HGO	0.5	0.4	0.4	n.d	0.3	0.4	0.4	0.4	0.4	0.4	0.5	0.5	0.3	0.5	0.4	0.4	0.4	0.4	HGO	0.4	0.3	0.5	0.4	0.4	0.5	0.4	0.5	0.5	0.4	0.4	0.3	0.4	0.4	0.5	0.4	0.4	0.5		
CAO	68.8	72.2	72.6	71.9	71.9	72.1	72.0	72.2	72.5	73.1	72.1	72.2	72.5	73.1	70.0	72.5	71.9	71.9	CAO	72.0	72.5	72.7	72.6	72.7	72.7	72.7	72.0	71.9	72.3	71.9	72.2	71.8	72.3	72.9	71.6	72.1	73.4		
NA2O	n.d	n.d	n.d	n.d	n.d	n.d	n.d	0.4	n.d	n.d	0.4	0.3	n.d	n.d	n.d	n.d	n.d	n.d	NA2O	n.d	n.d	n.d	n.d	n.d	0.3	n.d	n.d	n.d	n.d	n.d	n.d	0.3	n.d	n.d	n.d	n.d	n.d	n.d	
K2O	0.9	n.d	0.1	n.d	n.d	n.d	n.d	n.d	n.d	n.d	n.d	n.d	n.d	n.d	n.d	n.d	n.d	n.d	K2O	n.d	n.d	n.d	n.d	n.d	0.1	n.d	n.d	0.1	n.d	n.d									
P205	n.d	n.d	n.d	n.d	n.d	n.d	n.d	n.d	n.d	n.d	n.d	n.d	n.d	n.d	n.d	n.d	n.d	n.d	P205	n.d	n.d																		
SO3	1.4	0.3	0.4	0.3	0.4	0.4	0.3	0.5	0.3	0.3	0.3	n.d	n.d	n.d	n.d	n.d	0.6	0.3	SO3	n.d	0.9	n.d	n.d																
TOTAL	98.9	98.9	99.7	98.8	98.8	99.3	99.2	100.1	100.0	100.2	100.6	99.3	99.0	100.5	98.9	99.0	98.8	98.9	TOTAL	99.1	99.2	100.0	99.4	100.0	100.4	99.2	99.4	98.9	99.6	98.9	99.5	99.0	98.7	99.7	99.1	98.9	100.5		
Code Spot	ATE 2	ATE 3	ATE 5	ATE 6	ATE 15	ATE 16	ATE 17	ATE 19	ATE 20	ATE 22	ATE 23	ATE 26	ATE 30	ATE 31	ATE 32	ATE 33	ATE 35	ATE 36	Code Spot	ATE 17	ATE 18	ATE 20	ATE 25	ATE 26	ATE 27	ATE 1	ATE 2	ATE 3	ATE 5	ATE 6	ATE 7	ATE 8	ATE 10	ATE 11	ATE 12	ATE 13	ATE 15		
S102	25.3	24.9	25.1	24.6	24.5	23.6	24.9	24.9	24.2	24.2	24.5	24.3	24.9	24.6	25.3	24.9	25.2	24.6	S102	24.2	24.5	23.7	24.8	24.7	24.4	22.6	24.1	23.6	24.0	23.3	21.5	23.9	24.1	24.1	24.1	23.4	24.2		
AL203	0.8	1.0	0.9	0.9	1.1	1.1	0.8	0.8	1.1	1.0	0.8	1.1	1.0	0.8	0.8	1.0	0.9	0.9	AL203	1.4	1.2	1.3	1.1	0.9	1.2	2.5	0.8	1.3	1.3	1.3	1.3	1.0	1.1	1.3	1.0	1.6	1.0		
T102	n.d	n.d	n.d	n.d	n.d	n.d	n.d	n.d	n.d	n.d	n.d	n.d	n.d	n.d	n.d	n.d	n.d	n.d	T102	n.d	n.d	0.3	n.d	0.4	n.d														
FE203	0.5	0.9	0.6	1.0	1.1	0.9	0.7	0.5	0.8	1.3	1.0	0.7	0.9	0.9	0.5	0.9	0.6	1.0	FE203	1.3	1.0	1.1	0.9	1.1	1.0	1.6	0.9	1.1	1.4	0.9	1.1	0.9	1.1	1.1	1.7	0.8			
NMO	n.d	n.d	n.d	n.d	n.d	n.d	n.d	n.d	n.d	n.d	n.d	n.d	n.d	n.d	n.d	n.d	n.d	n.d	NMO	n.d	n.d																		
HGO	0.3	0.5	0.3	0.3	0.4	0.3	0.4	0.4	0.4	0.5	0.4	0.4	0.4	0.4	0.3	0.5	0.3	0.3	HGO	0.4	0.5	0.5	0.4	0.3	0.4	0.5	0.4	0.4	0.4	0.5	0.5	0.3	0.4	0.5	0.3	0.4	0.3		
CAO	72.9	72.3	72.5	72.0	72.5	72.2	72.7	72.4	72.3	71.8	72.0	72.5	72.4	71.9	72.9	72.3	72.5	72.0	CAO	71.7	72.5	72.1	73.3	73.4	73.1	70.2	70.5	70.7	71.4	72.1	68.5	72.4	72.4	71.5	72.4	71.1	72.5		
NA2O	n.d	0.5	n.d	n.d	n.d	n.d	n.d	n.d	n.d	n.d	n.d	n.d	n.d	n.d	n.d	0.5	n.d	n.d	NA2O	n.d	0.5	0.7	n.d	n.d	0.6	n.d	0.4	n.d	n.d	n.d	n.d								
K2O	n.d	n.d	n.d	0.2	n.d	0.2	n.d	0.2	0.2	0.2	0.3	n.d	0.3	n.d	n.d	0.3	n.d	0.2	K2O	n.d	n.d	n.d	n.d	n.d	n.d	0.3	n.d	n.d	n.d	n.d	1.5	n.d	n.d	n.d	n.d	n.d	n.d		
P205	n.d	n.d	n.d	n.d	n.d	0.6	n.d	P205	n.d	0.6	n.d	n.d																											
SO3	n.d	0.3	n.d	0.3	n.d	n.d	n.d	n.d	n.d	0.3	0.4	0.3	0.4	0.3	n.d	0.3	n.d	0.3	SO3	n.d	0.2	n.d	n.d	n.d	n.d	1.3	1.7	1.3	0.6	0.6	4.3	0.5	0.4	0.7	0.5	0.7	0.4		
TOTAL	99.8	100.4	99.4	99.3	99.6	98.9	99.5	99.2	99.0	99.3	99.4	99.3	100.3	98.9	99.8	100.4	99.5	99.3	TOTAL	99.0	99.9	99.0	100.5	100.4	100.1	99.0	99.5	99.1	99.1	99.1	99.3	99.0	99.7	99.2	99.4	98.9	99.2		
Code Spot	ATE 1	ATE 3	ATE 5	ATE 6	ATE 7	ATE 9	ATE 10	ATE 11	ATE 12	ATE 13	ATE 16	ATE 17	ATE 18	ATE 21	ATE 1	ATE 2	ATE 3	ATE 4	Code Spot	ATE 16	ATE 17	ATE 18	ATE 19	ATE 20	ATE 23	ATE 25	ATE 26	ATE 3	ATE 4	ATE 6	ATE 7	ATE 8	ATE 10	ATE 11	ATE 12	ATE 19	ATE 21		
S102	24.6	25.0	23.9	24.5	25.9	25.2	24.9	24.6	24.8	25.3	25.1	24.9	24.3	25.4	24.2	24.3	24.7	25.1	S102	23.7	24.0	24.2	24.1	24.6	24.4	24.4	24.1	24.3	25.0	24.3	24.8	24.8	24.5	24.8	24.7	24.8	24.4	24.4	
AL203	1.0	1.0	1.6	0.9	0.7	0.8	1.0	0.9	0.9	0.8	0.8	0.9	1.1	0.8	1.5	1.2	0.7	1.0	AL203	1.4	1.2	1.1	1.1	1.3	1.2	0.9	1.1	1.2	0.9	1.1	1.1	1.1	1.0	1.1	1.1	1.1	1.2	1.0	
T102	0.3	n.d	n.d	n.d	n.d	0.3	n.d	n.d	n.d	n.d	n.d	0.3	n.d	n.d	0.3	n.d	n.d	n.d	T102	n.d	0.4	n.d	n.d	0.2	n.d	n.d	n.d	n.d	n.d	n.d	n.d								
FE203	0.9	0.9	1.3	0.8	0.6	0.9	0.7	0.8	0.6	0.8	0.9	1.0	0.7	1.2	0.9	0.8	1.0	FE203	0.6	0.9	0.9	1.2	1.2	1.0	1.0	1.0	1.1	1.1	0.9	1.0	0.9	1.0	0.8	0.7	0.9	0.6	0.6		
NMO	n.d	n.d	n.d	n.d	n.d	n.d	n.d	n.d	n.d	n.d	n.d	n.d	n.d	n.d	n.d	n.d	n.d	n.d	NMO	n.d	n.d	n.d																	
HGO	0.5	0.5	0.5	0.3	0.3	0.7	0.6	0.4	0.5	0.5	0.6	0.4	0.3	0.4	0.5	0.4	0.5	0.6	HGO	0.5	0.4	0.4	0.5	0.5	0.5	0.4	0.4	0.5	0.4	0.4	0.3	0.5	0.5	0.3	0.5	0.5	0.4	0.4	
CAO	72.8	72.7	71.3	72.6	73.2	71.5	72.0	72.1	72.8	72.7	72.9	72.7	72.8	73.0	71.0	72.6	73.0	71.9	CAO	71.5	72.5	71.9	71.1	71.8	72.1	72.8	71.8	71.7	72.3	72.6	71.8	72.6	72.4	72.1	72.8	72.1	72.9		
NA2O	n.d	0.4	0.5	n.d	n.d	n.d	0.2	n.d	NA2O	n.d	n.d	n.d	0.5	n.d	n.d	n.d	n.d	n.d	0.4	n.d	n.d																		
K2O	n.d	n.d	n.d	n.d	n.d	n.d	n.d	n.d	n.d	n.d	n.d	n.d	n.d	n.d	n.d	0.1	n.d	n.d	n.d	K2O	0.3	n.d	0.1	n.d	n.d	n.d	n.d	n.d	0.2	n.d	n.d								
P205	n.d	n.d	n.d	n.d	n.d	n.d	n.d	n.d	n.d	n.d	n.d	n.d	n.d	n.d	n.d	0.3	n.d	n.d	n.d	P205	n.d	n.d	n.d																
SO3	n.d	n.d	n.d	n.d	n.d	n.d	n.d	n.d	n.d	n.d	n.d	n.d	n.d	n.d	0.3	n.d	n.d	0.3	SO3	0.8	0.7	0.6	0.6	0.6	n.d	0.4	0.6	0.3	n.d	n.d									
TOTAL	100.1	100.5	99.1	99.1	100.9	99.1	99.6	98.7	99.8	99.9	100.2	100.1	99.5	100.6	99.1	99.4	100.0	99.6	TOTAL	98.8	99.7	99.1	99.1	100.0	99.2	99.9	99.0	99.5	100.2	99.5	99.0	100.1	99.4	99.3	100.6	99.5	99.3		

(Table 12-6 continued). Electron Microprobe analyses of cement clinker mineral phases from Works B of SRC with PFA addition.

Code Spot	ATE 22	ATE 24	ATE 24	ATE 26	ATE 1	ATE 2	ATE 3	ATE 4	ATE 6	ATE 7	ATE 8	ATE 9	ATE 10	ATE 13	ATE 14	ATE 15	ATE 18	ATE 19	Code Spot	BTE 22	BTE 2	BTE 14	BTE 15	BTE 17	BTE 18	BTE 23	FER 12	FER 19	FER 23	FER 24	FER 10	FER 14	FER 18	FER 21	FER 24	FER 25	FER 15
S102	23.7	24.7	24.5	24.5	24.0	24.5	24.6	23.9	24.4	25.7	24.5	24.9	24.4	23.9	22.9	24.0	24.6	24.3	S102	31.5	33.0	31.9	30.7	34.4	31.8	29.9	14.6	3.6	11.4	17.3	3.9	4.7	3.3	3.4	3.0	6.1	8.6
AL203	2.7	1.0	0.8	1.0	1.2	0.9	1.1	1.4	1.1	1.1	1.0	0.8	0.8	1.7	1.9	1.2	1.0	1.0	AL203	2.3	0.3	1.5	1.8	n.d	1.5	1.9	12.1	17.5	12.3	5.8	17.1	15.2	17.3	16.6	19.0	16.6	13.4
TiO2	n.d	n.d	n.d	n.d	n.d	n.d	n.d	0.2	n.d	n.d	TiO2	0.2	n.d	n.d	n.d	n.d	0.2	n.d	n.d	0.3	0.4	0.3	0.8	0.7	0.8	1.0	0.7	0.4	0.8								
FE203	1.3	1.0	1.0	1.0	0.8	0.9	0.7	1.1	0.9	1.1	0.9	0.7	0.8	1.2	2.2	0.8	1.1	1.2	FE203	1.0	0.4	1.2	1.4	0.6	1.2	1.5	14.1	26.8	21.6	11.0	27.0	26.6	26.6	28.9	27.8	24.7	23.1
MNO	n.d	n.d	n.d	n.d	n.d	n.d	n.d	n.d	n.d	n.d	MNO	n.d	0.3	n.d	0.5	0.5	0.5	n.d	0.4	n.d	n.d																
NGO	0.6	0.4	0.5	0.5	0.4	0.5	0.4	0.4	0.3	0.3	0.5	0.4	0.5	0.4	0.6	0.5	0.5	0.3	NGO	0.2	n.d	0.3	0.3	n.d	0.4	0.4	0.8	1.4	1.1	0.8	1.3	1.7	1.7	1.4	1.8	1.3	1.4
CAO	70.8	73.1	71.9	71.9	72.3	72.6	72.5	73.2	72.5	70.3	72.1	73.6	72.7	72.1	71.4	72.8	72.6	72.6	CAO	59.3	64.1	65.5	64.0	64.7	64.0	64.2	54.7	49.7	51.8	63.5	50.2	47.5	47.5	47.7	47.1	50.8	53.0
NA2O	n.d	n.d	n.d	n.d	n.d	n.d	n.d	n.d	n.d	n.d	NA2O	1.3	n.d	n.d	0.5	n.d	0.3	0.4	0.4	0.6	n.d	n.d	0.4	n.d	n.d	n.d	n.d	n.d	0.1								
K2O	n.d	0.2	n.d	n.d	0.1	0.4	n.d	n.d	n.d	n.d	K2O	1.5	0.7	0.1	0.5	0.3	0.3	0.5	1.1	0.5	0.2	n.d	n.d	0.2	0.2	n.d	n.d	0.2	n.d								
P2O5	n.d	n.d	n.d	n.d	n.d	n.d	n.d	n.d	n.d	n.d	P2O5	n.d	n.d	n.d	n.d	n.d	0.4	n.d																			
SO3	n.d	n.d	n.d	0.2	n.d	n.d	n.d	n.d	n.d	0.4	n.d	n.d	n.d	0.7	n.d	n.d	n.d	n.d	SO3	2.5	0.9	n.d	0.9	n.d	n.d	1.1	3.0	0.6	0.3	n.d	n.d	n.d	n.d	0.2	n.d	n.d	n.d
TOTAL	99.1	100.2	98.7	99.1	98.7	99.4	99.3	100.0	99.2	99.1	99.0	100.4	99.3	100.4	99.0	99.5	100.0	99.4	TOTAL	99.8	99.4	100.5	100.1	100.0	100.1	99.9	100.8	101.0	99.4	98.7	101.2	99.1	99.9	99.2	99.8	100.1	100.4
Code Spot	ATE 20	ATE 21	ATE 22	ATE 24	ATE 25	ATE 26	BTE 14	BTE 21	BTE 22	BTE 8	BTE 9	BTE 11	BTE 12	BTE 38	BTE 39	BTE 8	BTE 14	BTE 19	Code Spot	FER 22	FER 7	FER 12	FER 16	FER 24	FER 11	FER 12	FER 23	FER 14	FER 24	FER 9	FER 13	FER 20	FER 25	FER 27	FER 5	FER 11	FER 16
S102	23.9	25.0	24.0	24.4	24.8	24.5	32.5	30.3	28.7	30.0	30.5	30.8	31.4	30.1	30.5	31.8	30.9	28.0	S102	5.0	4.5	5.1	2.6	3.5	14.2	5.4	2.5	6.8	7.0	4.4	7.6	10.8	13.4	11.3	9.0	6.0	5.4
AL203	1.2	1.2	1.2	1.2	0.9	1.0	0.7	1.7	2.2	1.7	1.7	1.6	1.3	1.7	1.7	1.3	1.4	1.1	AL203	22.2	19.1	16.0	18.3	15.3	10.7	16.7	19.4	14.2	14.9	18.2	14.6	13.5	10.5	11.7	16.2	16.6	16.2
TiO2	n.d	0.3	n.d	n.d	0.3	0.3	n.d	n.d	0.3	n.d	TiO2	0.4	0.6	0.6	0.7	1.2	0.6	0.6	0.4	0.4	0.6	0.7	0.7	0.5	0.3	0.4	0.4	0.5	0.7								
FE203	1.4	1.1	1.0	0.8	0.9	0.9	1.1	1.8	2.3	1.7	1.6	1.8	1.5	1.7	1.6	1.1	1.4	1.3	FE203	16.0	24.0	27.3	28.1	29.5	18.2	25.9	27.9	24.5	24.0	25.9	25.9	20.1	13.7	18.9	21.5	25.0	25.8
MNO	n.d	n.d	n.d	n.d	n.d	n.d	n.d	n.d	n.d	n.d	MNO	n.d	n.d	0.4	0.3	0.6	n.d	0.4	0.3	n.d	0.4	n.d	0.6	0.4	n.d	n.d	n.d	n.d	n.d								
NGO	0.4	0.3	0.3	0.4	0.4	0.4	n.d	0.3	0.4	0.3	0.5	0.3	0.2	0.3	0.5	n.d	0.3	0.3	NGO	1.2	1.5	1.4	1.5	1.4	1.0	1.5	1.5	1.1	1.5	1.5	1.2	1.2	1.6	1.3	1.5		
CAO	72.7	71.1	72.1	72.6	72.7	72.2	64.8	63.5	63.0	63.0	63.3	63.4	63.2	63.1	63.3	64.7	64.6	68.3	CAO	52.9	48.9	49.4	47.8	48.0	54.0	48.7	48.4	50.8	52.6	49.4	49.3	52.7	61.0	56.2	52.0	50.0	49.7
NA2O	n.d	n.d	n.d	n.d	n.d	n.d	0.5	0.4	0.7	0.7	0.5	0.4	0.5	0.7	0.5	n.d	0.5	0.4	NA2O	1.2	0.6	n.d	n.d	n.d	n.d	n.d	n.d	0.4	n.d	0.4	0.4	n.d	n.d	n.d	n.d	n.d	n.d
K2O	n.d	n.d	0.3	n.d	n.d	0.2	0.3	0.4	0.5	0.5	0.4	0.4	0.5	0.5	0.4	0.3	0.3	0.2	K2O	0.3	n.d	0.4	n.d	0.3	n.d	n.d	0.2	0.1	0.2								
P2O5	n.d	n.d	n.d	n.d	n.d	n.d	n.d	n.d	n.d	n.d	P2O5	n.d																									
SO3	0.2	0.3	0.5	n.d	n.d	n.d	0.6	1.5	1.3	1.0	0.9	1.0	0.5	1.0	0.9	0.7	0.6	0.5	SO3	n.d	n.d	n.d	n.d	n.d	0.5	0.3	n.d	2.0	n.d	0.6	0.5	0.3	n.d	0.3	n.d	0.3	
TOTAL	99.4	99.0	99.4	99.4	99.7	99.2	100.5	99.9	99.1	99.2	99.4	99.7	99.4	99.4	99.4	99.9	100.3	100.1	TOTAL	99.2	99.2	100.2	99.3	99.5	99.2	99.1	100.4	100.3	101.0	100.1	101.6	100.4	100.4	99.7	101.2	99.5	99.8
Code Spot	BTE 20	BTE 20	BTE 21	BTE 22	BTE 23	BTE 2	BTE 4	BTE 5	BTE 8	BTE 9	BTE 10	BTE 15	BTE 16	BTE 19	BTE 21	BTE 9	BTE 21	Code Spot	ALU 13	ALU 4	ALU 12																
S102	31.2	30.9	31.4	31.1	31.0	30.7	30.4	28.6	31.0	32.2	30.2	29.6	29.4	31.4	32.6	29.4	32.2	S102	4.1	4.1	4.5																
AL203	2.0	1.7	1.5	1.7	1.5	1.5	1.9	3.1	1.1	0.9	1.8	1.9	1.7	1.4	0.4	1.9	0.3	AL203	18.3	19.6	20.0																
TiO2	n.d	0.3	0.3	0.3	n.d	n.d	n.d	0.3	n.d	n.d	n.d	n.d	n.d	n.d	n.d	n.d	n.d	TiO2	n.d	n.d	0.3																
FE203	1.4	1.2	1.5	1.6	1.4	1.8	1.6	2.1	1.1	1.3	1.9	1.9	1.6	1.1	0.8	1.6	0.5	0.8	FE203	25.7	22.9	23.6															
MNO	n.d	n.d	n.d	n.d	n.d	n.d	n.d	n.d	n.d	MNO	n.d	n.d	n.d																								
NGO	0.3	0.3	0.4	0.3	0.2	0.3	n.d	0.3	n.d	0.2	0.2	0.4	0.3	n.d	0.3	n.d	n.d	NGO	1.2	1.3	1.2																
CAO	63.8	63.1	64.1	63.9	63.9	63.3	63.6	63.6	64.9	65.0	63.7	64.0	63.9	64.9	64.7	64.4	64.1	64.4	CAO	49.6	50.2	50.5															
NA2O	0.8	0.7	0.3	0.4	0.3	0.5	n.d	n.d	n.d	n.d	0.5	0.4	0.4	n.d	0.3	n.d	0.5	n.d	NA2O	n.d	n.d	n.d															
K2O	0.2	0.6	0.4	0.4	0.6	0.5	0.4	0.3	n.d	0.3	0.5	0.5	0.3	0.2	0.4	0.4	0.4	K2O	0.6	0.2	0.1																
P2O5	n.d	n.d	n.d	n.d	n.d	n.d	n.d	n.d	n.d	P2O5	n.d	n.d	n.d																								
SO3	0.8	0.5	0.4	0.7	0.6	0.9	1.4	0.9	0.4	0.4	0.9	0.9	1.5	0.5	n.d	1.5	1.0	0.6	SO3	0.8	1.2	n.d															
TOTAL	100.5	99.3	100.3	100.4	99.5	99.5	99.3	99.2	98.5	99.8	99.5	99.4	99.4	99.9	99.2	99.5	99.7	99.7	TOTAL	100.3	99.5	100.2															





(Table 12-6). Electron Microprobe analyses of cement clinker mineral phases from Works C DPC.

Code Spot	ATE 1	ATE 2	ATE 3	ATE 4	ATE 5	ATE 7	ATE 9	ATE 10	ATE 13	ATE 14	ATE 15	ATE 16	ATE 17	ATE 20	ATE 23	ATE 24	ATE 25	ATE 29	Code Spot	ATE B4	ATE B8	ATE B9	ATE 92	ATE 94	ATE 95	ATE 96	ATE 97	ATE 98	ATE 99	ATE 100	ATE 101	ATE 103	ATE 104	ATE 105	ATE 106	ATE 108	ATE 109	
S102	24.2	24.4	24.5	24.6	24.5	24.0	24.5	24.6	22.5	24.5	24.8	24.1	24.0	24.6	22.6	27.0	24.2	24.6	S102	25.1	24.8	23.6	24.7	24.2	23.9	24.5	24.2	24.4	24.3	24.7	24.7	24.7	23.9	24.3	25.0	23.3	25.0	
AL203	1.6	1.1	1.7	1.2	1.3	1.6	1.5	1.3	3.7	1.3	1.2	1.4	1.8	1.1	5.2	1.4	1.4	1.5	AL203	0.8	1.1	1.2	1.1	1.1	1.4	1.1	1.8	1.2	1.4	1.1	0.9	1.1	1.3	2.4	0.9	2.1	1.2	
T102	n.d	n.d	0.4	n.d	n.d	n.d	n.d	n.d	0.4	n.d	n.d	0.3	0.3	n.d	n.d	n.d	0.3		T102	n.d	0.5	n.d																
FE203	n.d	n.d	0.6	0.4	0.5	0.5	n.d	0.5	1.4	0.4	0.5	0.6	0.7	0.6	0.9	0.4	n.d	0.5	FE203	0.5	n.d	0.3	0.5	0.6	0.5	n.d	0.6	n.d	0.5	n.d	0.5	n.d	0.8	0.7	n.d	0.7	n.d	
MNO	n.d	MNO	n.d	n.d	n.d	n.d	n.d	n.d	0.3	n.d																												
MGO	0.7	0.5	0.8	0.6	0.8	0.7	0.5	0.4	0.8	0.6	0.8	0.8	0.5	0.7	0.7	0.3	0.5	0.9	MGO	0.6	0.5	0.5	0.6	0.9	0.5	0.4	0.5	0.4	0.7	0.4	0.8	0.4	0.5	0.9	0.4	0.6	0.5	
CAO	73.0	72.8	72.3	73.0	73.1	73.5	73.0	73.1	70.6	72.7	72.9	72.2	72.8	72.6	69.1	69.9	72.8	72.0	CAO	72.1	72.7	71.0	73.4	70.8	72.0	72.6	72.5	73.0	72.0	72.2	72.0	73.2	71.3	72.8	72.2	72.5		
NA2O	n.d	n.d	n.d	n.d	n.d	0.4	n.d	n.d	0.3	0.4	n.d	n.d	n.d	n.d	n.d	0.6	n.d	0.3	NA2O	n.d	n.d	0.5	n.d	n.d	n.d	0.4	n.d	n.d	n.d	0.5	n.d	n.d	n.d	n.d	n.d	n.d		
K2O	n.d	0.2	n.d	n.d	K2O	n.d	n.d	0.7	n.d	0.4	n.d	n.d	n.d	n.d	0.2	n.d																						
P2O5	n.d	P2O5	n.d																																			
SO3	n.d	0.4	n.d	n.d	n.d	n.d	n.d	0.5	0.3	n.d	n.d	SO3	n.d	n.d	1.2	n.d	0.7	0.3	0.2	n.d	n.d	0.3	0.6	n.d	n.d	n.d	n.d	n.d	n.d									
TOTAL	99.5	98.8	100.3	99.8	100.2	100.7	99.5	99.9	100.1	99.9	100.2	99.4	100.1	99.6	99.6	99.5	98.9	100.1	TOTAL	99.1	99.1	99.0	100.3	98.7	98.6	99.5	99.6	99.0	99.2	99.4	99.4	98.7	99.6	99.5	99.4	99.2		
Code Spot	ATE 30	ATE 31	ATE 34	ATE 36	ATE 41	ATE 43	ATE 44	ATE 46	ATE 47	ATE 48	ATE 49	ATE 50	ATE 51	ATE 53	ATE 54	ATE 55	ATE 62	ATE 63	Code Spot	ATE 110	ATE 111	ATE 112	ATE 113	ATE 115	ATE 116	ATE 117	ATE 118	ATE 119	ATE 120	ATE 121	ATE 123	ATE 124	ATE 125	ATE 127	ATE 128	ATE 129	ATE 130	
S102	24.3	25.0	23.7	23.8	24.3	24.4	24.7	24.3	24.3	24.1	23.9	25.7	23.6	24.6	24.1	24.2	24.5	24.1	S102	23.7	24.2	24.4	24.4	24.5	23.5	24.3	23.7	22.8	24.1	23.8	24.3	24.1	24.5	24.9	24.7	24.3	24.3	
AL203	4.3	1.6	1.4	1.7	1.7	1.0	1.1	1.2	1.1	1.3	1.7	1.7	1.6	1.1	1.2	1.5	0.9	1.2	AL203	1.8	1.8	1.3	1.3	0.9	2.0	1.5	1.6	2.2	1.8	1.7	1.8	1.4	1.5	0.9	1.1	1.1	1.1	
T102	0.3	n.d	0.3	n.d	0.3	n.d	n.d	n.d	n.d	n.d	0.3	0.1	n.d	n.d	n.d	n.d	n.d	n.d	T102	0.3	n.d	0.3	n.d															
FE203	0.4	n.d	0.8	0.8	0.6	0.4	0.4	n.d	n.d	n.d	0.5	0.5	0.7	n.d	0.5	0.8	0.4	0.5	FE203	0.8	1.0	0.6	0.4	0.7	0.8	n.d	0.6	0.8	0.5	0.7	0.5	0.4	0.4	n.d	n.d	0.4	0.4	
MNO	n.d	MNO	n.d																																			
MGO	1.1	0.9	0.7	0.6	0.6	0.8	0.5	0.7	0.5	0.8	0.7	0.5	0.6	0.5	0.6	0.8	0.7	0.5	MGO	0.6	1.1	0.8	0.6	0.6	0.5	1.8	0.7	0.9	0.7	0.4	0.7	0.7	0.7	0.4	0.9	0.7	0.7	
CAO	69.0	71.7	72.0	72.2	71.8	72.2	72.4	72.9	72.8	72.5	69.6	72.4	72.6	72.3	72.1	72.0	72.9		CAO	71.8	70.6	72.0	72.1	72.4	72.3	71.8	72.0	70.9	71.8	72.1	71.6	72.6	72.6	72.4	72.8	72.1	72.3	
NA2O	n.d	0.4	n.d	NA2O	n.d	0.4	n.d	0.4	0.4																													
K2O	0.1	n.d	0.3	0.2	0.1	n.d	n.d	n.d	n.d	0.1	0.2	0.3	n.d	n.d	n.d	n.d	0.2	n.d	K2O	n.d	0.2	n.d																
P2O5	n.d	P2O5	n.d	n.d																																		
SO3	0.1	0.3	0.3	0.3	n.d	n.d	0.3	0.2	n.d	n.d	0.8	n.d	SO3	n.d	0.5	n.d	n.d	n.d	0.3	n.d	n.d	n.d	n.d															
TOTAL	99.6	99.5	99.5	99.6	99.4	98.8	99.2	98.8	98.8	99.1	99.5	99.4	99.0	98.8	99.1	99.4	98.7	99.6	TOTAL	99.0	98.7	99.1	98.8	99.1	99.1	99.4	98.6	98.7	98.9	99.0	98.9	99.2	100.0	98.6	99.5	99.0	99.2	
Code Spot	ATE 64	ATE 65	ATE 66	ATE 67	ATE 69	ATE 70	ATE 71	ATE 72	ATE 73	ATE 74	ATE 75	ATE 76	ATE 78	ATE 79	ATE 80	ATE 81	ATE 82	ATE 83	Code Spot	ATE 131	ATE 132	ATE 133	ATE 134	ATE 135	ATE 136	ATE 137	ATE 138	ATE 139	ATE 140	ATE 141	ATE 142	ATE 143	ATE 144	ATE 145	ATE 147	ATE 148	ATE 149	
S102	24.3	24.3	24.6	23.8	24.2	25.1	24.0	24.2	24.2	24.7	24.2	24.3	24.6	24.9	24.4	24.7	24.3	25.2	S102	23.9	23.1	24.9	24.1	23.7	24.4	24.1	23.9	24.2	23.5	24.1	24.3	24.1	24.7	24.1	24.0	24.3	24.3	
AL203	1.1	1.2	0.9	2.1	1.3	0.9	1.6	1.8	1.2	1.1	1.8	1.0	0.9	0.8	1.4	1.4	2.6	1.0	AL203	1.5	2.1	1.2	1.5	1.9	1.6	1.4	1.6	1.2	1.6	1.4	1.3	1.3	1.1	1.3	1.7	1.3	1.5	
T102	n.d	n.d	n.d	0.3	n.d	n.d	0.3	n.d	T102	n.d	0.3	n.d	n.d	n.d	n.d	n.d	0.2	n.d																				
FE203	0.4	0.5	0.5	0.6	0.5	n.d	0.5	0.3	0.5	0.5	0.5	0.3	0.5	n.d	0.5	0.5	0.8	0.4	FE203	0.5	0.6	n.d	0.6	0.8	0.5	0.4	0.5	0.4	0.4	0.5	0.3	0.5	0.4	0.6	0.5	n.d	0.4	
MNO	n.d	MNO	n.d																																			
MGO	0.4	0.6	0.9	0.8	0.6	0.6	0.8	1.0	0.4	0.5	0.9	0.6	0.5	0.6	0.4	0.7	1.2	0.5	MGO	0.6	0.8	0.8	1.0	0.7	0.9	0.6	0.6	0.8	1.0	0.7	0.5	0.5	0.8	0.8	0.6	0.7	0.7	
CAO	72.8	73.5	72.1	71.2	72.4	72.5	71.6	71.3	72.4	72.1	71.4	72.2	72.5	72.1	72.2	70.8	72.3		CAO	72.4	72.6	72.6	71.1	72.6	71.4	72.8	72.2	72.5	71.9	72.9	73.9	72.7	72.5	71.7	73.5	72.8	72.5	
NA2O	n.d	n.d	n.d	0.4	n.d	0.4	0.4	n.d	n.d	n.d	n.d	0.5	n.d	n.d	n.d	n.d	n.d	n.d	NA2O	n.d	n.d	n.d	n.d	0.4	n.d													
K2O	0.2	n.d	n.d	0.2	n.d	n.d	n.d	n.d	0.2	n.d	K2O	n.d	0.1	n.d	0.2	n.d	0.3	n.d	n.d	n.d	n.d																	
P2O5	n.d	P2O5	n.d																																			
SO3	n.d	n.d	n.d	0.3	n.d	n.d	n.d	n.d	n.d	n.d	0.3	0.3	n.d	n.d	n.d	n.d	0.3	n.d	SO3																			

(Table 12-9 continued). Electron Microprobe analyses of cement clinker mineral phases from Works C OPC.

Code Spot	ATE 150	ATE 151	ATE 153	ATE 154	ATE 155	ATE 156	ATE 158	ATE 159	ATE 160	ATE 161	ATE 162	ATE 163	ATE 165	ATE 166	ATE 167	ATE 171	ATE 173	ATE 174	Code Spot	FER 177	ALU 90	ALU 28	ALU 38	ALU 107	ALU 181	Code Spot	ALU 229	ALU 242	FER 243	FER 244								
S102	24.0	24.2	24.2	24.5	24.3	24.2	24.3	24.2	23.9	24.1	24.6	24.1	24.1	23.7	23.0	24.5	24.2	24.2	S102	7.6	5.7	3.9	4.8	4.4	4.5	S102	11.4	2.7	2.5	3.8								
AL203	1.5	1.5	1.2	1.2	1.1	1.2	1.0	1.1	1.8	1.5	1.6	1.2	1.5	1.5	1.9	1.8	1.2	1.0	AL203	21.4	25.6	30.0	26.0	26.6	25.6	AL203	18.6	26.9	25.7	24.3								
T102	n.d	n.d	n.d	n.d	0.3	n.d	0.3	n.d	0.3	n.d	n.d	T102	0.7	0.5	0.5	0.6	0.9	0.6	T102	0.7	0.9	1.3	0.9															
FE203	n.d	0.5	0.7	0.5	0.5	0.5	0.4	0.3	0.7	0.5	0.8	0.5	0.5	0.5	0.7	0.6	0.4	n.d	FE203	11.8	0.9	5.2	8.5	8.4	9.8	FE203	10.6	11.3	15.7	13.4								
MNO	n.d	MNO	n.d	n.d	n.d	0.3	n.d	n.d	MNO	n.d	n.d	0.5	0.4																									
MGO	0.6	0.4	0.6	0.5	0.5	0.5	0.5	0.5	0.5	0.7	0.7	0.6	0.9	0.7	0.8	0.6	0.7	0.7	MGO	2.0	2.8	1.2	1.0	1.1	1.3	MGO	2.9	1.9	1.8	1.7								
CAO	73.0	72.6	72.1	72.3	73.5	72.6	73.2	72.4	72.0	72.9	71.8	73.1	72.6	73.0	72.2	72.0	72.4	72.3	CAO	54.4	54.9	58.2	57.8	56.9	56.4	CAO	54.1	52.9	50.7	52.3								
MA20	n.d	0.4	n.d	n.d	n.d	n.d	n.d	0.4	0.5	n.d	n.d	MA20	n.d	0.5	n.d	n.d	0.4	0.4	MA20	n.d	n.d	n.d	n.d															
K20	n.d	0.3	K20	0.2	n.d	0.2	n.d	n.d	0.3	K20	0.2	0.6	0.5	0.4																								
P205	n.d	P205	n.d	n.d	n.d	n.d	n.d	n.d	P205	n.d	n.d	n.d	n.d																									
S03	n.d	0.3	n.d	n.d	n.d	n.d	n.d	0.3	n.d	n.d	n.d	n.d	n.d	0.2	0.3	n.d	n.d	0.3	S03	0.4	0.4	n.d	0.3	n.d	0.4	S03	1.2	1.5	1.5	1.7								
TOTAL	99.1	99.5	98.8	99.0	100.2	99.0	99.4	99.2	98.9	99.7	99.5	99.5	99.6	99.9	99.3	100.3	98.9	98.8	TOTAL	98.5	91.3	99.2	99.3	98.7	99.3	TOTAL	99.70	98.70	100.20	98.90								
Code Spot	ATE 175	ATE 176	ATE 178	ATE 179	ATE 182	ATE 183	ATE 185	ATE 187	BTE 11	BTE 12	BTE 19	BTE 22	BTE 26	BTE 35	BTE 39	BTE 40	BTE 68	BTE 91	Code Spot	ATE 202	ATE 204	ATE 208	ATE 211	ATE 213	ATE 214	ATE 216	ATE 218	ATE 219	ATE 221	ATE 222	ATE 223	ATE 224	ATE 226	ATE 227	ATE 230	ATE 233	ATE 234	
S102	24.6	23.7	23.7	23.6	24.8	24.5	24.1	23.1	29.1	28.8	32.1	29.9	29.7	29.8	30.4	29.9	30.5	30.2	S102	23.1	24.3	23.8	23.0	23.5	24.1	23.9	23.8	23.2	24.5	24.6	24.1	24.7	25.4	24.4	24.3	24.7	24.0	
AL203	1.4	1.6	1.5	1.9	1.0	0.9	1.0	1.5	2.5	2.4	1.7	2.2	2.1	2.2	2.1	2.1	1.7	1.9	AL203	2.9	0.8	1.2	3.5	2.9	1.3	1.8	2.1	2.2	1.1	1.3	1.3	1.2	1.7	2.4	1.2	1.3	1.2	
T102	n.d	0.3	n.d	0.3	0.3	T102	0.3	n.d	0.3	0.4	n.d	0.3	0.4	n.d	0.3	0.3	0.3	0.2	0.3	n.d	n.d	n.d	0.3	0.2														
FE203	0.5	0.9	0.5	0.5	n.d	0.5	n.d	0.6	1.0	0.9	0.6	0.8	0.9	0.7	0.4	0.7	0.9	0.8	FE203	0.7	0.4	0.4	1.2	0.7	0.5	0.4	0.8	0.9	n.d	0.4	0.6	0.3	0.5	0.8	0.6	0.5	n.d	
MNO	n.d	0.3	n.d	MNO	n.d	n.d	n.d	n.d	n.d	n.d	n.d	n.d	n.d	n.d	n.d																							
MGO	0.5	0.6	0.8	1.0	0.5	0.6	0.5	0.6	0.4	0.2	n.d	n.d	n.d	0.2	0.3	0.2	n.d	n.d	MGO	0.9	0.7	0.8	0.9	0.7	0.5	0.6	0.6	0.8	0.6	0.5	0.7	0.5	0.5	0.6	0.6	0.7	0.5	
CAO	72.4	71.8	72.3	71.9	72.4	72.5	73.2	72.8	64.2	64.5	64.7	64.5	64.3	64.4	63.9	64.3	64.8		CAO	70.2	72.3	71.3	70.6	71.4	72.8	71.8	71.2	70.7	72.7	72.0	72.3	72.1	70.0	70.6	71.9	72.4	71.7	
MA20	n.d	0.4	n.d	n.d	n.d	0.5	n.d	n.d	n.d		MA20	n.d	n.d	n.d	n.d	n.d	n.d	n.d	n.d	n.d	n.d	n.d																
K20	n.d	n.d	0.2	n.d	n.d	n.d	n.d	0.2	0.3	0.3	0.2	0.4	0.4	0.4	0.3	0.4	0.3	0.3	K20	n.d	n.d	n.d	n.d	n.d	n.d	n.d	n.d	n.d	n.d	n.d	n.d							
P205	n.d	0.3	n.d	P205	n.d	n.d	n.d	n.d	n.d	n.d	n.d	n.d	n.d	n.d	n.d	n.d																						
S03	n.d	0.4	n.d	n.d	0.3	n.d	n.d	n.d	1.9	2.1	0.8	1.7	1.8	1.9	1.4	1.8	1.0	1.4	S03	0.3	n.d	n.d	0.3	n.d	n.d	n.d	n.d	n.d	n.d	n.d	0.3	0.5	n.d	n.d	n.d	n.d	0.3	
TOTAL	99.4	99.0	99.0	98.9	99.0	99.0	98.8	99.2	99.6	99.2	100.4	99.5	99.4	99.3	99.7	99.1	99.2	99.7	TOTAL	98.90	99.00	98.20	100.50	99.60	99.90	99.40	98.90	98.70	99.70	99.50	99.60	99.90	99.20	99.40	99.10	100.20	98.40	
Code Spot	BTE 114	BTE 146	BTE 176	BTE 184	FER 8	FER 27	FER 45	FER 77	FER 86	FER 87	FER 93	FER 102	FER 122	FER 126	FER 157	FER 164	FER 168	FER 172	Code Spot	ATE 235	ATE 236	ATE 237	ATE 238	BTE 201	BTE 203	BTE 205	BTE 206	BTE 207	BTE 209	BTE 210	BTE 228	BTE 231	BTE 232	BTE 239	BTE 240	BTE 241	FER 217	
S102	30.7	28.5	29.0	29.9	4.6	4.4	13.4	4.4	7.8	4.4	4.6	7.1	6.1	4.4	4.4	5.8	4.3	5.3	S102	24.1	24.4	23.0	23.8	28.8	28.4	29.5	29.6	28.9	28.1	29.8	28.3	28.4	29.3	28.1	28.9	28.9	9.8	
AL203	2.0	2.9	2.4	2.3	23.4	22.5	13.9	24.6	22.2	26.7	26.4	24.4	20.3	25.4	24.9	23.4	25.0	23.5	AL203	1.0	1.3	2.4	2.0	2.9	3.7	2.1	2.2	2.7	3.2	1.9	3.1	2.1	2.2	2.4	2.9	2.5	19.3	
T102	0.4	0.4	0.3	n.d	1.2	1.2	0.9	1.2	0.9	0.8	0.9	0.9	1.1	0.8	0.9	1.7	0.9	0.8	T102	n.d	0.3	0.3	0.4	0.5	0.4	0.5	0.4	0.4	n.d	0.4	0.4	0.4	0.3	n.d	0.4	0.8		
FE203	0.7	1.2	1.0	0.5	14.5	17.5	11.3	10.9	9.5	9.1	8.4	11.5	15.8	12.6	14.4	12.8	12.9	12.3	FE203	0.5	0.4	1.3	0.7	1.0	0.9	0.9	0.6	1.0	1.3	0.5	1.1	0.6	0.6	0.8	0.8	0.7	9.6	
MNO	n.d	n.d	n.d	n.d	0.3	0.7	0.5	0.3	n.d	n.d	0.3	n.d	MNO	n.d	n.d	n.d	n.d	n.d	n.d	n.d	n.d	n.d	n.d	n.d	0.3													
MGO	0.4	0.3	n.d	0.3	1.7	2.1	1.7	1.5	1.4	1.4	1.4	2.3	2.6	2.1	2.1	1.8	2.5	1.7	MGO	0.6	0.7	1.0	0.5	0.5	0.3	0.4	0.5	0.3	0.4	n.d	0.4	0.2	n.d	n.d	n.d	0.4	1.5	
CAO	64.0	63.9	64.5	64.0	53.6	50.7	56.3	55.7	56.5	56.2	57.6	52.8	50.1	53.7	51.6	52.3	52.0	52.6	CAO	71.9	71.9	70.3	71.5	63.2	63.3	62.9	63.7	63.0	63.4	63.8	63.2	64.3	63.3	62.8	63.6	64.6	52.6	
MA20	n.d	n.d	n.d	0.6	0.4	n.d	n.d	0.4	0.4	0.5	n.d	0.5	0.7	n.d	n.d	n.d	n.d	0.6	MA20	0.4	n.d	0.5	n.d	n.d	0.4	0.5	n.d	0.4	n.d	n.d	n.d	n.d	n.d	n.d	0.2	n.d		
K20	0.3	0.3	0.3	0.4	0.2	n.d	0.2	0.3	n.d	n.d	0.2	0.5	n.d	0.2	0.2	0.3	0.6		K20	n.d	n.d	n.d	n.d	0.4	0.2	0.2	0.2	0.4	0.4	0.2	0.2	0.4	0.3	0.7	0.2	0.2	n.d	
P205	n.d	P205	n.d	n.d	n.d	n.d	n.d	n.d	0.3	n.d	n.d																											
S03	1.1	1.7	1.7	1.4	0.6	0.3	0.9	n.d	0.5	n.d	0.3	0.9	1.9	n.d	n.d	0.5	0.9	2.0	S03	0.3	0.2	0.4	0.3	1.9	1.9	1.8	2.3	2.2	2.3	1.9	2.0	1.2	2.0	3.3	1.8	2.0	n.d	
TOTAL	99.6	99.2	99.2	99.4	100.5	99.4	99.1	99.2	99.5	99.1	99.9	100.6	99.1	99.0	98.5	99.5	98.8	99.4	TOTAL	64.0	65.0	65.0	64.0	1.10	1.20													



(Table 12-9 continued). Electron Microprobe analyses of cement clinker mineral phases from Works D OPC .

Code Spot	ATE 206	ATE 209	ATE 211	ATE 212	ATE 213	ATE 214	ATE 215	ATE 221	ATE 222	BTE 5	BTE 7	BTE 19	BTE 20	BTE 22	BTE 31	BTE 45	BTE 46	BTE 92	Code Spot	FER 149	FER 157	FER 185	FER 186	FER 189	FER 190	FER 197	FER 198	ALU 71	ALU 130	ALU 180	ALU 187	ALU 193	ALU 200		
S102	25.0	24.2	24.7	24.3	25.1	25.2	25.1	21.2	24.5	30.6	30.4	30.4	29.7	30.2	31.0	30.8	31.1	31.6	S102	8.3	2.9	4.7	6.3	3.1	4.1	4.3	5.3	3.7	3.5	2.5	3.4	3.3	4.0		
AL203	0.8	1.4	0.8	1.5	0.9	0.7	0.9	6.0	1.7	2.1	2.0	2.0	2.6	1.6	2.2	1.6	1.6	1.4	AL203	16.7	21.5	18.9	17.5	20.2	19.0	20.6	18.8	29.0	30.1	31.0	30.1	30.5	29.9		
T102	n.d	0.5	n.d	0.3	n.d	n.d	n.d	n.d	n.d	0.3	0.4	0.4	0.5	0.6	0.3	0.3	0.3	0.3	T102	1.4	1.6	2.1	2.2	2.7	2.6	1.1	1.8	0.3	n.d	n.d	0.3	n.d			
FE203	0.5	1.0	0.4	1.4	0.5	0.4	0.4	3.0	1.1	0.9	1.1	0.9	1.4	1.2	1.4	1.0	1.1	0.7	FE203	19.2	21.7	21.0	20.5	23.4	22.8	20.2	19.9	3.6	5.9	4.6	5.5	4.6	4.0		
NMO	n.d	n.d	n.d	n.d	n.d	n.d	0.3	n.d	NMO	0.4	n.d	0.3	0.6	n.d	0.4	0.3	0.5	n.d	n.d	n.d	n.d	n.d													
HGO	0.8	0.8	0.6	1.1	0.6	0.8	1.4	1.3	0.9	0.4	0.4	0.3	0.3	0.4	0.4	0.5	0.5	0.4	HGO	2.4	2.6	2.7	2.3	2.7	2.5	2.6	2.6	0.4	0.8	0.9	0.8	0.6	0.8		
CAO	73.4	72.0	71.7	71.2	72.3	71.8	70.8	67.1	71.7	64.3	64.3	62.3	63.9	63.6	63.7	63.1	64.7		CAO	50.8	48.7	49.6	51.1	48.8	48.3	50.2	49.4	56.7	57.6	58.9	58.7	58.9	59.8		
NA2O	0.3	n.d	0.6	n.d	0.5	0.3	n.d	n.d	0.4	n.d	n.d	NA2O	n.d	6.2	0.8	0.7	0.6	0.9	0.9																
K2O	n.d	0.2	n.d	0.8	0.8	0.7	1.0	0.7	0.7	0.8	1.0	0.3	K2O	0.1	n.d	n.d	n.d	n.d	n.d	0.2	n.d	0.5	0.4	0.6	0.4	0.5	0.8								
P205	n.d	0.3	n.d	n.d	0.5	0.3	0.3	0.3	0.3	n.d	P205	n.d	n.d	n.d	n.d	n.d	n.d	n.d																	
SO3	n.d	0.8	0.7	1.0	1.5	0.6	n.d	n.d	n.d	n.d	SO3	n.d	n.d	n.d	n.d	n.d	n.d																		
TOTAL	100.8	99.9	98.2	99.8	99.4	98.9	98.9	98.8	99.9	100.8	99.0	100.5	98.6	99.7	99.9	99.4	99.0	99.4	TOTAL	99.3	99.0	99.3	100.5	100.9	99.7	99.5	98.3	100.4	99.1	99.2	99.5	99.6	100.2		
Code Spot	BTE 103	BTE 116	BTE 138	BTE 146	BTE 150	BTE 151	BTE 154	BTE 182	BTE 188	BTE 191	BTE 201	BTE 204	BTE 216	BTE 217	BTE 218	BTE 219	FER 2	FER 9																	
S102	30.7	31.5	31.0	31.5	31.0	31.0	32.3	30.6	31.6	31.2	30.8	31.7	32.2	31.9	31.0	30.8	4.4	6.8																	
AL203	2.4	1.7	1.8	1.6	1.5	1.8	1.2	2.4	1.9	1.5	1.9	1.5	1.7	1.4	1.7	1.6	22.7	19.0																	
T102	0.4	0.3	0.4	0.3	n.d	0.3	n.d	0.4	n.d	0.4	0.5	0.4	0.4	0.4	0.5	0.3	0.9	1.0																	
FE203	1.4	0.8	0.5	0.7	0.9	0.8	0.6	0.9	1.0	0.8	1.0	0.7	0.9	1.0	1.4	1.0	18.9	18.7																	
NMO	n.d	0.4																																	
HGO	0.5	0.4	0.5	0.3	0.2	0.2	0.2	0.3	0.3	0.4	0.2	0.2	0.4	0.4	0.4	0.3	2.5	2.5																	
CAO	63.3	64.1	64.3	63.5	63.9	63.7	65.0	64.1	63.8	63.4	64.0	64.2	63.0	64.1	63.8	62.7	49.9	49.4																	
NA2O	n.d	0.4	n.d	0.4	n.d	0.7	0.4	0.5	0.5	n.d	n.d																								
K2O	0.4	0.4	n.d	0.8	0.9	0.9	0.5	0.3	0.3	0.5	n.d	n.d	1.1	0.7	0.9	1.1	0.3	1.6																	
P205	n.d	0.3	n.d	n.d	n.d	n.d	n.d	0.3	n.d	n.d	0.4	0.3	n.d	n.d	n.d	0.5	n.d	n.d																	
SO3	n.d	n.d	n.d	0.4	n.d	0.3	n.d	0.7	0.7	n.d	1.4																								
TOTAL	99.1	99.9	98.5	99.5	98.4	99.0	99.8	99.3	98.9	97.8	98.7	99.1	100.4	100.3	100.9	99.5	99.6	100.8																	
Code Spot	FER 17	FER 23	FER 30	FER 40	FER 42	FER 43	FER 52	FER 77	FER 78	FER 100	FER 101	FER 102	FER 104	FER 121	FER 122	FER 126	FER 132	FER 134																	
S102	4.6	5.3	2.9	4.2	6.6	3.6	3.6	4.7	4.6	4.0	4.7	4.4	4.0	5.0	5.4	4.0	3.4	4.0																	
AL203	23.1	22.2	22.4	25.5	19.3	20.8	19.3	17.2	17.5	21.2	24.4	25.1	25.2	21.5	18.9	20.7	23.0	18.0																	
T102	1.1	1.0	1.2	0.9	1.0	1.6	2.0	2.9	3.0	1.4	0.9	0.9	0.8	1.2	1.5	1.4	0.5	2.6																	
FE203	16.0	17.5	21.5	12.4	15.4	21.2	22.4	21.6	21.1	20.6	11.5	10.1	17.1	20.5	20.1	21.1	20.8	21.1																	
NMO	n.d	n.d	n.d	n.d	n.d	n.d	0.4	n.d	0.3	n.d	0.4	0.3	0.3	0.4	0.4	0.5	n.d	0.9																	
HGO	2.5	2.8	2.6	1.7	6.6	2.5	3.1	3.9	2.7	3.4	1.6	1.7	4.1	2.7	2.5	2.8	3.1	2.8																	
CAO	51.1	51.4	48.8	53.1	49.4	49.0	48.7	47.8	48.6	48.8	54.6	55.4	47.4	49.3	49.1	48.8	49.4	48.6																	
NA2O	0.4	0.5	n.d	0.6	n.d	0.8	0.5	n.d	n.d	0.4	n.d																								
K2O	0.3	0.2	n.d	0.7	0.5	0.2	n.d	0.2	n.d	n.d	0.2	0.4	0.4	0.2	n.d	n.d	n.d	n.d																	
P205	n.d																																		
SO3	n.d																																		
TOTAL	99.1	100.9	99.4	99.1	98.8	98.9	99.5	98.3	97.8	99.4	98.3	99.1	99.8	100.8	97.9	99.7	100.2	98.0																	

(Table 12-10). Electron Microprobe analyses of cement clinker mineral phases from Works E OPC.

Code Spot	ATE 1	ATE 2	ATE 3	ATE 4	ATE 5	ATE 6	ATE 10	ATE 12	ATE 13	ATE 14	ATE 15	ATE 16	ATE 17	ATE 19	ATE 20	ATE 21	ATE 22	ATE 23	Code Spot	ATE 64	ATE 65	ATE 66	ATE 67	ATE 70	ATE 71	ATE 72	ATE 73	ATE 74	ATE 75	ATE 76	ATE 77	ATE 78	ATE 79	ATE 80	ATE 84	ATE 87	ATE 88		
S102	23.9	25.3	24.8	25.3	24.8	26.5	25.1	25.3	25.4	25.0	24.9	23.8	23.2	25.3	22.5	24.6	25.0	25.1	S102	25.0	25.4	21.6	25.3	25.0	24.6	24.5	24.6	25.1	25.1	25.1	24.9	24.7	25.7	24.9	24.9	24.8	25.3		
AL203	1.8	0.7	0.9	0.9	0.8	1.0	0.9	1.0	0.8	0.7	0.8	1.8	1.8	0.8	4.1	0.8	0.6	0.8	AL203	0.6	1.0	5.0	0.9	0.9	0.9	1.1	0.9	1.0	0.8	0.9	0.9	1.4	1.1	1.1	0.9	1.1	0.9		
T102	n.d	0.4	n.d	n.d	n.d	n.d	n.d	T102	n.d	n.d	0.4	n.d	n.d	n.d	0.4	0.3	n.d	n.d	0.3	n.d	n.d	n.d	n.d	n.d	0.3	n.d													
FE203	1.0	0.5	0.6	0.4	0.8	0.7	0.5	0.4	0.5	0.7	0.6	1.4	1.0	0.4	2.1	0.5	0.5	0.5	FE203	0.5	n.d	2.2	0.8	0.4	0.5	0.8	0.4	0.3	n.d	0.4	0.5	0.4	n.d	0.5	0.6	n.d			
NMO	n.d	NMO	n.d	0.3	n.d	0.3																																	
NGO	1.5	1.3	1.1	1.3	1.2	1.0	1.0	1.3	1.0	1.0	1.0	1.3	1.2	1.3	1.4	1.1	1.0	1.1	NGO	1.1	1.0	2.6	1.1	1.2	1.1	1.1	1.2	0.9	1.0	1.0	1.0	1.0	1.1	1.1	1.2	1.1	1.4		
CAO	71.1	72.5	71.5	71.3	72.0	69.9	72.2	72.5	71.0	71.8	71.7	71.2	70.1	72.7	69.2	72.3	72.2	71.9	CAO	72.2	72.9	66.9	72.0	72.2	73.1	72.4	71.5	72.2	72.9	72.6	71.7	72.3	71.7	72.0	72.7	72.0	72.5		
NA2O	n.d	NA2O	n.d	n.d	0.4	n.d	n.d	n.d	n.d	0.4	n.d	n.d																											
K2O	n.d	n.d	n.d	0.2	n.d	0.2	n.d	n.d	n.d	n.d	n.d	n.d	0.8	n.d	0.3	n.d	n.d	n.d	K2O	n.d	n.d	0.2	n.d	n.d	n.d	n.d	0.2	n.d	0.2	n.d	n.d	0.2	n.d	n.d	n.d	n.d	n.d	n.d	
P2O5	n.d	P2O5	n.d	n.d																																			
SO3	n.d	0.8	n.d	0.3	n.d	n.d	n.d	SO3	n.d	0.3	n.d	n.d																											
TOTAL	99.3	100.3	98.9	99.4	99.6	99.3	99.7	100.5	98.7	99.2	99.0	99.5	99.3	100.5	99.9	99.3	99.3	99.4	TOTAL	99.4	100.3	99.3	100.1	99.7	100.2	100.3	99.8	99.5	100.0	99.9	98.9	99.9	100.2	99.1	100.5	99.9	100.4		
Code Spot	ATE 24	ATE 25	ATE 26	ATE 27	ATE 28	ATE 29	ATE 28	ATE 30	ATE 31	ATE 32	ATE 34	ATE 35	ATE 36	ATE 37	ATE 38	ATE 39	ATE 41	ATE 42	Code Spot	ATE 89	ATE 90	ATE 91	ATE 92	ATE 93	ATE 94	ATE 95	ATE 96	ATE 97	ATE 98	ATE 99	ATE 101	ATE 103	ATE 104	ATE 105	ATE 106	ATE 107	ATE 108		
S102	25.0	24.9	25.1	24.8	25.0	25.3	25.0	24.9	25.2	24.9	24.7	25.0	25.1	26.0	25.0	25.0	25.0	25.0	S102	23.9	26.6	25.2	25.0	25.0	25.3	25.1	25.0	25.7	25.1	24.8	24.1	25.3	25.3	25.4	25.0	25.1	24.8		
AL203	0.8	0.8	0.8	0.7	0.7	1.0	1.0	0.8	0.8	0.7	1.1	0.8	0.6	0.6	0.9	0.9	0.7	0.9	AL203	1.6	1.2	0.8	1.0	1.6	1.0	0.7	0.9	1.0	1.1	1.1	1.7	1.2	0.8	0.9	1.0	1.1	0.7		
T102	n.d	T102	n.d	n.d																																			
FE203	0.6	0.6	0.4	0.4	n.d	n.d	n.d	n.d	0.7	0.4	0.4	n.d	0.5	0.4	n.d	n.d	n.d	0.4	FE203	0.6	0.4	n.d	0.3	0.8	n.d	0.4	n.d	n.d	0.7	n.d	0.8	0.4	n.d	n.d	0.4	0.5	0.4		
NMO	n.d	NMO	n.d	n.d																																			
NGO	1.2	1.3	1.1	0.8	1.0	1.0	1.0	1.2	1.0	1.2	0.9	1.1	0.9	1.0	1.0	1.0	1.1	NGO	1.0	0.9	1.0	1.0	1.3	1.0	1.2	1.1	1.0	1.0	0.9	1.6	1.0	1.0	1.0	1.2	1.0	1.1			
CAO	71.8	72.1	72.8	72.1	72.5	72.5	72.5	72.6	71.9	71.6	71.7	72.5	72.3	71.1	72.0	72.6	72.2	71.5	CAO	71.3	69.7	71.9	72.0	71.3	71.9	72.5	72.0	72.7	72.6	72.5	70.8	71.8	72.5	71.9	72.6	72.5	72.1		
NA2O	n.d	NA2O	0.4	n.d	0.5	n.d	n.d	n.d	n.d	n.d	n.d																												
K2O	n.d	0.2	0.2	0.2	n.d	n.d	n.d	n.d	n.d	0.3	n.d	n.d	n.d	0.3	n.d	n.d	n.d	n.d	K2O	n.d	n.d																		
P2O5	n.d	P2O5	n.d	n.d	n.d																																		
SO3	n.d	SO3	0.4	n.d	0.2	n.d	n.d	n.d	n.d	n.d	n.d																												
TOTAL	99.4	99.9	100.4	99.0	99.2	99.8	99.5	99.3	99.8	98.9	99.1	99.2	99.4	99.5	98.8	99.5	98.9	98.9	TOTAL	99.2	98.8	98.9	99.3	100.0	99.2	99.9	99.0	100.4	100.5	99.3	99.7	99.9	99.6	99.2	100.2	100.2	99.1		
Code Spot	ATE 44	ATE 45	ATE 46	ATE 47	ATE 48	ATE 50	ATE 51	ATE 52	ATE 53	ATE 54	ATE 55	ATE 56	ATE 57	ATE 58	ATE 60	ATE 61	ATE 62	ATE 63	Code Spot	ATE 109	ATE 110	ATE 111	ATE 112	ATE 113	ATE 114	ATE 115	ATE 120	ATE 121	ATE 122	ATE 123	ATE 125	ATE 126	ATE 127	ATE 128	ATE 129	ATE 130	ATE 131		
S102	25.0	24.7	25.1	24.6	24.9	25.0	24.8	25.0	25.2	26.4	24.5	24.1	25.1	24.7	25.4	25.2	25.1	25.3	S102	24.7	25.0	24.9	25.5	24.9	25.2	24.9	24.4	25.2	24.7	25.0	24.0	25.1	25.6	25.0	25.4	25.0	24.7		
AL203	0.9	0.9	0.7	0.8	0.8	0.8	0.7	0.7	0.9	0.8	0.9	1.2	0.7	0.9	0.8	0.8	0.8	0.6	AL203	0.7	0.8	1.0	0.7	0.9	0.8	0.9	1.2	0.9	0.9	0.9	1.6	0.7	0.8	0.9	0.7	0.8	0.7		
T102	n.d	0.3	n.d	n.d	n.d	n.d	0.3	n.d	n.d	n.d	T102	n.d	0.2	n.d	n.d	n.d	n.d	n.d	0.2	n.d	n.d	n.d	0.2	n.d	0.2	n.d	n.d	n.d	n.d										
FE203	0.4	0.6	0.6	0.5	0.4	0.4	0.5	0.4	0.4	n.d	0.6	0.5	0.5	0.6	0.4	n.d	0.5	0.4	FE203	0.5	0.4	n.d	n.d	0.5	0.6	n.d	0.5	n.d	0.6	0.6	0.7	0.4	n.d	0.4	n.d	0.4	0.5		
NMO	n.d	NMO	n.d	n.d																																			
NGO	1.1	1.0	1.1	1.0	1.1	0.9	1.0	0.9	1.0	1.0	1.0	1.2	1.0	0.9	1.1	1.0	1.0	1.0	NGO	1.1	1.1	1.2	1.0	1.1	1.1	1.2	1.1	1.0	1.2	1.2	1.2	1.0	1.1	1.0	1.0	1.2	1.0		
CAO	71.5	71.7	71.8	71.5	71.9	71.9	71.5	72.0	71.5	70.6	71.8	72.2	72.3	71.6	72.5	72.7	72.7	72.6	CAO	72.1	72.2	72.0	71.6	71.9	71.8	72.2	71.0	71.8	72.2	71.6	71.5	72.3	72.3	72.6	72.3	72.0	71.7		
NA2O	n.d	NA2O	n.d	n.d	n.d	0.4	n.d	n.d	0.4	n.d	n.d																												
K2O	n.d	0.3	0.2	0.3	0.2	n.d	0.2	0.2	0.2	0.2	n.d	n.d	n.d	0.3	n.d	n.d	n.d	n.d	K2O	n.d	n.d	n.d	0.2	0.2	0.2	0.2	0.2	0.2	0.2	0.2	0.2	0.2	0.2	0.2	0.1	n.d	0.2		
P2O5	n.d	P2O5	n.d	n.d	n.d	n.d	n.d	n.d	0.6	n.d	n.d																												
SO3	n.d	0.3	n.d	SO3	n.d	n.d																																	
TOTAL	98.9	99.5	99.5	98.7	99.3	99.0	98.7	99.2	99.2	99.3	98.8	99.2	99.6	99.0	100.5	99.7	100.1	99.9	TOTAL	99.1	99.7	99.1	99.4	99.5	99.7	99.4	99.6	98.9	99.8	99.2	99.4	99.5	100.0	99.9	99.5	99.4	98.8		





(Table 12-n). Electron Microprobe analyses of cement clinker mineral phases from Works G OPC .

Code Spot	ATE 1	ATE 2	ATE 3	ATE 4	ATE 6	ATE 8	ATE 9	ATE 12	ATE 14	ATE 16	ATE 17	ATE 19	ATE 21	ATE 22	ATE 23	ATE 26	ATE 29	ATE 30	Code Spot	ATE 92	ATE 93	ATE 94	ATE 95	ATE 96	ATE 97	ATE 98	ATE 99	ATE 100	ATE 101	ATE 102	ATE 104	ATE 105	ATE 106	ATE 107	ATE 108	ATE 109	ATE 110		
S102	24.1	24.8	24.2	25.2	25.0	22.9	24.4	24.4	24.4	24.3	24.4	24.0	23.9	24.7	24.2	24.4	24.8	24.7	S102	24.9	24.4	24.4	24.5	24.5	24.9	22.6	23.0	24.6	24.8	24.5	24.1	24.7	24.2	25.0	24.3	24.3	24.8		
AL203	1.4	0.9	1.2	1.6	1.0	3.0	1.1	0.7	0.9	0.8	1.1	1.3	1.4	1.1	2.8	1.5	0.8	0.8	AL203	0.8	1.0	0.8	1.2	1.1	0.8	5.3	4.1	0.8	0.6	1.6	2.9	0.7	6.8	1.0	1.0	1.4	0.6		
T102	n.d	0.2	0.3	0.4	n.d	0.2	0.3	n.d	0.3	n.d	0.2	0.2	0.4	n.d	0.4	n.d	n.d	n.d	T102	n.d	n.d	n.d	n.d	n.d	0.3	0.3	n.d	n.d	0.3	0.4	n.d	0.3	n.d	n.d	0.4	n.d			
FE203	0.5	0.4	0.5	1.1	0.5	0.7	0.3	0.4	n.d	0.5	0.6	0.7	0.8	0.5	1.0	0.7	0.5	0.5	FE203	0.6	0.5	n.d	n.d	0.4	0.5	n.d	1.8	2.0	0.5	n.d	1.0	1.6	n.d	1.8	0.5	0.4	0.8	0.5	
WMO	n.d	0.3	n.d	0.3	n.d	WMO	n.d																																
MGO	0.4	0.5	0.7	1.1	0.8	1.1	0.5	0.5	0.6	0.4	0.8	0.5	0.6	0.5	0.9	1.0	0.7	0.7	MGO	0.7	0.6	0.6	0.7	0.6	0.4	1.0	0.9	0.6	0.6	0.8	1.0	0.4	1.1	0.6	0.5	0.6	0.6		
CAO	73.0	72.4	72.0	69.4	72.5	70.5	72.9	73.2	72.8	72.8	72.1	72.1	72.0	73.0	69.9	70.8	72.7	72.8	CAO	72.3	72.9	73.1	72.6	72.2	72.6	67.9	68.7	72.0	73.4	70.8	65.7	72.9	64.4	72.7	72.6	71.9	72.6		
NA2O	n.d	n.d	n.d	n.d	n.d	0.6	0.5	n.d	n.d	n.d	0.3	n.d	0.3	n.d	0.4	n.d	n.d	n.d	NA2O	n.d	0.4	n.d	0.4	0.4	n.d	0.4	n.d	n.d	n.d	n.d									
K2O	n.d	n.d	0.4	0.2	n.d	0.2	n.d	0.2	n.d	n.d	n.d	n.d	n.d	n.d	0.3	0.2	n.d	n.d	K2O	n.d	n.d	n.d	n.d	n.d	n.d	0.2	n.d	n.d	0.1	0.2	n.d	0.6	n.d	n.d	n.d	n.d			
P205	n.d	n.d	0.3	n.d	n.d	n.d	n.d	n.d	n.d	0.3	n.d	0.4	P205	n.d	0.5	n.d	n.d																						
SO3	n.d	n.d	0.5	n.d	SO3	n.d																																	
TOTAL	99.4	99.5	100.1	99.0	99.8	99.2	100.0	99.4	99.0	99.1	99.8	98.8	99.4	99.8	99.5	99.0	99.5	99.9	TOTAL	99.3	99.4	98.9	99.4	98.9	99.0	99.1	99.0	98.9	99.4	99.5	99.3	98.7	99.6	99.8	99.3	99.4	99.1		
Code Spot	ATE 32	ATE 33	ATE 34	ATE 35	ATE 42	ATE 43	ATE 44	ATE 47	ATE 48	ATE 49	ATE 50	ATE 51	ATE 53	ATE 54	ATE 55	ATE 56	ATE 57	ATE 59	Code Spot	ATE 111	ATE 112	ATE 113	ATE 114	ATE 117	ATE 118	ATE 120	ATE 121	ATE 123	ATE 124	ATE 125	ATE 126	ATE 127	ATE 129	ATE 130	ATE 131	ATE 133	ATE 134		
S102	24.3	24.5	24.2	24.7	24.7	24.5	25.2	24.8	24.8	24.6	24.7	24.6	24.6	24.3	24.5	24.5	24.5	24.6	S102	25.7	24.7	24.8	25.3	24.8	24.0	24.5	23.8	24.6	25.6	24.6	23.5	24.3	24.7	24.2	24.2	24.8	24.6		
AL203	0.9	1.2	1.1	0.7	1.0	1.2	0.9	0.9	0.9	0.9	0.7	0.9	1.1	1.0	0.9	0.8	0.8	0.9	AL203	0.9	0.9	1.1	0.8	1.2	1.3	0.8	3.6	0.8	0.8	0.9	3.7	0.9	0.9	1.0	1.1	1.0	1.1		
T102	n.d	0.3	n.d	n.d	n.d	0.3	n.d	0.3	n.d	0.2	T102	n.d	n.d	n.d	n.d	0.3	n.d	n.d	0.3	n.d	n.d	0.4	n.d	n.d	n.d	0.4	n.d	n.d											
FE203	0.5	0.8	0.7	0.6	0.6	0.8	0.3	0.5	0.5	0.4	0.5	0.4	0.5	0.4	0.4	0.6	0.7	0.7	FE203	n.d	n.d	0.6	n.d	0.7	0.4	n.d	1.9	0.4	n.d	0.4	3.0	0.4	0.6	0.4	0.6	0.4	0.3		
WMO	n.d	WMO	n.d																																				
MGO	0.5	0.5	0.5	0.5	0.3	0.5	0.5	0.7	0.7	0.5	0.6	0.4	0.5	0.4	0.5	0.4	0.5	0.6	MGO	0.4	0.5	0.5	0.6	0.7	0.6	0.5	0.9	0.4	0.5	0.5	0.9	0.6	0.6	0.5	0.5	0.5	0.5		
CAO	73.1	72.5	72.3	72.2	72.1	72.8	72.6	72.6	72.6	72.4	72.2	72.6	72.7	72.5	72.3	72.7	72.5	72.6	CAO	71.7	72.9	72.9	73.1	71.1	72.4	72.7	68.0	73.2	72.8	72.7	68.0	72.6	72.9	72.6	72.1	72.7	73.0		
NA2O	0.5	n.d	0.4	n.d	n.d	n.d	NA2O	n.d	0.3	0.3	n.d	n.d	n.d																										
K2O	n.d	n.d	n.d	0.2	0.2	0.2	n.d	0.2	n.d	n.d	0.2	n.d	0.2	n.d	n.d	n.d	n.d	n.d	K2O	n.d	0.2	n.d	n.d	0.4	0.1	n.d	n.d	n.d	n.d	n.d	n.d								
P205	n.d	n.d	n.d	n.d	0.4	0.4	0.3	n.d	n.d	n.d	0.3	0.3	n.d	n.d	n.d	n.d	n.d	n.d	P205	n.d	n.d	n.d	0.4	0.2	n.d	0.2	n.d	n.d	n.d	n.d	n.d								
SO3	n.d	SO3	n.d																																				
TOTAL	99.8	99.8	98.8	98.9	99.3	100.3	100.0	99.5	99.5	98.8	99.2	99.2	99.4	98.9	99.0	99.1	98.9	99.6	TOTAL	98.7	99.0	99.9	100.2	99.0	98.7	98.5	98.7	99.4	99.7	99.1	99.9	98.9	99.7	99.2	99.2	99.4	99.5		
Code Spot	ATE 60	ATE 61	ATE 63	ATE 64	ATE 65	ATE 66	ATE 67	ATE 78	ATE 79	ATE 80	ATE 81	ATE 83	ATE 84	ATE 85	ATE 86	ATE 87	ATE 89	ATE 90	Code Spot	ATE 135	ATE 136	ATE 137	ATE 138	ATE 140	ATE 141	ATE 142	ATE 144	ATE 146	ATE 147	ATE 148	ATE 149	ATE 151	ATE 152	ATE 154	ATE 156	ATE 157	ATE 158		
S102	24.8	23.6	24.3	24.6	24.8	26.0	24.8	24.8	24.9	24.5	24.9	24.8	24.6	24.5	25.0	24.6	24.5	25.0	S102	24.5	23.1	24.8	24.8	24.6	24.9	24.6	24.0	24.5	24.6	24.8	24.7	24.3	24.6	24.9	24.9	24.9	24.9		
AL203	0.8	2.2	1.1	0.9	0.8	0.9	0.9	1.2	0.7	1.0	1.1	0.9	0.8	1.3	0.9	1.0	0.8	0.8	AL203	1.3	4.0	0.9	0.9	0.7	0.6	1.2	1.4	1.1	1.0	0.8	0.7	0.8	0.9	1.3	0.9	1.0	0.9		
T102	n.d	0.3	n.d	n.d	n.d	T102	n.d	0.2	n.d	n.d	n.d	n.d	0.3	0.5	n.d	n.d	n.d	n.d	0.4	n.d	n.d	0.4	n.d	n.d															
FE203	0.5	1.0	0.3	0.3	0.5	0.6	0.5	0.6	0.3	0.5	0.4	0.6	0.3	0.5	0.3	0.5	0.3	0.3	FE203	0.8	1.5	0.4	n.d	0.5	0.4	0.3	0.8	0.6	0.6	0.6	0.4	0.5	0.7	0.4	0.4	0.4	0.4		
WMO	n.d	WMO	n.d	n.d																																			
MGO	0.5	0.7	0.6	0.6	0.6	0.4	0.5	0.4	0.5	0.5	0.6	0.7	0.7	0.4	0.5	0.4	0.6	0.4	MGO	0.7	0.8	0.5	0.4	0.5	0.5	0.6	0.5	0.6	0.5	0.6	0.5	0.4	0.5	0.6	0.7	0.8	0.6		
CAO	72.6	71.5	72.6	72.5	73.2	72.0	72.3	72.7	72.9	72.6	73.1	72.7	72.0	72.9	71.9	72.6	72.3	73.2	CAO	71.5	70.8	72.3	72.6	72.6	73.1	72.7	71.6	72.3	72.1	72.3	72.4	72.7	72.7	72.4	71.5	72.2	72.4		
NA2O	n.d	n.d	0.4	0.4	0.5	n.d	0.3	n.d	n.d	n.d	n.d	n.d	0.6	n.d	n.d	0.5	n.d	n.d	NA2O	n.d	0.3	n.d																	
K2O	0.2	0.3	0.2	n.d	n.d	0.2	n.d	0.2	n.d	n.d	K2O	n.d	0.3	0.2	n.d	n.d	n.d																						
P205	n.d	n.d	0.6	n.d	n.d	n.d	n.d	n.d	n.d	0.3	n.d	0.4	P205	n.d	n.d	n.d	n.d	n.d	0.2	n.d	n.d	n.d	n.d	n.d	n.d	0.3	n.d	n.d	n.d	n.d	n.d	n.d							
SO3	n.d	n.d	n.d	n.d	n.d	0.3	n.d	SO3	n.d	n.d																													
TOTAL	99.4	99.3	100.1	99.3	100.4	99.8	99.3	99.7	99.6	99.1	100.2	99.5	99.3	99.4	99.1	99.1	99.2	100.1	TOTAL	98.8	99.6	98.9	98.7	98.9	99.7	99.7	98.8	99.3	98.8	99.1	98.9	98.9	99.2	100.4	98.9	99.6	99.2		

(Table 12-12 continued). Electron Microprobe analyses of cement clinker mineral phase from Works G DPC .

Code Spot	ATE 160	ATE 161	ATE 162	ATE 163	ATE 165	ATE 166	ATE 167	ATE 168	ATE 169	ATE 171	ATE 173	ATE 175	ATE 176	ATE 178	ATE 179	ATE 182	ATE 183	ATE 184	Code Spot	ATE 239	ATE 242	ATE 243	BTE 25	BTE 128	BTE 240	BTE 241	BTE 244	BTE 245	BTE 247	BTE 248	BTE 249	ALU 177	ALU 15	ALU 18	ALU 20	ALU 24	ALU 27	
S102	24.0	24.8	25.6	24.6	24.8	24.9	24.4	24.5	24.1	25.0	25.4	24.5	27.1	24.5	24.6	24.4	24.3	24.3	S102	26.1	24.9	24.9	32.2	30.2	31.2	31.2	30.7	31.8	32.6	31.3	29.4	3.8	3.9	19.3	3.8	4.5	4.5	
AL203	1.0	1.0	0.9	0.8	0.8	0.9	1.0	0.7	1.2	2.0	1.1	1.2	1.2	0.8	0.8	0.9	0.8	2.7	AL203	1.0	0.8	0.8	1.4	1.9	1.8	1.5	1.9	1.7	1.3	1.8	2.8	27.3	29.0	9.3	29.0	27.7	28.5	
T102	n.d	0.2	n.d	n.d	0.2	n.d	n.d	0.2	n.d	n.d	n.d	T102	0.4	0.3	n.d	n.d	0.4	n.d	0.3	0.3	0.4	n.d	0.3	0.6	0.9	0.2	n.d	n.d	0.4	0.2								
FE203	0.6	0.5	0.5	0.7	0.4	0.5	0.5	0.6	0.5	0.6	0.6	0.5	0.6	n.d	0.6	0.5	0.5	1.1	FE203	0.4	n.d	0.4	0.6	1.0	0.8	0.8	1.0	0.7	0.7	0.8	1.9	13.1	5.7	1.7	5.3	6.3	5.6	
MNO	n.d	MNO	n.d	n.d	n.d	n.d	n.d	n.d	n.d	n.d	n.d	n.d	n.d	0.3	n.d	n.d	n.d	n.d	n.d																			
MGO	0.9	0.4	0.7	0.6	0.5	0.9	0.5	0.5	0.8	1.0	1.0	0.4	0.5	0.5	0.5	0.2	0.5	0.9	MGO	0.4	0.5	0.6	0.4	0.4	0.3	0.5	0.3	0.3	0.5	0.7	1.7	1.2	0.7	0.8	0.8	0.6	0.6	
CAO	73.1	72.2	72.4	72.1	72.9	71.6	72.3	73.2	71.6	70.5	71.7	72.8	69.0	73.3	72.2	71.9	72.8	70.1	CAO	70.3	73.2	72.4	63.9	64.0	63.6	63.8	62.9	63.3	64.2	63.5	62.3	49.3	56.5	67.6	58.3	56.8	57.2	
NA2O	n.d	n.d	n.d	0.4	n.d	0.3	n.d	0.4	n.d	0.4	n.d	0.3	n.d	n.d	n.d	0.4	n.d	0.3	NA2O	n.d	n.d	n.d	n.d	0.6	0.4	n.d	n.d	0.5	n.d	0.4	0.7	0.7	1.5	0.4	1.1	1.3	1.6	
K2O	0.2	n.d	n.d	0.2	0.2	0.2	0.2	0.2	n.d	0.3	0.2	n.d	0.4	n.d	0.1	0.2	0.2	0.2	K2O	0.2	n.d	n.d	0.5	0.8	0.8	0.7	0.9	0.9	0.7	0.8	0.9	1.6	1.2	0.3	0.7	1.2	1.1	
P2O5	n.d	n.d	n.d	n.d	0.3	n.d	P2O5	n.d	0.5	n.d	n.d	0.7	0.3	0.5	0.8	0.7	n.d	0.5	0.3	n.d	n.d	n.d	n.d	n.d	n.d													
SO3	n.d	SO3	n.d	n.d	n.d	n.d	n.d	n.d	n.d	n.d	n.d	n.d	n.d	n.d	n.d	n.d	n.d	n.d	n.d	n.d																		
TOTAL	99.8	98.9	100.1	99.4	99.9	99.3	98.9	99.7	98.8	99.4	100.0	99.6	99.1	99.1	98.8	98.7	99.1	99.6	TOTAL	98.8	100.2	99.1	99.0	100.0	99.2	99.1	99.0	100.3	99.8	99.9	99.6	98.7	99.2	99.3	99.0	99.0	99.3	
Code Spot	ATE 185	ATE 186	ATE 187	ATE 188	ATE 190	ATE 191	ATE 192	ATE 193	ATE 194	ATE 196	ATE 197	ATE 198	ATE 199	ATE 200	ATE 201	ATE 202	ATE 204	ATE 205	Code Spot	ALU 31	ALU 41	ALU 46	ALU 52	ALU 82	ALU 88	ALU 91	ALU 103	ALU 116	ALU 150	ALU 153	ALU 155	ALU 159	ALU 170	ALU 174	ALU 180	ALU 189	ALU 195	
S102	24.1	24.3	24.3	24.9	24.4	24.8	24.6	24.7	24.7	24.9	24.4	24.5	24.5	24.3	24.1	24.1			S102	18.6	4.8	4.6	4.5	4.2	6.1	4.8	3.9	6.3	10.0	7.1	4.4	5.0	6.0	6.2	4.4	4.3	5.2	
AL203	1.2	0.8	0.8	0.7	1.0	0.7	0.9	1.6	1.2	0.9	1.1	1.3	1.2	0.8	1.6	1.3	2.0	2.2	AL203	13.4	29.5	29.5	30.4	27.3	24.7	25.8	26.4	25.1	22.4	26.2	28.8	28.0	26.8	26.3	26.2	25.7	25.1	
T102	n.d	0.2	0.3	n.d	0.2	0.3	0.3	n.d	n.d	n.d	n.d	n.d	T102	0.8	n.d	n.d	n.d	0.7	0.6	0.8	0.8	0.7	0.8	0.6	0.3	0.4	0.3	0.7	0.8	0.7	0.7							
FE203	0.6	0.4	n.d	0.4	0.5	0.5	0.6	0.5	0.5	0.4	0.4	0.6	0.6	0.6	0.7	0.7	0.6	0.6	FE203	3.6	4.1	4.3	4.5	7.5	8.3	9.9	8.3	7.4	9.7	5.8	5.6	5.9	5.4	5.8	12.4	10.1	10.3	
MNO	n.d	MNO	n.d	n.d	n.d	n.d	n.d	n.d	n.d	n.d	n.d	n.d	n.d	n.d	n.d	n.d	n.d	n.d	n.d	n.d																		
MGO	0.6	0.5	0.4	0.5	0.5	0.6	0.6	0.9	0.7	0.4	0.6	0.6	0.6	0.5	0.6	1.3	0.7	0.8	MGO	1.3	0.4	0.8	0.6	1.3	1.2	1.6	1.1	1.3	2.8	0.6	0.8	0.6	0.5	0.6	1.8	2.2	2.0	
CAO	72.4	72.6	73.6	72.5	72.6	73.3	71.7	70.9	72.7	72.4	73.1	71.7	71.7	73.4	72.2	71.2	71.2	71.7	CAO	66.8	57.2	57.0	57.9	56.8	57.6	55.7	56.8	57.7	53.3	57.5	56.9	56.5	57.0	56.7	52.6	53.4	54.9	
NA2O	n.d	0.3	n.d	n.d	n.d	n.d	n.d	0.5	NA2O	0.5	1.1	1.1	1.1	1.0	1.1	0.9	1.0	0.8	0.6	1.3	1.1	1.4	1.1	1.4	0.6	1.0	0.6											
K2O	0.2	n.d	n.d	0.2	0.2	n.d	0.2	0.2	n.d	n.d	n.d	0.2	0.2	n.d	0.2	0.2	0.2	0.2	K2O	0.3	1.8	1.7	1.6	0.5	0.4	0.4	0.5	0.3	0.4	1.6	1.6	1.5	1.5	1.5	1.5	0.7	0.9	0.8
P2O5	0.3	n.d	n.d	n.d	0.3	n.d	0.2	0.3	n.d	n.d	0.2	n.d	P2O5	n.d	n.d	n.d	n.d	n.d	n.d	n.d	n.d	n.d	n.d	n.d	n.d	n.d	n.d	n.d	n.d	n.d	n.d							
SO3	n.d	SO3	n.d	n.d	n.d	n.d	n.d	n.d	n.d	n.d	n.d	n.d	n.d	n.d	n.d	n.d	n.d	n.d	n.d	n.d																		
TOTAL	99.4	98.6	99.1	99.2	99.5	99.9	98.8	99.2	100.1	98.8	100.5	99.4	99.1	99.8	99.8	99.0	98.8	100.1	TOTAL	99.3	98.9	99.0	100.6	99.3	100.0	99.9	98.8	99.6	100.0	100.7	99.5	99.3	98.6	99.2	99.5	98.3	99.6	
Code Spot	ATE 206	ATE 207	ATE 208	ATE 210	ATE 211	ATE 212	ATE 213	ATE 215	ATE 216	ATE 218	ATE 219	ATE 220	ATE 221	ATE 231	ATE 232	ATE 235	ATE 236	ATE 238	Code Spot	ALU 217	ALU 237	FER 11	FER 13	FER 28	FER 58	FER 115	FER 119	FER 122	FER 132	FER 143	FER 172	FER 203	FER 209	FER 214	FER 234	FER 251	FER 164	
S102	27.7	24.9	24.7	24.9	24.7	24.9	24.6	24.6	25.0	25.2	25.1	24.5	24.9	24.5	24.6	25.0	24.5	24.1	S102	3.9	4.6	3.6	7.8	3.7	13.4	4.9	4.1	4.3	4.2	4.3	6.1	3.7	4.1	13.8	3.0	3.9	6.8	
AL203	1.2	0.8	1.0	0.7	1.0	1.0	1.2	0.9	0.6	0.8	0.8	0.7	1.0	0.9	1.0	1.0	0.8	2.0	AL203	28.8	27.8	17.7	18.2	18.5	10.7	18.2	20.9	23.5	24.8	25.9	19.6	21.5	21.1	12.6	20.7	22.0	21.2	
T102	n.d	0.3	0.3	0.3	0.3	n.d	T102	0.3	0.6	3.0	1.1	2.6	1.7	1.7	2.0	1.1	1.3	1.2	1.9	2.1	1.9	0.8	2.9	2.1	1.3													
FE203	0.4	n.d	0.4	0.6	0.6	0.5	0.4	0.5	0.4	n.d	0.4	n.d	n.d	0.5	0.4	n.d	0.4	1.0	FE203	6.1	7.1	21.7	18.1	21.7	14.3	20.7	21.0	14.2	15.0	14.0	17.3	19.9	19.3	14.7	21.9	19.4	12.2	
MNO	n.d	MNO	n.d	n.d	0.9	n.d	1.0	n.d	0.5	0.6	n.d	n.d	0.4	0.5	0.4	0.6	n.d	n.d	0.6	n.d																		
MGO	0.4	0.4	0.4	0.7	0.6	1.0	0.6	0.4	0.6	0.5	0.5	0.8	0.7	0.6	0.5	0.5	0.7	1.0	MGO	0.9	0.9	3.1	2.1	2.7	1.7	3.5	2.5	2.3	2.8	2.7	2.1	2.4	2.3	2.1	3.0	2.6	1.5	
CAO	69.5	73.3	72.4	71.7	72.6	71.8	72.7	72.5	72.0	73.5	73.3	72.8	72.9	71.8	72.1	72.7	72.2	70.7	CAO	57.7	56.4	48.8	51.0	48.4	56.5	50.6	48.8	53.4	50.4	49.3	51.7	49.2	49.4	56.0	48.3	49.5	53.8	
NA2O	n.d	0.4	NA2O	1.1	1.0	n.d	n.d	n.d	0.5	n.d	0.7	0.4	0.6	0.4	n.d	n.d	n.d	n.d	n.d	n.d																		
K2O	0.3	n.d	n.d	0.3	n.d	0.4	0.2	0.3	0.2	0.2	0.2	0.2	0.2	n.d	n.d	n.d	n.d	n.d	K2O	1.1	0.8	n.d	0.2	n.d	0.2	n.d	n.d	0.2	0.6	0.6	0.7	0.3	n.d	0.5	n.d			

- ABDUL-MAULA, S. and ODLER, I. (1982). Effects of oxidic composition on hydration and strength development of laboratory made Portland Cements. World Cem. Tech., June, 216-222.
- ALDOUS, R., (1983). The hydraulic behaviour of rhombohedral alite. Cement & Concrete Res., 13, 89-96.
- ALDRIDGE, L.P. and EARDLEY, R.P. (1973). Effects of analytical errors on the Bogue calculation of compound composition. Cement Tech., Sep/Oct, 4, 177-182.
- ALDRIDGE, L.P., (1982).a. Accuracy and precision of an X-ray diffraction method for analysing Portland Cement. Cement & Concrete Res., 12, 447-454.
- ALDRIDGE, L.P., (1982).b. Accuracy and precision of phase analysis in Portland Cement by Bogue, Microscopic and X-ray diffraction method. Cement & Concrete Res., 12, 381-398.
- ALEXANDER, K.M., (1972). The relationship between strength and the composition and fineness of cement. Cement & Concrete Res., 2, 663.
- BARNES, P., JEFFERY, J.W., and SARKAR, S.L. (1978). Composition of Portland Cement belites. Cement & Concrete Res., 18, 559-564.
- BEAUPRE, E., (1981). Analysis of ash content and BTU of coal. Internat. Lab., Jan/Feb, 47-53.
- BEITZ, L., MULLER, E. and PLESCH, R.,. The chemical analysis of cement and its raw materials by means of the MRS. 300 multichannel X-ray spectrometer. Siemens analytical application note 154.
- BIGARÉ, M., GUINIER, A., MAZIERES, C., REGOURD, M., YANNAQUIS, N., EYSEL, W., HAHN, Th., and WOERMANN, E., (1967). Polymorphism of Tricalcium Silicate and its solid solutions. J. Am. Ceram. Soc., Vol 50, 11, 609-619.
- BIRCHALL, J.D., HOWARD, A.J. and DOUBLE, D.D. (1980). Some general considerations of a membrane/osmosis model for Portland Cement hydration. Cement & Concrete Res., 10, 145-155.
- BLAINE, R.L., ARNI, H.T. and DEFORE, M.R., (1968). Inter-relations between cement and concrete properties. Part 3, Building Science series 8., Nat. Bur. of Stand.
- BOGUE, R.H., (1929). Cement Recalculation. Ind. and Eng. Chem., 1, 192.
- BOGUE, R.H. and LERCH, W., (1934). Hydration of Portland Cement compounds. Ind. Eng. Chem., 26, No 8, 837-847.
- BOIKOVA, A.I. and TORCPOV, N.A., (1964). Stoichiometry and Polymorphism of Tricalcium silicate. Dokl. Akad. Nauk. SSSR., 156, No. 6, 1428-1431.
- BOIKOVA, A.I., DOMANSKY, A.I., PARAMONAVA, V.A., STAVITSKAJA, G.P. and NIKVSHCHENKO, V.M., (1977). Influence of  $\text{Na}_2\text{O}$  on the structure and properties of  $3\text{CaO} \cdot \text{Al}_2\text{O}_3$ . Cement & Concrete Res., 7, 483.

- BROWN, L.S., (1948). Microscopical study of clinker. Chapter 4, Portland Cement Ass., Chicago, Illinois.
- BROWN MILLER, L.T. and BOGUE, R.H., (1932). The system  $\text{CaO-Na}_2\text{O-Al}_2\text{O}_3$ , Am. J. Sci., 23, 501-524.
- BUTT, Y.M. and TIMASHEV, V.V. (1962). Effects of phase composition of Portland Cement clinkers on the binding properties of cement. Trudy Niitsementa., 17, 85.
- BUTT, Y.M. (1971). Effects of gypsum and alkalis on cement. Isement, 4, 14.
- BUTT, Y.M., TIMASHEV, V.V. and OSOKIN, A.P. (1974). Mechanism of clinker formation process and the modification of its structure. Proc. Vith. Int. Congress on The Chemistry of Cement., (Moscow). P1., 132-154.
- CERVANTES LEE, F. and GLASSER, F.P. (1979). Investigation of the polymorphic forms of  $\text{C}_3\text{A}$ . J. Appl. Cryst., 12, 538.
- CHATTERJEE, A.K. (1979). Phase composition microstructure, quality and burning of Portland Cement clinker- a review of phenomenological interrelations. World Cement Tech. (May/June) Part 1 and 2, 124-135, 165-173.
- CHAYES, F. and FAIRBURN, (1951). A test of the precision of thin section analysis by point count. Am. Miner., 36, 704-712.
- CHROMY, S. (1967). High temperature microscopic investigation of tricalcium and dicalcium silicate phases in Portland Cement. J. Am. Ceram. Soc., 50, 677.
- CHROMY, S. (1970). The inversion of the to modifications of dicalcium silicate. Zement Kalk Gips., 23, 8, 382-389.
- COPELAND, L.E., BRUNAUER, S., KANTRO, D.L., SCHULTZ, E.G. and WEISE, C.H. (1959). Quantitative determination of the four major phases of Portland Cement by combined X-ray and chemical analysis. Anal. Chem., 31, 1521-1530.
- COPELAND, L.E. and KANTRO, D.L. (1960). Kinetics of the hydration of Portland Cement. Proc. Symp. Chem. Cement. Washington, 1, 443-453.
- DORN, J.D. (1978). Microscopic methods for burnability improvement. Cement & Concrete Res., 8, 635-646.
- DOUBLE, D.D. (1981). Cement - A respectable material. Nature, Vol 289, 348-349.

- DUNHAM, A.C. and WILKINSON, F.C.F. (1978). Accuracy, precision and detection limits of energy dispersive electron-microprobe analyser of silicates. X-Ray Spect., 7, 2, 50-56.
- EGOROV, G.B. and BELOV, L.V. (1975). Mathematical modelling of the reactivity of clinkers. Cement, 3, 18-19.
- ERAMIN, N.I., EGEREVA, A.I., DMITRIEVA, A. and FIRFAROVA, I.B. (1970). Solid solutions of  $2\text{CaO} \cdot \text{SiO}_2$  with some metal oxides. 2h., Prikl. Khim., (Leningrad), 43, 1, 18-24.
- FLETCHER, K.E. (1965). The effect of  $\text{Fe}^{3+}$  and  $\text{Al}^{3+}$  on the polymorphism of tricalcium silicate. Trans. Brit. Ceram. Soc., 64, 377-385.
- FLETCHER, K.E. (1968). The analysis of belite in Portland Cement clinker by means of an electron-probe microanalyser. Mag. Concrete Res., 20, 64, 167-170.
- FLETCHER, K.E., MIDDLEY, H.G. and MOORE, A.E. (1965). Data on the binary system  $3\text{CaO} \cdot \text{Al}_2\text{O}_3 \cdot \text{Na}_2\text{O} \cdot 8\text{CaO} \cdot 3\text{Al}_2\text{O}_3$  within the system  $\text{CaO}-\text{Al}_2\text{O}_3-\text{Na}_2\text{O}$ . Mag. Concrete Res., 17, 53, 171-176.
- FLINT, E.P. (1939). Mineralizers in cement. Rock Products, Oct., 40-42.
- FOREST, J. (1967). Study of local encrustation in cement rotary kilns and belites. Silicates Industriels, 32, 11, 373-384.
- GESAUER, J. and KRISTMANN, M. (1979). The influence of the composition of industrial clinker on cement and concrete properties. World Cem. Tech., March.
- GHOSE, A. and BARNES, P. (1979). Electron microprobe analysis of Portland Cement clinker. Cem. Concrete Res., 9, 6, 747-755.
- GHOSE, A. and BARNES, P. (1980). Distribution of minor elements in cement clinkers - macroscopic and microscopic variations. World Cem. Tech., Nov., 441-443.
- GHOSE, A. and BARNES, P. (1981). An unusual form of belite in Portland Cement clinker. J. Am. Ceram. Soc., 63, C120.
- GOUDA, A.R.G. (1980). Fluxes conserve energy in cement manufacture. Rock Products, April, 52-56.
- GOURDIN, P., DEMOULIAN, E., HAWTHORN, F. and VERNTE, C. (1980). Proc. VIIIth. Inter. Cong. Chem. Cement, (Paris), II, 223-228.
- GRYMEK, J. (1959). Influencing the formation of alite in Portland Cement clinker. Silikattechnik, 10, 81-86.
- GUNIER, A. and REGOURD, M. (1968). Structure of Portland Cement minerals. Proc. Vth. Inter. Cong. Chem. Cement, (Tokyo), 1, 1-32.

- GUTT,W.(1968). Manufacture of Portland Cement from phosphatic raw materials. Proc. Vth. Inter. Cong. Chem. Cement.(Tokyo)., 1,93.
- GUTT,W.(1971). Manufacture of cement from industrial byproducts. Current paper, 19/71,Build. Res. Est., Watford, U.K.
- GUTT,W. (1974). The use of byproducts in concrete. Current paper 53/74, Build. Res. Est.,Watford U.K.
- GUTT,W. and NURSE,R.W.(1974). The phase composition of portland cement clinker. Current paper 96/74, Build. Res. Est., Watford U.K.
- GUTT,W. and OSBORNE,G.J.(1966). The system  $2CaO-SiO_2-CaF_2$ . Trans.Brit. Ceram. Soc.,65,521-534.
- GUTT,W. and SMITH,M.A.(1968). Studies of the role of calcium sulphate in the manufacture of Portland Cement clinker . Trans. Brit. Ceram. Soc.,67,10,487.
- GUTT,W. and SMITH,M.A.(1974). Studies of phosphatic portland cements. Current paper 95/74, Build. Res. Est.,Watford U.K.
- GUTTMANN,A. and GILLIE,F.(1931). A final statement on the alite problem. Zement,20,144-147.
- HAN,K.S.,GARD,J.A. and GLASSER,F.P.(1981). Composition of stable and metastable  $C_3A$  solid solution crystallized from simulated clinker melts. Cement & Concrete Res.,11,79,84.
- HARADA,A.T.,OHTA,M. and TAKAGI,S.(1978). The morphology of hydrated alite polymorphs. J. Ceram. Soc. Japan,86,195-202.
- HAHN,T.,EYSEL,W. and WOERMANN,(1968). Crystal chemistry of tricalcium silicate solid solution. Proc. Vth. Intern. Symp. Chem. Cement. Tokyo,1,61-66.
- HALSTEAD,P.E. and MOORE,A.E.(1962). The composition and crystallography of an anhydrous calcium alumino-sulphate occurring in expanding cement. J. Appl. Chem.,12,4,413-417.
- HANSEN,W.C.,BROWNMILLER,L.T. and BOGUE,R.H.(1928). Studies on the system calcium oxide-alumina-ferric oxide, J. Am. Chem. Soc.,50,396-406.
- HANSEN,W.C.(1968). Potential compound composition of Portland Cement clinker. Jnl. Mats.,3,1,100-106.
- HEILMANN,T.(1952). The influence of the fineness of cement raw mixes on their burnability . Proc. IIIrd. Inter. Symp. Chem. Cement, (London),711-749.
- HEILMANN,T.(1960). Reactions of coal ash with portland cement clinker during the burning process. Proc. IVth Intern. Symp. Chem. Cement,(Washington),1,87.

- HJORTH, L. (1971). C.E.R.I.L.H. report, No. 25963.
- HOFMANNER, F. (1975). Microstructure of portland cement clinker .Report from Holderbank Management and Consulting Limited . Switzerland.
- HORNAIN, H. (1971). Sur la répartition des éléments de transition et leur influence sur quelques propriétés du clinker et du cement . Rev. Mat. Const., 671, 203-218.
- HORNAIN, H. (1971). b. Sur la composition de l'aluminate tricalcique. Rev. Mat. Const., 211, 60-64.
- HORNAIN, H. (1973). Analyse à la microsonde de la phase ferritique du clinker . Rev. Mat. Const., 680, May, 4-13.
- INSLEY, H. (1936). Structural Characteristics of some constituents of Portland Cement clinker. Jnl. Res. Nat. Stand. , 17, 353-361.
- INSLEY, H., FLINT, E.P., NEWMAN, E.S. and SWENSON, J.A. (1938). Relations of composition and heat of solution of Portland cement clinker. Jnl. Res. Nat. Bur. Stand., 21, 353-365.
- INSLEY, H. and FRÉCHETTE, D. (1955). Microscopy of ceramic and cements. London Academic Press. (2nd printing.).
- JAWED, I. and SKALNY, J. (1977). Alkalies in cement : A review. Part 1, Cement & Concrete Res., 7, 719-730.
- JAWED, I. and SKALNY, J. (1978). Alkalies in cement : A review. Part 2, Cement & Concrete Res., 8, 37-52.
- JEFFERSON, D.P. (1978). Geology and the cement industry. Industrial Geology, Ed. KNILL, J.L., Oxford University Press .
- JEFFERY, J.W. (1952). The tricalcium silicate phase . Proc. IIIrd. Intern. Symp. Chem. Cement , London, 38.
- JOHANSEN, V. (1977). Influence of alkalis on the strength development of cement. Proc . Symp. on the effects of alkalis on the properties of concrete. Cement & Concrete Association .London.
- KANTRO, D.L., COPELAND, L.E., WEISE, C.H. and BRUNAUER, S. (1964). Quantitative determination of the major phases in Portland Cement by X-ray diffraction methods. Jour. P.C.A., Res. and Dev Labs., January , 20-40.
- KATO, A. (1959). The possibility of the entry of  $\text{SiO}_2$  into the clinker ferrite phase to form a solid solution . Semento Gijutsu Nenpo., XIII, 1-2.
- KLIEGER, P. (1957). Long-time study of cement performance in concrete (Chapter 10). In progress report on strength and elastic properties of concrete. Jnl. Am. Concr. Inst., 54, 12, 481-504.

- KONDO, R. and YOSHIDA, K. (1968). Miscibilities of special elements in tricalcium silicate and alite and the hydration properties of  $C_3S$  solid solution. Proc. Vth. Intern. Symp. Chem., Tokyo, 1, 300-322.
- KNÖFEL, D. (1977). Modifying some properties of Portland Cement clinker and Portland Cement by means of  $TiO_2$ . Zement-Kalk-Gips., 4, 191-196.
- KNÖFEL, D. (1978). Modifying some properties of Portland Cement clinker and Portland Cement by means of  $ZnO$  and  $ZnS$ . Zement-Kalk-Gips., 3, 157-161.
- KNÖFEL, D. (1979). Relationships between chemistry phase content and strength in Portland Cement. Zement-Kalk-Gips., 9, 448-454.
- KRISTMANN, M. (1977). Portland cement clinker mineralogical and chemical investigations. (Part I and II). Cement & Concrete Res., 7, 649-658.
- LEA, F.M., and PARKER, T.W. (1934). Investigations on a portion of the quaternary system  $CaO-Al_2O_3-SiO_2-Fe_2O_3$ . The quaternary subsystem  $CaO-C_2S-C_5A_3-C_4AF$ . Proc. Roy. Soc. (Lond.) Series A, 36.
- LEA, F.M. (1970). The chemistry of cement and concrete, Pub. E. Arnold, London.
- LEHMANN, H., LOCHER, F.W. and THORNEMANN, P. (1964). Der Einfluss der Kalkstein korngroße auf die Klinker mineral bildung im Temperaturbereich von  $850^{\circ}C$  bis  $1450^{\circ}C$ . Tonind. Ztg. 88, 21/22, 489., 23/24, 537
- LUDWIG, R. and RICHARTZ, W. (1978). Fluxes for X-ray fluorescence analysis of substances in the cement industry. Zement-Kalk-Gips., 11, 550-557.
- MAJUMDAR, A.J. (1965). The ferrite phase in cements. Trans. Brit. Ceram. Soc., 64, 2, 105-119.
- MAKI, I. (1973). Microscopy of cement. Cement & Concrete Res., 3, 295.
- MAKI, I. and CHROMY, S. (1978). Microscopic study on the polymorphism of  $Ca_3SiO_5$ . Cement & Concrete Res., 8, 407-414.
- MAKI, I. and GOTO, K. (1982). Factors influencing the phase constitution of alite in Portland Cement clinker. Cement & Concrete Res., 12, 3, 301-308.
- MANDER, J.E. (1977). Effect of alkalis on properties of concrete. Proc. Symp. Chem. Cement. Sep. (1976). London. Cement & Concrete Association, 27.
- MANDER, J.E., ADAMS, L.D. and LARKIN, E.E. (1974). A method for determination of some minor compounds in Portland Cement and clinker by X-ray diffraction. Cement & Concrete Res., 4, 533-544.
- METZGER, A. (1953). The presence of Bredigite  $Ca_2SiO_4$  in Portland Cement clinker. Zement-Kalk-Gips., 42, 269-270.

- MIDGLEY, H.G. (1957). A compilation of X-ray diffraction data of cement minerals. Mag. Concrete Res. March, 17-24.
- MIDGLEY, H.G. (1958). The composition of the ferrite phase in Portland Cement. Mag. Concrete Res., 10, 20, 13-16.
- MIDGLEY, H.G. (1964). The chemistry of cement 1. Ed. TAYLOR, H.F.W., New York, Academic Press, 89.
- MIDGLEY, H.G. (1968). a. The composition of alite (Tricalcium Silicate) in a Portland Cement clinker. Mag. Concrete Res., 20, 62, 41-44.
- MIDGLEY, H.G. (1968). b. The minor elements in alite (Tricalcium Silicate) and belite (Dicalcium Silicate) from some Portland Cement clinkers as determined by electron probe X-ray microanalysis. Proc. Vth. Intern. Symp. Chem. Cement. (Tokyo), Part 1, 226-233.
- MIDGLEY, H.G. (1970). Compound calculation of the phases in Portland Cement clinker. Cement Tech., 2, 4, 79-84.
- MIDGLEY, H.G. (1974). The polymorphism of calcium orthosilicate. Proc. VIth. Intern. Symp. Chem. Cement. (Moscow). Part 1.
- MIDGLEY, H.G. and BENNETT, M. (1971). A microprobe analysis of Larnite and Bredigite from Scawt Hill, Larne, Northern Ireland. Cement & Concrete Res., 1, 413-418.
- MIDGLEY, H.G. and FLETCHER, K.E. (1963). The role of alumina and magnesia in the polymorphism of tricalcium silicate. Trans. Brit. Ceram. Soc., 62, 917-937.
- MIDGLEY, H.G. and MOORE, A.E. (1970). The ferrite phase in Portland Cement clinker. Cement Tech., Sep/Oct., 152-156.
- MIDGLEY, H.G., ROSAMANN, D. and FLETCHER, K.E. (1960). X-ray diffraction examination of Portland Cement clinker. Proc. IVth. Intern. Symp. Chem. Cement., Part 1, 69-81.
- MOORE, A.E. (1965). Examination of a Portland Cement clinker by electron probe micro-analysis. Silicates Industriels. 30, 8, 445-450.
- MOORE, A.E. (1966). Tricalcium aluminate and related phases in Portland Cement. Mag. Concrete Res., 18, 55, 59-64.
- MULLER HESSE, H. and SCHWIETE, H.E. (1956). On the solid solution of MgO in some cement clinker minerals. Zement-Kalk-Gips., 9, 9, 386-389.
- NEWKIRK, T.F. and THWAITE, R.D. (1958). Pseudo-ternary system calcium oxide - monocalcium aluminate - dicalcium ferrite. Jour. Res. NBS. 16, 4, 233-245.
- NEWKIRK, T.F. and THWAITE, R.D. (1958). System  $\text{CaO-CaO-Al}_2\text{O}_3-2\text{CaO}\cdot\text{Fe}_2\text{O}_3$  From "Phase diagrams for Ceramists". By, LEVIN, E.M., ROBBINS, C.R. and McMURDIE, H.F., Ed. RESEN, M.K., Pub, American Ceramic Society (1964).
- NIESEL, K. and THORMANN, P. (1967). The stability fields of dicalcium silicate modifications. Tonind. Zeitung. 91, 9, 362-369.

- NURSE, R.W. (1952). The dicalcium silicate phase. Proc. IIIrd. Intern. Symp. Chem. Cement. (London), 56-77.
- NURSE, R.W. (1960). Phase equilibria and constitution of Portland Cement clinker. Proc IVth. Intern. Symp. Chem. Cement. (Washington), Nat. Bur. Stand. (U.S.A.), Monograph 43 (1962), 9-37.
- NURSE, R.W., WELCH, J.H. and MAJUMDAR, A.J. (1965). The CaO-Al<sub>2</sub>O<sub>3</sub> systems in a moisture free atmosphere. Trans. Brit. Ceram. Soc., 64, 9, 409-418.
- ODLER, I. and WONNEMANN, R. (1983). Effects of alkalis on Portland cement hydration ., I. Alkali oxides incorporated into the crystalline lattice of clinker minerals . Cement & Concrete Res., 13, 4, 477.
- OKROKOV, S.D. and VOLKONSKII, B.V. (1975). Interrelation of composition, structure and properties of clinker., Zement, 6, 8-10.
- ONO, Y., KAWAMURA, S. and SODAY, Y. (1968). Microscopic observations of alite and belite and hydraulic strength of cement . Proc. Vth. Intern. Symp. Chem. Cement. (Tokyo). 1, 275-285.
- OSBAECK, B. (1979). The influence of alkalis on the strength properties of Portland Cement. Zement-Kalk-Gips., 2, 72-77.
- OSBORN, E.F. and MUAN, A. (1960). System CaO-Al<sub>2</sub>O<sub>3</sub>-SiO<sub>2</sub> Revised and Redrawn in "Phase Diagrams for Ceramists". By, LEVIN, E.M., ROBBINS, C.R. and McMURDIE, H.F., Ed. RESEN, M.K., Pub. American Ceramic Society (1964).
- PETERSON, O. (1967). Investigation of Portland Cement clinker with the microprobe. Zement-Kalk-Gips., 2, 61-64.
- POLLITT, H.W. and BROWN, A.W. (1968). The distribution of alkalis in Portland Cement clinker. Proc. Vth. Intern. Symp. Chem. Cement (Tokyo), Part 1, 322-333.
- POPOVICS, S. (1967). A model for the kinetics of the hardening of Portland Cement . Highway Res. Board, Washington, D.C. 192, 14-35.
- POPOVICS, S. (1976). Phenomenological approach to the role of C<sub>3</sub>A in the hardening of Portland Cement pastes. Cement & Concrete Res. 6, 343-350.
- POPOVICS, S. (1981). Extended model for estimating the strength - development capacity of Portland Cement. Mag. Concrete Res., 33, 116, 147-153.
- PRITTS, I.M. and DAUGHERTY, K.E. (1976). The effects of stabilizing agents on the hydration rate of  $\beta$  C<sub>2</sub>S. Cement & Concrete Res. 6, 783-796.
- REGOURD, M. (1978). Crystallization and reactivity of tricalcium aluminate in Portland in Portland Cement., II . Cemento. 75, 323.
- REGOURD, M., CHROMY, S., HJORTH, L., MORTUREUX, B. and GUINIER, A. (1973). X-ray diffraction studies on C<sub>3</sub>A in cement. J. Appl. Cryst., 6, 355.

- REGOURD, M. and GUINIER, A. (1974). The crystal chemistry of the constituents of Portland Cement clinker. Proc. VIth. Intern. Symp. Chem. Cement., Vol 1. (Moscow), 25-52.
- ROBSON, T.D. (1968). The chemistry of calcium aluminate and their relating compounds. Proc. Vth. Intern. Symp. Chem. Cement. (Tokyo), Part 1., 349-365.
- SARKAR, S.L. (1977). Dicalcium Silicate. Unpublished Ph.D. Thesis., University of London.
- SASAKI, T. (1960). X-ray study on the inversion of the crystal form of dicalcium silicate, especially on the effect of stabilizing agents., Semento Gijutsu Nenpo. XIV., 22-23.
- SCHAULT, C.M. and ROY, D.M. (1965). Crystalline solution in  $3\text{CaO} \cdot \text{Al}_2\text{O}_3$  on the join  $\text{Ca}_3\text{Al}_2\text{O}_6$ - $\text{Ca}_3\text{Fe}_2\text{O}_6$ . Nature. 206, 4986, 819.
- SCHWARTZ, J. (1967). Contribution to the investigation of aluminous ferrite phase in Portland Cement clinker. Thesis, C.N.A.M. Paris.
- SHIN, G.Y. and GLASSER, F.P. (1983). Interdependence of sodium and potassium substitution in tricalcium aluminate. Cement & Concrete Res., 13, 135-140.
- SKALNY, J., MANDER, J.E. and MEYERHOFF, M.H., (1975). S.E.M. study of partially dissolved clinkers. Cement & Concrete Res., 5, 119-128.
- SMITH, D.K. (1962). Crystallographic changes with the substitution of aluminium for iron in dicalcium ferrite. Acta. Cryst., 15, 1146-1152.
- SMITH, D.K., MAJUMDAR A.J. and ORDWAY, F. (1961). Re-examination of the polymorphism of dicalcium silicate. J. Am. Ceram. Soc., 44, 8, 405-411.
- SMITH, D.K., MAJUMDAR, A.J. and ORDWAY, F. (1965). The crystal structure of  $\gamma$  dicalcium silicate. Acta. Cryst., 18, 787-795.
- SOROKA, I. (1979). Portland Cement paste and concrete. Macmillan Press, London.
- SPRUNG, S. and RECHENBERG, W. (1977). Effects of alkalis on properties of concrete. Proc. IIIrd. Symp. Chem. Cement. London, Cement & Concrete Ass., 109.
- SUDAKAS, L.G., KAPLYA, A.F., FEDIK, A.A. and SHEIKO, A.N. (1975). Dependence of the quality of cement on the structural peculiarities of clinker, Isement, 2, 19-20.

- SUZUKAWA, Y. (1956). The alkali phases in Portland Cement : II The potassium phase. Zement-Kalk-Gips, 9, 390-396.
- SYLLA, M. (1978). Effects of the kiln atmosphere in the burning of cement clinker. Zement-Kalk-Gips, 6, 291-293.
- TARTE, P. (1965). Al-Fe Isomorphous substitution in  $3\text{CaO}-\text{Al}_2\text{O}_3$  and the interaction between the so called  $\text{C}_3\text{A}$  and  $\text{C}_4\text{AF}$  phases. Nature, 207, 5000, 973-974.
- TAYLOR, H. (1964). Chemistry of cements. Academic Press, London.
- THILO, E. and FUNK, H. (1953). Effects of small amounts of alkalis on the  $\beta$ - $\gamma$  inversion of  $\text{C}_2\text{S}$ . Z. Anorg. Allgem. Chem., 273, 1-2, 28-40.
- TSUBOI, T. and OGAWA, T. (1972). Application of the microscope to the sintering process of cement clinker. Zement-Kalk-Gips, 6, 292-294.
- VARMA, S.P. and WALL, C.D. (1981). A monoclinic tricalcium aluminate ( $\text{C}_3\text{A}$ ) in a commercial Portland Cement clinker. Cement & Concrete Res., 11, 567-574.
- WELCH, J.H. (1960). Reported by NURSE, R.W., Proc. IVth. Intern. Symp. Chem. Cement. (Washington). 1, 36.
- WELCH, J.H. and GUTT, W. (1960). The effect of minor components on the hydraulicity of the calcium silicates. Proc. IVth. Intern. Symp. Chem. Cement. (Washington). 1, 59-68.
- WOERMANN, E. (1960). The decomposition of alite in technical Portland Cement clinker. Proc. IVth. Intern. Symp. Chem. Cement. (Washington). Part 1, 119.
- WOERMANN, E., HAHN, Th. and EYSEL, W. (1963). Chemical and structural investigation on the solid solutions of tricalcium silicate. I. Zement-Kalk-Gips, 16, 370-375.
- WOERMANN, E., HAHN, Th. and EYSEL, W. (1965). Solid solution of Mg in  $\text{Ca}_2\text{Fe}_2\text{O}_5$  and  $\text{Ca}_2\text{FeAlO}_5$ . Am. Ceram. Soc., Bull., 44, 299.
- WOERMANN, E., HAHN, Th. and EYSEL, W. (1979). Substitution of alkalis in tricalcium silicate. Cement & Concrete Res., 9, 6, 701-711.
- WOLF, F. and HILLE, J. (1959). Stabilization of  $\beta$  -  $\text{Ca}_2\text{SiO}_4$  by elemental carbon. Silikattechnik, 10, 530-536.
- YAMAGUCHI, G. and TAKAGI, S. (1968). The analysis of Portland Cement clinker. Proc. Vth. Intern. Symp. Chem. Cement. (Tokyo). Part 1, 181-225.
- YAMAGUCHI, G., VCHIKAWA, S. (1962). Influence of sodium oxide upon the formation and the crystal structure of tricalcium silicate solid solution in the system  $\text{CaO}-\text{SiO}_2-\text{Al}_2\text{O}_3-\text{Fe}_2\text{O}_3$ . J. Ceram. Assoc. Japan, 70, 209-220.
- YAMAUCHI, T. (1937). The system  $\text{CaO}-\text{Fe}_2\text{O}_3$ . J. Japan Ceram. Assoc., 45, 279.
- YANNAQUIS, N. and GUINIER, A. (1959). Polymorphic  $\beta$ - $\gamma$  transition of calcium orthosilicate. Bull. Soc. Franc. Min. Crist., 82, 126-136.

## Standards

### British Standards

BS 12 :1978 Specification for ordinary and rapid hardening

Portland cement. HMSO

BS 1370:1979 Low heat Portland cement. HMSO

BS 4027:1980 Sulphate-resisting Portland cement.HMSO.

BS 4550: Methods of testing cement, Part1 :1978 sampling ; Part 2  
: 1970

Chemical tests ; Part 3 : 1978 Physical tests. HMSO.

### American Standards

ASTM C151 Autoclave test for unsoundness.